GRIFFITH UNIVERSITY

The Co-Transcriptional Response of Intracellular Group B Streptococcus (GBS) and Monocytes

Author

Prince, Darren William

Published

2019-10-31

Thesis Type

Thesis (PhD Doctorate)

School

School of Medical Science

DOI

10.25904/1912/1117

Downloaded from

http://hdl.handle.net/10072/389087

Griffith Research Online

https://research-repository.griffith.edu.au

The Co-Transcriptional Response of Intracellular Group B Streptococcus (GBS) and Monocytes

Darren William Prince

Bachelor of Science with Honours (1st)

Submitted in fulfilment of the requirements of the degree of Doctor of Philosophy

School of Medical Science

Griffith University

May 2019

Abstract

Group B Streptococcus (GBS) is a species of gram positive bacteria representing a significant human pathogen; namely, as the most prolific cause of neonatal disease and mortality globally, but also increasingly reported in adult disease (especially among the elderly and those with compromised immune systems). The first chapter of this thesis reviews the extensive literature covering GBS; with a focus on classification and disease. Selected virulence factors are also discussed. In chapter 2, eight strains of GBS were selected for whole genome sequencing by Third Generation, Pacific Biosystems (PacBio) sequencing technology. A protocol was optimised to provide sufficient, high quality genomic preparations from multiple strains of GBS – suitable for the PacBio technology. Using a sequenced strain of GBS from chapter 2, an infection model was optimised in chapter 3 for the purpose of providing quality RNA for co-transcript analysis. U937 human monocytes were infected with GBS (strain 874391) and the host/pathogen RNA prepared from the same reaction (monocytes with internalised GBS) – with an emphasis on yielding sufficient pathogen RNA; which can sometime be an impediment for co-transcript studies. Pathogen RNA derived from the optimised infection protocol was demonstrated to amplify with RT-qPCR for 12 tested GBS genes (*cylE, 1010, rib, czcD, pil2B, cpsE, scpB, htp, cfb, copA, hvgA and maeA*). In chapter 4, RT-qPCR was used to analyse differential gene expression from the mixed, host/pathogen RNA. Twelve human genes and 12 GBS genes were assessed for differential gene expression. Seven of the tested human genes (*IL8*, *IL1A*, *IL1B*, *IL10*, *TNF*, *LMO2* and *MCP-1*) and 6 of the tested GBS genes (*scpB, 1010, rib, czcD, htp, hvgA*) were significantly upregulated in RNA derived from the infection samples. Of the GBS genes tested, *htp* was the most upregulated. An *htp* knockout mutant of GBS strain 874391 (Δ*htp*) was constructed for chapter 5 of this thesis to assess the impact of *htp* transcription on GBS survival in an infection context. The infection assays optimised in chapter 3 were performed with the Δ*htp* GBS construct. Contrary to expectation, the Δ*htp* GBS construct survived the internalised environment of the monocytes in significantly higher numbers than the wild-type over 48 hours of infection.

Declaration of Originality

This work has not previously been submitted for a degree or diploma in any university. To the best of my knowledge and belief, the thesis contains no material previously published or written by another person except where due reference is made in the thesis itself.

Darren Prince

May 2019.

Table of Contents

Abstract **2**
Declaration of Originality **3**
Table of Contents **4**
List of Tables **9**
List of Figures **11**
Acknowledgements **16**
List of Abbreviations **18**
Publications Related to this Thesis **21**
CHAPTER 1: Introduction and Literature Review **22**
1.1 Introduction 22
Streptococcus 22
Classification 24
Streptococcus agalactiae (Group B Streptococcus) 25
Capsular Serotype 25
Multilocus Sequence Type (MLST) 27
1.2 Disease & Epidemiology 30
Overview 30
Historical Perspective 30
GBS Disease in Neonates, Children and Non-pregnant Adults 32
Clinical Presentations of GBS Disease 34
Meningitis and Meningitis Sequelae 34
Bacteraemia and Sepsis 35
Early Onset Neonatal Disease (EOD) 39
Late Onset Neonatal Disease 43
Carriage and Disease in Adults 44
Selected Virulence Factors 46
Serine-Rich Repeat Proteins 46
β-hemolysin/cytolysin (β-h/c) 50
Streptococcal Group B, C5a-Peptidase (scpB) 51
Polysaccharide Capsule 53
Pili 55
Metal Ion Transport Systems 56
1.3 Genetics 57

The GBS Genome 57
Bacterial Transcriptomes and RNA-seq 60
Host-Pathogen Co-transcriptomes 61
CHAPTER 2: Genome Sequencing of *Streptococcus agalactiae* 874391 66
2.1 Introduction 66
Aims of this study 69
2.2 Materials and Methods 70
2.2.1 General Procedures 70
2.2.1.1 Preparation of Tryptone-soya, horse-blood agar plates 71
2.2.1.2 Preparation of Todd-Hewitt Broth with Yeast (THY) bacterial growth media 71
2.2.1.3 Propagation of GBS on TSA-blood agar plates 71
2.2.1.4 Bacterial growth in THY 71
2.2.1.5 Serial Dilutions of bacterial cultures and bacterial colony counts 71
2.2.1.6 Gel Electrophoresis for DNA and RNA 72
2.2.1.7 Spectrophotometric and Fluorescence Assessment of Nucleic Acid Quality and Quantity 72
2.2.1.8 Sequence Analysis and Bioinformatics 72
Results 2.3 73
2.3.1 Genomic Preparations 73
2.3.2 Genomic preparations of GBS – Final protocol for PacBio sequencing 73
Pellet collections 73
gDNA Preparations 74
2.3.3 gDNA Preparation Data 75
2.3.4 Genome Assembly 76
2.4 Discussion 78
CHAPTER 3: Optimisation of an *in vitro* infection model of human monocytes with *Streptococcus agalactiae* for co-transcript analyisis 80
3.1 Introduction 80
3.1.1 Background 80
3.1.2 Aims of this study 82
3.2 Materials and Methods 82
3.2.1 General Procedures 82
3.2.1.1 Cell Culture Media (500ml) 82
3.2.1.2 Revival and Propagation of U937 Monocyte Cells 82
3.2.1.3 Passaging U937 Monocyte Cells 83
3.2.1.4 Statistics 83

3.2.2 Experimental Procedures 84
3.3 Results 84
3.3.1 Infection Model – Optimised Protocol for RT-qPCR 84
3.3.2 Summary results of optimisation experiments 88
3.4 Discussion 93
CHAPTER 4: Co-transcriptional analysis of GBS-infected U937 monocytes using RT-qPCR 96
4.1 Introduction 96
4.1.1 Aims of this study 98
4.2 Materials and Methods 99
4.2.1 Cell Collection, RNA preparations, DNA Contamination Testing and cDNA synthesis 99
4.2.2 *Mycoplasma* Test of U937 Monocytes 100
4.2.3 Testing cDNA Dilutions in RT-qPCR for Amplification of GBS and U937 Monocyte Gene Targets 101
4.2.4 RT-qPCR Gene Expression Analysis 101
4.3 Results 104
4.3.1 Cell Collection, RNA preparations, DNA Contamination Testing and cDNA synthesis 104
4.3.2 *Mycoplasma* Test of U937 Monocytes 106
4.3.3 Testing cDNA Dilutions in RT-qPCR 106
4.3.4 RT-qPCR Gene Expression Analysis 111
4.3.4.1 Human Genes 111
4.3.4.2 Bacterial Genes 114
4.4 Discussion 117
CHAPTER 5: The role of GBS *Htp* in intracellular survival in monocytes 124
5.1 Introduction 124
5.1.1 Aims of this study 126
5.2 Materials and Methods 127
5.2.1 General Procedures 127
5.2.1.1 THY/Spec100 selective growth media 127
5.2.1.2 THY/Spec100 selective growth agar gel plates 127
5.2.1.3 THY/CM10 selective growth media 127
5.2.1.4 THY/CM10 selective growth agar gel plates 127
5.2.2 Experimental Procedures 128
5.2.2.1 Plasmid Construct for mutating *htp* 128
5.2.2.2 Cross-over induction to generate Δ*htp* mutants 129
5.2.2.3 Genomic Preparations of transformants 131
5.2.2.4 PCR confirmation of the Δ*htp* mutant 132

5.2.2.5 Gel Extraction for DNA sequencing 132
5.2.2.6 GBS Growth Assay 132
5.2.2.7 Infection Assays 133
5.2.2.8 Statistical Analysis 133
5.3 Results 134
5.3.1 Confirmation of *htp* mutant construct 134
5.3.2 Infection Assays 137
5.4 Discussion 140
CHAPTER 6: Conclusion 144
References 150
Appendix 1 – Genomic Preparation Optimisations 183
Experiment 1: Quantify bacterial growth from overnight THY cultures of GBS 183
Experiment 2: Pilot DNA extraction from GBS strain 0058 184
Experiment 3: DNA extraction from GBS strain 0247 187
Experiment 4: gDNA extractions from larger pellets of GBS strains 189
Experiment 5: Genomic preparations using bacterial cells isolated during the mid-log phase of growth 191
Experiment 6: Protocol refinements for genomic preparations using bacterial cells isolated during the mid-log phase of growth 196
Appendix 2 – Infection Assay Optimisations 199
Experiment 1: Infection 1. Pilot Infection Experiment – Adhesion and Invasion assays 199
Experiment 2: Infection 2. Centrifugation to Enhance the Host-Pathogen Interaction 203
Experiment 3: Infection 3. Centrifugation to Enhance the Host-Pathogen Interaction (ii) 204
Experiment 4: Infection 4. Centrifugation to Enhance the Host-Pathogen Interaction (iii) 206
Experiment 5: Effectiveness of Antibiotics against GBS 874391 209
Experiment 6: Effectiveness of Antibiotics against GBS 874391 (ii) 211
Experiment 7: Effectiveness of Antibiotics against GBS 874391 (iii) 213
Experiment 8: Infections 5 and 6. Centrifugation to Enhance the Host-Pathogen Interaction (iv) 216
Experiment 9: Infections 7 to 11. Assess Monocyte Viability 218
Experiment 10: Infections 12 to 14. Centrifugation to Preserve Monocyte Viability 225
Experiment 11: Infections 15 to 17. Scaling Up the Infection Protocol 231
Experiment 12: Pilot Testing the Optimised Protocol with a GBS-only control 233
Experiment 13: GBS-only Mock-Infection 234
Experiment 14: Extracting RNA from cells stored in TRIzol 240
Experiment 15: Test RNA for Bacterial DNA Contamination 243

Experiment 16: Test RNA for Eukaryotic DNA Contamination 247
Experiment 17: Optimisation of PCR Procedures for *β-actin* primers 248
Experiment 18: Optimisation of PCR Procedures for alternative *β-actin* primers 253
Experiment 19: Sequencing of putative *β-actin* amplicon 259
Experiment 20: Design and testing *GAPDH* primers 263
Experiment 21: Upscaling the GBS-only Control 270
Experiment 22: RNA Preparations by Column Extraction 271
Experiment 23: RNA Extraction, DNAse Treatment, cDNA Synthesis and preliminary RT-qPCR 274
Experiment 24: Optimising RNA extraction from monocytes 282
Appendix 3 – Ancillary Information 285

List of Tables

TABLE 2.01: GBS (*S. agalactiae*) Strains used in this study; including uropathogenic S. agalactiae (UPSA), asymptomatic *S. agalactiae* and asymptomatic bacteriuria- causing (ABSA) strains. 70
TABLE 2.02: Final gDNA preparations of 8 GBS strains sent for PacBio sequencing. 75
TABLE 4.01: Primers used for *Mycoplasma* testing by standard PCR. 100
TABLE 4.02: Human primers used in this study. 102
TABLE 4.03: Amplification plots generated by Quantstudio Real-Time PCR Software for four dilutions of cDNA on *dnaN* for 4 mixed (Infection) samples. 107
TABLE 4.04: Amplification plots generated by Quantstudio Real-Time PCR Software for four dilutions of cDNA on *cylE* for 4 Mixed (infection) samples and 2 GBS-only samples. 108
TABLE 4.05: Amplification plots generated by Quantstudio Real-Time PCR Software for four dilutions of cDNA on *cylE*. 110
TABLE 4.06: Statistical summary of gene expression change of infected U937 monocytes against the baseline control of uninfected U937 monocytes using the *GAPDH* housekeeping gene as the reference. 112
TABLE 4.07: Statistical summary of gene expression change of infected U937 monocytes against the baseline control of uninfected U937 monocytes using the *ACTB* housekeeping gene as the reference. 113
TABLE 4.08: Statistical summary of gene expression change intracellular GBS 874391 against the baseline control of non-infection GBS 874391 using the *rpoB* gene as the reference. 115
TABLE 4.09: Statistical summary of gene expression change intracellular GBS 874391 against the baseline control of non-infection GBS 874391 using the *dnaN* gene as the reference. 116
TABLE 5.01: Bacterial strains and plasmids used in this study. 128
TABLE 5.02: Chloramphenicol cassette Insertion ratio for each putative mutant strain of GBS.... 134
TABLE 5.03: Eppendorf Biospectrometer (1mm) absorbance readings of DNA isolations from 10 putative *htp* mutants. 135
TABLE 5.04: Comparative stationary-phase growth of GBS mutant and wild-type strains in THY after 17 hours of incubation. 137
TABLE 5.05: MOI calculations for each of the 4 independent infection assays. 137
TABLE AP1.01: CFU/ml of 8 GBS strains after 16 hours incubation at 37°C in THY media..... 184
TABLE AP1.02: Nanodrop absorbance quantification of each gDNA preparation from 8 pellets of GBS 0058. 186
TABLE AP1.03: Nanodrop absorbance quantification of pooled gDNA from 8 preparations of GBS 0058. 186
TABLE AP1.04: Nanodrop absorbance quantification of 4 gDNA preparations from GBS 0247..... 187
TABLE AP1.05: Nanodrop absorbance quantification of pooled gDNA from 4 preparations of GBS 0247. 188
TABLE AP1.06: Absorbance quantifications of pooled gDNA from multiple preparations of GBS. 188
TABLE AP1.07: Averaged data for the gDNA extracted from 3 pellets of each GBS strain – quantified by absorption on the Eppendorf Biospectrometer. 190
TABLE AP1.08: Pooled preparations of GBS strains (extracted from both original & large pellets) absorbance quantified on the Eppendorf Biospectrometer. 190
TABLE AP1.09: Genomic preparations of GBS using cells collected during the mid-log growth phase. 193

TABLE AP1.10: Pooled and Absorbance measured genomic preparations of GBS using mid-log growth cells. 193
TABLE AP1.11: Comparison of DNA quantity measurements using absorbance and fluorescence (Qubit) based methods, from experiment 5 (mid-exponential growth phase). 194
TABLE AP1.12: BioSpec absorbance quantification of gDNA preparations for 4 GBS strains, 2 treatments per strain, and 2 elutions per treatment. 197
TABLE AP2.01: GBS counts from infections and Eppendorf Biospectrometer (1mm) absorbance readings from individual RNA isolations. 242
TABLE AP2.01: RNA Column Extraction 3. Absorbance measures of RNA yield from GBS cells incubated under various media conditions. 272
TABLE AP2.02: RNA Column Extraction 4. Absorbance measures of RNA yield from varying numbers of GBS incubated in sRPMI with 1% FBS..... 273
TABLE AP2.03: The 12 GBS genes used in this study for RT-qPCR and their primers. 276
TABLE AP2.04: Summary of RNA derived from 12 GBS-only samples..... 277
Table A: *GAPDH* primers designed for this study to test infection-derived RNA for human DNA contamination. 285
TABLE B: Monocyte cell viability after bead-beating..... 286
TABLE C: Summary statistics of 4 bead-beating experiments (i.e. summary data from TABLE B). 286
TABLE D: Cell collection data from infection model optimisations. 287
TABLE E: RNA isolation, quantification and cDNA synthesis data from infection model optimisations..... 287
TABLE F: Results Summary generated by Quantstudio Real-Time PCR Software for dnaN amplification of various cDNA dilutions from 4 infection samples..... 288
TABLE G: Results Summary generated by Quantstudio Real-Time PCR Software for cylE amplification of various cDNA dilutions from 4 infection samples and 2 GBS-only samples. 289
TABLE H: Results Summary tables generated by Quantstudio Real-Time PCR Software for all human genes over 5 separate runs of qPCR. 290
TABLE I: Results Summary tables generated by Quantstudio Real-Time PCR Software for all GBS genes over 6 separate runs of qPCR. 304
TABLE J: Assembled contig of *htp* mutant GV6_177 – FASTA file format..... 322
TABLE K: Assembled contig of *htp* mutant GV12_8 – FASTA file format..... 323
TABLE L: Assembled contig of WT GBS 874391 – FASTA file format. 324

List of Figures

FIGURE 2.01: Agarose gel showing genomic integrity of 1µg gDNA final preparations (absorbance quantified) from 8 GBS strains. 75
FIGURE 2.02: Agarose gel showing genomic integrity of 1µg re-prepared GBS 0058. 76
FIGURE 2.03: Histogram of mapped read lengths used by the SMRT software to generate an assembled genome for GBS 0058. 76
FIGURE 2.04: Coverage plot for the assembled genome of GBS 0058 generated by the SMRT software. 77
FIGURE 3.01: The effect of varying pre-incubation centrifuging times on the GBS CFU/ml recovered from monocytes after 5hrs antibiotic treatments. 88
FIGURE 3.02: The effect of varying pre-incubation centrifuging times on monocyte survival (cells/ml) and viability (%) after 5hrs antibiotic treatments. 89
FIGURE 3.03: GBS Time Kill – Six Hour Assays. 90
FIGURE 3.05: RT-qPCR performed on GBS-only cDNA samples. 92
FIGURE 3.06: RT-qPCR performed on a single sample of mixed cDNA amplifying GBS housekeeping genes. 92
FIGURE 4.01: Agarose gel showing PCR results for a single Infection/Mixed RNA sample 266 (M266) tested for bacterial and human DNA contamination (*spb1* and *GAPDH* respectively). 104
FIGURE 4.02: Agarose gel showing PCR results for 3 Infection/Mixed RNA samples (M286, M296 and M306) - tested for bacterial and human DNA contamination (*spb1* and *GAPDH* respectively). 105
FIGURE 4.03: Agarose gel showing PCR results for 6 Monocyte/U937-only samples (U237A1, U237A2, U237A3, U247A1, U247A2 and U247A3) - tested for human DNA contamination (*GAPDH*). 105
FIGURE 4.04: Agarose gel showing PCR results for Mycoplasma testing of the U937 monocytes used for the infection assays in this study. 106
FIGURE 4.05: Fold gene expression change of the infected U937 monocytes against the baseline transcript control of uninfected U937 monocytes - with *GAPDH* as the reference gene. 112
FIGURE 4.06: Fold gene expression change of the infected U937 monocytes against the baseline transcript control of uninfected U937 monocytes - with *ACTB* as the reference gene. 113
FIGURE 4.07: Fold change of bacterial genes in the GBS-infected U937 monocyte group compared to control GBS incubations without monocytes, using *rpoB* as the reference gene. 115
FIGURE 4.08: Fold change of bacterial genes in the GBS-infected U937 monocyte group compared to control GBS incubations without monocytes, using *dnaN* as the reference gene. 116
FIGURE 5.01: GBS 874391 htp mutation. 129
FIGURE 5.02: Agarose gel showing the PCR-generated amplicons of 10 putative mutants using the *htp*_CHK primers. 135
FIGURE 5.03: Sequence Assemblies generated using of 2 primer sets on the Δ*htp* strain GV_6_177 against the chloramphenicol cassette (pLZ12). 136
FIGURE 5.04: Sequence Assemblies generated using of 2 primer sets on the Δ*htp* strain GV_12_8 against the chloramphenicol cassette (pLZ12). 136
FIGURE 5.05: Sequence Assemblies generated using of 2 primer sets on the wild-type GBS 874391 against the *htp* gene (CHF17_01323). 136
FIGURE 5.06: Four independent infection assays comparing monocyte-internalised GBS (both wild-type and Δ*htp*) over 48 hours of infection. 138

FIGURE 5.07: Pooled means from 4 independent infection assays comparing monocyte-internalised GBS (both wild-type and Δ*htp*) over 48 hours of infection. 139
FIGURE AP1.01: Agarose gel showing 1µg gDNA from 8 GBS strains as indicated. 191
FIGURE AP1.02: Agarose gel showing separation of 1µg gDNA from 8 GBS strains as indicated, isolated from cells in mid-exponential (mid-log) growth phase. 194
FIGURE AP1.03: Agarose gel showing separation of 1µg gDNA (fluorescence quantified) from 8 GBS strains as indicated. 195
FIGURE AP1.04: Agarose gel showing separation of 1µg gDNA from GBS strains 874391 and 0834 as indicated, isolated from cells in mid-exponential growth phase, comparing 2 elutions of preparations derived from heat/vortexing vs bead-beating methods. 197
FIGURE AP1.05: Agarose gel showing separation of 1µg gDNA from GBS strains 874391 and 0843 as indicated, isolated from cells in mid-exponential growth phase, comparing 2 elutions of preparations derived from 1 minute vs 5 minutes bead-beating methods. 198
FIGURE AP2.01: Infection 1 – U937 Monocytes infected with GBS 874391 at an MOI of 35. 202
FIGURE AP2.02: Infection 2 - GBS recovered from centrifuged vs non-centrifuged monocytes infected with GBS 874391 at an MOI of 79. 204
FIGURE AP2.03: Infection 3 - GBS recovered from centrifuged vs non-centrifuged monocytes infected with GBS 874391 at an MOI of 285. 206
FIGURE AP2.04: Infection 4 - GBS recovered from centrifuged vs non-centrifuged monocytes infected with GBS 874391 at an MOI of 285. 207
FIGURE AP2.05: Infection 3 - GBS recovered from first and final wash supernatants. 208
FIGURE AP2.06: GBS Time Kill Assay 1. 210
FIGURE AP2.07: GBS Time Kill Assay 2. 211
FIGURE AP2.08: GBS Time Kill Assay 3. 212
FIGURE AP2.09: GBS Time Kill Assay 4. 213
FIGURE AP2.10: GBS Time Kill – Six Hour Assay 1. 214
FIGURE AP2.11: GBS Time Kill – Six Hour Assay 2. 215
FIGURE AP2.12: Infection 5. GBS recovered from centrifuged vs non-centrifuged monocytes infected with GBS 874391 at an MOI of 1308; including the final wash supernatant at time point 6. 217
FIGURE AP2.13: Infection 6. GBS recovered from centrifuged monocytes infected at an MOI of 285; and including the first and final pre-processing wash supernatants. 218
FIGURE AP2.14: Infection 7. GBS recovered from centrifuged monocytes infected at an MOI of 212; and including the first and final pre-processing wash supernatants. 220
FIGURE AP2.15: Infection 8. GBS recovered from centrifuged monocytes infected at an MOI of 168; and including the first and final pre-processing wash supernatants. 220
FIGURE AP2.16: Infection 9. GBS recovered from centrifuged monocytes infected at an MOI of 168; and including the second and final pre-processing wash supernatants. 221
FIGURE AP2.17: Infection 10. GBS recovered from monocytes infected with GBS 874391 at an MOI of 101; and including the second and final pre-processing wash supernatants. 222
FIGURE AP2.18: Infection 10. Counts of viable infected monocytes over the infection period. 222
FIGURE AP2.19: Infection 11. GBS recovered from monocytes infected with GBS 874391 at an MOI of 79; and including the second and final pre-processing wash supernatants. 223
FIGURE AP2.20: Infection 11. Counts of viable infected monocytes over the infection period. 224
FIGURE AP2.21: Infection 12. GBS recovered from infected monocytes and final wash supernatants for three, pre-incubation conditions; no-centrifuge, 5 minute centrifuge and 50 minute centrifuge. 226

FIGURE AP2.22: Infection 12. Monocyte and GBS cell count/ml after 5 hours of antibiotic treatment. 226
FIGURE AP2.23: Infection 13. GBS recovered from infected monocytes and final wash supernatants for three, pre-incubation conditions; no-centrifuge, 5 minute centrifuge and 50 minute centrifuge. 227
FIGURE AP2.24: Infection 13. Monocyte and GBS cell count/ml after 5 hours of antibiotic treatment. 228
FIGURE AP2.25: Infection 14. GBS recovered from infected monocytes and final wash supernatants for three, pre-incubation conditions; no-centrifuge, 5 minute centrifuge and 50 minute centrifuge. 228
FIGURE AP2.26: Infection 14. Monocyte and GBS cell count/ml after 5 hours of antibiotic treatment. 229
FIGURE AP2.27: The effect of varying pre-incubation centrifuging times on the GBS CFU/ml recovered from monocytes after 5hrs antibiotic treatments..... 230
FIGURE AP2.28: The effect of varying pre-incubation centrifuging times on monocyte survival (cells/ml) and viability (%) after 5hrs antibiotic treatments. 230
FIGURE AP2.29: GBS counts (CFU/ml) and Monocyte counts (cells/ml) from three, 24ml infections. 232
FIGURE AP2.30: Mock-infection 1. GBS-only control in 10% bRPMI diluted in water..... 234
FIGURE AP2.31: Mock-infection 2. Testing GBS survival and proliferation in bRPMI diluted in PBS. 236
FIGURE AP2.32: Mock-infection 3. Testing GBS survival and proliferation in 1X bRPMI, sRPMI, and sRPMI with 10% FBS..... 236
FIGURE AP2.33: Mock-infection 4. Testing GBS survival and proliferation in sRPMI containing various dilutions of FBS. 237
FIGURE AP2.34: Mock-infection 5. Testing GBS survival and proliferation in sRPMI containing various dilutions of FBS over six hours – with the addition a bRPMI and sRPMI treatment. 237
FIGURE AP2.35: Mock-infection 6. Testing GBS survival and proliferation in sRPMI containing heavier dilutions of FBS and additionally, the same concentrations of FBS in 1:10 dilutions of sRPMI. 238
FIGURE AP2.36: Mock-infection 7. Testing GBS survival and proliferation in sRPMI containing heavier dilutions of FBS..... 239
FIGURE AP2.37: Mock-infection 8. Testing GBS survival and proliferation in sRPMI containing heavier dilutions of FBS..... 239
FIGURE AP2.38: Quantified RNA Extractions from TRIzol Reagent; Mixed (blue) and GBS-only (red) samples. 241
FIGURE AP2.39: Agarose gel showing separation of eukaryotic ribosomal subunits from 2µg RNA isolated from 12 selected infection samples. 243
FIGURE AP2.40: Agarose gels of 2 independent PCRs testing for the presence of bacterial DNA in selected infection samples. 245
FIGURE AP2.41: Agarose gel of PCR rerun of 10 infection samples that previously demonstrated possible overlap with the amplified region of interest..... 245
FIGURE AP2.42: Agarose gel showing bacterial DNA contamination of RNA isolated from 4 GBS-only control treatments. 246
FIGURE AP2.43: Agarose gel of PCR results for 4 DNA-contaminated RNA samples after treatment with the Turbo DNAfree Kit. 246
FIGURE AP2.44: Agarose gel of PCR testing for Human genomic DNA contamination of RNA isolated from 12 selected infections. 248

FIGURE AP2.45: PCR Optimisations 1 and 2. Agarose gels showing the results of 2 independent PCRs each testing the same 12 infection samples with β-actin primers - for gDNA contamination. 250
FIGURE AP2.46: PCR Optimisation 3. Agarose gels showing PCR results for 12 infection samples with *β-actin* primers – testing for gDNA contamination. 250
FIGURE AP2.47: PCR Optimisation 4. Agarose gel showing PCR optimisation results (optimising for annealing temperature and $MgCl_2$) for *β-actin* primers on a gDNA template. 251
FIGURE AP2.48: PCR Optimisation 5. Agarose gel showing PCR optimisation results (further optimising for annealing temperature and $MgCl_2$) for *β-actin* primers on a gDNA template. 252
FIGURE AP2.49: PCR Optimisation 6 – Agarose gel showing PCR optimisation for alternative *β-actin* primers on gDNA for annealing temperature and $MgCl_2$. 254
FIGURE AP2.50: PCR Optimisation 7 - Agarose gel showing PCR optimisation for alternative *β-actin* primers on cDNA for annealing temperature and $MgCl_2$. 255
FIGURE AP2.51: PCR Optimisation 8 - Agarose gel showing PCR optimisation for alternative *β-actin* primers on gDNA for annealing temperature, $MgCl_2$ concentration and PCR extension time. 256
FIGURE AP2.52: Optimisation 9 – Agarose gel showing PCR optimisation results for alternate *β-actin* primers in 2mM $MgCl_2$ at annealing temperatures 64°C & 66°C for DMSO (% volume). 257
FIGURE AP2.53: Optimisation 10 – Agarose gel of PCR products comparing Primary genomic DNA (PgDNA) against mixed genomic DNA (MgDNA). 258
FIGURE AP2.54: Agarose gels of putative PCR-generated *β-actin* amplicons (Gel A: MgDNA. Gel B: cDNA) for gel-extraction and sequencing. 260
FIGURE AP2.55: cDNA sequence assembly generated in Sequencher 5.3. 260
FIGURE AP2.56: gDNA sequence assembly generated in Sequencher 5.3. 261
FIGURE AP2.57: Agarose gel of putative PCR-generated *β-actin* amplicons (gDNA) for gel-extraction and sequencing. 261
FIGURE AP2.58: cDNA (from first gel extraction) sequence assembly generated in Sequencher 5.3. 262
FIGURE AP2.59: gDNA (from repeated gel extraction) sequence assembly generated in Sequencher 5.3. 262
FIGURE AP2.60: Unidirectional assembly of gDNA sequences generated in Sequencher 5.3. 262
FIGURE AP2.61: Map of where the amplicons fit along the human GAPDH gene based on the newly designed primers. 264
FIGURE AP2.62: Agarose gel showing putative *GAPDH* PCR-generated amplicons from newly designed primer sets on mixed gDNA. 265
FIGURE AP2.63: Agarose gel showing putative *GAPDH* PCR-generated amplicons using newly designed primers 4, 7a and 7b on both gDNA and cDNA. 266
FIGURE AP2.64: Agarose gels testing 14 RNA samples for DNA contamination using 2 newly designed *GAPDH* primer sets. 267
FIGURE AP2.65: Agarose gels testing the sensitivity of the *GAPDH* primer set 7a to detect human DNA contamination in RNA samples. 268
FIGURE AP2.66: Agarose gels testing the sensitivity of the *GAPDH* primer set 7a to detect human DNA contamination in RNA samples after being treated with DNase. 269
FIGURE AP2.67: RNA Column Extraction 4. Trend line demonstrating the correlation between cell numbers and RNA yield for 6-hour incubated, GBS-only treatment in sRPMI with 1% FBS. 273
FIGURE AP2.68: Agarose gel showing spb1 DNA contamination test of 12 GBS-only RNA samples. 277
FIGURE AP2.69: Agarose gel showing DNA contamination test of 5 GBS-only RNA samples after undergoing DNase treatment. 278

FIGURE AP2.70: Experion gel image showing prokaryotic ribosomal RNA. 278
FIGURE AP2.71: RT-qPCR performed on GBS-only cDNA samples. 280
FIGURE AP2.72: RT-qPCR performed on a single sample of mixed cDNA amplifying GBS housekeeping genes. 281
FIGURE AP2.73: U937 monocyte cell count data for viability estimates after bead-beating. 283
FIGURE AP2.74: Mean and standard deviation for cell count of viable monocyte across four independent bead-beating experiments. 283

Acknowledgements

I would firstly like to express appreciation to my supervisors, Professor Glen Ulett and Doctor Matthew Sullivan for the opportunity to pursue my PhD as part of this laboratory team; and for their invaluable patience, wisdom, knowledge and guidance passed on to me throughout the course of this project.

I would like to thank the Menzies Health Institute at Griffith University for use of their laboratory facilities. I also appreciate the financial support from the Australian Government through their Research Training Support Scholarship program – without which my completion this project would not have been possible.

I would also like to thank Doctor Deepak Ipe for his technical advice and moral support; especially during the early stages of my candidature.

Thanks also to and for their contributions to the GBS gene assembly as published in Genome Announcements (Sullivan *et al.*, 2017a).

Special thanks to Research Assistant Dean Gosling, firstly for his role in constructing the mutant bacterial strain used in this project, but also for keeping the lab In good spirits; despite the challenges involved in having to look after the rest of us.

I would also like to thank the rest of the lab team, Doctor Kelvin Goh, Lahiru Katupitiya, Michelle Chamoun and Dhruba Achyra for the many and varied ways in which you all contributed to the maintenance of my sanity throughout our time together.

I am deeply grateful for the love, patience, advice and support of my family and friends throughout the course of my studies; namely my Dad, Darryl, my sister and her family Cindi, Craig, Catelyn and Jessica Peers, to Ross Blyth, Dina Bryan, Kathryn Lee, Tracie Cheng and Anna Chruscik.

I would like to pay special tribute to my Mum, Elizabeth Brown, and to my Nanna Coleman, both of whom passed away during my studies. It is only by their unwavering examples of love, support, kindness and generosity of spirit that I have developed into the person I am today. You are both deeply missed.

List of Abbreviations

Δhtp	*htp* knockout mutant strain of GBS 874391
µl	Microliters
µg	Micrograms
aa	Amino acid
ABC	ATP Binding Cassette
ABSA	Asymptomatic, bacteriuria-causing *S. agalactiae*
ABX	Antibiotics
ACTB	Beta-actin
AUC	Area Under the Curve
β-actin	Beta-actin
β-h/c	Beta-hemolysin/cytolysin
BBB	Blood Brain Barrier
bp	Base Pair
bRPMI	Basal RPMI cell culture media
CAMP	Christie–Atkins–Munch-Petersen
CC	Clonal Complex of GBS
cDNA	Copy DNA
CFU	Colony Forming Units
Cm	Chloramphenicol
Cm^R	Chloramphenicol resistance
CM10	Media containing 10µg/ml Chloramphenicol
cRPMI	Complete RPMI cell culture media
CXCL-1	C-X-C motif ligand 1
czcD	Cobalt-zinc-cadmium resistance protein

DAPI	4',6-diamino-2-phenylindole, dihydrochloride
DEVANI	Design of a Vaccine Against Neonatal Infection
DNA	Deoxyribonucleic acid
dNTPs	Deoxynucleotide triphosphates
E	Exponent in exponential notation (e.g. 5.3E7 = 5.3 x 10^7)
ECM	Extracellular Matrix
EOD	Early Onset Disease
GBS	Group B Streptococcus
GAPDH	Glyceraldehyde 3-phosphate dehydrogenase
gDNA	Genomic DNA
GU	Genitourinary
Htp	Histidine Triad Proteins
HvgA	Hypervirulent GBS Adhesin
IL	Interleukin
LOD	Late Onset Disease
LMO2	Host LIM domain only 2
MCP-1	Host Monocyte chemoattractant protein 1
MgDNA	Mixed genomic DNA isolated from GBS-infected monocytes
ml	Millilitres
MLST	Multilocus Sequence Type
NET	Neutrophil Extracellular Traps
NTC	No Template Control
PacBio	Pacific Biosciences
PgDNA	Primary genomic DNA isolated from human cells
PCR	Polymerase Chain Reaction

Rib	Resistance to proteases, immunity, group B
ROS	Reactive Oxygen Species
RPMI	Roswell Park Memorial Institute (RPMI) 1640 Medium
rpoB	gene encoding the beta subunit of a bacterial RNA polymerase
SMRT	Single Molecule Real Time
ScpB	Streptococcal Group B, C5a-Peptidase
SOPS	Standard Operating Procedures
Spec	Spectinomycin antibiotic
$Spec^R$	Spectinomycin resistance
Spec100	Media containing 100µg/ml Spectinomycin
sRPMI	Supplemented RPMI cell culture media
Srr	Serine-Rich Repeat proteins
ST	Sequence Type (same as MLST)
T	Time point - hours (e.g. T=4 is 4 hours)
T^S	Temperature Sensitive
THY	Todd-Hewitt Broth with yeast
TNF	Tumor Necrosis Factor
TRAIL	Tumor necrosis factor-Related Apoptosis-Inducing Ligand
TSA-Blood	Tryptone-soya, horse blood
ULOD	Ultra-late onset disease
UPSA	Uropathogenic *S. agalactiae*
UTI	Urinary Tract Infection
WT	Wild-type bacterial strain

Publications Related to this Thesis

Sullivan MJ, Forde BM, Prince DW, Ipe DS, Ben Zakour NL, Davies MR, Dougan G, Beatson SA, Ulett GC (2017). “Complete Genome Sequence of Serotype III *Streptococcus agalactiae* Sequence Type 17 Strain 874391”, Genome Announcements, Volume 5, Issue 42, e01107-17.

CHAPTER 1: Introduction and Literature Review

1.1 Introduction

Streptococcus agalactiae (that is, Group B Streptococci or GBS) is a common bacterial colonizer (i.e. normal flora) of the human gastro-intestinal and genitourinary tracts (Bliss *et al.*, 2002, Easmon, 1986). Originally discovered as a veterinary pathogen (Keefe, 1997, Plastridge, 1958, Lancefield, 1934), *S. agalactiae* is now considered a significant pathogenic agent of various human diseases. *S. agalactiae* is most notably implicated in neonatal sepsis and meningitis (Dermer *et al.*, 2004), but is also increasingly associated with adult disease – especially in the elderly and immunocompromised (Eickhoff *et al.*, 1964, Harper, 1971, Farley *et al.*, 1993, Verghese *et al.*, 1986). Infection by *S. agalactiae* is facilitated by a broad range of virulence factors ranging from adhesins/invasins, to toxins, as well as strategies to circumvent host immunity (Rajagopal, 2009). Continued advances in genetic sequencing technologies, including the ability to reveal whole genomes and transcriptomes, have significantly contributed to our knowledge of bacterial infectious mechanisms (Edwards & Holt, 2013, Loman *et al.*, 2012). Therefore the knowledge base available for research into medical treatments and vaccines has greatly benefited from the contributions of these new technologies.

Streptococcus

Streptococcus (from the Greek Streptos - meaning chain, and coccos - meaning berry) is a genus of bacteria named for their ellipsoid (elongated spheroid) cells arranged in pairs or chain-like structures. The first use of the term “Streptococcus” is commonly attributed to Theodor Billroth (Billroth, 1874) following his microscope observations of chain-forming cocci (Ferretti & Kohler, 2016, Wilson, 1987). However, Buchanan (Buchanan, 1917) argues that Rosenbach (Rosenbach, 1884) should be the designated author of *Streptococcus*; as the first author to record using the term specifically for the genus. The two-dimensional chains of Streptococcal bacteria result from the

tendency of their ovoid cells to divide repeatedly along a single, parallel plane, along the shortest circumferential axis of the ellipsoid cell, which is in contrast to truly spherical cocci (such as *Staphylococcus*) which can divide along multiple planes; permitting tetrad motifs and/or three-dimensional clusters of cells (Zapun *et al.*, 2008).

Bacterial chain length in streptococci has the potential to influence virulence; depending on the host environment (Evans *et al.*, 2014). Several studies have reported a relationship between capsular synthesis and streptococcal chain lengths. Miller *et al.* (Miller & Neely, 2005) reported variable chain lengths associated with capsular mutants of *Streptococcus iniae*. Hanson *et al.* (Hanson *et al.*, 2012) found that interrupting the expression of the capsule synthesis gene, *cpsA*, in *S. agalactiae* resulted in longer chains. Pneumococcal studies have found that the expression of a polysaccharide capsule, whilst essential for virulence, inhibits the alibility of the bacteria to adhere to host cells (Cundell *et al.*, 1995, Hammerschmidt *et al.*, 2005, Weiser *et al.*, 2003, Talbot *et al.*, 1996, Adamou *et al.*, 1998). Increased chain length may provide bacteria a measure to overcome the adhesion inefficiency resulting from the presence of a capsule (Rodriguez *et al.*, 2012). However, smaller chain lengths may reduce the capacity of the host immune system to mark bacterial cells for phagocytosis through complement evasion (Dalia & Weiser, 2011).

The methods of cell division and separation (i.e. determining the structure of cell aggregation and chain length) are better studied in rod-shaped bacteria than in cocci (Pinho *et al.*, 2013). A diverse range of murein hydrolases (a class of enzyme which breaks down the peptidoglycan walls of bacteria, thereby facilitating cell division and separation) have been described; predominantly from *Escherichia coli* and the genus *Bacillis* (Vollmer *et al.*, 2008, Smith *et al.*, 2000, Shockman *et al.*, 1996, Holtje & Tuomanen, 1991). In Streptococcal species, the murein hydrolase designated PcsB (for Protein Cell-wall Separator in group B streptococcus) has been implicated as an integral component in the regulation of both cell division and cell separation (Bartual *et al.*, 2014, Caliot *et al.*, 2012, Barendt *et al.*, 2009, Vollmer *et al.*, 2008, Ng *et al.*, 2004, Ng *et al.*, 2003, Reinscheid *et al.*, 2001,

Chia *et al.*, 2001); with atypical expression of PcsB leading to irregularities in cell morphology, cell-division regime and chain length. Caliot *et al.* (Caliot *et al.*, 2012) discovered that deleting the gene for the capsular carbohydrate of *S. agalactiae* (GBC – *gbc0*) disrupts the normal distribution of PcsB leading to irregularities in cell division and separation. Utilizing a variety of *Streptococcus sanguinus* mutant strains, Evans *et al.* (Evans *et al.*, 2014) detected correlations between cellular chain length, and a variety of designated 'clusters of orthologous gene' function groups (COGS – (Tatusov *et al.*, 2001)); suggesting that the length of cellular chains in *Streptococcus* is dependent upon a complex interplay between a variety of functionally diverse genes.

Classification

Almost all *Streptococcus* are gram-positive, catalase-negative, non-motile, mesophilic, facultative or obligate anaerobes; individual cells are approximately 1µm in size (Patterson, 1996). Belonging to the Streptococcaceae family, *Streptococcus* are classified in the Order Lactobacillales (lactic acid bacteria or LAB) for their capacity to tolerate lower pH environments; facilitating their survival in the presence of organic acids (Sonomoto & Yokota, 2011). Streptococci are further classified into the Class Bacilli, and in the Phylum Firmicutes (Latin for strong skin or shell); owing to their robust, gram-positive cell wall (Vos *et al.*, 2011). *Streptococcus* can be broadly categorised according to their haemolytic activities as evident on blood agar (Brown, 1919). Gamma-haemolytic streptococci grow colonies on blood agar but are not haemolytic, whereas Alpha-haemolytic strains oxidise the iron in haemoglobin molecules; leading to a greenish colour around colonies on blood agar. Many streptococcal strains are Beta-haemolytic; completely rupturing red blood cells, resulting in an observable clearing of these red cells around the colonies on blood agar. Haemolytic streptococci are further commonly differentiated into Lancefield serotypes (Groups) based on the precipitation reaction between serologically-specific bacterial-surface carbohydrates (C substance) and Group-specific anti-C sera (Lancefield, 1928, Lancefield, 1933); with each Group designated by an uppercase letter (Lancefield, 1933, Lancefield, 1934). Lancefield groupings were initially correlated to the

isolation source of the bacteria (i.e. Group A streptococci were isolated primarily from humans, Group B from cows, Group C from other animals, Group D from cheese and Group E from "certified" milk) (Lancefield, 1933). However, over time, pathogenic streptococci from multiple Lancefield groups have become increasingly implicated in human infections (Skoff *et al.*, 2009, Phares *et al.*, 2008, Dermer *et al.*, 2004).

Streptococcus agalactiae (Group B Streptococcus)

Capsular Serotype

Wild-type strains of *S. agalactiae* express a polysaccharide capsule (Cieslewicz *et al.*, 2005). Individual strains of *S. agalactiae* are commonly sub-classified according to capsular serotype. Polysaccharide-based serotypes are designated by Roman numerals to distinguish them from protein-based antigens (Henrichsen *et al.*, 1984). Paralleling pneumococcal nomenclature, Lancefield (Lancefield, 1934) identified three serotypes of GBS based on capsular polysaccharide molecules; serotypes I, II and III (Lancefield *et al.*, 1975, Lancefield, 1934). Some unexpected, overlapping serological reactions can prompt cross-precipitation however, and resulted in the further distinction between serotypes Ia and Ib (Lancefield, 1938). Furthermore, some strains of GBS are considered nontypeable; lacking any known, type-specific, polysaccharide or protein-based antigenic identifier (Wilkinson, 1977, Pattison *et al.*, 1955a, Kong *et al.*, 2008). It should be noted that these capsular substances are distinct from the C substance used to distinguish the major Groups of streptococcal species, which are identical throughout all GBS, originate on the cell-wall surface of streptococcal cells as opposed to the capsule surface and, according to Wilkinson (Wilkinson, 1977), have a distinct precipitation response time compared to the capsular antigens used to characterise GBS serotypes. Improvements in molecular techniques have increasingly led to the characterisation of many isolates previously designated nontypeable and presumed to express capsules at low levels (Kong *et al.*, 2008, Poyart *et al.*, 2007, Ulett *et al.*, 2009). Some GBS isolates do not express capsule (Creti *et al.*,

2012). The absence of capsule in GBS is often attributed to a mutation in the *cspE* capsule gene (Rosini *et al.*, 2015, Ramaswamy *et al.*, 2006). Creti *et al.* (Creti *et al.*, 2012) described a GBS strain lacking the capsular operon.

Currently, there are ten capsular serotypes described for GBS (i.e. serotypes Ia & Ib and serotypes II to IX); with identification of each serotype based on the antigenic properties of GBS capsules (Afshar *et al.*, 2011, Slotved *et al.*, 2007, Sheppard *et al.*, 2016). Importantly, in the context of pathogenesis, there are several GBS capsular serotypes that are disproportionately associated with disease in humans. Serotypes Ia, Ib, II, III & V account for the overwhelming majority of GBS disease in humans (Skoff *et al.*, 2009, Edmond *et al.*, 2012, Edwards & Baker, 2005, Hickman *et al.*, 1999); for example, in one study, up to 96% of clinical isolates were represented by these serotypes (Phares *et al.*, 2008). Expression of serotype III capsules, in particular, has been positively correlated with increased virulence (Rubens *et al.*, 1987). Serotype III is the most common serotype associated with both early and late onset neonatal disease and meningitis (Baker & Barrett, 1974, Hauge *et al.*, 1996, Baker, 1980, Edwards *et al.*, 2011). GBS Serotype III is also in adult GBS disease (Tyrrell *et al.*, 2000), however serotype V is the most common etiological agent causing disease in non-pregnant adults (Blumberg *et al.*, 1996, Phares *et al.*, 2008, Farley, 2001, Flores *et al.*, 2015).

Differences in molecular structures of the capsule are defined by genes in the *cps* locus (Cieslewicz *et al.*, 2005); with *cpsA* playing a primary transcriptional role in the expression of this locus (Cieslewicz *et al.*, 2001).

Serotype III GBS isolates have been further classified into three primary lineages based on the restriction digest patterns (RDP) of *Hin*dIII digestion of chromosomal DNA from 62 serotype III strains of GBS; designated serotypes III-1, III-2 and III-3 (Takahashi *et al.*, 1998). The majority of invasive disease-causing isolates in this study were GBS serotype III-3. Serotype III-3 GBS have larger capsules with higher sialic acid content compared to serotype III-1 and III-2 isolates – sialic acids are believed

to contribute to virulence by a) mimicking antigens that are present on human cells (Hayrinen *et al.*, 1989), and b) inhibiting phagocytosis by interfering with host complement proteins (Edwards *et al.*, 1982, Marques *et al.*, 1992). However, whilst serotype III GBS are disproportionately overrepresented in human disease, research by Jones *et al.* (Jones *et al.*, 2006) suggests that factors apart from the capsule are largely responsible for the increased virulence of serotype III strains.

The GBS capsular polysaccharides are prominent vaccine targets (Edwards, 2008). However, Bellais *et al.* (Bellais *et al.*, 2012) reported the capacity of a pathogenic isolate to switch its serotype from III to IV via the exchange of a 35.5kb segment of chromosomal DNA containing the *cps* gene. The potential for GBS to switch serotypes represents a potential method to evade serotype-targeted vaccines (Bellais *et al.*, 2012).

Multilocus Sequence Type (MLST)

Jones *et al.* (Jones *et al.*, 2003) reported an alternative profiling method to distinguish between lineages of GBS; Multilocus Sequence Typing (MLST) or Sequence Type (ST). This widely used method characterises seven housekeeping genes (*adhP*, *atr*, *glcK*, *glnA*, *pheS*, *sdhA*, and *tkt*) in order to generate a reference profile for each isolate. ST characterisation does not necessarily correlate to capsular serotype (Jones *et al.*, 2003). Several of these ST genotypes have been characterised as hypervirulent; with ST-17 (serotype RDP III-3) in particular associated with more serious manifestations of invasive disease in both human infection and mouse models (Seifert *et al.*, 2006, Lamy *et al.*, 2006, Bellais *et al.*, 2012, Bisharat *et al.*, 2004, Davies *et al.*, 2004, Tazi *et al.*, 2012, Dramsi *et al.*, 2012, Poyart *et al.*, 2008). ST-17 is frequently associated with neonatal disease (Jones *et al.*, 2003) and is possibly a more precise determinant of virulence in serotype III isolates than the serotype III capsular antigens (Jones *et al.*, 2006). Bisherat *et al.* (Bisharat *et al.*, 2004) found that, unlike other ST lineages of GBS isolates of human origin, ST-17 isolates cluster more closely with strains of bovine origin; indicating that ST-17 may have recently arisen in human populations from a

bovine strain of GBS. This hypothesis is supported by a genome sequencing study that showed introduction of tetracycline antibiotics in the 1940s prompted the movement of bovine GBS into humans (Da Cunha *et al.*, 2014), to be discussed subsequently.

Jones *et al.* (Jones *et al.*, 2003) further grouped GBS ST lineages into clonal complexes (CC) on the basis of genetic identity over at least six of the seven loci (Jones *et al.*, 2006). Clonal complex 17 (CC17), which contains ST-17, is also strongly associated with hypervirulence (Teatero *et al.*, 2016, Sorensen *et al.*, 2010). As characterised by ST-17, CC17 strains isolated from humans express two of the three pili identified in GBS, the HvgA protein and a unique protein adhesin (Srr-2), however these strains lack the adhesins Srr-1 and FbsC found in other CC strains (Tazi *et al.*, 2012, Buscetta *et al.*, 2014, Seifert *et al.*, 2006). The function, structure and relevance of these, and other, virulence factors are addressed in detail in the subsequent chapter "Selected Virulence Factors". CC1 (mostly serotype V) GBS are more frquently implicated in adult disease (Flores *et al.*, 2015, Blumberg *et al.*, 1996, Phares *et al.*, 2008). Several recent Canadian studies have reported large proportions of adult invasive disease associated with CC17, serotype III strains, along with an increase in the incidence of CC1, serotype IV GBS associated infections in adults (Teatero *et al.*, 2015, Teatero *et al.*, 2014). Using whole genome analysis, Teatero *et al.* (Teatero *et al.*, 2016) found the core genome of CC17 to be highly conserved and clustered independently of etiological manifestation (i.e. regardless of whether isolated from child or adult disease), suggesting that any variation within CC17 is the result of horizontal gene transfer (including by mobile genetic elements) between the members of a single population expanding from a single clone pool. Campisi *et al.* (Campisi *et al.*, 2016) reported that an emerging GBS serotype IV, CC23 pathogen (ST-452) has a genome comprised of two sections, each demonstrating near identical homology with two strains from separate clonal complexes, CC23 ST-24 and CC17 ST-291; indicating that ST-452 arose from a massive recombination event between these two other strains.

GBS classification based on MLST is further complicated by horizontal gene transfer. Some of the MLST profiles designated in Jones *et al.* (Jones *et al.*, 2003) represented multiple capsular serotypes. This raises the question as to whether either capsular serotyping or MLST can be reliably considered indicative of relatedness – which has broad implications for epidemiological and phenotypical studies of GBS. The capacity for large-scale genetic recombination from horizontal gene transfer has been previously described for GBS (Campisi *et al.*, 2016, Brochet *et al.*, 2008). With regards to capsular serotype, it has been reported that horizontal exchange of a single gene is enough to alter the serotype of GBS (Chaffin *et al.*, 2000, Bellais *et al.*, 2012). Luan *et al.* (Luan *et al.*, 2005) found CC17 to be exclusively represented by serotype III however, serotype variation was found to be common throughout all other GBS CCs – indicating frequent recombinations of genes encoding capsular serotypes. In a study comparing the fully sequenced genomes of 8 strains of GBS, Tettelin *et al.* (Tettelin *et al.*, 2005) reported that the most conserved genomes in the study were between GBS strains of disparate serotypes and MLSTs. Brochet *et al.* (Brochet *et al.*, 2008) demonstrated the capacity of GBS to exchange chromosomal segments as large as 334kb – thereby distorting the picture of GBS phylogenetic relationships. Da Cunha *et al.* (Da Cunha *et al.*, 2014) reported exchanges of genomic fragments within clonal complexes involving as much as 47% of the genome. Whilst investigating the distinction between serotypes Ia and Ib, as early as 1938, Lancefield (Lancefield, 1938) noted that similarity of chemical reactivity cannot necessarily be assumed to inform phylogenetic relatedness. Jones *et al.* (Jones *et al.*, 2003) suggests that phylogenetic ambiguity may be resolved as DNA sequencing technologies progress, however, in the context of an open genome incorporating horizontal gene transfer (Tettelin *et al.*, 2005), caution is recommended when inferring phylogenetic relationships between GBS strains.

1.2 Disease & Epidemiology

Overview

Historical Perspective

Originally characterised as a veterinarian pathogen, namely implicated in bovine mastitis (Stableforth, 1938, Keefe, 1997, Plastridge, 1958, Lancefield, 1934), GBS is now recognised as a major cause of human disease. GBS is also a common commensal microbe found in the human gut (Easmon, 1986). Asymptomatic GBS colonisations are frequently reported in the human genitourinary (GU) tract; with carriage in pregnant women having serious implications for neonatal infections that can arise as a result of vertical transmission of GBS (Easmon, 1986, Finch *et al.*, 1976). GBS has been cultured from the bowels of surgical patients, is more frequently recovered from anorectal than genitourinary sites in the same patients and is disproportionally prevalent in female infection (Anthony *et al.*, 1983, Dillon *et al.*, 1982, Badri *et al.*, 1977, Barnham, 1983). Based on these lines of evidence, the lower gastrointestinal tract is broadly considered to be the primary site of GBS colonisation in humans.

GBS disease is common in both humans and cattle, and despite the frequent human contact with cattle and/or dairy products, molecular analysis indicates that bovine lineages of GBS are overtly distinct from human strains. It is therefore unlikely that either cohort serves as a major disease reservoir for the other (Bohnsack *et al.*, 2004, Finch & Martin, 1984). This is supported by the increase in incidence of GBS disease in the western world coinciding with near-ubiquitous milk pasteurisation practices and a decline in direct public contact with cattle (Edwards *et al.*, 2011). El Ghoroury (El Ghoroury, 1950) noted a clear distinction between human and bovine GBS when it comes to their capacity to ferment lactose, salicin and glycerol, as well as their respective ability to reduce methylene blue in milk. Pattison *et al.* (Pattison *et al.*, 1955b) identified a distinction between

serotype patterns represented by bovine and human isolates. Finch and Martin (Finch & Martin, 1984) further identified biochemical markers distinguishing bovine from human strains of GBS, including bacitracin susceptibility, haemolytic activity, pigment production and lactose utilisation. All human isolates of GBS appear to harbour the *scpb-lmb* transposon locus, whereas this locus seems to be lacking in most bovine strains (Franken *et al.*, 2001). The majority of GBS strains isolated from humans can be grouped within five clonal complexes (CC1, CC9/10/12, CC17, CC19 and CC23) – with an additional clonal complex (CC26) more commonly reported in Africa (Brochet *et al.*, 2009, Sorensen *et al.*, 2010, Luan *et al.*, 2005). However no human isolates have been reported for the predominant bovine clonal complex 67 (CC67) (Sorensen *et al.*, 2010). Differences between human and bovine strains have also been described for surface proteins, including surface protein X that is associated with virulence in bovine mastitis but is rarely expressed in human strains (Wibawan & Lammler, 1990). An allelic analysis of RDP III-1 to 4 strains proposed evidence for an ancestral lineage between human and bovine strains, but ultimately concluded the lineages to be "largely unrelated" (Bohnsack *et al.*, 2004). More recent genomic insights have offered alternative views of the relationship between human and bovine GBS (Da Cunha *et al.*, 2014).

Da Cunha *et al.* (Da Cunha *et al.*, 2014) has proposed, based on genome analysis of 229 GBS strains, collected from 4 continents over 58 years, that the rise in human disease may be related to human use of the broad-spectrum antibiotic tetracycline since 1948 (Nelson & Levy, 2011). Genomic analysis indicates that tetracycline usage may have created a genetic bottleneck leading to the replacement of the previously diverse human strains of GBS with tetracycline resistant, pathogenic strains – and in particular, the hypervirulent CC17 complex that plays such a large role in neonatal disease (Da Cunha *et al.*, 2014). Tetracycline resistance (TcR) was first reported in *Shigella* in Japan in 1953 (Watanabe, 1963). The increasing prevalence of TcR in *Enterobacteriaceae*, *Staphylococcus*, bacteroides and streptococcal species was evident by the late 1960s (Nelson & Levy, 2011, Sabath, 1969). TcR in GBS was reported in 1964 (Eickhoff *et al.*, 1964). In contrast to other CCs, no CC17

strain has been found to lack in TcR-conferring, integrative and conjugative elements (ICEs) which, when correlated to the low incidence of GBS human disease reported prior to the use of tetracycline, indicates that CC17 was a rarer complex before the broad-scale usage of tetracycline in human health (Da Cunha *et al.*, 2014). A reduction in antibiotic use would typically be reflected in a decline in resistance due to a lessening of the selective pressure and increased cost associated with maintaining resistance (Lipsitch, 2001), however TcR appears to be fixed and maintained in human strains of GBS, despite a decline in the use of tetracycline to treat human diseases (Da Cunha *et al.*, 2014).

GBS Disease in Neonates, Children and Non-pregnant Adults

Since the first report of GBS as a human pathogen by Fry in 1938 (Fry, 1938), GBS has revealed itself to be the most significant cause of potentially fatal neonatal disease worldwide (Baker, 1977, Gotoff, 1977, Anthony & Okada, 1977). Franciosi *et al.* (Franciosi *et al.*, 1973) and Baker & Barret (Baker & Barrett, 1973) recognised two distinct syndromes of GBS neonatal disease; acute/early and delayed/late onset. Early Onset neonatal Disease (EOD) describes a manifestation of GBS pathology within the first seven days after birth and is often associated with sepsis, meningitis, respiratory and pulmonary distress (Anthony & Okada, 1977, Wu *et al.*, 2004). Subsequent manifestation of GBS disease, up to 90 days, is classified as Late Onset Disease (LOD) and is more commonly associated with bacteraemia and a significantly higher incidence of meningitis than EOD (Anthony & Okada, 1977, Wu *et al.*, 2004). In 2008, the European Commission Seventh Framework (EC FP7) instigated the DEVANI (Design of a Vaccine Against Neonatal Infection - http://www.devaniproject.org) program for the purpose of developing strategies to specifically combat GBS in neonatal disease across Europe (Afshar *et al.*, 2011).

GBS infection/disease in children beyond early infancy is more likely to be associated with an underlying medical condition. Urinary tract infections (UTIs) and tonsillitis are more commonly

reported in older children in contrast to sepsis and meningitis that are more commonly observed in younger infants with EOD or LOD (Wu *et al.*, 2004). Symptoms in these older children can be less pathognomonic than disease in their younger counterparts (including meningitis sequelae - (Visintin *et al.*, 2010)), however GBS disease is less likely to be fatal in older children (Bonadio *et al.*, 1992).

The increase in incidence of GBS disease in non-pregnant adults in developed countries in the past two decades is a cause for concern for the health care sector (Skoff *et al.*, 2009, Farley *et al.*, 1993, Edwards & Baker, 2005). A two year surveillance study conducted in Atlanta (Georgia, US) reported that GBS in non-pregnant adults accounted for almost a third of all GBS disease; with a 21% mortality rate in non-pregnant adults representing 67% of the overall mortality rate from all GBS disease reported during the study period (Farley *et al.*, 1993). This study identified both advancing age and immunocompromisation from other co-morbidities (e.g. diabetes, cancer, Human Immunodeficiency Virus (HIV) and infections from additional organisms) as the primary risk factor for GBS disease in this cohort. This finding is consistent with Munoz *et al.* (Munoz *et al.*, 1992) who reported an association between GBS UTIs in adults and other, underlying medical conditions. Farley *et al.* (Farley *et al.*, 1993) found ethnicity to be a factor associated with GBS disease, with the prevalence of GBS invasive disease more than twice as high in black adults than in white adults; the discrepancy between blacks and whites becoming more significant with advancing age. However Farley *et al.* (Farley *et al.*, 1993) recognised the possibility of this ethnic disparity being an artefact of health and socioeconomic factors. In adults, GBS causes a diverse range of diseases, including of the soft tissues, respiratory system, circulatory system, skin, bone, abdomen, central nervous systems (CNS) and urinary tract (Farley *et al.*, 1993, Munoz *et al.*, 1992, Skoff *et al.*, 2009). Farley *et al.* (Farley *et al.*, 1993) estimated 17% of the invasive GBS in the studied adult cohort were nosocomially acquired.

The recent appearance and increasing incidence of previously unreported serotypes of GBS in human disease is of further concern. Until the characterisation of serotypes IV and V in the mid-

1980s, only serotypes Ia, Ib, II and III were commonly isolated from disease cases (Jelinkova & Motlova, 1985); with serotypes Ia and III, in particular, consistently overrepresented (Edwards *et al.*, 2011). However, as early as 1990, a multistate US study reported a growing proportion of other GBS serotypes contributing to the overall disease burden in the US (Wenger *et al.*, 1990). Serotypes IV and V are now recognised as major contributors to the global disease burden of GBS (Blumberg *et al.*, 1996, Campisi *et al.*, 2016, Skoff *et al.*, 2009, Bergseng *et al.*, 2008, Meehan *et al.*, 2014, Teatero *et al.*, 2014, Teatero *et al.*, 2015, Ferrieri *et al.*, 2013, Palmeiro *et al.*, 2010, Dutra *et al.*, 2014). Consistent with the increased reporting of serotype IV GBS disease, Diedrick *et.al.* (Diedrick *et al.*, 2010) reported an increasing incidence of colonizing serotype IV GBS in a US survey; including the characterisation of a new MLST 452.

Clinical Presentations of GBS Disease

Meningitis and Meningitis Sequelae

In the US alone, an estimated 4100 cases of bacterial meningitis, including 500 deaths, were reported per annum between 2003 and 2007 (Thigpen *et al.*, 2011). There is a broad range of potential sequelae associated with neonatal bacterial meningitis (Visintin *et al.*, 2010, Edmond *et al.*, 2010). Many studies have reported associations between infant meningitis and conditions extending beyond infancy, including impairments to hearing and vision, delays in speech and language development, poor educational outcomes, psychosocial and behavioural problems, hydrocephalus, skin, bone and joint damage, pain and joint stiffness, renal compromise, seizure disorders such as epilepsy, cerebral palsy and other neuro-motor disabilities (Visintin *et al.*, 2010, Halket *et al.*, 2003, Stevens *et al.*, 2003, de Louvois *et al.*, 2007, de Louvois *et al.*, 2005, Fortnum, 1992, Fortnum & Davis, 1993, Ramakrishnan *et al.*, 2009, Wellman *et al.*, 2003). The UK's National Institute for Health and Care Excellence Clinical Guidelines 102 (CG102), Chapter 7, further identifies, reviews and analyses more than 20 such studies from Europe, Australia and North America, between 1995 and

2010, investigating the negative, long-term outcomes of bacterial meningitis throughout childhood and up to the age of 16. Ramakrishnan *et al.* (Ramakrishnan *et al.*, 2009) reviewed an analysed 37 articles relating to meningitis sequelae covering 21 African nations and children up to the age of 15. Where these studies investigated the etiological agents of the meningitis, GBS consistently rated highly in terms of the severity of the meningitis sequelae (CG102). Neonatal meningitis studies therefore tend to focus on GBS and *Escherichia coli* pathogenic sources of disease (Carter *et al.*, 2003).

A global meta-data analysis in 2010 covering 132 papers found that low-income nations suffered the greatest burden of long-term disabling bacterial meningitis sequelae; with the risk of major sequelae in African and Asian regions being more than twice that of the represented European regions (Edmond *et al.*, 2010). However, the majority of studies of infant meningitis sequelae focus on wealthy countries; where there is greater access to medical information for researchers, better quality healthcare for patients, and a lower overall risk of infection (Carter *et al.*, 2003, Victora *et al.*, 2003, Caudron *et al.*, 2008). The mechanisms by which bacterial pathogens, including GBS, penetrate the blood-brain barrier to cause meningitis are reviewed elsewhere (Dando *et al.*, 2014).

Bacteraemia and Sepsis

Bacteraemia describes the presence of viable bacteria in circulatory blood and is clinically defined by a positive blood culture (Bone, 1991). Sepsis defines the host's systemic and dysregulated response to microbial invasion, namely of the bloodstream, and often leads to organ failure and death (Ayres, 1985, Singer *et al.*, 2016). Circulatory manifestations of sepsis include hypotension, hypocapnia, elevated or reduced white blood cell counts, decreased platelet counts, vasodilation, increased vascular capacity and cardiac output (Ayres, 1985). A study of invasive GBS disease in men found that GBS can gain access to the blood via the respiratory tract, urinary tract, through the skin and intravenous delivery sites (Verghese *et al.*, 1986).

The mammalian blood stream provides the host with a raft of defensive mechanisms conferring host defence against many pathogens. However there are some pathogens, including GBS, with a demonstrated capacity to enter and survive the blood stream. This ability provides the bacteria with access to potential sites of infection throughout the host's body. Proliferation within the blood stream itself can result in systemic and septic infections. GBS has several virulence factors that promote its survival in blood, including factors that mediate molecular mimicry, and evasion of soluble and cellular defence mechanisms in the blood.

Sialic acid represents a family of 9-carbon, monosaccharide molecules linked to the outer glycan chains of all vertebrate cells (Varki, 2008). Sialic acid is also highly expressed in the capsule of GBS – allowing GBS to mimic host cells, camouflaging the bacteria from host defences (Carlin *et al.*, 2009). For example, these capsular residues can bind to neutrophil Siglec-9, dampening the antibacterial activity of neutrophils (Carlin *et al.*, 2009). Sialic acids also hinder the attachment of Complement 3 proteins to the bacterial surface, impairing the functional activity of phagocytes as well as the downstream, cytolytic activity of the complement cascade (Marques *et al.*, 1992).

Complement Protein 5a (C5a) recruits neutrophils to an infection site, inducing opsonophagocytic destruction of invading microbes (Manthey *et al.*, 2009). GBS expresses the protease designated ScpB (discussed in more detail below) which has a demonstrated capacity to preferentially cleave human C5a, thereby dampening neutrophil recruitment (Takahashi *et al.*, 1995, Bohnsack *et al.*, 1997).

Neutrophils, as short-lived, blood-based phagocytic cells, are the most abundant leucocytes in mammalian circulatory systems, and are considered the primary responders to a site of inflammation (Kolaczkowska & Kubes, 2013, de Oliveira *et al.*, 2016). Of interest is their capacity to release fibres of DNA into the extracellular environment forming neutrophil extracellular traps (NETs); adhesive fibrous structures that localise and concentrate pathogenic cells and molecules for

degradation and phagocytosis (Brinkmann *et al.*, 2004). DNases/nucleases are enzymes that degrade nucleic acids, such as those comprising NETs, by cleaving nucleotide chains at their phosphodiester bonds (Yang, 2011). Ferrieri *et al.* (Ferrieri *et al.*, 1980) first reported these enzymes in GBS in 1980. Derre-Bobillot *et al.* (Derre-Bobillot *et al.*, 2013) first demonstrated the use of a GBS nuclease (Nuclease A or NucA) in the degradation and evasion of NETs; confirming the role of NucA in the persistence of GBS infection and severity of disease. Bonsor *et al.* (Bonsor *et al.*, 2008) has further proposed as a means of virulence, the possibility of nucleases entering cells to degrade intra-cellular nucleic acids such as RNA and DNA.

The pore-forming exotoxin β-hemolysin/cytolysin (β-h/c) that is responsible for β–haemolysis is another, highly recognised and multifunctional virulence factor expressed by GBS (discussed in detail below). The β-h/c genes have been mapped to the *cyl* operon (Spellerberg *et al.*, 1999a). Carey *et al.* (Carey *et al.*, 2014) reports neutrophils as the primary responders to the presence of β-h/c in a murine model, and further reports that NETs may be induced by β-h/c to facilitate the destruction of neutrophils. Comparing wild-type and *cylE* mutant strains of GBS in both macrophage and neutrophil killing assays, Lui *et al.* (Liu *et al.*, 2004) found that strains lacking β-h/c were more readily cleared by the immune cells, than the wild-type strains expressing β-h/c. Rajagapol *et al.* (Rajagopal *et al.*, 2006) found that a serine/threonine kinase (Stk1) promoted survival of GBS in blood through the positive regulation of β-h/c. Hensler *et al.* (Hensler *et al.*, 2008) demonstrated the potential of β-h/c to interfere with cardiac function through undermining the viability of cardiomyocytes.

Group B Streptococcus immunogenic bacterial adhesin (BibA) is another cell surface protein that is highly conserved throughout GBS (Santi *et al.*, 2007). A study comparing wild-type GBS with *bibA*-knockout mutants demonstrated that BibA is essential for attachment to human cervical and lung epithelial cells, as well as conferring resistance to opsonisation and neutrophil phagocytosis (Santi *et al.*, 2007).

Monocytes are another type of phagocytic white blood cell and are a precursor cell to tissue-based macrophages (Volkman & Gowans, 1965, Ebert & Florey, 1939, Gordon & Taylor, 2005). Besides phagocytosis, monocytes are also recruited around the site of infection due to their capacity to release cytotoxic substances such as Reactive Oxygen Species (ROS) and Nitric Oxide (NO) (Mangan *et al.*, 1993). Peotta *et al.* (Peotta *et al.*, 2001) investigated the inflammatory response of monocytes and macrophages in response to GBS challenge; finding that certain inflammatory markers (CD16 and CD68) were significantly more highly expressed in the mature differentiated cells than in the monocytes; indicating a potentially lower efficiency of bacterial clearing in the undifferentiated, less mature, monocytes.

Interleukin 6 (IL-6) is a cytokine which acts in a predominantly pro-inflammatory manner to drive immune activity (i.e. recruitment of neutrophils and monocytes to the site of infection) in response to the identification of infectious stimuli (Gabay, 2006, Scheller *et al.*, 2011). Heumann *et al.* (Heumann *et al.*, 1994) observed in gram-positive bacteria, the capacity to induce the secretion of IL-6 by human monocytes. Vallejo *et al.* (Vallejo *et al.*, 1996) demonstrated this capacity for GBS in human neonatal monocytes; determining that the Group B antigen plays a more significant role in IL-6 stimulation than the presence of a capsule, or its associated serotype III polysaccharide. Currie *et al.* (Currie *et al.*, 2011) compared the immune responses to GBS challenge in whole blood from healthy adults, preterm and term neonates finding that the IL-6 and monocyte responses were roughly on par between the healthy adults and term babies, however the secretion of both IL-6 and Tumour Necrosis Factor (TNF) by monocytes in preterm neonates were significantly diminished by comparison. This is consistent with the findings of a similar previous study reporting defective production of IL-6 in preterm infants versus term infants and adults (Yachie *et al.*, 1992).

Tumor necrosis factor-Related Apoptosis-Inducing Ligand (TRAIL) is a ligand functioning to induce the apoptosis cascade in a diverse range of human cell types (Wiley *et al.*, 1995). Halaas *et al.*

(Halaas *et al.*, 2004) reported that GBS can stimulate TRAIL in monocytes -triggering apoptosis and thereby undermining the effectiveness of bacterial clearing from the blood by monocytes.

The ability to survive the intracellular environments of phagocytes adds another dimension to the survival capacity of GBS. Valenti-Weigand *et al.* (Valenti-Weigand *et al.*, 1996) described entry of GBS into mouse-macrophage-like cells within 5 minutes of infection, remaining fully viable for at least eight hours and surviving in the cells for 24 hours. Cornacchione *et al.* (Cornacchione *et al.*, 1998) reported a group III strain of GBS persisting in murine macrophages for 48 hours; attributing this survival to the ability of GBS to impair protein kinase C (PKC), a component in the activation pathway of interferon-γ (INF-γ). These findings are consistent with those of subsequent studies that demonstrated prolonged survival of GBS inside macrophages (Ulett *et al.*, 2003, Ulett & Adderson, 2005). Whilst β-h/c is necessary to induce cytoskeleton alterations disrupting macrophage activity (Fettucciari *et al.*, 2011), Sagar *et al.* (Sagar *et al.*, 2013) found that non-haemolytic, mutant strains of GBS survived in human THP-1 macrophage-like cells more readily than their haemolytic wild-type strains through reduced stimulation of TNF-α; indicating the need for GBS to regulate β-h/c expression to promote survival in the intracellular environment. Cumley *et al.* (Cumley *et al.*, 2012) demonstrated that acidification of the phagosome is necessary for GBS survival in phagocytes, and that this acidification is regulated by GBS's CovR/S two-component system.

Early Onset Neonatal Disease (EOD)

EOD describes neonatal GBS disease which most commonly manifests within the first 48 hours postpartum, however the same clinical syndrome can arise in the neonate for the following 5 days (Gibbs *et al.*, 2004). Early reports of EOD recorded mortality rates as high as 90% for neonates with very low (≤1kg) birth weights (Boyer *et al.*, 1983a).

EOD is thought to result primarily from maternal transfer of the bacteria; either by aspiration during birth, or earlier through carriage-ascending amniotic infections (Boyer *et al.*, 1983b, Eickhoff *et al.*,

1964, Harper, 1971, Baker & Barrett, 1973, Doran & Nizet, 2004, Edwards *et al.*, 2011). This is supported by studies revealing identical serotypes and/or genotypes of GBS being isolated from both mother and child (Boyer *et al.*, 1983b, Harper, 1971, Helmig *et al.*, 1993, Melchers *et al.*, 2003). A positive GBS culture during pregnancy predicts a 16% to 73% GBS transmission rate between mother and neonate; correlated to the weight of maternal GBS carriage (Ancona *et al.*, 1980, Boyer *et al.*, 1983b). Prenatal maternal colonisation presents a roughly 25-fold higher risk of EOD presenting in the neonate (Boyer & Gotoff, 1985).

Frequently infecting the lungs as the portal of entry, GBS is a common cause of neonatal pneumonia (Tseng & Kandall, 1974, Vollman *et al.*, 1976). Infant respiratory distress characterised by tachypnoea (rapid breathing) and cyanosis (skin discolouration due to lack of oxygen), are often the first symptoms of EOD (Jacob *et al.*, 1980, Payne *et al.*, 1988, Hemming *et al.*, 1976). Hemming *et al.* (Hemming *et al.*, 1976) found GBS bronchopneumonia in the autopsy results of all tested samples from neonates succumbing to EOD. From the lungs, the bacteria can gain access to the bloodstream. It is the capacity of GBS to enter and survive the blood which has systemic implications for GBS infection. Untreated bacteraemia permitting GBS to proliferate in the blood can lead to septicaemia and sepsis. Through the blood, GBS can disseminate throughout the body causing disease in various locations. GBS crossing the BBB is a common cause of neonatal meningitis (Dando *et al.*, 2014). Edwards *et al.* (Edwards *et al.*, 2011) lists a range of less-common GBS ailments for both EOD and LOD across many sites of infection including various infections of the abdomen, brain, skin and soft tissue, cardiovascular system, eyes, ears, sinuses, respiratory system and urinary tract.

Intuitively, the heavier the maternal carriage of GBS, the more likely the transfer of GBS to the neonate. Boyer *et al.* (Boyer *et al.*, 1983b) reported a 65% transmission rate when the maternal carriage was “high density” (+++), in contrast to low density carriage (+) with a vertical transmission rate of just 17%. Ancona *et al.* (Ancona *et al.*, 1980) reports a total transmission rate of 67% associated with heavy (3+) maternal carriage against a combined 36% for moderate (2+) to light (1+)

maternal carriage. The detection at birth of vertical GBS acquisition was 48% for heavy maternal carriage, 24% for moderate carriage and 4% for light carriage; with 72% of those infants with positive cultures at discharge being born to 3+ mothers, in contrast to only 12% born to 2+ and 1+ mothers combined (Ancona *et al.*, 1980). Furthermore, infections at neonatal mucosal sites were found to be more frequent when the maternal GBS carriage was heavy (Ancona *et al.*, 1980).

Beyond maternal carriage, several maternal and neonatal risk factors have been identified for EOD. Premature delivery is commonly associated with EOD; as is prolonged membrane rupture and varying indicators of maternal infection (Schuchat *et al.*, 2000, Dillon *et al.*, 1987, Seaward *et al.*, 1998, Benitz *et al.*, 1999, Malek *et al.*, 2005). In addition to preterm labour and heavy maternal colonisation, low birth weight, chorioamnionitis (inflammation of foetal membranes) and maternal bacteriuria are also reportedly risk factors for EOD (Benitz *et al.*, 1999, Boyer *et al.*, 1983a, Malek *et al.*, 2005). However, between 6% and 40% of EOD can arise in the absence of these perinatal complications (Boyer *et al.*, 1983a, Malek *et al.*, 2005), suggesting additional, unknown risk factors.

Whilst the overwhelming majority of EOD is considered to stem from maternal transmission, there are reports of nosocomial and community acquisition, although less frequent. Paredes *et al.* (Paredes *et al.*, 1977) interpreted the increase in neonatal colonisation between the first 20 hours and nursery discharge (22.5% to 65.4%), in contrast to changes in maternal carriage (27.7% to 31.1%) between admission and discharge, to be highly indicative of nosocomial, rather than maternal, transmission. Easmon *et, al.* (Easmon *et al.*, 1981) found that one-third of the GBS-infected babies in a post-natal care ward had been born to mothers who were culture-negative throughout pregnancy and labour – leading to the discovery of non-maternal sources of GBS transfer; including contamination by other mothers in the same ward and a colonised staff member.

Studies show an increased prevalence of GBS EOD disproportionally affects neonates of African descent (including Caribbean and African-American) when compared against disease rates in other

ethnic populations (Schuchat & Wenger, 1994, Zangwill *et al.*, 1992). This is consistent with higher rates of GBS colonisation reported in black women (Hickman *et al.*, 1999, Katz *et al.*, 1994, Newton *et al.*, 1996). In one US (Houston) study, carriage rates in black women were 40.6%, compared to 20.3% in whites and 26.9% in Hispanics (Hickman *et al.*, 1999). This is reflected in another US (Alabama) study finding carriage rates in pregnant black women were 35.71%; significantly higher than the 19.84% carriage rate for pregnant non-black women – concluding race to be a significant predictor of GBS colonisation (Taylor *et al.*, 2002). A meta-analysis of literature from developing nations spanning from 1975 to 1996 found Mid-East/Nth African and Sub-Saharan African GBS carriage rates to be 22% and 19% respectively - in comparison to the 12% and 14% carriage rates found in Pakistan/India and the Americas respectively (Stoll & Schuchat, 1998). Schuchat (Schuchat, 1998) suggests that other risk factors, such as low birth rates and prematurity, which are also more common in births to black mothers, may further contribute to the increased prevalence of GBS EOD in black neonates. Newton (Newton *et al.*, 1996) proposes the possibility that differences in mucosal surface receptors between races, or that some other race-specific physiology may account for the colonisation disparity observed between differing ethnicities; as opposed to the hypothesis of race-associated socio-economic differences or behaviours such as sexual activity.

The introduction of intrapartum antibiotic prophylaxis in the early 1990s and antenatal/perinatal culture screening as standard practice during the late 1990s has resulted in a substantial decrease in early onset neonatal disease. National strategic guidelines for the prevention of GBS EOD were first issued for the United States in 1996 (Schuchat *et al.*, 1996). Utilising Centers for Disease Control and Prevention (CDC) records, Jordan *et al.* (Jordan *et al.*, 2008) estimates a drop in EOD incidence in the United States approaching 80% (from ~1.7/1000 down to ~0.4/1000 cases per live births) between 1990 and 2003. A global meta-analysis revealed that the application of antibiotic prophylaxis reduced the incidence of EOD by roughly 70% (from 0.75/1000 live births down to 0.23/1000 live

births) (Edmond *et al.*, 2010). Unfortunately, the incidence of LOD in neonates has remained unaffected by the implementation of these guidelines (Jordan *et al.*, 2008).

Late Onset Neonatal Disease

Late onset GBS disease is generally characterised by the appearance of symptoms between seven days and three months (Franciosi *et al.*, 1973, Baker & Barrett, 1973). Recent reports of LOD symptoms manifesting after 90 days have generated the designation ultra-late onset disease (ULOD) (Guilbert *et al.*, 2010).

GBS serotype III is overwhelmingly the most frequent serotype reported in LOD cases. Using compiled data from several studies, Edwards *et al.* (Edwards *et al.*, 2011) estimates the incidence of serotype III in LOD to be 64%; compared to 31% to 36% for other cohorts (with the exception of non-pregnant adults at 16%).

Whilst EOD is commonly associated with a variety of obstetrical complications, these are not generally implicated as factors in the development of LOD, with the exception of premature delivery - commonly reported as the prevailing risk factor for LOD (Fluegge *et al.*, 2006, Lin *et al.*, 2003). Ferrieri *et al.* (Ferrieri *et al.*, 2013) reported LOD to be at least two times more likely to be associated with preterm delivery than EOD; with roughly 75% of infants diagnosed with EOD being born full term. A six year French study found that a lower gestational age contributed more significantly to ULOD, than to LOD; concluding LOD and ULOD are likely the same clinical syndrome - with gestational age representing the only significant distinction between the two cohorts (Guilbert *et al.*, 2010).

Despite having a lower natural base incidence rate than EOD, LOD incidence has not paralleled the significant reduction in EOD stemming from the introduction of screening and antibiotic therapy guidelines (Jordan *et al.*, 2008, Poyart *et al.*, 2008). Aber *et al.* (Aber *et al.*, 1976) observed that 41%

of infants colonised with GBS were born to culture-negative mothers, and that babies born to GBS culture-negative mothers tended to acquire GBS later than those born to culture-positive mothers – indicating a likely nosocomial source of infection rather than maternal. A six month study of a special care baby unit and two postnatal wards identified hospital staff and mothers sharing the same ward as likely sources of LOD (Easmon *et al.*, 1981). Several studies have found similar patterns in nursery settings suggesting non-maternal sources of infection (Anthony *et al.*, 1979, Boyer *et al.*, 1980, Paredes *et al.*, 1977, Steere *et al.*, 1975, MacFarquhar *et al.*, 2010, Al-Maani *et al.*, 2014). In finding clinical strains of GBS on a patient monitor, Al-Maani *et al.* (Al-Maani *et al.*, 2014) confirmed the health care environment as a potential reservoir of GBS infections in neonates. Community acquisition of GBS is also reported for neonates, albeit rarely (Gardner *et al.*, 1980). In many cases however, intrapartum and post-partum transferal of GBS from mother to infant can still be regarded as a likely source of LOD (Weems Jr *et al.*, 1986), including GBS acquisition through breastfeeding (Godambe *et al.*, 2005, Lanari *et al.*, 2007, Christiansen & Leth, 2011, Widger *et al.*, 2010).

Carriage and Disease in Adults

GBS genital carriage in non-pregnant adults has been associated with several risk factors including; being young and female, increased sexual experience and intercourse frequency; especially leading up to the collection date, multiple sexual partners, number of pregnancies, the first half of the menstrual cycle, African American ethnicity, use of tampons and intrauterine contraceptive devices, diabetes, decreased hand washing and the consumption of milk and fish (Meyn *et al.*, 2002, Manning *et al.*, 2004, Bliss *et al.*, 2002, Baker *et al.*, 1977, Foxman *et al.*, 2007, Christensen *et al.*, 1984). In a study investigating the association between colonisation factors and GBS capsular serotypes, Foxman *et al.* (Foxman *et al.*, 2007) was one of the first to quantify a link between vaginal acquisition of GBS (serotypes Ia and Ib) and fish consumption; as well as associating serotype V GBS colonisation with increased sexual activity. Global studies have reported the prevalence of GBS maternal colonisation to range from 12% to 26% with diverse proportions of carriage readily associated with

geographic study regions; and as high as 37% in black women when ethnicity is accounted for (Campbell *et al.*, 2000, Stoll & Schuchat, 1998). A Europe-wide meta-study reported the range of colonisation in pregnant women between 6.5% and 36% (Barcaite *et al.*, 2008). Pharyngeal carriage rates reported for adult cohorts tend to be lower; between 4% and 12% (Chretien *et al.*, 1979, Ferrieri & Blair, 1977).

GBS disease in adults is identified in a broad range of syndromes and symptoms and has recently been reported to account for over 90% of the GBS disease burden in the United States; over 18s accounting for 2602 of 2886 cases (CDC, 2014). As in childhood GBS disease, bacteraemia, pneumonia and meningitis are frequently reported in adult GBS disease (Schuchat, 1998, Jackson *et al.*, 1995). Skin and soft tissue infections (such as cellulitis, osteomyelitis, septic arthritis, UTIs, ulcer and wound infections) are also commonly reported for GBS; as are endocarditis, peritonitis and empyema (Jackson *et al.*, 1995, Schwartz *et al.*, 1991, Farley *et al.*, 1993, Farley, 2001, Kaseman *et al.*, 2013).

GBS disease in non-pregnant adults is usually associated with increasing age and/or the presence of an underlying medical condition. A one year Boston City Hospital survey study was one of the first to report a link between GBS disease in elderly adults with diseases such as diabetes and pyelonephritis (Eickhoff *et al.*, 1964, Harper, 1971). Farley *et al.* (Farley, 2001) added cirrhosis and neurological impairment to the risk factors associated with GBS invasive disease in adults. In a later study, Farley *et al.* (Farley *et al.*, 1993) noted that GBS disease was commonly associated with infections from varying microbial organisms, as well as immune-compromise from conditions such as cancer and HIV. Verghese *et al.* (Verghese *et al.*, 1986) found that 43% of bacteraemia cases in their study were polymicrobial, and that 70% were nosocomially acquired.

Selected Virulence Factors

Serine-Rich Repeat Proteins

Serine-rich repeat (Srr) proteins represent a family of surface molecules expressed in several species of gram-positive bacteria (reviewed in (Lizcano *et al.*, 2012). See also Table 1 in (Takamatsu *et al.*, 2005)). The ability of these proteins to adhere to host cell surfaces was first identified in oral streptococci *Streptococcus gordonii* and *Streptococcus sanguis* (Wu *et al.*, 1998, Takamatsu *et al.*, 2005). Having purified the protein from growth media, Wu *et al.* (Wu *et al.*, 1998) characterised a heavily glycosylated adhesin (designated fimbriae-associated protein 1 – Fap1) in *Streptococcus sanguis* (formerly *parasanguis*); each with two distinct regions containing large amounts of threonine and serine. Stephenson *et al.* (Stephenson *et al.*, 2002) confirmed that Fap1 is essential for *S. sanguis* adhesion to host cells *in vitro*. *S. gordonii* was found to express two homologous serine-rich adhesins (HAS and GspB) which mediate specific binding to human platelets (Takamatsu *et al.*, 2005). As platelets are abundant in blood, the capacity to bind to platelets has serious implications for systematic infections. A homologous serine-rich surface protein in *Staphylococcus aureus* (SraP) has also been found to mediate binding to human platelets (Siboo *et al.*, 2005). As a protein of unknown function, the Srr protein in GBS was originally designated Gbs1529 (Glaser *et al.*, 2002). This surface molecule was subsequently identified as belonging to the serine-rich adhesin protein family and redesignated Srr-1 (Seifert *et al.*, 2006).

GBS Srr proteins can vary in size but are typically characterised around the 1100-1300 amino-acid range – which is significantly shorter than Srr proteins found in other streptococcal species such as HSA (2178 aa) and GspB (3072 aa) in *S. gordonii*, Fap1 (2570 aa) in *S. sanguis* and PsrP (4776 aa) in *Streptococcus pneumoniae* (Seifert *et al.*, 2006, Lizcano *et al.*, 2012). Starting at the N-terminal end, this protein consists of a short signalling peptide (~50-90 aa) followed by two non-repeat sequences straddling the first serine-rich region in which the proportion of Ser/Thr exceeds 40% (Chaze *et al.*, 2014, Seifert *et al.*, 2006). The specific binding domain (to extracellular substances) lies roughly

between amino-acids 300 and 650, followed by a long (>700 residue) serine rich region (>70% Ser/Thr including 140 repetitions) and attached to a membrane-spanning region via the LPxTG motif (Fischetti *et al.*, 1990). It is thought that the enzyme Sortase A uses the LPxTG motif to covalently distribute proteins onto the peptidoglycan (Bierne & Dramsi, 2012, Dramsi & Bierne, 2016). Within the Binding domain there exists a 13 amino-acid sequence demonstrated to lock fibrinogen into place during adhesion to brain microvascular endothelial cells, thereby facilitating the persistence of GBS in meningitis (Ponnuraj *et al.*, 2003, Seo *et al.*, 2013, Seo *et al.*, 2012). Wang *et al.* (Wang *et al.*, 2014) showed that the absence of this "latch" domain decreased the capacity of GBS binding to both cervical and vaginal epithelial cells.

Two serine-rich repeat proteins have been identified in GBS; Srr-1 and Srr-2 (Seifert *et al.*, 2006). These two proteins, whilst structurally similar, share less than 20% overall genetic identity; and less than 36% identity from the signalling peptide to the binding region - whereas Srr-1 proteins isolated from different strains of GBS share more than 89% identity across the same region (Seifert *et al.*, 2006). Six *et al.* (Six *et al.*, 2015) found less than 20% amino-acid identity between Srr-1 and Srr-2 across the short serine-rich region of the proteins, and less than 15% identity across the long serine-rich region (<30% homology across both regions). To date, Srr-2 is only found in serotype III, ST-17 strains of GBS and has been implicated in the hypervirulence of many these strains (Seifert *et al.*, 2006). By contrast, Srr-1 is commonly isolated from multiple GBS serotypes (Samen *et al.*, 2007, Wang *et al.*, 2014, van Sorge *et al.*, 2009). Both Srr-1 and Srr-2 operons encode glycosytranferases and membrane translocation genes downstream of the *srr* loci however, importantly, *Srr-1* also encodes a regulatory gene (*rga*) upstream of this loci which is not present in the *Srr-2* operon (Six *et al.*, 2015). This lack of specific regulation likely accounts for the excess expression of Srr-2 observed on the surface of ST-17 cells when compared to Srr-1 .Using surface plasmon resonance spectrometry, Seo *et al.* (Seo *et al.*, 2013) demonstrated a 10-fold higher affinity for Srr-2 to fibrinogen *in-vitro* compared to Srr-1. Six *et al.* (Six *et al.*, 2015) found that Srr-2 is expressed on

more cells (>90%), and in significantly higher amounts on the surface of ST-17 cells (Median Mean Fluorescence Intensity (MFI) = 10.1), than Srr-1 is expressed on the cells of non-ST-17 strains (>30% of cells with a median MFI of 4). A single serotype V, ST-26 strain (NCTC 10/84) in this study proved the exception, expressing copious amounts of Srr-1 on its cell surface (MFI = 17.6); much more than its other non-ST-17 counterparts. This strain has been previously recognised as hypervirulent due to its overproduction of β-hemolysin/cytolysin and its observed virulence in animal models; and is considered atypical of non-ST-17 strains (Hooven *et al.*, 2014, Dramsi *et al.*, 2012).

Keratins are the most abundant structural proteins found in epithelial cells; primarily acting as cytoplasmic scaffolds supporting the cells from both mechanical and non-mechanical stresses (Coulombe & Omary, 2002). Several studies have described pathogenic bacteria utilising keratin for binding, colonization and invasion of epithelial cells (Batchelor *et al.*, 2004, Carlson *et al.*, 2002, O'Brien *et al.*, 2002, Sajjan *et al.*, 2000, Sojar *et al.*, 2002, Tamura & Nittayajarn, 2000, Viswanathan *et al.*, 2004, Walsh *et al.*, 2004). The capacity of bacteria to interact with keratin has implications for the potential infection of highly keratinized epithelial sites such as respiratory and vaginal epithelia (Tamura & Nittayajarn, 2000). Using a lung-derived epithelial cell line (A549), Tamura & Nittayajarn (Tamura & Nittayajarn, 2000) reported gram-positive streptococci (including GBS) binding to two forms of cytokeratin 8 (CK8), not through capsular binding, but rather via cell surface proteins. Samen *et al.* (Samen *et al.*, 2007) characterised a 157 amino-acid binding region of Srr-1 to a 255 amino-acid region of human keratin 4 (K4). Samen *et al.* (Samen *et al.*, 2007) further reported the participation of GBS Srr-1 in keratin binding to larynx epithelial (HEp-2) cells.

More recently, a fibrinogen-binding region was also identified in Srr proteins (Seo *et al.*, 2013, Seo *et al.*, 2012). Further investigation across multiple GBS serotypes found that corresponding Srr-1 mutant strains exhibited a significant decrease in their capacity to bind to fibrinogen as well as a 50% reduction in adhesion to cervical and vaginal epithelial cells compared to the parental wild-type strains (Wang *et al.*, 2014); i.e. implicating Srr-1 in vaginal colonisation. Srr-1 has been further

implicated in both attachment to and invasion of brain endothelial tissue; thereby facilitating meningitis (van Sorge *et al.*, 2009, Seo *et al.*, 2012). Both Srr-1 and Srr-2 proteins have a demonstrated binding affinity to fibrinogen however Srr-2 binds to fibrinogen with significantly greater affinity (Seo *et al.*, 2013). It is therefore likely that the expression of Srr-2 contributes to the increased virulence of ST-17 strains of GBS; resulting from elevated levels of fibrinogen binding observed when compared against the fibrinogen-binding affinity of their non-ST-17, Srr-1 expressing, counterparts (Dramsi *et al.*, 2012, Seo *et al.*, 2013).

Srr-2 has also been found to bind to plasminogen, a zymogen (biologically inactive precursor) of plasmin which is found abundantly in blood and the extracellular environment (Six *et al.*, 2015). The primary role of plasmin is to degrade fibrin, thereby regulating blood clots by breaking fibrin down into soluble fragments. However the involvement of plasmin has also been described in a variety of other biological functions; including the facilitation of cell migration, degradation of the extra-cellular matrix, degradation of laminin, degradation of fibronectin, and may also play an activation role in the degradation of collagen (Aisina & Mukhametova, 2014, Stoppelli, 2013). Plasminogen binding has been previously reported for GBS and the proteolytic activity of activated plasmin proposed as a means by which GBS cross the blood-brain-barrier; causing meningitis (Six *et al.*, 2015, Boone *et al.*, 2011, Boone & Tyrrell, 2012, Magalhaes *et al.*, 2013, Magalhaes *et al.*, 2007, Wiles *et al.*, 2010). In contrast to Srr-2, Six *et.al.* (Six *et al.*, 2015) found that Srr-1 does not have any specific binding affinity to plasminogen. Notably, previous studies reported plasminogen binding in non-ST-17 GBS strains; serotype V strain NCS13 (Boone *et al.*, 2011, Boone & Tyrrell, 2012), serotype V strain 2603V/R (Wiles *et al.*, 2010) and serotype III (ST-23) strain NEM316 (Magalhaes *et al.*, 2013). Boone *et al.* (Boone *et al.*, 2011, Boone & Tyrrell, 2012) attributed the plasminogen binding activity of strain NCS13 to a surface enzyme phosphoglycerate kinase (PGK). Wiles *et al.* (Wiles *et al.*, 2010) characterised a GBS surface-bound plasminogen binding protein called “Skizzle”. Plasminogen binding activity in GBS is therefore not exclusive to Srr-2, however the unregulated activity of Srr-2 in

plasminogen binding likely contributes to the hypervirulence of ST-17 strains; especially regarding their propensity to cause meningitis. Notably, when compared to the clearance rates of an Srr-1 mutant, van Sorge *et al.* (van Sorge *et al.*, 2009) reported that Srr-1 does not play a role in GBS survival in human blood.

β-hemolysin/cytolysin (β-h/c)

Originally reported in the 1930s (Todd, 1934), β-h/c remained largely ignored until the rise of GBS disease in humans (Liu & Nizet, 2006). β-h/c is a surface-associated toxin that is implicated in a variety of virulence pathways between host and pathogen; including intracellular invasion, neutrophil recruitment, phagocyte resistance, triggering the sepsis cascade, cell damage and apoptosis (Liu & Nizet, 2004, Liu *et al.*, 2004, Nizet, 2002). The function of β-h/c is usually activated through direct interaction between GBS and host cells (Platt, 1995).

Through inducing pore-formation, the cytolytic activity of β-h/c has been reported for a variety of cell types ranging from red blood cells (erythrocytes) and fibroblasts to lung epithelial and endothelial cells to brain endothelial cells and including neutrophils and macrophages (Tapsall & Phillips, 1991, Nizet *et al.*, 1996, Gibson *et al.*, 1999, Nizet *et al.*, 1997, Liu *et al.*, 2004, Doran *et al.*, 2002, Ring *et al.*, 2000). It is the destruction of red blood cells which produces characteristic halos of clearance around GBS colonies on blood agar (Brown, 1919). Partially purified β-h/c was shown to lyse 80% of erythrocytes (1% concentration in suspension) in as little as 3 minutes at 37^{o}C (Marchlewicz & Duncan, 1981). Pores generated by β-h/c are considered relatively large, inducing the rapid release of rubidium ions and haemoglobin from the red blood cells (Marchlewicz & Duncan, 1981). Inoue *et al.* (Inoue *et al.*, 1976) estimated that lysing a single sheep erythrocyte requires the activity of 5 β-h/c molecules. Flux of water and macromolecules across cell membranes resulting from β-h/c pore damage have also been reported (Nizet *et al.*, 1996, Gibson *et al.*, 1999).

In recognition of its cytolytic activity, the operon transcribing β-h/c was designated *cyl* (Spellerberg *et al.*, 1999a). This operon accounts for several *cyl* genes however only the *cylE* gene has been found to be essential for β-h/c expression (Pritzlaff *et al.*, 2001). Lamy *et al.* (Lamy *et al.*, 2004) found *covS/R* to be a negative regulator of β-h/c through noting that knockout *covS/R* mutants had significantly reduced β-h/c activity, and that *covR* demonstrated a binding affinity with the *cyl* operon. The repression of *cylE* by *covR* induces activation of another pore-forming toxin, designated CAMP factor (Lamy *et al.*, 2004, Jiang *et al.*, 2005, Rajagopal *et al.*, 2006). *CovS* strengthens β-h/c expression through phosphorylating *covR* at an aspartate residue (Lamy *et al.*, 2004, Jiang *et al.*, 2008, Lin *et al.*, 2009). The serine/threonine kinase Stk1 has also been shown to phosphorylate *covR*, but at a serine residue; undermining aspartate phosphorylation - thereby reducing both *covR* activity and CAMP activation (Lin *et al.*, 2009).

Synthesis of β-h/c has been frequently associated with the production of a polyene pigment co-expressed on the surface of haemolytic GBS cells (Rosa-Fraile *et al.*, 2014, Liu & Nizet, 2004) (Spellerberg *et al.*, 2000, Tapsall, 1986). This pigment is reported to contribute to immune evasion through promoting biochemical resistance to reactive oxygen species (ROS) produced by host phagocytes (Liu & Nizet, 2004, Liu *et al.*, 2004, Fang, 2004). Hyper-haemolytic strains of GBS characteristically display increased pigmentation whereas non-haemolytic strains of GBS tend to lack pigmentation altogether (Spellerberg *et al.*, 1999a, Nizet *et al.*, 1996, Pritzlaff *et al.*, 2001).

Streptococcal Group B, C5a-Peptidase (scpB)

The complement system represents an early innate host response to the presence of foreign cells (Colten, 1986, Kerr, 1981). Through a series of protein-cell interactions, the complement cascade mediates a variety of rapid host reactions to the challenge of a foreign cell. Complement performs two primary functions; 1) Opsonisation of the foreign cell and 2) destruction of the cell through lysis (Esser, 1994, Kinoshita, 1991). Complement protein 3b (C3b) mediates phagocytosis through

opsonisation (attachment of phagocytic-recognised antigens to the cell membrane) of the invading cell (Ehlenberger & Nussenzweig, 1977). Further along the complement cascade, the complement 5 protein (C5) is cleaved into complement components 5b and 5a (C5b and C5a respectively). C5b adheres to the membrane of foreign cells; initiating the membrane attack complex (MAC); a complex of proteins forming transmembrane pores in the invading cell; causing ion flux between intracellular and extracellular environments, cell lysis and cell death (Serna *et al.*, 2016, Hadders *et al.*, 2012, Morgan, 1999, Podack, 1984).

Pathogenic bacteria employ a large variety of both active and passive counter-complement strategies to circumvent the anti-microbial action of the complement cascade; often by mimicking, interacting with or lysing complement proteins; including complement activation regulators, and complement cascade protein degraders, recruiters and inhibitors (reviewed in (Sarma & Ward, 2011, Lambris *et al.*, 2008, Rooijakkers & van Strijp, 2007, Zipfel *et al.*, 2007)). The thick peptidoglycan surface of gram positive bacteria has also been demonstrated to passively inhibit perforation by complement MAC (Joiner *et al.*, 1983).

Human C5a, a 74 amino-acid glycoprotein derivative of C5, is involved in a variety of host-defence responses (Manthey *et al.*, 2009, Monk *et al.*, 2007, Guo & Ward, 2005) including; as an anaphylatoxin – stimulating a rapid inflammatory response including the release of histamine from mast cells (el-Lati *et al.*, 1994, Lagunoff *et al.*, 1983), and as a primary chemoattractant in the recruitment of inflammatory cells such as macrophages, monocytes and neutrophils (Soruri *et al.*, 2003, Bohnsack *et al.*, 1997, Marder *et al.*, 1985, Snyderman *et al.*, 1975). Due to its pleiotropic nature, C5a has also been implicated in vasodilation (Schumacher *et al.*, 1991), differentiation of monocytes into dendritic cells (Soruri *et al.*, 2003), neutrophil activation and granular release (Hu *et al.*, 2015), the stimulation of leukotrienes in lung tissue (Stimler *et al.*, 1982), the induction of tissue-remodelling molecules (Takafuji *et al.*, 2003), regulatory interactions with the coagulation system (Amara *et al.*, 2008) and adaptive immune system (Hawlisch *et al.*, 2004)and is suspected to be a

factor in in a broad range of peptide interactions; including some leading to pathological conditions (Guo & Ward, 2005).

GBS expresses a surface protease that inactivates, and thereby undermines the defensive role C5a plays in the host response to pathogenic challenge (Bohnsack *et al.*, 1997). Group B Streptococcal C5a-Peptidase (ScpB or C5a-ase) inhibits C5a-mediated neutrophil recruitment to the site of infection by cleaving the C5a protein (Bohnsack *et al.*, 1991, Hill *et al.*, 1988). ScpB has also been implicated as an important adhesin and invasin (Cheng *et al.*, 2002). By anchoring to absorbed fibronectin (Hull *et al.*, 2008, Tamura *et al.*, 2006, Beckmann *et al.*, 2002), ScpB facilitates adhesion and infiltration of host cells, as well as mitigating the natural opsonisation activity of fibronectin (Hosein & Bianco, 1985, Bevilacqua *et al.*, 1981).

Polysaccharide Capsule

Most wild-type strains of GBS are encapsulated. The capsule is recognised as an important virulence factor, contributing significantly to the survival and prevalence of GBS in the host environment (Kasper, 1986). GBS that do not express a capsule have a significant deficiency in their capacity to infect and produce disease in the host (Rubens *et al.*, 1987, Wessels *et al.*, 1989, Martin *et al.*, 1992, Wessels *et al.*, 1992). Baker and Kasper (Baker & Kasper, 1976) demonstrated that antibodies specific to GBS capsule acquired through placental transfer can confer vital protection to the neonate against GBS disease. GBS capsules are therefore considered important candidates for GBS vaccines (Johri *et al.*, 2006, Paoletti & Kasper, 2003, Marques *et al.*, 1994).

As previously discussed, the outer residue on the GBS capsule includes sialic acid, mimicking the host cells and thereby contributing to immune evasion (Carlin *et al.*, 2009). Capsular mutants of GBS have been shown to elicit a stronger immune response (i.e. cytokine release) than capsular-expressing strains (Doran *et al.*, 2003). Multiple acapsular GBS mutants were reported to be more susceptible to opsonisation and phagocytosis by human leukocytes than the parent, wild-type strain

(Marques *et al.*, 1992). An increase in the size and density of the capsule has been correlated to inhibition of C3 deposition (Marques *et al.*, 1992). Studies comparing parent and acapsular mutant strains of GBS in murine models have demonstrated that the acapsular strains are cleared more readily from lung tissue, more heavily associated with macrophages, contribute less to bacteraemia, and have an at-least 100-fold greater median lethal dose (LD_{50}), than the capsular parental strains (Martin *et al.*, 1992, Wessels *et al.*, 1992).

Regulation of capsular expression appears to be strain specific. RogB has been identified as a negative regulator of the GBS capsular operon (*cps*), however the gene for RogB is not found in all strains of GBS (Gutekunst *et al.*, 2003, Rajagopal, 2009); including being absent in some pathogenic GBS strains (Tettelin *et al.*, 2005). When present in the GBS genome, RogB contributes to virulence as a positive regulator of *fbsA* (a GBS adhesion), as well as promoting adherence and resistance to antimicrobial peptides by promoting pili expression (Dramsi *et al.*, 2006). CovR/S has been identified as a potential activator of the capsular operon, but this activity is not observed consistently across strains (Lamy *et al.*, 2004). It has also been revealed that GBS capsular expression can be amended by *O*-acetylation (Lewis *et al.*, 2004), which has been previously shown to modify immune responses in other bacteria such as *Neisseria meningitidis* and *Streptococcus pneumoniae* (Berry *et al.*, 2002, McNeely *et al.*, 1998). A mutation in the *neuA* gene has been found to increase *O*-acetylation of the GBS capsule (Lewis *et al.*, 2007).

Some studies have reported that the presence of a capsule can inhibit the adherence and invasion of GBS to various host cells (Hulse *et al.*, 1993, Tamura *et al.*, 1994, Nizet *et al.*, 1997), which lends weight to the proposal that GBS capsule expression is regulated as a response to the extracellular environment (Rajagopal, 2009).

Pili

Despite the research emphasis on GBS over the past half century, pili were not recognised in GBS until 2005 (Lauer *et al.*, 2005). Pili are hairlike structures that promote GBS adhesion and invasion of host pulmonary cells, and epithelial cells including lung, cervical and brain microvascular epithelial cells (Sharma *et al.*, 2013, Maisey *et al.*, 2007, Pezzicoli *et al.*, 2008, Krishnan *et al.*, 2007). In GBS, pili are also reported to play a role in the formation of bacterial aggregations and biofilms (Konto-Ghiorghi *et al.*, 2009).

The GBS pilus is anchored to the cell wall by Sortase A (SrtA) via an LPxTG domain (Konto-Ghiorghi *et al.*, 2009). Three structural subunits encode the GBS pilus; one major pilin, PilB (GBS1477), is the structural backbone of the pilus, and the two minor pilins, PilA (GBS1478) and PilC (GBS1474) (Dramsi *et al.*, 2006). PilA aligns along the PilB backbone and serves as the major adherent element of the pilus (Konto-Ghiorghi *et al.*, 2009). Whilst PilB is the major structural element of the pilus, it is not required for adhesion, whereas both PilA and PilC were indispensable for this function (Konto-Ghiorghi *et al.*, 2009, Krishnan *et al.*, 2007, Dramsi *et al.*, 2006). However, PilB was demonstrated to provide resistance to phagocytic clearing as well as promoting bloodstream survival in the mouse model (Maisey *et al.*, 2008). PilC was found to be unnecessary in the process of biofilm formation (Konto-Ghiorghi *et al.*, 2009). Banjeree *et al.* (Banerjee *et al.*, 2011) reported a further potential role for PilA, inducing neutrophil recruitment - which increases the permeability of the blood-brain-barrier (BBB) creating an opportunity for GBS invasion.

The genes encoding GBS pili are found in two disparate loci known as pili-islands 1 (PI-1) and 2 (PI-2) – with PI-2 divided into two variants PI-2a and PI-2b (Rosini *et al.*, 2006). RogB and Rga have been found to positively regulate expression of PI-2a, but not the other pili-islands (Dramsi *et al.*, 2006, Samen *et al.*, 2011). The expression of RogB has been shown to be regulated by RovS; a well-characterised global regulator of virulence genes in GBS (Samen *et al.*, 2006). Jiang *et al.* (Jiang *et al.*,

2012) found that PI-1 is regulated by several factors; including, an AraC-type regulator, Ape1, the two-component CsrRS system, as well as environmental pH.

Metal Ion Transport Systems

Transition metal ions (such as manganese, iron, cobalt, nickel, copper and zinc) perform a range of structural, chemical and metabolic functions necessary for cell viability and proliferation (Hood & Skaar, 2012). Zinc, for example, was early recognised as "indispensable" for biological function; now recognised to be involved in a vast variety of cellular activities including cell-cycle and DNA synthesis roles, as a protein co-factor in thousands of proteins, and as playing a role in transcript regulation (Maret, 2013, Beyersmann, 2002). The ability to maintain optimal concentrations of essential metal ions (metal homeostasis) is therefore crucial to bacterial survival and virulence (Ma *et al.*, 2009, Chandrangsu *et al.*, 2017). During infections, host immune cells have been reported to either saturate the bacteria with excess/toxic concentrations of metals (Djoko *et al.*, 2015), or alternatively, starve the bacteria of access to these biologically essential resources (Hood & Skaar, 2012). Complex mechanisms are employed by bacteria to maintain an optimal balance of metal ions within the cell, including; efflux systems to pump excess ions out of the cell to mitigate cytotoxic concentrations, and uptake systems to acquire metal ions during periods of scarcity (Porcheron *et al.*, 2013, Waldron & Robinson, 2009). Examples of streptococcal metal ion transport systems include the zinc transporters cobalt-zinc-cadmium resistance proteins (CzcD) and histidine triad proteins (Htp), the copper export system (cop operon), and ATP Binding Cassette (ABC) ion transporters (Ong *et al.*, 2014b, Loisel *et al.*, 2011, Neubert *et al.*, 2017, Klein & Lewinson, 2011).

1.3 Genetics

The GBS Genome

Sequencing technologies have progressed exponentially since the first full bacterial genome was reported in 1995 (Loman & Pallen, 2015, Loman *et al.*, 2012, Fleischmann *et al.*, 1995). The advent of next generation sequencing in the mid-2000s has seen a rapid increase in the amount of completed genomes reported in scientific literature; owing largely to the reduced sequencing cost (per base), and the increased efficiency of the higher throughput technologies (Caboche *et al.*, 2014, Mardis, 2013). This rise in genomic sequencing is particularly evident in the reporting of bacterial genomes (Loman & Pallen, 2015, Loman *et al.*, 2012). The National Center for Biotechnology Information (NCBI) database currently (Apr, 2019) holds 13,994 fully resolved prokaryote genomes including 108 belonging to strains of GBS (https://www.ncbi.nlm.nih.gov/genome/genomes/186).

Sanger sequencing, developed in the 1970s, is a highly accurate, but costly, laborious and time-inefficient method of genome construction when compared against newer, Next (i.e. second and third) Generation sequencing technologies (Mardis, 2013). Second generation sequencing technologies, such as Illumina's HiSeq, permit *de novo* assemblies of genomes by contributing copious short reads (e.g. 4 billion, 125-base reads output for a HiSeq 2500) to the analysis (Mardis, 2013). However, the short-read restraint of second generation sequencing can limit the capacity to fully resolve genomes containing long repeat regions; especially when the repeated regions are larger than the maximum sequenced read length (Koren *et al.*, 2013, Goodwin *et al.*, 2016, Rhoads & Au, 2015). Third generation sequencing technologies, such as PacBio's (RSII) Single Molecule Real Time (SMRT) sequencers, overcome this limitation by sequencing native, large fragment lengths of genomic DNA; with median fragments ≥10kb and some fragments reported larger than 60kb (Buermans & den Dunnen, 2014). Third generation sequencing is therefore more appropriate for

GBS genomes as GBS is known to carry large repeat regions in its genome, including those genes encoding the serine rich repeat proteins discussed earlier (Rhoads & Au, 2015).

GBS genomes vary in size, but tend to straddle the 2 mega-base pair (Mbp) range (https://www.ncbi.nlm.nih.gov/genome/genomes/186). Using shotgun Sanger sequencing, Glaser *et al.* (Glaser *et al.*, 2002) characterised the genome of a septicaemia, fatality-causing GBS strain (NEM316 serotype III), finding a 2.2Mb circular genome with 2118 protein-coding genes and known virulence factors located almost exclusively in one of the 14 reported gene islands. As serotype V is increasingly implicated in invasive disease in non-pregnant adults, Tettelin *et al.* (Tettelin *et al.*, 2002) characterised the genome of a serotype V GBS strain (2603V/R), finding a 2.16Mb circular genome and, by genetic comparison to multiple strains, significant heterogeneity across GBS, even within the same serotype. In seeking to clarify the role of serotype III in LOD, Herbert *et al.* (Herbert *et al.*, 2005) compared the whole genome sequences of these two strains (NEM316 and 2603V/R), noting that the main regions of heterogeneity are located in both the capsular genes and genetic islands; concluding that the genes contained in these regions are the most likely to contribute to virulence in LOD.

In adding the genomes of six newly sequenced pathogenic strains to the two, already characterised strains of pathogenic GBS, Tettelin *et al.* (Tettelin *et al.*, 2005) elucidated the concepts of core, dispensable and pan genomes. The core genome represents those genes which are found in every sequenced strain of the bacteria, whereas the dispensable genome describes those genes which are lacking in at least one of the sequenced strains – but also include those which may be present in only one strain; and the pan genome a combination of the two – i.e. constituting all genes present in all strains (Tettelin *et al.*, 2005). From the eight strains analysed, Tettelin *et al.* (Tettelin *et al.*, 2005) found a core genome for GBS of around 1806 genes (approximately 80% of each genome) comprised mainly of housekeeping, cell envelope, regulatory, transport and protein-binding genes. The remaining dispensable genome is largely uncharacterised, but contains a relative abundance of

mobile and extrachromosomal elements. Tettelin *et al.* (Tettelin *et al.*, 2005) concluded that GBS has a continually increasing, open genome; predicting an additional 33 genes will be added to the GBS pan genome for every new sequence – as genes are constantly being acquired by GBS through horizontal gene transfer.

Adding strain A909 (serotype Ia) to the existing, available genomes (NEM316 and 2603VR), Brochet *et al.* (Brochet *et al.*, 2006) found that differing serotypes of GBS have a heterogeneous genomic backbone – especially in regions pertaining to capsule synthesis and cell surface proteins. In a later study they demonstrated the ability of GBS to transfer and integrate large (334kb) chromosome fragments through conjugation; concluding that the GBS chromosome is a mosaic derived from various disparate ancestors (Brochet *et al.*, 2008).

Sheppard *et al.* (Sheppard *et al.*, 2016) compared the efficiency of whole genome sequencing (WGS) with the standard latex agglutination method of serotyping for all ten known serotypes of GBS; finding WGS to be highly accurate. The cost of serotyping GBS from a single clinical sample using WGS renders the method currently impracticable, however as the costs of WGS fall, it may eventually be possible to replace the standard methods with fast and accurate genomic serotyping (Sheppard *et al.*, 2016).

The increased accessibility to whole bacterial genomes has contributed to target vaccination research for several pathogens (De Groot & Rappuoli, 2004, Kaushik & Sehgal, 2008, Bambini & Rappuoli, 2009). In exposing the heterogeneous nature of the GBS dispensable genome, Tettelin *et al.* (Tettelin *et al.*, 2005) demonstrated one of the main challenges facing GBS vaccine research; given the diversity of the GBS genome (Tettelin *et al.*, 2006), vaccines based on the limited knowledge of too few genomes may be broadly ineffective against persisting strains of GBS in the longer term. Tettelin *et al.* (Tettelin *et al.*, 2006) noted that current US vaccine research only targeted the GBS serotypes that account for most US infections, but not those identified from other

regions. Targets from the core genome would be ideal for a universal vaccine, but only a small amount of targets have been identified in the core genome of GBS (Tettelin *et al.*, 2006).

Bacterial Transcriptomes and RNA-seq

Whilst the power of genomic analysis lies in elucidating the repertoire of genes available to each organism, quantifying the transcriptome (transcribed RNA) can illuminate which strategies are being employed by the organism in response to specific environmental conditions (Wang *et al.*, 2009, Adams, 2008, Morozova & Marra, 2008). Powerful high-throughput Next Generation sequencing technologies, such as RNA-seq, have provided opportunities for the analysis of bacterial transcriptomes (Croucher & Thomson, 2010).

RNA-seq has a particular advantage over microarray technology in that RNA-seq provides absolute transcript numbers, providing a more accurate references of gene-expression scale, magnitude and resolution (t Hoen *et al.*, 2008, Llorens *et al.*, 2011, Schultze *et al.*, 2015). In the process of RNA-seq, once mRNAs and sRNAs have been extracted from the sample and enriched from processed RNA such as ribosomal and transfer RNAs (Giannoukos *et al.*, 2012, Sharma *et al.*, 2010), it is reverse-transcribed into a cDNA library for sequencing (Croucher & Thomson, 2010). When the sample of interest is compared to controls, it can be determined which genes have been transcriptionally up or down regulated by the organism in response to the experimental context (Wang *et al.*, 2009). As well as revealing what annotated virulence strategies a pathogen is employing against its host, examining the transcriptome may also unveil novel regulators of virulence (Raghavan *et al.*, 2011a, Raghavan *et al.*, 2011b). It is possible, though computationally challenging, to construct a transcriptome *de novo* using RNA-seq, however utilising a reference-based strategy is preferred if a reference genome is available (Tjaden, 2015, Martin & Wang, 2011). Whilst the current method involves converting the extracted RNA into a cDNA library for sequencing, future technologies may permit the direct sequencing of RNA molecules (Goodwin *et al.*, 2016).

Small RNAs (sRNAs) in bacteria are commonly understood to act as post-transcriptional regulators of gene expression (Gottesman & Storz, 2011). Combining strand-specific RNA-seq with differential RNA-seq (dRNA-seq) across varying growth conditions, Rosinski-Chupin *et al.* (Rosinski-Chupin *et al.*, 2015) identified 120 novel small RNAs in GBS strain NEM316. Rosinski-Chupin *et al.* (Rosinski-Chupin *et al.*, 2015) further demonstrated the pervasiveness of reiterative transcription in this strain – suggesting a novel regulatory strategy. Flores *et al.* (Flores *et al.*, 2015) incorporated RNA-seq into their study, demonstrating the differential expression of genes across mutant strains of GBS when compared against a wild-type strain. Whilst RNA-seq is now commonly used to characterise bacterial transcriptomes (Sharma & Vogel, 2014), few other studies were found utilising RNA-seq in GBS. Richards *et al.* (Richards *et al.*, 2013) used RNA-seq to compare the transcriptomes of human and bovine strains of GBS, revealing the upregulation of lactose metabolism in bovine strains; thereby indicating the importance of lactose metabolism in GBS adaptation to the bovine host environment. Wang *et al.* (Wang *et al.*, 2016) used RNA-seq on fish (tilapia) to examine the potential impact of climate change on fish health; finding that the fish's immune response became compromised in warmer water, rendering them more susceptible to GBS infections.

Host-Pathogen Co-transcriptomes

Until recently, transcriptomic analyses of host and pathogen could only be accomplished in separate host and pathogen experiments (e.g. (Ordas *et al.*, 2011, Xiang *et al.*, 2010, Xiu *et al.*, 2015)), however the power of RNA-seq has now been adapted to investigate host-pathogen interactions simultaneously. Co-transcriptome (or dual transcriptome) protocols have been developed allowing characterising the transcriptomes of both host and pathogenic cells in a context of direct antagonism (i.e. infection of host cells with pathogenic cells) (Ravasi *et al.*, 2016, Avraham *et al.*, 2016). This new measure provides us with the opportunity to quantify the reaction of each cell type in response to the specific challenges associated with the presence of the antagonist.

To overcome the challenge of host RNA saturation in the infection sample, Bent *et al.* (Bent *et al.*, 2013) reported a protocol for enriching pathogen RNA in the sample. Mouse macrophage-like P388 cells were infected separately with bacterial and viral pathogens. Unlike commercially available pathogen enrichment kits which probed sequences for known genes, the authors of this study claim their technique to be unbiased. They reported a roughly 20-fold enrichment for the viral RNA and the elucidation of several hundred extra bacterial genes for transcriptomic analysis. In attempting to further enrich bacterial RNA from the host-pathogen sample, Ferreira-Machado *et al.* (Ferreira-Machado *et al.*, 2015) tried ultrasonics, centrifugation and a combination of both. The study reported increasing the sequencing depth rather than using these methods; reporting that the methods yielding the highest bacterial RNA degraded the RNA quality beyond usefulness.

The following is a brief review of the use of dual RNA-seq reported for host (plant, human, mouse cells) pathogen (parasite, viral, bacterial, fungal) interactions. Starting with the plant hosts, Kawahara *et al.* (Kawahara *et al.*, 2012) was an early implementer of the dual transcriptome technique, utilizing RNA-seq to analyse the mixed-transcriptome of rice (*Oryza sativa*) and a fungal pathogen (*Magnaporthe oryzae*) to investigate the mechanisms of fungal attack and rice defence. More recently, Zhou *et al.* (Zhou *et al.*, 2016) used this dual RNA-seq method to characterise the co-transcriptome of maize challenged with the pathogenic Rice black-streaked dwarf virus (RBSDV) to unveil the viral pathways of disease.

In challenging mouse macrophages with the pathogenic fungus, *Candida albicans*, Tierney *et al.* (Tierney *et al.*, 2012) was able to elucidate a complex network of host-pathogen interactions resulting from host-pathogen contact; including the characterisation of previously unknown molecular pathways. A dual RNA-seq study challenging the human HeLa cell line with *Salmonella* showed the importance of pathogenic sRNAs (especially PinT) in altering the capacity of the host to respond to intracellular infection (Westermann *et al.*, 2012). Humphrys *et al.* (Humphrys *et al.*, 2013) proposed a method to enrich the bacterial and host RNAs from each other; challenging human

epithelial (HEp-2) cells with the human pathogenic bacteria *Chlamydia trachomatis*. The study characterized the poorly understood mechanisms of early Chlamydial infection (i.e. 1hr post infection), noting the initial priority of *C. trachomatis* for nutrient recruitment, and the dampening of immune response in the host transcript.

Mavromatis *et al.* (Mavromatis *et al.*, 2015) infected mouse macrophages with two strains of uropathogenic *Escherichia coli* (UPEC); strain 83972 which is highly susceptible to macrophage killing, and strain UTI89 which has been shown to be resistant to macrophage killing (Bokil *et al.*, 2011). The macrophages responded similarly to both UPEC strains, differentially expressing 603 common genes for both UPEC strains; in general, upregulating immune signalling pathways and downregulating cell-cycle functionality (Mavromatis *et al.*, 2015). Strain UTI89 differentially regulated 124 genes not characterised in the 83972 transcriptome – speaking to a unique transcriptional program in UTI89 adapted to survive the intracellular environments of macrophages. In contrast to the macrophage transcriptome, few transcripts in either UPEC strain were downregulated.

Enriched dual RNA-seq was used to characterise the co-transcriptome profile of the human macrophage-like THP-1 cell line infected with a tuberculosis surrogate pathogen, *Mycobacterium bovis* (Rienksma *et al.*, 2015). Notably, the THP-1 cells upregulated cholesterol biosynthesis presumably to compensate for the reported upregulation of cholesterol degrading pathways in the *M. bovis* transcriptome.

Baddal *et al.* (Baddal *et al.*, 2015) challenged well-differentiated normal human bronchial epithelial (WD-NHBE) cells with the bacterial pathogen, nontypeable *Haemophilus influenza* (NTHi) which causes a wide range of human diseases. The study found differential regulation of genes related to virulence, biosynthetic pathways, transport and stress response in the bacteria, and in genes related to pathogen recognition, cytoskeleton synthesis and maintenance, junctional complexes,

extracellular matrix proteins and inflammatory response in the host cells; characterising an intricate 'conversation' entailing host-pathogen responses and counter-responses.

Concurrent RNA-seq was also performed on a mixed RNA sample to characterise the host-pathogen interactions of mouse macrophages challenged by the parasitic pathogen *Leishmania major* (Dillon *et al.*, 2015). The macrophages differentially expressed 6897 genes at 4 hours post-infection, ranging from 29-fold downregulated to 56-fold upregulated – 93% of which were unique to this time point. This study also reported significant differential regulation of almost 3000 genes across different stages of the parasitic life cycle. Fernandes *et al.* (Fernandes *et al.*, 2016) profiled the dual transcriptome of *Leishmania* in human macrophages, noting an aggressive early response of the macrophages to initial challenge, which is later tempered as the parasite finds a niche inside the phagocytic cells.

To demonstrate the viability and sensitivity of the software package RNA CoMPASS in the analysis of dual transcriptomes, Xu *et al.* (Xu *et al.*, 2014) analysed the co-transcriptome of lymphoblastoid cell lines (LCLs) generated through infection of naïve B-cells with Epstein Barr virus (EBV), with B-cells from Burkitt's lymphomas (BL). The software was sensitive enough to differentiate between the LCLs and BL cells; including the identification of EBV in all LCLs. Even though EBV is also implicated in BL tumorigenesis, the gene expression profile of EBV in BL were found to be distinct from EBV in LCLs. The multifunctional regulator MYC was found to be one of the most highly active pathways in BL, relative to LCLs.

Heath *et al.* (Heath *et al.*, 2015) infected human pleural mesothelial cells (PMC) with *Streptococcus pneumoniae* (Spn) to profile the co-transcriptome. The study found that upon infection, Spn upregulates genes related to adherence and metabolism. PMC upregulates genes related to stress responses and cell survival, but interestingly, did not upregulate genes related to the innate immune system. Aprianto *et al.* (Aprianto *et al.*, 2016) utilised a dual RNA-Seq approach to characterise the

co-transcriptome of early pneumococcal infections of epithelial cells; reporting that adherent (but not soluble) bacteria repress both the expression of the host immune response and the synthesis of antimicrobial peptides, as well as stimulating the acquisition of non-glucose sugars from epithelial mucus. More recently, Aprianto *et al.* (Aprianto *et al.*, 2018) generated a co-expression matrix of pneumococcal infections by applying RNA-Seq to 22 distinct, infection-relavent conditions. To date, no dual RNA-seq profiles are reported for GBS challenge to any model cell type.

CHAPTER 2: Genome Sequencing of *Streptococcus agalactiae* 874391

2.1 Introduction

Streptococcus agalactiae (Group B Streptococcus or GBS) is a common etiological agent responsible for a variety of human infections and diseases, including infections of the human genitourinary (GU) tract (Dermer *et al.*, 2004, Eickhoff *et al.*, 1964, Harper, 1971, Farley *et al.*, 1993, Verghese *et al.*, 1986). Urinary tract infections (UTIs) have been shown to disproportionally affect females over males (Foxman & Brown, 2003, Foxman, 2010) and an increasing number are ascribed to GBS (Stamm, 2002). GBS GU infections in pregnant mothers are considered the primary route of transmission for neonatal sepsis and meningitis – the leading cause of neonatal death globally (Baker, 1977, Gotoff, 1977, Anthony & Okada, 1977).

GBS is a highly diverse species of bacteria. This diversity promotes their survival and proliferation GBS in a broad range of host environments; including described infections for a variety of mammals, reptiles, amphibians and fish (Delannoy *et al.*, 2013, Eisenberg *et al.*, 2017). This bacteria can interact with the host as commensal, asymptomatic or pathogenic infections (Bliss *et al.*, 2002, Easmon, 1986, Finch *et al.*, 1976). There are three primary methods of classifying GBS; 1) Capsular Serotyping – 10 serotypes (Ia, Ib and II to IX) are currently described based on an antigenic response of capsular polysaccharides (Lancefield *et al.*, 1975, Lancefield, 1934, Afshar *et al.*, 2011, Slotved *et al.*, 2007, Sheppard *et al.*, 2016), 2) Restriction Digest Patterns – a sub classification of serotype III based on differences in where the *Hind*III enzyme cuts the GBS chromosome (Nagano *et al.*, 1991), and 3) Multilocus Sequence Typing (MLST or ST) – creates a profile for GBS based on a seven gene backbone of housekeeping genes (Jones *et al.*, 2003). This includes the hypervirulent ST-17 sequence type (Teatero *et al.*, 2016, Sorensen *et al.*, 2010). GBS can be further grouped into clonal

complexes based on close genetic identity between 6 of the 7 genes used in MLST (Jones *et al.*, 2006). Analysis has shown capsular serotype to be unrelated to MLST (Tettelin *et al.*, 2005).

The genome of GBS reflects its phenotypic diversity. This has been attributed to several factors including; 1) GBS having an open genome permitting horizontal gene transfer (Tettelin *et al.*, 2005) and 2) the demonstrated ability of GBS to exchange large fragments of its genome. Tettelin (Tettelin *et al.*, 2005) described the concept of the GBS pan genome; predicting that 33 genes would be added to GBS every time a new genome was annotated. One study showed that GBS could exchange genomic fragments larger than 300kb (Brochet *et al.*, 2008). Within clonal complexes, GBS was shown to be able to exchange up to 47% of its genome (Da Cunha *et al.*, 2014). This inherent genomic flexibility resulted in a bacterial species with a highly diverse phenotype.

Sanger sequencing was the mainstay sequencing protocol from the 1970s to the mid-2000s (Rocha *et al.*, 2013). Few whole genomes were generated over this period because the method was expensive (per bp) and time inefficient (Mardis, 2011, Metzker, 2010, Shendure & Ji, 2008). Second generation sequencing, with its time-efficient preparations and relatively inexpensive cost (per bp) has made whole genome sequencing an increasingly realistic prospect for research. As such, over the past 15 years, sequencing of bacterial genomes has become commonplace (Land *et al.*, 2015). At the time of writing, GenBank contains 1076 partially assembled genomes for GBS alone (Source: Genome Assembly and Annotation report, Downloaded November 9th, 2018). However, many such assemblies are considered incomplete (Land *et al.*, 2015), and according to the GenBank Genome Assembly and Annotation report for GBS (Downloaded November 9th, 2018), only 102 of the 1076 genome assemblies for GBS are complete (9.5%).

One of the main limitations for second generation sequencing is that genome assemblies must be generated from short reads (<300bp per read). This is only a problem when the genome contains long repeat motifs – as it can be difficult (or impossible) to determine the correct assembly location for a read when that sequence is shorter than the repeat (Koren *et al.*, 2013, Goodwin *et al.*, 2016,

Rhoads & Au, 2015). As such, assemblies based entirely on second generation sequencing technologies of organisms with long repeats cannot be considered complete. GBS is known to have several long repeat motifs in its genome – including the Serine-Rich Repeat which translates a well-defined virulence factor in GBS.

Pacific Biosciences (RSII) Sequencing (PacBio or third generation sequencing) overcomes the aforementioned limitation by recording movies of the sequencing process (Levene *et al.*, 2003, Lundquist *et al.*, 2008); in contrast to the parallel digital image-capture methods used by second generation technologies. Basing each sequence on the individual movies removes the read-size limitation undermining confidence in genomes based exclusively on second generation sequencing methods. Thus, PacBio sequencing is the preferred modern method of bacterial genome sequencing (often used in combination with sequence data previously derived from second generation sequencing methods).

Given the extensive diversity of bacteria, there are several factors to consider when attempting to extract a high quality, high yields of genomic DNA from bacterial cells. Intuitively, to maximise the DNA yield, more bacterial cells should be submitted to the extraction process. The highest number of cells will be available from bacteria in the stationary phase of growth (Kolter *et al.*, 1993). However, in the stationary phase, there is high competition for nutrients, cell death, toxic waste and degrading enzymes – all of which can undermine the quality of the DNA (Kolter *et al.*, 1993, Jaishankar & Srivastava, 2017). A potential solution is to extract the DNA from the cells prior to them reaching stationary phase; likely reducing the amount of cells (and thereby the amount of DNA) available for extraction. Bacterial cells have a range of surface protection (e.g. capsules, cell-wall structure etc.) inhibiting access to the intracellular genetic material (Salton & Kim, 1996). Researchers can utilise a range of physical/mechanical and/or chemical/enzymatic means to break down these external barriers (Gill *et al.*, 2016). Researchers also have to decide on the appropriate DNA extraction methods. Some methods that yield high concentrations of DNA (e.g. Guanidinium

Thiocyanate-Phenol-Chloroform methods) can retain chemical contaminants in the DNA (Tan & Yiap, 2009). Spin-column extraction methods are generally considered to be cleaner, less labour-intensive, more reproducible methods of DNA extraction; though still generally a more expensive solution (Tan & Yiap, 2009).

Aims of this study

GBS represents a highly diverse species of bacteria with a highly diverse genome. The first aim of this Chapter was to establish a protocol to generate high quality genomic DNA from diverse strains of GBS - that would produce genomic preparations suitable for Pacific Bio sequencing (considering the expenditure on Pacific Bio sequencing, and the requirement for 20µg of high integrity, high purity genomic DNA). This requires optimising a protocol to identify the optimal genomic DNA extraction method for whole genome sequencing. A high quality GBS genome is desired to provide scaffold information; facilitating the co-transcript analysis GBS-infected monocytes performed in Chapter 4 of this thesis. A second aim of this Chapter was to analyse the sequenced data and assemble completed a genome for a ST-17 GBS strain 874391.

2.2 Materials and Methods

For simplicity and readability of this thesis, a decision was taken to include Structured Sections of General Procedures and subheadings that describe experiment-specific Procedures, Observations, and Interpretations; with experiments described sequentially. For the same reasons, it was further decided to include tables within chapters.

2.2.1 General Procedures

TABLE 2.01: GBS (S. agalactiae) Strains used in this study; including uropathogenic S. agalactiae (UPSA), asymptomatic S. agalactiae and asymptomatic bacteriuria- causing (ABSA) strains.
NT designates isolates which have no associated serotype and are currently considered non-typable.

Strain	**Source**	**Pathology**	**Serotype**	**MLST (Clonal Complex)**	**References**
UPSA 0058	Urine	UTI	Ia	23 (23)	Ipe *et al.* (2016) *Infection & Immunity*, Vol. 84, p. 308.
UPSA 0247	Urine	UTI - cystitis	III	unknown	Tan *et al.* (2012) *Infection & Immunity*, Vol. 80, pp. 3145-3160.
UPSA 0714	Urine	UTI	III	17 (17)	Ipe *et al.* (2016) *Infection & Immunity*, Vol. 84, p. 308.
ABSA 0729	Urine	asymptomatic	NT	452 (24)	Ipe *et al.* (2016) *Infection & Immunity*, Vol. 84, p. 308.
UPSA 0807	Urine	UTI - cystitis	V	1 (1)	Ipe *et al.* (2016) *Infection & Immunity*, Vol. 84, p. 308.
ABSA 0834	Urine	asymptomatic	III	182(19)	Ipe *et al.* (2016) *Infection & Immunity*, Vol. 84, p. 308.
ABSA 1014	Urine	asymptomatic	II	28 (19)	Ipe *et al.* (2016) *Infection & Immunity*, Vol. 84, p. 308.
874391	Vaginal isolate	asymptomatic	III	17 (17)	Takahashi *et al.* (1993) *J. Med. Microbiology*, Vol. 38, pp. 191-196. Seifert *et al.* (2006) *Microbiology*, Vol. 152, pp. 1029-1040.

2.2.1.1 Preparation of Tryptone-soya, horse-blood agar plates

Using a Supernova magnetic stirrer, 30g/L Triptone-Soya Broth powder (OXOID) was dissolved into R0 water in a glass bottle until homogenous. While stirring, 15g/L Bacteriological agar was added. The liquid mix was then autoclaved for 30 minutes at 121^{o}C. The autoclaved liquid was returned to the stirrer and cooled while stirring to 49^{o}C. At 49^{o}C, 50ml/L horse blood was added to the mix and immediately poured into petri dishes (20-25ml per dish). Agar was allowed to set and dry open for 90 minutes. Plates were wrapped in cling wrap and stored at 4^{o}C until use.

2.2.1.2 Preparation of Todd-Hewitt Broth with Yeast (THY) bacterial growth media

Using a Supernova magnetic stirrer, 36.4g/L Todd-Hewitt Broth powder (OXOID) and 5g/L Yeast Extract powder (OXOID) were stirred into a glass bottle or flask until homogenous. The liquid was autoclaved for 30 minutes at 121^{o}C and stored at room temperature.

2.2.1.3 Propagation of GBS on TSA-blood agar plates

With a sterilized inoculation loop, freezer stock of a single bacterial strain was streaked over the TSA-blood agar plate and incubated at 37^{o}C overnight. Beta-haemolytic blood clearing around GBS colonies was observed to confirm GBS. Plates were stored at 4^{o}C until use (to allay bacterial growth).

2.2.1.4 Bacterial growth in THY

Using a sterilized inoculation loop, a single bacterial colony from a TSA-blood agar plate containing GBS colonies was inoculated into THY growth media (10ml THY in a 50ml tube or 100ml THY in a 500ml conical flask). The inoculum was incubated at 37^{o}C for 16-17 hours while shaking (200rpm).

2.2.1.5 Serial Dilutions of bacterial cultures and bacterial colony counts

Ten-fold serial dilutions of bacterial cultures were performed in PBS to a dilution factor 1:1E7. Pipette 5µl of dilutions Droplets of 5µl for each dilution between 1:1E3 and 1:1E7 was pipetted, in

triplicate, onto TSA-blood agar plates and incubated at 37^{o}C overnight. Triplicates at the lowest dilution factor (i.e. highest bacterial concentration) which were countable, were counted and averaged across the triplicates. Averages were multiplied to colony forming units per ml (CFU/ml).

2.2.1.6 Gel Electrophoresis for DNA and RNA

Desired percentage (w/v) of Agarose gel powder was added to TAE (Tris, Acetic acid, EDTA) buffer and microwaved until homogeneous. For every 10ml TAE, 1µl SYBRsafe (Invitrogen) red stain was added and hand mixed thoroughly before being poured into the mould, covered and allowed to set for at least 15 minutes. The set gel was placed in gel dock, the samples and 1kb Plus Ladder (New England Biolabs) loaded into the appropriate wells and electrophoresis performed for desired time at desired voltage. Gels were viewed and imaged on a Gel Dock EZ Imager (Bio-Rad).

2.2.1.7 Spectrophotometric and Fluorescence Assessment of Nucleic Acid Quality and Quantity

Quantity by elution concentration was determined initially by spectral absorbance measured on a Nanodrop Spectrophotometer or Eppendorf Biospectrometer. Subsequently, Qubit fluorescence reagents were used to determine genomic DNA (gDNA) quantity more accurately using the Biospectrometer. Absorbance measures also provided data pertaining to protein, salt and nucleotide (non-DNA) contamination present in the DNA. The structural integrity of the prepared gDNA was observed using gel electrophoresis.

2.2.1.8 Sequence Analysis and Bioinformatics

FASTA files were assembled using multiple iterations of the SMRT 2.0 software package which was performed on the Gowonda HPC core cluster (Griffith University). After each iteration, the assembled genome was examined for sequence crossover using Gepard 1.40 and the assembled FASTA file altered using artemis software. Then the file was returned to SMRT 2.0 for reassembly.

This was repeated until there was no sequence crossover evident and zero variants returned by the SMRT software.

Results 2.3

2.3.1 Genomic Preparations

Extensive optimisations were performed to generate high yield, high quality genomic DNA preparations from eight strains of GBS for PacBio sequencing. The experimental details of these optimisations are located in Appendix 1.

2.3.2 Genomic preparations of GBS – Final protocol for PacBio sequencing

Pellet collections

Two conical flasks of 50ml THY (pre-warmed at 37°C) were each inoculated with 50µl of a 10ml overnight culture. The new, diluted culture was incubated at 37°C, shaking. Samples were tested every hour on a Thermo-Scientific Spectronic 200 – aiming for a reading OD_{600} between 0.4 and 0.8.

The culture (100ml) was divided into ten 10ml aliquots (15ml tubes) and centrifuged for 10 minutes at 7,197g. After discarding supernatant, pellets were resuspended in 10ml PBS to wash the cells from the THY media and re-centrifuged. All-but 0.5ml of the supernatant was discarded, and the remaining PBS used to resuspend the pellets. Cells were transferred to clean 1.5ml tubes and centrifuged at 15,000g for 1 minute. Supernatants were removed by pipette and the pellets stored at -20°C.

gDNA Preparations

The UltraClean Microbial DNA Isolation Kit instructions were generally followed to extract gDNA from GBS cell pellets using the following methods. Three pellets were processed through each column.

Bacterial pellets were thawed on ice. Lysosyme (15mg/ml) was added to the Microbead Solution prior to use in order to assist bacterial cell wall digestion. 300µl of the Lysosyme/Microbead Solution was used to resuspend 3 thawed pellets into a single reaction. The resuspended cells were then mixed gently by vortex (10 seconds). 10µl of Mutanolysin (100 units @ 10units/µl) and 40mg (2µl from 20mg/ml) RNaseA was added to each digest and the mix vortexed for 5 seconds. The mixes were then incubated for 90 minutes at 37^{o}C before being transferred to the Microbead Tubes where 50µl of Solution MD1 (pre-heated to 65^{o}C) were added to each tube. The mixes were then horizontally bead-beaten for 1 minute at 30 beats per second using a TissueLyser II.

The lysates were then centrifuged for 30 seconds at 10,000g. After carefully transferring the supernatants to 2ml collection tubes, 100µl of Solution MD2 was added to each supernatant, and the mix vortexed for 5 seconds before incubating in ice for 5 minutes. Following a further 1 minute centrifuge at 10,000g, the supernatants were transferred to clean 2ml collection tubes and 900µl of Solution MD3 added to each supernatant and vortexed for 5 seconds.

700µl of each supernatant was aliquoted into the spin filter and centrifuged for 30 seconds at 10,000g. After discarding the flowthrough, the remaining supernatant mix was loaded (700µl or less at a time) into the spin filter and centrifuged as above. 300µl of Solution MD4 was then loaded into each membrane and centrifuged for 30 seconds at 10,000g. After discarding the flowthrough, the tubes were re-centrifuged for 1 minute at 10,000g to remove residual MD4 Solution from the tube.

50µl of nuclease-free Ultrapure Distilled Water (Invitrogen) was added to each membrane and incubated at room temperature for 2-5 minutes. DNA was eluted by centrifuge for 60 seconds at 10,000g. If required, multiple genomic DNA preparations were pooled. Elutes were stored at 4^{o}C

overnight or -20°C for longer periods. 20µg was sent to the Doherty Institute (Melbourne University) for PacBio sequencing.

2.3.3 gDNA Preparation Data

TABLE 2.02: Final gDNA preparations of 8 GBS strains sent for PacBio sequencing.

Strain	Absorbance gDNA ng/µl	$A_{260/280}$	$A_{260/230}$	Fluorescence gDNA ng/µl	Total µg
GBS 0058	202.1	1.84	2.33	187.1	56.1
GBS 0247	231.6	1.82	2.37	236.6	47.3
GBS 0714	124.3	1.92	1.39	98.8	29.6
GBS 0729	203.0	1.82	2.36	187.1	37.4
GBS 0807	103.8	1.85	1.79	79.2	23.8
GBS 0834	157.4	1.83	2.32	138.3	27.7
GBS 1014	195.1	1.83	2.35	148.7	29.7
GBS 874391	252.3	1.83	2.33	242.4	48.5

Note: Total µg calculated on eluted volumes multiplied by fluorescence readings.

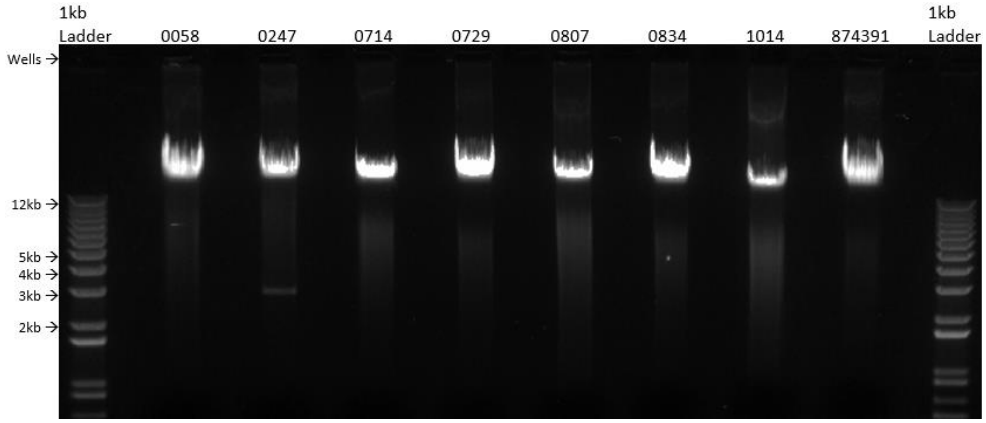

FIGURE 2.01: Agarose gel showing genomic integrity of 1µg gDNA final preparations (absorbance quantified) from 8 GBS strains.

The ladder used was 1kb Plus DNA ladder (Invitrogen) with relevant sizes as indicated in kilobases (kb).

There is minor smearing evident for all 8 preparations, however, the preparations otherwise exhibit high integrity gDNA. Due to a contamination event, GBS 0058 was re-prepared (FIGURE 2.02).

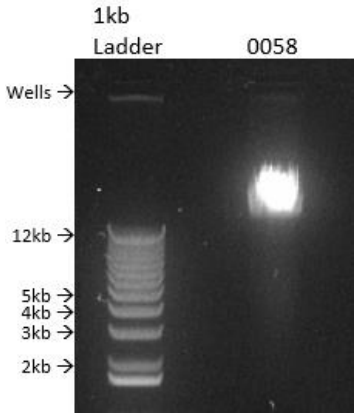

FIGURE 2.02: Agarose gel showing genomic integrity of 1µg re-prepared GBS 0058.

2.3.4 Genome Assembly

Sequence read data was provided by The Doherty Institute (The University of Melbourne). After 5 passes through SMRT 2.0 software, a 2,053,346 base-pair genome was assembled for GBS 0058. The mean read length for the PacBio sequencing was reported to be 16,256 bases. The average regional depth of coverage was reported to be 465.68. The majority of coverage was for reads between around 5kb to 20kb – with most reads within that size range hovering around the 250-fold coverage mark. Some reads for the GBS 0058 assembly were reported to be in excess of 80kb in length (FIGURE 2.08).

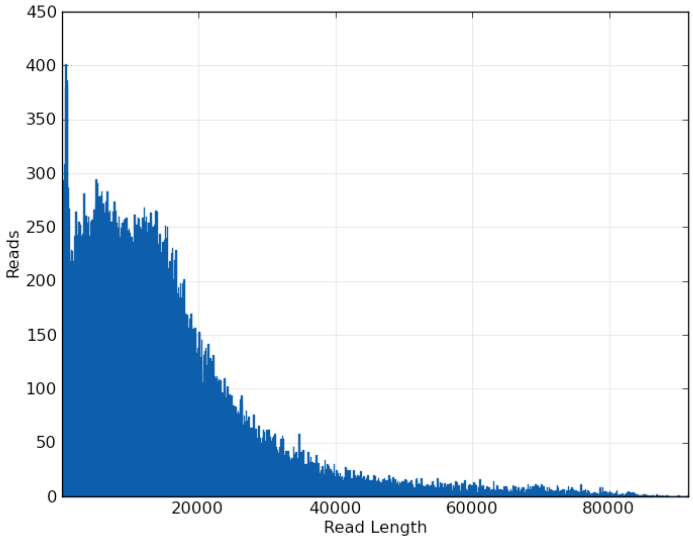

FIGURE 2.03: Histogram of mapped read lengths used by the SMRT software to generate an assembled genome for GBS 0058.
Reads contributing to the genome assembly of GBS 0058 - generated by PacBio sequencing.

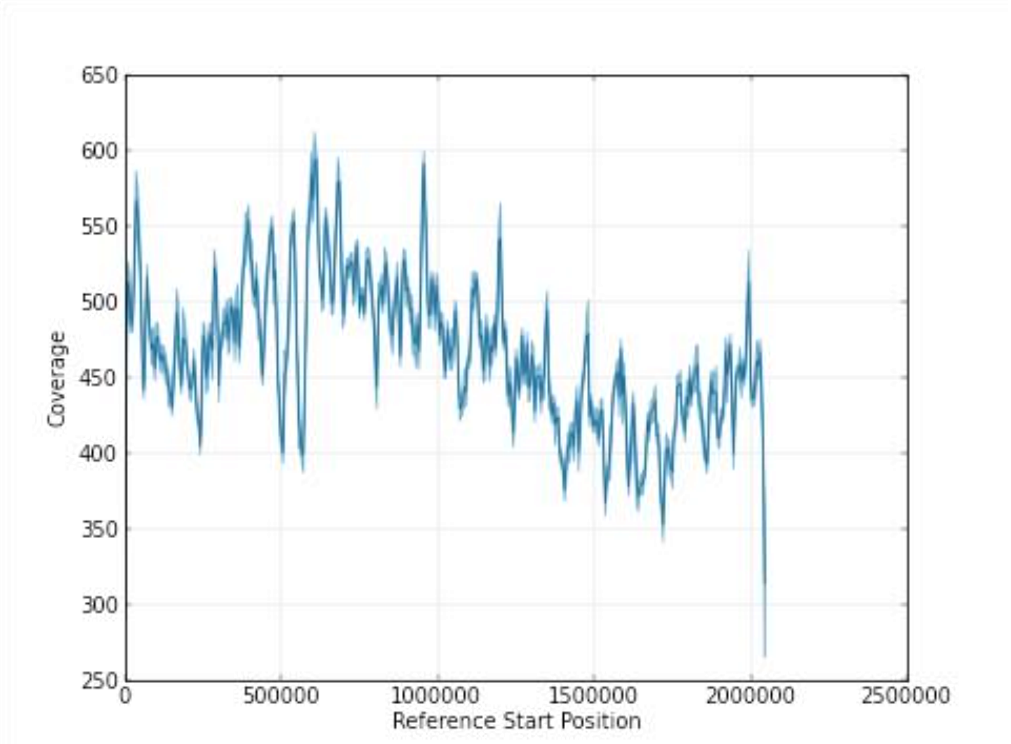

FIGURE 2.04: Coverage plot for the assembled genome of GBS 0058 generated by the SMRT software.

The blue line indicates how much each region of the final assembly was repeated in the PacBio sequence dataset. Note that the y-axis begins at 250-fold coverage.

The fold coverage exceeded 250-fold for all of the regions of this assembly. The highest coverage was over 600-fold. Only the region around the putative origin point fell below 350-fold coverage.

The seven remaining GBS sequences were assembled by Dr Matthew Sullivan (Menzies Health Institute – Griffith University), Dr Brian Forde and A/Prof Scott Beatson (School of Chemistry and Molecular Biosciences – University of Queensland).

2.4 Discussion

GBS is a genomically diverse species with an open genome facilitating the acquisition of new genes and the exchange of large genomic fragments (Tettelin *et al.*, 2005, Brochet *et al.*, 2008, Da Cunha *et al.*, 2014). Unique strains of GBS are therefore expected respond uniquely to external stimuli; including genomic extraction protocols - resulting in varying efficiencies of genomic preparations between strains. This study developed a protocol that could be used to generate high purity, high integrity genomic preparations for different strains of infectious GBS previously isolated from the genitourinary tract.

GBS cells were initially collected during the stationary phase, but subsequently, the mid-log phase of cellular growth; which was shown to be necessary to mitigate any influence of degrading enzymes present at the stationary growth phase. The UltraClean Microbial DNA Isolation Kit (MO BIO Laboratories) was effective, but required several modifications; Lysosyme, Mutanolysin and RNase were necessary to the digest the bacterial cell wall and the bead-beating was reduced from 10 minutes to 1 minute to avoid nucleic acid degradation. Elutions were performed twice through each membrane with Ultrapure Distilled Water (Invitrogen) (instead of the kit-provided elution buffer) and centrifuged for 60 seconds (instead of the kit-recommended 30 seconds) to improve yield. These many modifications enabled the preparation of highly pure, good yields of GBS gDNA, suitable for PacBio sequencing.

Focussing on GBS 0058, the average read lengths for the PacBio sequencing ranged between 10 and 20kb; with some of the reads exceeding 80kb. Utilizing the freely available software packages Gepard 1.4 and artemis on a Windows desktop and SMRT 2.0 on Griffith University's High Performance Computing Facility (Gowanda), complete GBS assemblies were attained from the PacBio sequences.

Illumina (2nd generation) sequencing is considered robust due to the copious amounts of data generated. However, this method is limited to short reads, which can fail to account for long repeats in the sequenced genome. PacBio sequencing overcomes this limitation by generating much longer sequence reads. It is becoming increasingly common to complete genomes by combining the robust data from the Illumina method with the long-read PacBio data. The PacBio sequence assembly data from this study was combined with pre-existing Illumina assemblies – leading to the announcement of a complete genome for GBS 874391 (Sullivan *et al.*, 2017a). The genome characteristics of GBS 874391 are consistent with the reports of other pathogenic strains of GBS; characterised by a circular genome around 2Mbp in length, a GC content around 35%, and around 2000 coding sequences (CDS) (Sullivan *et al.*, 2017a, Liu *et al.*, 2012, de Aguiar *et al.*, 2016, Glaser *et al.*, 2002); including the key virulence factors common to pathogenic strains of GBS and a clustered regularly interspaced short palindromic repeat (CRISPR) array (Sullivan *et al.*, 2017a).

CHAPTER 3: Optimisation of an *in vitro* infection model of human monocytes with *Streptococcus agalactiae* for co-transcript analysis

3.1 Introduction

3.1.1 Background

GBS has a large assortment of virulence factors that promote survival and proliferation of the bacteria in blood. These include; β-hemolysin/cytolysin (β-h/c) – a haemolytic toxin that breaks down red blood cells, ScpB – a peptidase that specifically targets Complement protein 5a (C5a) for inactivation, sialic acid expression that promotes host mimicry and immune evasion, Nuclease A that provides a defence against neutrophil extracellular traps, and TRAIL stimulation that induces apoptosis in monocytes (Rajagopal, 2009). GBS may gain access to mammalian blood streams via respiratory tracts, urinary tracts, through the skin, as well as through sites of intravenous entry (Verghese *et al.*, 1986). Neonatal aspiration of GBS during birth is considered a primary route of infection leads to bacteraemia and subsequent early onset neonatal disease (Boyer *et al.*, 1983b, Eickhoff *et al.*, 1964, Doran & Nizet, 2004, Baker & Barrett, 1973). Survival in the blood gives GBS systemic access to infect a range of tissue sites, however, GBS can also survive and proliferate in the blood stream, causing bacteraemia and sepsis (Edwards *et al.*, 2016). Furthermore, GBS exhibits a capacity to survive the intracellular environment of immune cells (Valenti-Weigand *et al.*, 1996, Cornacchione *et al.*, 1998, Sagar *et al.*, 2013, Cumley *et al.*, 2012).

The mammalian blood stream has a raft of host defence strategies to clear pathogenic agents (Medzhitov & Janeway, 2000). Phagocytes (principally, polymorphonuclear leukocytes) are key innate immune cells that detect and eliminate foreign materials from sites of infection (Dale *et al.*, 2008). The primary mechanism of phagocytic bacterial clearing (phagocytosis) involves the

phagocyte engulfing the foreign material (e.g. bacterial cells), then destroying the engulfed material with Reactive Oxygen Species (ROS) (Kolaczkowska & Kubes, 2013, Dupre-Crochet *et al.*, 2013, Badwey & Karnovsky, 1980). Neutrophils are the phagocytes which are most abundant in human blood and are considered the initial immune responders to sites of infection (Kolaczkowska & Kubes, 2013). Monocytes are another type of blood-borne phagocyte recruited to sites of infection (Yona & Jung, 2010, Hawiger, 2001). Monocytes can differentiate into macrophages following diapedesis and translocation from the blood to other tissues to clear foreign materials (Yona & Jung, 2010).

A commonly used human monocyte cell line, U937, is useful for host-pathogen interaction studies due to this cell line sharing phenotypic properties with monocytes; including the secretion of specific cytokines and chemokines (Lehmann, 1998, Anderson & Abraham, 1980). The U937 cell line was originally isolated from a 37-year-old male histiocytic lymphoma patient in 1974 (Sundstrom & Nilsson, 1976). It is considered generally more mature and robust than the comparable THP-1 cell line (Chanput *et al.*, 2015). *In vitro*, U937 cells can be differentiated into macrophage-like cells (Hass *et al.*, 1989, Minta & Pambrun, 1985, Olsson *et al.*, 1983).

Methodological and technological advances in DNA sequencing in recent years have permitted simultaneous characterisation of host-pathogen transcripts derived from single reactions (Ravasi *et al.*, 2016, Avraham *et al.*, 2016). Prior to these advances, transcript studies were generally limited to analysing the response of the host and the pathogen independently (e.g. (Ordas *et al.*, 2011, Xiang *et al.*, 2010, Xiu *et al.*, 2015)). The ability to characterise co-transcripts in single reactions allows the study of mechanisms of cell interactions in the context of direct antagonism (Ravasi *et al.*, 2016, Avraham *et al.*, 2016). Through elucidating transcriptional factors used by host and pathogen cells in co-culture, targets for medical intervention and novel aspects of host-pathogen interactions may be revealed. However the major challenge of co-transcript studies has been saturation of the sample with host RNA. Co-transcript studies therefore require extensive protocol optimisation to ensure sufficient quality and quantity of pathogen RNA is available for downstream analysis.

3.1.2 Aims of this study

This study aimed to develop a monocyte/GBS intracellular infection model capable of generating enough pathogen and human RNA for downstream transcript analysis either by RT-qPCR or RNAseq. Within this Aim, this study sought to characterise the optimal infection environment, incubation conditions (time, media, scale), cell collection and RNA extraction methods.

3.2 Materials and Methods

3.2.1 General Procedures

3.2.1.1 Cell Culture Media (500ml)

U937 cells were cultured in a 10% FBS Complete Roswell Park Memorial Institute 1640 (cRPMI). cRPMI was prepared by adding the following supplements in the following order to 417.5ml basal RPMI (bRPMI) (without L-Glutamine) (Gibco); 1mM Sodium Pyruvate (Gibco), 1X Minimum Essential Medium non-essential Amino Acids (MEM NEAA)(Gibco), 1X GlutaMAX (Gibco), 1X Pen/Strep antibiotics (Gibco), 12.5ml 1M HEPES (Gibco), 50ml Heat Inactivated Fetal Bovine Serum (FBS)(Gibco) and 25µM Beta-Mercaptoethanol (Gibco). The media was mixed gently and stored at 4^{o}C until use.

3.2.1.2 Revival and Propagation of U937 Monocyte Cells

To revive U937 monocytes from frozen stocks, 10ml of cRPMI was equalised in a 25cm^2 Cell Culture Flask (Corning) at 37^{o}C in 5% CO_2 for 30 minutes. 500µl of cells were thawed at 37^{o}C (quick thawing to mitigate crystal ice damage). 9.5ml of cRPMI (pre-warmed at 37^{o}C) was transferred to a 50ml tube. From that tube, 1ml of cRPMI was slowly added to the 500µl monocytes (media added to cells to mitigate osmotic shock). The mix was gently mixed with a 5ml serological pipette and added to the tube containing 8.5ml cRPMI. The cell mix was centrifuged for 5 minutes at 300g and the

supernatant carefully decanted. The cell pellet was resuspended in 10ml equalised cRPMI and transferred to a clean 25cm^2 Cell Culture Flask. After briefly mixing, 5ml of the cell mix was transferred to a new 25cm^2 Cell Culture Flask. Both flasks were incubated for 3 days at 37^{o}C in 5% CO_2 prior to passaging.

3.2.1.3 Passaging U937 Monocyte Cells

. Cells were observed for media colour (yellow media indicating nutrient depletion), clarity (clear media indicating that the cells are free of bacterial contamination), and cell proliferation prior to passage. For passaging, cRPMI media was incubated at 37^{o}C for at least 40 minutes prior to use.

Cells from the same passage were combined into a single 50ml tube and roughly 500µl of cells were aliquoted into a 1.5ml tube for counting. The cell mix was then centrifuged for 5 minutes at 300g. After decanting the supernatant, the cell pellet was resuspended in pre-warmed cRPMI (to the original volume). The split ratio was determined based on cell concentration and the greater volume of pre-warmed cRPMI media was added to a single Cell Culture Flask of appropriate size. The lessor volume of resuspended cells was mixed into the same flask. After gently mixing, half the culture volume was moved to a second flask. Both flasks were incubated for 2-5 days at 37^{o}C in 5% CO_2 until re-passaging (Freshney, 2000). Monocytes were counted using a NucleoCounter NC-200 (Chemometec), or haemocytometer. Total cells and viable cells were recorded. New passages were seeded from cultures with monocyte concentrations greater than 5E5 cells/ml.

3.2.1.4 Statistics

All statistics were performed using Graphpad Prism version 7.02. Central tendency bars and error bars in figures represent the Mean and Standard Error of the Mean (SEM), as the discreet figures represent means of replicated data points (technical replicates) over repeated experiments, unless otherwise stated.

3.2.2 Experimental Procedures

A general overarching consideration was that an identical method was required to work for three treatment conditions; the infection treatment, the monocyte control and the bacterial control. As host RNA generally saturates the RNA infection preparation, the optimisations focussed on attaining sufficient bacterial RNA for downstream analysis. Full details of the optimisation process, including experimental procedures, observations and interpretations for individual experiments, can be found in Appendix 2. The fully optimised protocol, from initial cell cultures through to RT-qPCR, is in the Results, section 3.3.1.

3.3 Results

3.3.1 Infection Model – Optimised Protocol for RT-qPCR

Preparing GBS and U937

GBS and U937 monocytes are prepared to achieve an MOI between 80 and 200.

Prepare GBS 874391 overnight culture in 10ml THY in accordance with the General Procedures (Bacterial growth in THY - CHAPTER 2, section 2.2.1.4). Wash GBS from the overnight culture media in PBS and resuspended in bRPMI for the infection challenge. Specifically, centrifuge the overnight culture for 15 minutes at 7197g, resuspend the pellet in 10ml PBS, and centrifuge again for 10 minutes at 7197g. Resuspend the resulting pellet a second time in 10ml PBS centrifuged for another 10 minutes at 7197g. Resuspend the pellet in 30ml bRPMI (to get between 3 and 3.5E9 CFU/ml). Retain 20µl of washed GBS for processing in accordance with the General Procedures (Serial Dilutions of bacterial cultures and bacterial colony counts – CHAPTER 2, section 2.2.1.5). Store the rest on ice prior to the infection.

Prepare cultured U937 monocytes between passage 3 and 25. Wash resuspended monocytes from the passage in PBS before being resuspended in sRPMI with 1%FBS (to a concentration between 3 and 3.5E6 cells/ml). Specifically, monocytes in cRPMI are centrifuged for 5 minutes at 500g and the pellet resuspended in 20ml of PBS. Repeat centrifuge and PBS resuspension. After another centrifuge, resuspend the pellet for the desired infection volume of cells - in sRPMI with 1%FBS and store on ice until the infection.

Infection and Collection

GBS-only: (to collect >1E7 GBS CFU/ml in ~7ml)

Into a 50ml tube, prepare 10ml per replicate of sRPMI media with 1%FBS. After removing 10µl of the media, inoculate with 10µl of washed GBS (to a final concentration between 3 and 3.5E6 CFU/ml). Centrifuge at room temperature for 5 minutes at 500g. Invert-mix the tube and aliquot 4ml of inoculum each into 2 wells of a 6-well cell culture plate. Incubate for 6 hours at 37°C in 5%CO_2. Combine the contents of both wells into a 15ml tube and, after gently mixing, separate into 4, 2ml tubes containing 1.7ml each (use the remaining for GBS serial dilutions and colony counts). Centrifuge the 4 tubes at 13,000g for 10 minutes. Resuspend first pellet in 700µl PBS and use this first resuspension to resuspend the remaining 3 pellets (i.e move resuspensions to subsequent pellets). Centrifuge at 13,000g for 2 minutes and remove the supernatant. Quick-freeze the pellet in dry ice for 30 minutes and transfer to a -80°C freezer until RNA isolation.

Monocyte-only

Into a 50ml tube, prepare 3-3.5E6 monocytes in 10ml of sRPMI media with 1%FBS. After removing 1ml of the media, inoculate with 1ml of bRPMI. Centrifuge at room temperature for 5 minutes at 500g. Invert-mix the tube and aliquot 4ml of inoculum each into 2 wells of a 6-well cell culture plate. Incubate at 37°C in 5%CO_2 for 1 hour before adding 50µg/ml Gentamicin and 2.5X Pen/Strep. Return to the incubator for another 5 hours at 37°C in 5%CO_2. Aliquot the contents of the two wells into a 15ml tube. After gently mixing, take 500µl into a 1.5ml tube for monocyte counts. Centrifuge the

remaining ~7.5ml for 5 minutes at 500g. Resuspend pellet in 1ml PBS and centrifuge for 5 minutes at 500g. Quick-freeze pellet in dry ice for 30 minutes and transfer to -80°C freezer until RNA isolation.

Infection

Into a 50ml tube, prepare 3-3.5E6 monocytes in 30ml of sRPMI media with 1%FBS. After removing 3ml of the monocytes, inoculate with 3ml of washed GBS (to a final concentration of GBS between 3 and 3.5E8 CFU/ml). Centrifuge at room temperature for 5 minutes at 500g. Invert-mix the tube and aliquot 4ml of inoculum each into 6 wells of a 6-well cell culture plate (24ml total). Incubate at 37°C in 5%CO_2 for 1 hour before adding 50µg/ml Gentamicin and 2.5X Pen/Strep. Return to the incubator for another 5 hours at 37°C in 5%CO_2. Aliquot the contents of all 6 wells into a 50ml tube and mix gently. Take 1ml for GBS serial dilutions and colony counts and a further 500µl for monocyte counts. Centrifuge remaining ~22.5ml for 5 minutes at 500g. Resuspend pellet in 1ml PBS and centrifuge for 5 minutes at 500g. Quick-freeze pellet in dry ice for 30 minutes and transfer to -80°C freezer until RNA isolation.

Column RNA Isolation

The Promega SV Total RNA Isolation System kit was used to column extract the GBS RNA. This kit incorporates and on-column DNase treatment. The cell pellet was thawed in ice before resuspension in 100µl RNase-free TE Buffer containing 30mg/ml Lysozyme followed by 100U Mutanolysin. The rest of the protocol followed the manufacturer's instructions. Elutions were performed with 100µl nuclease-free Ultrapure Distilled Water.

Testing and Resolving Bacterial DNA Contamination

Bacterial DNA contamination was tested by standard PCR generating an amplicon for the *spb1* gene. The PCR was performed using the Phusion High-Fidelity DNA polymerase (Thermo-Scientific) following the manufacture's protocol. The *spb1* primers used in this PCR were;

Forward 5'-ATTGCGACATGGGCTAAATC (Designation: 1279 F1)

Reverse 5'-TGAAGCTTTTGTGGAACCATG (Designation: 1279 R1)

- generating an amplicon of ~762bp for the *spb1* gene specific to ST17 strains of GBS.

The Turbo DNAfree Kit from Ambion (Life Technologies) was utilised according to the manufactures instructions to DNase-treat each sample where bacterial DNA contamination was detected. PCR was subsequently re-performed on the DNase-treated samples. Amplification was analysed by gel electrophoresis.

Any sample of RNA derived from monocytes was assumed to be contaminated with human DNA. PCR was therefore only performed on these samples after the Turbo DNase treatment. The *GAPDH* primers used in this PCR were;

Forward 5'-GGAAATGAGCTTGACAAAGTGG (Designation: Human_GAPDH-DWP-F7)

Reverse 5'-GAGCACAGGGTACTTTATTGATGG (Designation: Human_GAPDH-DWP-R7a)

- generating an amplicon of ~171bp for the human *GAPDH* gene.

cDNA Synthesis

cDNA synthesis is performed on all RNA samples using the SuperScript III Reverse Transcriptase kit (Invitrogen) in accordance with the manufacturer's instructions.

RT-qPCR

RT-qPCR was performed in 96-well plates on a Lightcycler 480 II (Roche) in 20µl reactions (in triplicate) using the SensiFAST SYBR No-ROX kit (BIOLINE) in accordance with the manufacturer's instructions. The cDNA templates are diluted 1:60 before use.

3.3.2 Summary results of optimisation experiments

Pre-incubation, centrifugation of infections

In an attempt to increase bacterial RNA yields from infected monocytes, a centrifugation stage was tested between the initial infection, and the incubation. Increasing the proximity between host and pathogen cells in the bottom of the tubes was expected to increase contact, and thereby GBS adhesion and invasion of the monocytes. Experiments were performed to determine whether or not a centrifugation step increases intracellular GBS yield from the monocytes, and to determine the optimal centrifugation time for preserving GBS yield, monocyte yield and monocyte viability. Details of centrifugation experiments are available in Appendix 2, Experiments 2, 3, 4, 8 and 10.

Adding a five minute centrifugation of the infection prior to incubating significantly increased intracellular GBS yield from the monocytes. However increasing the centrifugation time beyond five minutes (up to 50 minutes) did not significantly increase intracellular GBS yield from the monocytes. Across the treatments, no significant difference was found in either monocyte counts or monocyte viability (possibly due to the large spread of data for the 50-minute-centrifuge treatment), however the 5-minute-centrifuge treatment yielded significantly higher numbers of viable monocytes (P=0.0061) and higher viability (P=0.012) than the non-centrifuged treatment.

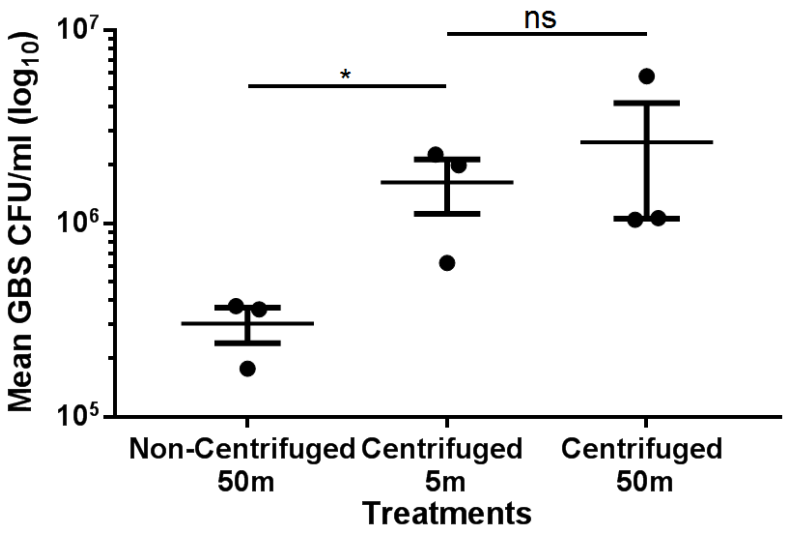

FIGURE 3.01: The effect of varying pre-incubation centrifuging times on the GBS CFU/ml recovered from monocytes after 5hrs antibiotic treatments.

Data represents values derived from three independent infections. Lines are Mean and SEM. Based on the t-test analysis, GBS counts for the non-Centrifuged treatment were significantly lower than for both the 5 minute centrifuge treatment (p=0.0144) and the 50 minute centrifuge treatment (p=0.0194). No statistical significance is reported for GBS counts between the 5 minute and 50 minute centrifuge treatments.

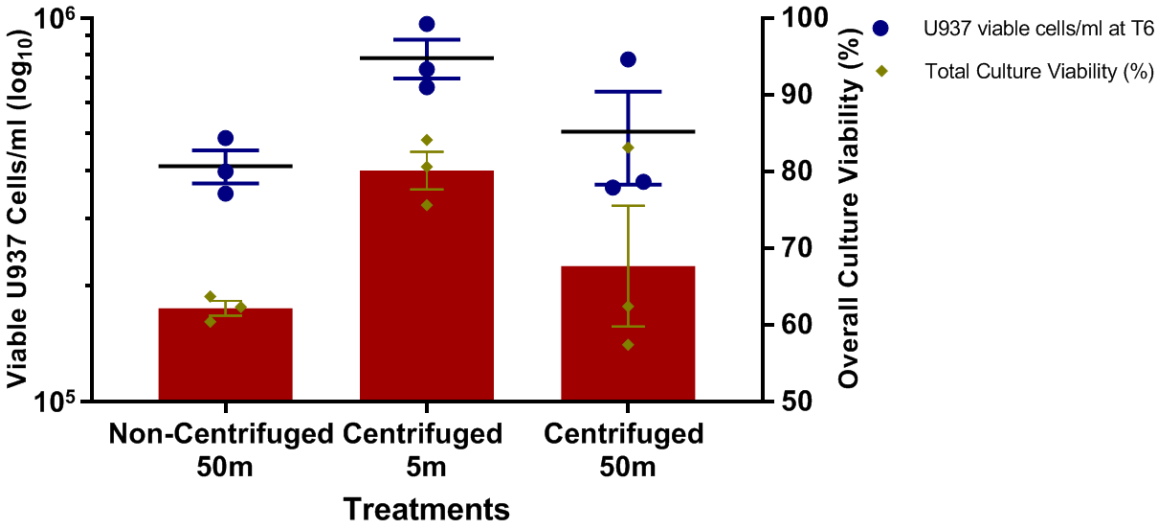

FIGURE 3.02: The effect of varying pre-incubation centrifuging times on monocyte survival (cells/ml) and viability (%) after 5hrs antibiotic treatments.

Data represents values derived from three independent infections. Data in blue represents the viable monocyte counts (Mean and SEM). Red bars represents the viable monocytes as a percentage of the total monocytes (cells/ml). T6 = 6 hours of infection (5 hours of ABX). Notably, the 5 minute centrifuge treatment was significantly higher than the non-centrifuge in both monocyte counts (p= 0.0061) and percentage viability (p= 0.012). No statistical significance was reported between the 50 minute centrifuge treatment and either of the other treatments.

Effectiveness of Antibiotics (ABX) against GBS 874391

Previous optimisation results (see Appendix 2, Experiment 4) raised the possibility of extracellular GBS survival during the infection period. Therefore, a series of antibiotic time-kill experiments were performed to assess the ability of the antibiotics to clear GBS 874391 from the extracellular environment. Antibiotics, previously prescribed for complete GBS clearing, were found to allow low levels of survival in GBS 874391. For comprehensive experimental details see Appendix 2, Experiments 5, 6 and 7. GBS survival was found to stabilise after three hours of ABX treatment, however only at numbers around 0.01% of those recovered from the intracellular environments of the monocytes from the experimental infections. At such comparatively low numbers, these surviving extracellular GBS are not expected to influence downstream applications (such as RT-

qPCR); especially considering that the infected monocytes are isolated from the media prior to RNA preparations.

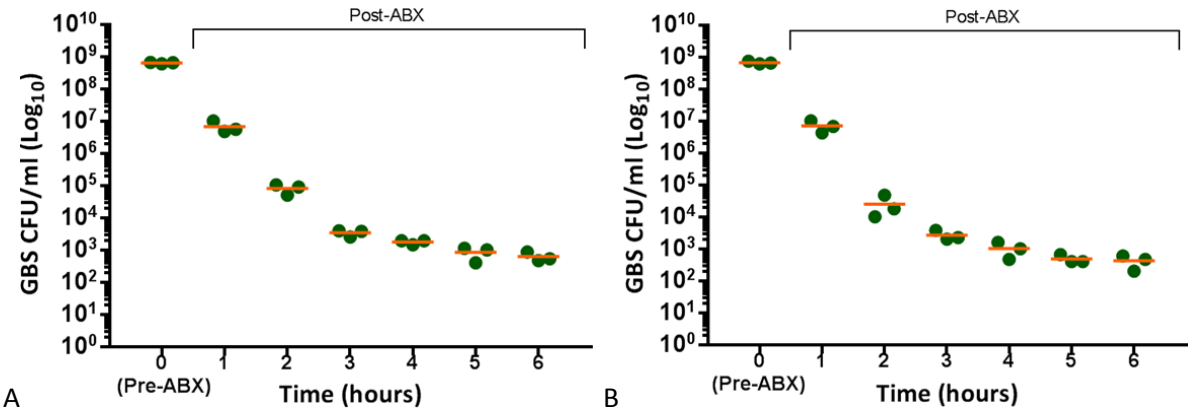

FIGURE 3.03: GBS Time Kill – Six Hour Assays.

Around 1E9 CFU/ml of GBS were exposed to a cocktail of Gentamycin and Pen/Step antibiotics for 6 hours. Surviving bacteria were enumerated by CFU/ml counts every hour. The lines show means of 3 technical replicates.

Infection Media Formulation, Cell Collections, RNA Extraction, RT-qPCR

A media formulation was required to be used in the infections, as well as provide appropriate survival conditions in the monocyte-only and GBS-only control treatments. The experiments initially focussed on the GBS-only control treatment as the infections were likely to produce limited numbers of GBS for RNA extraction (and comparison to the GBS-only control). Various cell collection and RNA extraction methods were also trialled throughout this optimisation process, and new primers designed to test the RNA for human (monocyte) DNA contamination. For comprehensive experimental details see Appendix 2, Experiments 12 to 23.

From ten tested GAPDH primers generated to test for human DNA contamination of extracted RNA, primer set 7a demonstrated specific banding and high sensitivity – detecting DNA contamination in 0.01µg of mixed RNA (RNA derived from GBS-infected monocytes).

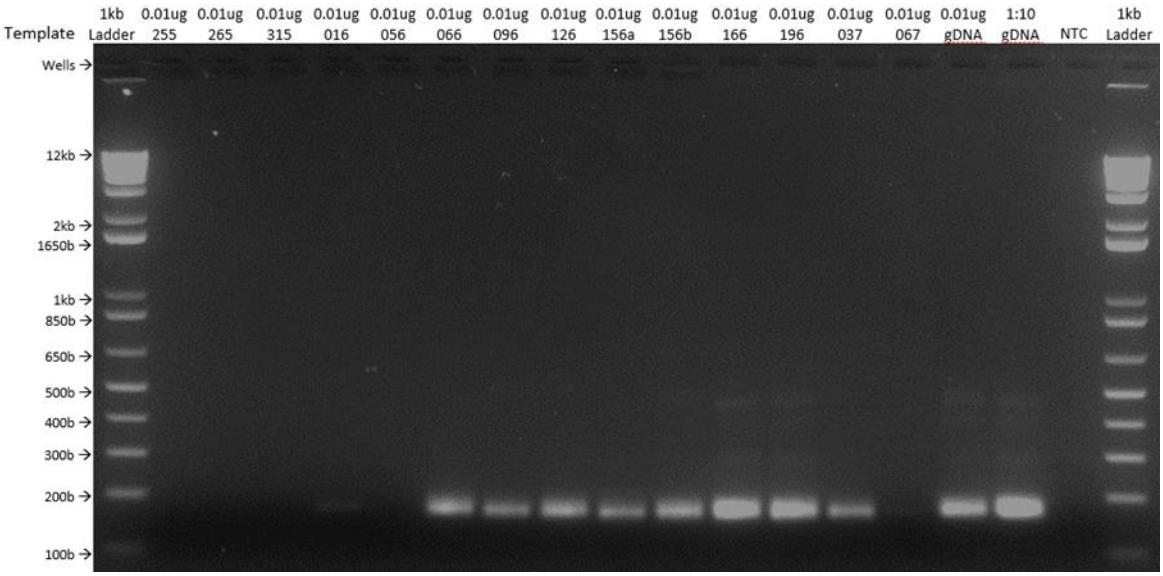

FIGURE 3.04: Agarose gels testing the sensitivity of the GAPDH primer set 7a to detect human DNA contamination in RNA samples.

Mixed gDNA (isolated from GBS-infected monocytes) was used as the positive control in both gels. The 14 RNA samples tested were also isolated from GBS-infected monocytes. Primer set 7a is expected to produce an amplicon 171bp in size. Gel shows the PCR results using primer set 7a on 0.01µg of RNA. The ladder used in both gels was the 1kb Plus DNA ladder (Invitrogen) with relevant sizes as indicated.

After extensive optimisation, a media formulation was developed containing complete RPMI media (cRPMI) with no L-Glutamine or ABX, and with the addition of 0.1%FBS (designated sRPMI). Lower concentrations of FBS were found to inhibit RNA yield; regardless of the number of GBS cells utilised in the preparation. Dilutions of cDNA from 12 GBS-only samples and 1 mixed sample (M266) generated amplification curves for 12 tested GBS genes in under 35 cycles.

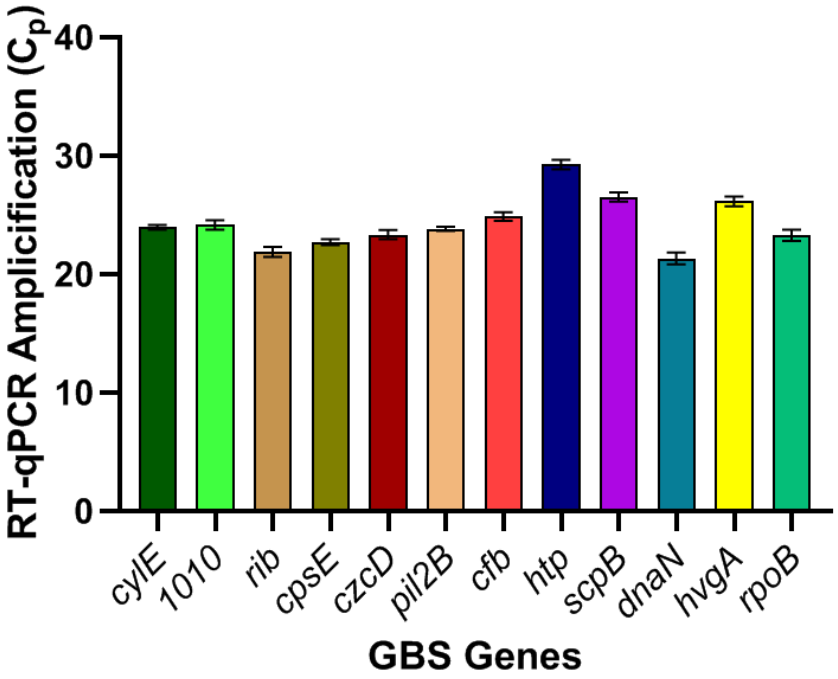

FIGURE 3.05: RT-qPCR performed on GBS-only cDNA samples.

RT-qPCR performed on Lightcycler 480. Each data point represents the mean of 3 technical replicates. Samples: n=12 for cylE and n=3 for the remaining genes. Graph shows mean and SEM. See Appendix 2, Figure AP2.71 for images of amplification curves.

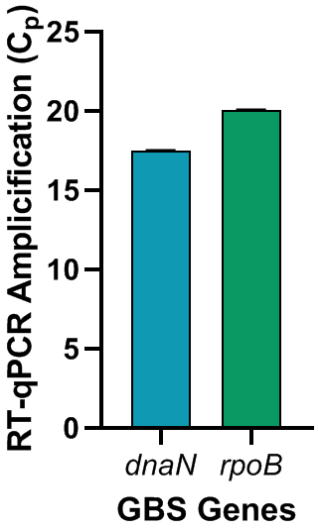

FIGURE 3.06: RT-qPCR performed on a single sample of mixed cDNA amplifying GBS housekeeping genes.

RT-qPCR performed on Lightcycler. Each data point represents the mean of 3 technical replicates. Samples: n=3 for both genes. Graph shows mean and SEM. See Appendix 2, Figure AP2.72 for images of amplification curves.

3.4 Discussion

A common difficulty for co-transcript studies has been the saturation of host RNA derived from the sample and the ability to recover sufficient usable pathogen RNA information to make the studies meaningful. The protocol has to be optimised for setting up the infection, for the infection conditions, cell collection, RNA isolation and quality testing – all in a single protocol that can be utilised consistent across the infection treatment, as well as the two control treatments. And this all has to be accomplished in an inherently antagonistic (phagocyte versus pathogen) context while preserving both sufficient bacterial numbers and minimising stress on the host cells.

A previous study found that centrifuging the infection prior to incubation could increase the association between the two cell types (Virok *et al.*, 2003). The current study found that the 45 minute centrifuge proposed by Virok increased the GBS recovery from intracellular bacteria, but caused significant stress to the monocytes – resulting in lower monocyte viability at the end of the infection period. Reducing the centrifuge to 5 minutes was found to preserve monocyte viability throughout the infection. It is notable that the MOI in this study ranged from 35 to 1308 and had to be iteratively optimised for consistency. Keeping the MOI under 200 was found to further contribute to monocyte stability.

It was unexpected to find that GBS 874391 survived the application of antibiotics since previous studies have found this mixture of Gentamicin and Pen/Strep to effectively clear GBS (Leclercq *et al.*, 2016) (Sullivan *et al.*, 2017b). Bacterial time-kill assays were performed demonstrating the efficiency of the ABX mix on the GBS. The time it took for the GBS numbers to stabilize in the ABX informed the optimal infection time to minimise stress on the challenges monocytes. GBS numbers (CFU) remaining in the ABX media was roughly $4\log_{10}$ lower than GBS recovered from the monocytes after six hours of infection (i.e. 0.01%) – and was therefore considered insufficient to influence the co-transcript data. Contrasting the healthy GBS colonies after five hours ABX to the stressed colonies

observed from only one hour of ABX incubation could be indicative of a repeatable, adaptive mutation (e.g. movement of a transposable unit) occurring in the GBS.

The *spb1* primers used to test RNA for bacterial DNA contamination successfully amplified the *spb1* gene for both GBS-only and infection samples. Despite several studies reporting the use of specific primers for the PCR amplification of *β-actin* (Castelruiz *et al.*, 1999, Sarobe *et al.*, 2002, Kethiri *et al.*, 2017, Bas *et al.*, 2004, Zhang *et al.*, 2012, Armakolas *et al.*, 2016), the two separate *β-actin* primer sets could not be optimised to reliably reveal eukaryotic DNA contamination. We are unable to explain the discordance between the non-specific binding in our PCR results using previously published *β-actin* primers. *GAPDH* is another eukaryotic housekeeping gene involved in a variety of cellular functions (Suzuki *et al.*, 2000, Tristan *et al.*, 2011). Ten *GAPDH* primer pairs were developed and tested. Two of these (*GAPDH* 4 and 7a) were considered viable. *GAPDH* 7a was determined to be the more sensitive of the two.

Studies have suggested that post infection centrifuges may have an impact the final transcripts (Chan *et al.*, 2007, Xue *et al.*, 2018). Since this study is focussing on blood infections, soluble (non-adherent) monocytes are the host cell. Therefore, post infection centrifuges are necessary to isolate the cells from the infection media. This potential influence must therefore be considered in the final transcript analysis.

A low nutrient media formulation was initially developed to provide a suitable pathogen control treatment, however, this media formulation limited the available GBS transcript – regardless of how many GBS contributed to the analysis. The concentration of FBS in the media had to be increased to allow sufficient, reliable transcription – yielding enough trustworthy RNA for the downstream applications.

Using the infection conditions optimised in this study an appropriate GBS-only control protocol was developed producing enough quality cDNA to be consistently amplified using RT-qPCR. All of the GBS genes used in this study demonstrated amplification by RT-qPCR. The subsequent study will assess

the viability of using this protocol to derive host and pathogen cDNA for a co-transcript analysis of GBS 874391-infected U937 monocytes.

CHAPTER 4: Co-transcriptional analysis of GBS-infected U937 monocytes using RT-qPCR

4.1 Introduction

According to the Central Dogma of Molecular Biology, proteins that form the fundamental units of organic life are encoded by information contained in nucleic acids (Crick, 1958, Crick, 1970). Watson's simplified, unidirectional version of this model proposed that the template of deoxyribonucleic acid (DNA) is first transcribed/copied into ribonucleic acid (RNA), before the information contained in the RNA is translated into proteins (Watson, 1965). Over time, refinements to our knowledge of molecular interactions have found Watson's version to be overly simplistic (Shapiro, 2009, Morange, 2008). Nevertheless, the fundamental premise that proteins are coded by an intermediate RNA molecule holds true for almost all protein coding genes (Koonin, 2012). RNA expression can therefore provide vital insights into cellular activity – revealing those factors which are important to the cell in a given context. This information can in-turn be used to refine the direction of subsequent research into therapeutic solutions.

Streptococcus agalactiae (Group B Streptococcus or GBS) is a bacterial species containing strains which are commonly pathogenic to humans; most significantly to the immunocompromised (neonates, the elderly, and others with pre-existing pathologies such as HIV and diabetes) (Dermer *et al.*, 2004, Eickhoff *et al.*, 1964, Farley, 2001). GBS is well known to harbour a vast variety of virulence factors including the capsule, proteinases, immune evasion mechanisms, cytotoxins, adhesins, nutrient acquisition and efflux regulators etc. (see Selected Virulence Factors, Chapter 1, for and overview of some of the better described virulence factors). The U937 cell line is a human cell culture line that has been regularly employed as a phagocyte research model due to its capacity to closely mimic the activities of human monocytes and macrophages (Lehmann, 1998, Anderson & Abraham, 1980, Sundstrom & Nilsson, 1976).

Many RNA studies focus on analysing the transcripts of either host or pathogen independently. For example, Mereghetti *et al.* (Mereghetti *et al.*, 2008) characterised the rapid response of the GBS (NEM316) transcript as the result of contact with whole human blood; notably finding that the GBS transcript adapts to human blood in a temperature dependant manner. Stitkiewicz and Musser (Sitkiewicz & Musser, 2009) investigated the transcript of GBS in a variety of growth medium conditions; elucidating that the GBS transriptome is highly adaptable to changing environments. Stitkiewicz *et al.* (Sitkiewicz *et al.*, 2009) further profiled the transcript response of GBS to human amniotic fluid; revealing significant changes to the expressions of multiple virulence factors. Bryan *et al.* (Bryan *et al.*, 2008) profiled multiple strains of GBS in varying concentrations of methionine; describing MtaR as having a global influence over GBS gene expression. Transcript studies provide valuable information to the research community, however it is also desirable to analyse the RNA transcripts of both host and pathogen from the same (i.e. infected) samples; i.e. co-transcript studies (Westermann *et al.*, 2012, Ravasi *et al.*, 2016, Avraham *et al.*, 2016). Such studies face challenges; including dealing with the problem of host RNA saturation in the infected sample.

In Chapter 3, an infection model was rigorously optimised to permit the RNA extraction from a hypervirulent ST17 strain of GBS bacteria (GBS 874391) in sufficient quantities and qualities to be amplified consistently in RT-qPCR - from an amount of bacterial cells expected to be retrieved from GBS-infected U937 monocytes. Here that model is expanded and utilised to examine the transcription profiles of both the infected monocytes and intracellular bacteria based on the analysis of differential gene expression for 12 human genes and 12 bacterial genes. A study previously analysed the co-transcript of *Streptococcus pneumoniae* and Human Pleural Mesothelial Cells (Heath *et al.*, 2015). To our knowledge, this is the first attempt to characterise a co-transcript of Group B Streptococcus with human monocytes.

4.1.1 Aims of this study

The primary aim of this study was to confirm the viability of the model optimised in Chapter 3 for use in Real-Time, Reverse-Transcriptase qPCR. It was especially important to ensure that bacterial RNA of sufficient quality and quantity could be generated from the *in vitro* infections in amounts that would amplify in RT-qPCR and enable robust differential gene expression analysis. In light of this goal, a secondary aim was to pre-emptively refine the optimised protocol to include a minimal impact, monocyte lysis step - providing the RNA isolation method with better access to the bacterial cells. A third aim was to compare the gene expression profile of GBS and monocytes in the infection model compared to the non-infection (separate) control conditions for twelve selected genes that relate to virulence and immune defence against bacterial infection.

4.2 Materials and Methods

4.2.1 Cell Collection, RNA preparations, DNA Contamination Testing and cDNA synthesis

Six of the GBS-only controls attained in Chapter 3 contributed to the analysis of this Chapter. Using the SV Total RNA Isolation Kit (Promega) for RNA extractions, the protocol developed in Chapter 3 was generally followed to the point of cDNA synthesis for four infection samples and six monocyte-only control samples. The following modifications were required to account for the larger cell pellets in the treatments containing monocytes. The bead-beating was added to provide the Mutanolysin access to the bacterial cells.

The initial RNA digest (in TE buffer with 30mg/ml lysozyme) was scaled up five-fold (from 100µl to 500µl). Pellet resuspensions were progressively performed 100µl at-a-time, each time moving 100µl the resuspension into a 2ml nuclease-free, cap-lock tube containing 50mg acid-washed glass beads (see section 4.2.1). Then, after a 10 second bead-beat (section 4.3.1), 50µl (500U) of Mutanolysin was added to the digest before the 90 minute incubation at 37^{o}C. After the incubation, the digest was moved to a 15ml tube and Lysis buffer added at 175µl for every 5E6 viable monocytes in the collected pellet. The Lysis mix was them passed through a 20 gauge needle ten times to shear genomic DNA. Twice the amount of Dilution buffer as Lysis buffer was added and mixed by inversion before dividing the mix into four 2ml RNase-free tubes for the 3 minute, 70^{o}C incubation. After centrifuging for 10 minutes at 13,000g in 4^{o}C, the supernatants were combined into a 15ml tube where 200µl of cold Ethanol was added for every 500µl of supernatant. The supernatant was then divided into ten spin columns before proceeding with the rest of the protocol according to Promega's instructions (and the CHAPTER 3 protocol, section 3.3.1).

Due to the large number of monocytes contributing to both infection samples and monocyte-only samples, they were assumed to have retained some DNA contamination. DNase treatments were

therefore routinely performed on these samples using the Turbo DNAfree kit from Ambion and following the manufacturer's instructions. The positive bacterial control was 8ng of genomic DNA from GBS 874391. The positive human control was 28ng of infection/Mixed genomic DNA.

The cDNA synthesis was performed on 5µg of RNA from each of the infection and monocyte-only samples using the SuperScript III Reverse Transcriptase kit in accordance with the manufacturer's instructions.

4.2.2 *Mycoplasma* Test of U937 Monocytes

If *Mycoplasma* are present in a cultured cell line, they may interact with the cells in a manner that undermines the reliability of any experimental outcomes. The absence of *Mycoplasma* from the cell line therefore needs to be confirmed for any study using cultured cell lines. Standard PCR was performed on post-passage supernatants from the U937 monocyte lineage used in this study (passage 17). The positive control was 2.3ng/µl of a *Mycoplasma fermentans* plasmid (pUC57 mini) provided by Dr Matthew Sullivan. The negative control was cRPMI.

TABLE 4.01: Primers used for Mycoplasma testing by standard PCR.

Organism	Primer Name	Primer 5' to 3'	Source
Mycoplasma (various species)	MCGp1_F1	ACACCATGGGAGCTGGTAAT	*Mycoplasma* Detection Kit (Takara)
	MCGp1_R1	CTTCATCGACTTTCAGACCCAAGGCAT	*Mycoplasma* Detection Kit (Takara)
	MycDeg1_F1	AMACCATGGGAGYTGGTAAT	Dr Matthew Sullivan
	MycDeg1_F2	CTTCWTCGVCTTYCAGACCCAAGGCAT	Dr Matthew Sullivan

Each 20µl reaction was comprised of the following; 4µl (1X) 5X HF Phusion Buffer (New England Biolabs), 0.4µl (200µM) 10mM dNTPs (Sigma), 1µl each (0.5µM) of both 10µM forward and reverse primers, 0.2µl (0.4 units) of Phusion DNA Polymerase (New England Biolabs), 1µl of template and the remaining 12.4µl of nuclease-free Ultrapure Distilled Water (Invitrogen).

PCR Program: 98°C for 30 seconds, then 35 cycles of [98°c for 10 seconds, 58°C for 30 seconds, 72°C for 30 seconds], followed by 10 minutes at 72°C, then 10°C until collected. Amplicons were resolved on a 2% gel over 50 minutes at 100V.

4.2.3 Testing cDNA Dilutions in RT-qPCR for Amplification of GBS and U937 Monocyte Gene Targets

To see how far the volume of cDNA could be stretched at the concentrations attained, three independent RT-qPCRs were performed using varying dilutions of the cDNA from the infection samples. The first RT-qPCR tested 1:10, 1:20:1:40 and 1:80 dilutions of infection cDNA on the bacterial housekeeping gene *dnaN*. The second RT-qPCR tested the same dilutions on the non-housekeeping gene *cylE*. The final RT-qPCR tested 1:10, 1:40, 1:160 and 1:320 dilutions of infection cDNA on the bacterial housekeeping gene *rpoB*.

To test the various dilutions, RT-qPCR was performed in 96-well, semi-skirted PCR plates (4titude) on a QuantStudio 6-Flex Real-Time PCR system. 20µl reactions were performed in triplicate for each condition (sample and dilution). Each 20µl reaction consisted of 10µl (1X) 2X SensiFAST SYBR No-Rox Mix (BIOLINE), 0.4µl (400nM) each of 20µM forward and reverse primers, 1µl of template, and the remaining made up with 8.2µl of nuclease-free Ultrapure Distilled Water. After sealing the plate, the plate was shaken for 15 seconds on a Platform Shaker (Ratek) and centrifuged at 800g for 2 minutes in 4°C. Amplification was performed using the 2-step cycling program - namely; 1 cycle at 95°C for 2 minutes, then 40 cycles alternating between 95°C for 5 seconds and 60°C for 30 seconds. Data analysis was performed using the QuantStudio Real-Time PCR Software (version 1.1).

4.2.4 RT-qPCR Gene Expression Analysis

Utilising 1:160 dilutions of all cDNA samples, six RT-qPCRs were performed to analyse the gene expression patterns of GBS 874391 using 12 bacterial genes (plus 2 housekeeping genes) and RT-qPCRs were performed to analyse the expression patterns of U937 monocytes using 12 human

genes (plus 2 housekeeping genes). The gene expression of four infection samples was compared that of four relevant control samples (GBS-only for the bacterial genes and monocyte-only for the human genes). The bacterial primers used in this study are the same as those used in Chapter 3 (see Appendix 2, TABLE AP2.03).

TABLE 4.02: Human primers used in this study.

Gene	Primer Name	Primers 5' to 3'	Function	Source
Beta-actin	027-ACTB_F	TCCTCCCTGGAGAAGAGCTA	Cytoskeleton (Houdekeeping)	Dando *etal* 2016. *Infection & Immunity* V84 No7 pp1941-1956
	028-ACTB_R	CGTGGATGCCACAGGACT		
Glyceraldehyde 3-phosphate dehydrogenase	029-GAPDH_F	AGCCACATCGCTCAGACAC	Energy synthesis (Housekeeping)	Dando *etal* 2016. *Infection & Immunity* V84 No7 pp1941-1956
	030-GAPDH_R	GCCCAATACGACCAAATCC		
Interleukin 1α	031-IL1A_F	CAAAAGGCGAAGAAGACTGAC	Pro-inflammatory cytokine	Dando *etal* 2016. *Infection & Immunity* V84 No7 pp1941-1956
	032-IL1A_R	GGAACTTTGGCCATCTTGAC		
Interleukin 1β	033-IL1B_F	AGCTGATGGCCCTAAACAGA	Pro-inflammatory cytokine	Dando *etal* 2016. *Infection & Immunity* V84 No7 pp1941-1956
	034-IL1B_R	TCGGAGATTCGTAGCTGGAT		
Interleukin 6	035-IL6_F	GGAGACTTGCCTGGTGAAAA	Pro-inflammatory cytokine	Stoner *etal* 2015. *PLoS ONE* V10 Iss6 e0128431
	036-IL6_R	CAGGGGTGGTTATTGCATCT		
Interleukin 8	037-IL8_F	AGCTCTGTGTGAAGGTGCAG	Pro-inflammatory chemokine	Stoner *etal* 2015. *PLoS ONE* V10 Iss6 e0128431
	038-IL8_R	AATTTCTGTGTTGGCGCAGT		
Interleukin 10	Human IL-10 Forward	GGAGAACCTGAAGACCCTCA	Anti-inflammatory cytokine	Forsberg *etal* 2002. *Gastroenterology* 123: pp667-678
	Human IL-10 Reverse	TGCTCTTGTTTTCACAGGGA		
Interleukin 12α	039-IL12A_F	CACTCCCAAAACCTGCTGAG	Pro-inflammatory cytokine	Dando *etal* 2016. *Infection & Immunity* V84 No7 pp1941-1956
	040-IL12A_R	TCTCTTCAGAAGTGCAAGGGTA		
Interleukin 12β	041-IL12B_F	AGATGGAATTTGGTCCACTGA	Pro-inflammatory cytokine	Dando *etal* 2016. *Infection & Immunity* V84 No7 pp1941-1956
	042-IL12B_R	GCAGGTGAAACGTCCAGAAT		
Interleukin 17α	043-IL17A_F	CCACCTCACCTTGGAATCTC	Pro-inflammatory cytokine	Dando *etal* 2016. *Infection & Immunity* V84 No7 pp1941-1956
	044-IL17A_R	GGTAGTCCACGTTCCCATCA		
Tumor necrosis factor	045-TNF	CGGTGCTTGTTCCTCAGC	Pro-inflammatory cytokine	Dando *etal* 2016. *Infection & Immunity* V84 No7 pp1941-1956
	046-TNF	GCCAGAGGGCTGATTAGAGA		
CXC chemokine ligand 1	047-CXCL1_F	TCCTGCATCCCCCATAGTTA	Pro-inflammatory chemokine	Dando *etal* 2016. *Infection & Immunity* V84 No7 pp1941-1956
	048-CXCL1_R	CTTCAGGAACAGCCACCAGT		
LIM domain only 2	049-LMO2_F	GATGGTAGACCTTTATTGGG	Erythroid differentiation (oncogene)	Virok *etal* 2003. *Infectious Diseases* V188 Issu9 pp 1310–1321
	050-LMO2_R	GCACATCTCTAGTTCGCA		
Monocyte chemoattractant protein 1	051-MCP-1_F	AACACTCACTCCACAACC	Leukocyte chemokine	Virok *etal* 2003. *Infectious Diseases* V188 Issu9 pp 1310–1321
	052-MCP-1_R	TCCCCAAGTCTCTGTATCTA		

For gene expression analysis, RT-qPCR was performed in 384-well, semi-skirted PCR plates (4titude) on a QuantStudio 6-Flex Real-Time PCR system. 10µl reactions were performed in quadruplicate for each condition (sample and gene). Each 10µl reaction consisted of 5µl (1X) 2X SensiFAST SYBR No-Rox Mix (BIOLINE), 0.2µl (400nM) each of 20µM forward and reverse primers, 1µl of template, and the remaining made up with 3.6µl of nuclease-free Ultrapure Distilled Water. After sealing the plate, the plate was shaken for 15 seconds on a Platform Shaker (Ratek) and centrifuged at 800g for 2 minutes in 4°C. Amplification was performed using the 2-step cycling program - namely; 1 cycle at 95°C for 2 minutes, then 40 cycles alternating between 95°C for 5 seconds and 60°C for 30 seconds.

Preliminary data analysis was performed using the QuantStudio Real-Time PCR Software (version 1.1). Non-amplifying outlier wells were excluded unless otherwise stated. Amplifying outlier wells were excluded on the basis of amplification separation from other like-replicates; confirmed by Grubb's Outlier statistical Test. Expression-fold change was calculated on the basis of comparing the replicate Ct means of four infection samples against four control samples (for 12 bacterial and 12 human genes). Preliminary expression analysis was performed on a Microsoft Excel spreadsheet template where the fold-change expression ratio was calculated on the basis of the following formula (which factors in any efficiency variations between the samples);

$$Ratio = \frac{(Target\ Gene\ Efficiency)^{\Delta Ct\ Target\ gene\ (Mean\ control\ Ct - Mean\ treatment\ Ct)}}{(Reference\ Gene\ Efficiency)^{\Delta Ct\ Reference\ gene\ (Mean\ control\ Ct - Mean\ treatment\ Ct)}}$$

(Pfaffl, 2001)

Ratios greater than 1 were considered to directly reflect a fold increase in gene expression. Ratios less than 1 were considered to reflect a fold decrease in gene expression (i.e. 0.5 indicated a two-fold decrease, 0.25 a three-fold decrease etc.). A column statistics t-test (against a hypothetical value of 1) was performed on the four fold-change values derived for each gene (Graphpad Prism version 7.02).

4.3 Results

4.3.1 Cell Collection, RNA preparations, DNA Contamination Testing and cDNA synthesis

Summary table of all sample data (infection and controls can be found in Appendix 3, TABLES D and E. RNA was extracted from 4 mixed (host/pathogen infection) samples (designated M266, M286, M296 and M306), 6 U937-only (host monocyte control) samples (designated U237A1, U237A2, U237A3, U247B1, U247B2 and U247B3), and 12 GBS-only (bacterial pathogen control) samples (designated G175A, G175B, G185A, G185B, G195A, G195B, G195C, G195D, G225A, G225B, G225C and G225D).

DNA contamination testing results for GBS-only controls can be found in Appendix 2 (FIGURES AP2.68 and AP2.69).

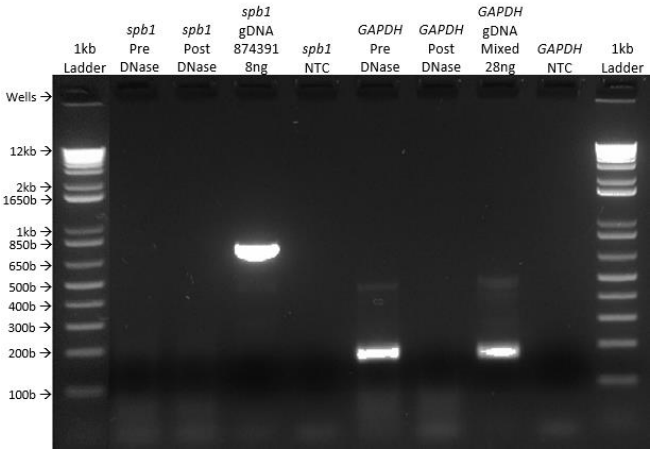

FIGURE 4.01: Agarose gel showing PCR results for a single Infection/Mixed RNA sample 266 (M266) tested for bacterial and human DNA contamination (spb1 and GAPDH respectively).
The expected amplicon size for the spb1 primer set is 762bp. The expected amplicon size for the GAPDH primer set is 171bp. GBS 874391 gDNA served as the positive control for spb1. gDNA isolated from an infection sample served as the positive control for GAPDH. Gel shows samples both before and after DNase treatments. The ladder used in both gels was the 1kb Plus DNA ladder (Invitrogen) with relevant sizes as indicated.

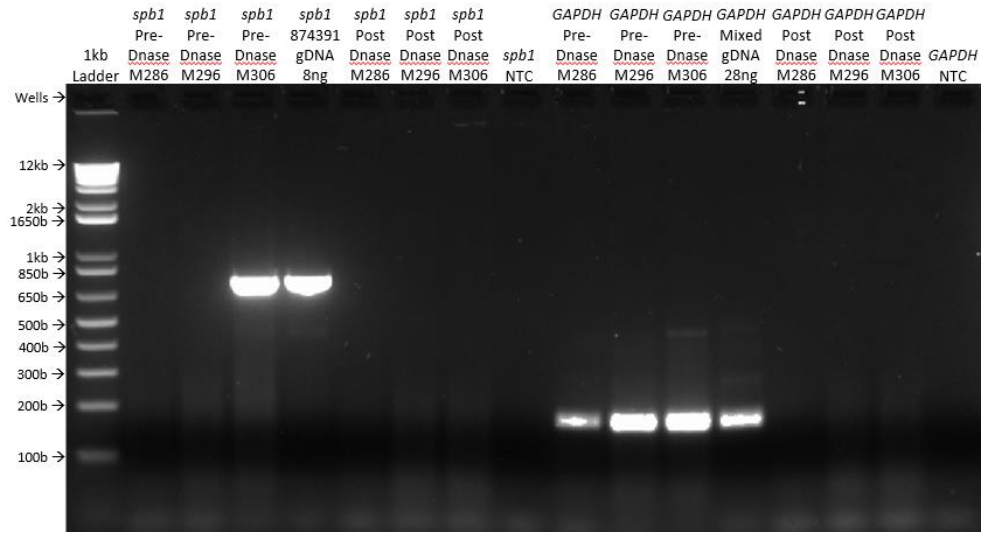

FIGURE 4.02: Agarose gel showing PCR results for 3 Infection/Mixed RNA samples (M286, M296 and M306) - tested for bacterial and human DNA contamination (spb1 and GAPDH respectively).
The expected amplicon size for the spb1 primer set is 762bp. The expected amplicon size for the GAPDH primer set is 171bp. GBS 874391 gDNA served as the positive control for spb1. gDNA isolated from an infection sample served as the positive control for GAPDH. Gel shows samples both before and after DNase treatments. The ladder used in both gels was the 1kb Plus DNA ladder (Invitrogen) with relevant sizes as indicated.

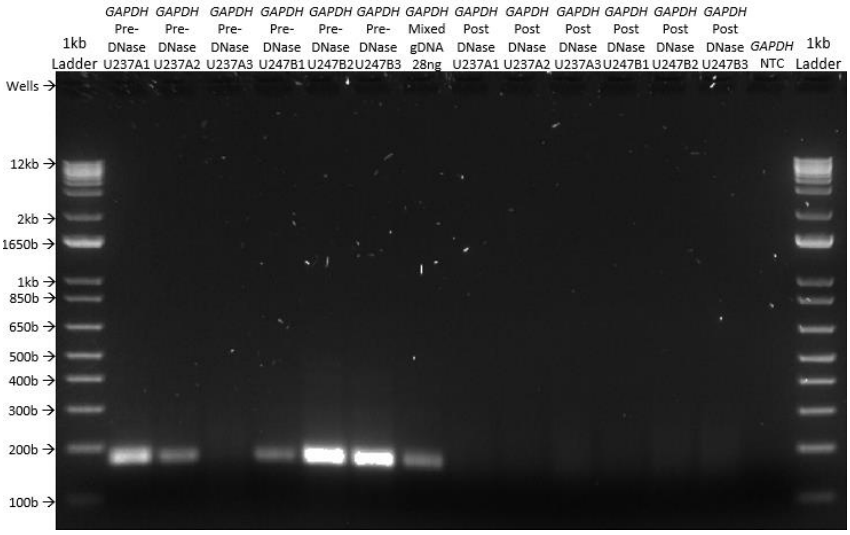

FIGURE 4.03: Agarose gel showing PCR results for 6 Monocyte/U937-only samples (U237A1, U237A2, U237A3, U247A1, U247A2 and U247A3) - tested for human DNA contamination (GAPDH).
The expected amplicon size for the GAPDH primer set is 171bp. gDNA isolated from an infection sample served as the positive control for GAPDH. Gel shows samples both before and after DNase treatments. The ladder used in both gels was the 1kb Plus DNA ladder (Invitrogen) with relevant sizes as indicated.

Human DNA contamination was detected in all but one sample (U237A3). Bacterial DNA contamination was only overtly detected in sample M306. All DNA contamination was resolved by the DNAse treatment.

4.3.2 *Mycoplasma* Test of U937 Monocytes

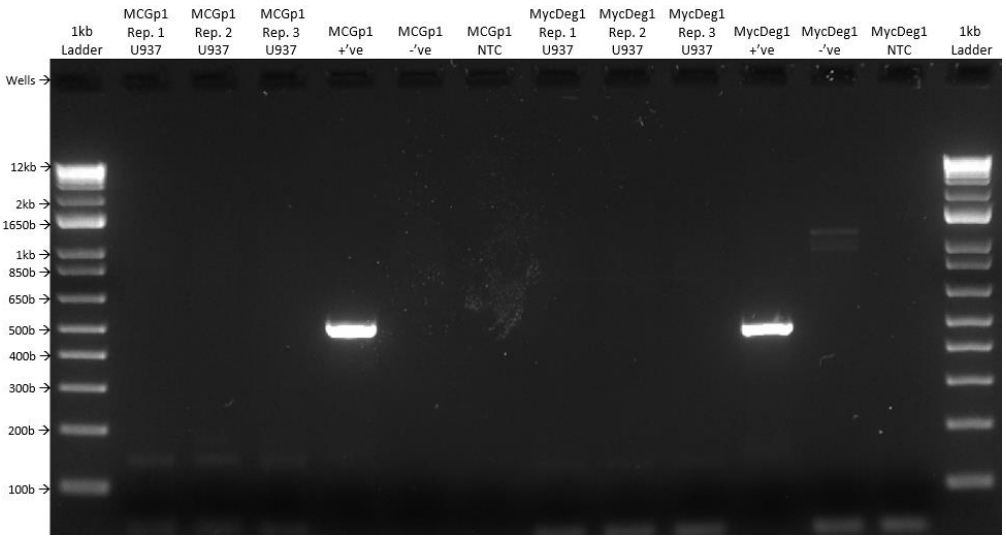

FIGURE 4.04: Agarose gel showing PCR results for Mycoplasma testing of the U937 monocytes used for the infection assays in this study.

Two primer sets (MCGp1 and MycDeg) used in PCR to detect any putative Mycoplasma in the supernatant of cultured U937 monocytes (3 technical replicates). Expected amplicon sizes vary depending on the species of Mycoplasma detected. A plasmid derived from Mycoplasma fermentans served as the positive control for both primer sets. The expected amplicon size for this species is 491bp. The ladder used in both gels was the 1kb Plus DNA ladder (Invitrogen) with relevant sizes as indicated.

Mycoplasma was only detected in the positive controls. No *Mycoplasma* contamination was detected in the monocytes contributing to this study.

4.3.3 Testing cDNA Dilutions in RT-qPCR

The Results Summary generated by Quantstudio Real-Time PCR Software for *dnaN* amplification in 4 infection samples can be found in Appendix 3, TABLE F. The Results Summary generated by Quantstudio Real-Time PCR Software for *cylE* amplification in 4 infection samples and 2 GBS-only controls can be found in Appendix 3, TABLE G.

TABLE 4.03: Amplification plots generated by Quantstudio Real-Time PCR Software for four dilutions of cDNA on dnaN for 4 mixed (Infection) samples.

Infection Sample	Amplification of cDNA dilutions of 1:10, 1:20, 1:40 and 1:80
M266	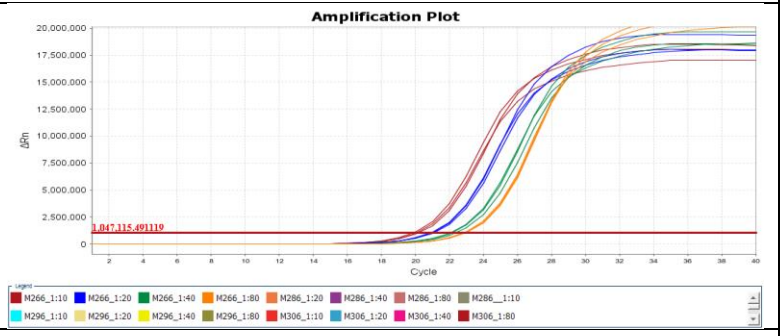
M286	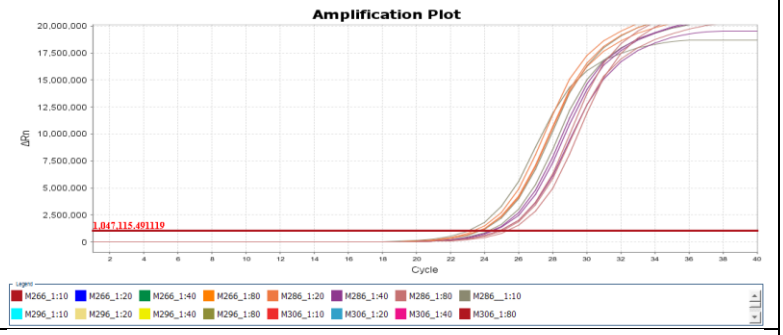
M296	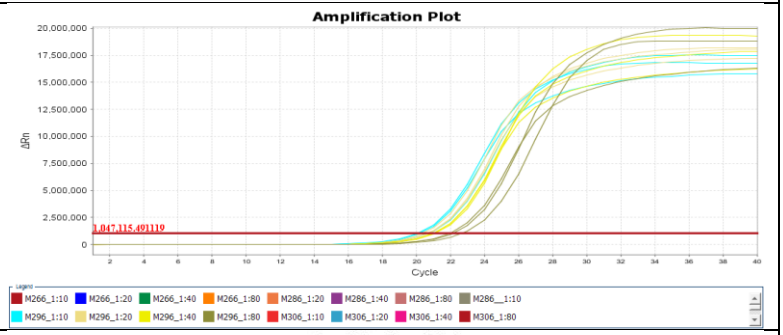
M306	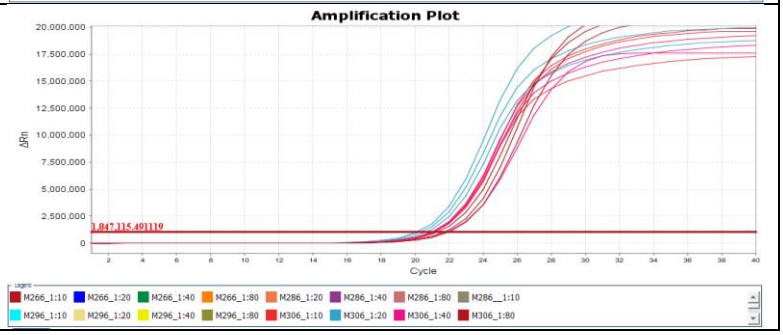

The highest mean Ct for three replicates of the 1:80 dilutions was 25.167 (sample M286). This is well under the detection limit of RT-qPCR. However, this is for a housekeeping gene (*dnaN*) which is putatively consistently expressed. The experiment was therefore repeated with the non-housekeeping gene *cylE* to ensure that detection is possible for genes expressed at lower levels (TABLE 4.04).

TABLE 4.04: Amplification plots generated by Quantstudio Real-Time PCR Software for four dilutions of cDNA on cylE for 4 Mixed (infection) samples and 2 GBS-only samples.

Sample	Amplification of cDNA dilutions of 1:10, 1:20, 1:40 and 1:80
M266 (Infection)	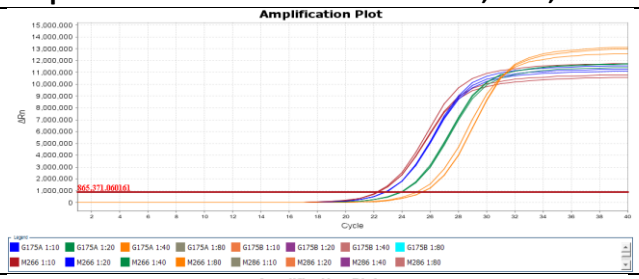
M286 (Infection)	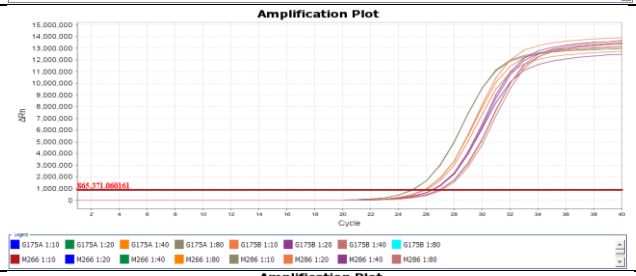
M296 (Infection)	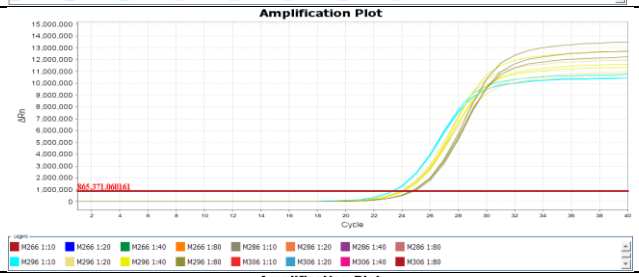
M306 (Infection)	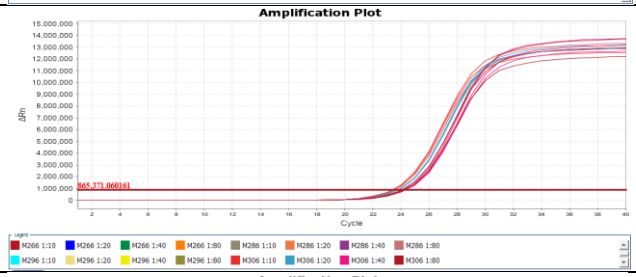
G175A (GBS-only control)	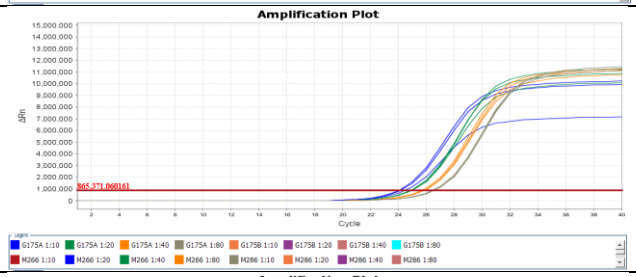
G175B (GBS-only control)	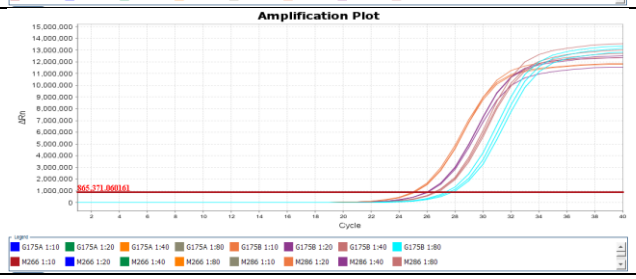

For the 1:80 cDNA dilutions, RT-qPCR amplification of *cylE* in the Mixed samples was detected at around 25 cycles, whereas the GBS-only samples amplified *cylE* at around 27 cycles – giving a preliminary indication of $2\log_2$ less *cylE* in the GBS-only samples. As robust amplification was detected in well-under 45 cycles, 1:160 and 1:320 cDNA dilutions were tested against the bacterial housekeeping gene *rpoB*.

The next analysis tested various dilutions (1:10, 1:40, 1:160 and 1:320) of cDNA derived from 4 mixed RNA samples (M266, M286, M296 and M306) and 2 GBS-only RNA samples (G175A and G175B) (TABLE 4.05) using primers for *cylE*.

TABLE 4.05: Amplification plots generated by Quantstudio Real-Time PCR Software for four dilutions of cDNA on cylE.

Four Mixed (infection) samples and two GBS-only samples.

Sample	Amplification of cDNA dilutions of 1:10, 1:40, 1:160 and 1:320
M266 (Infection)	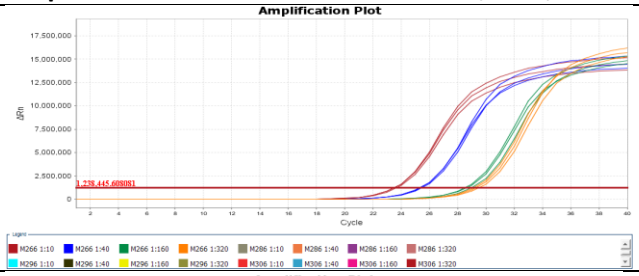
M286 (Infection)	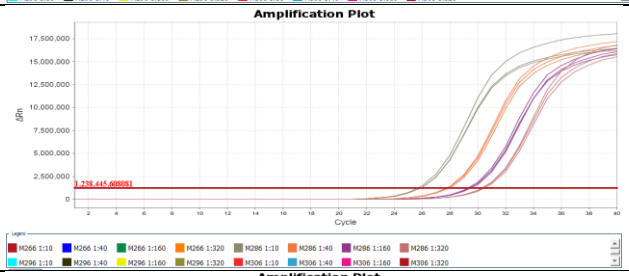
M296 (Infection)	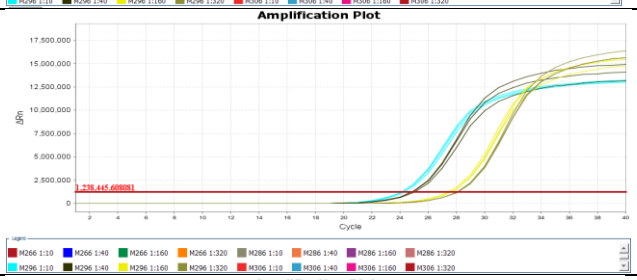
M306 (Infection)	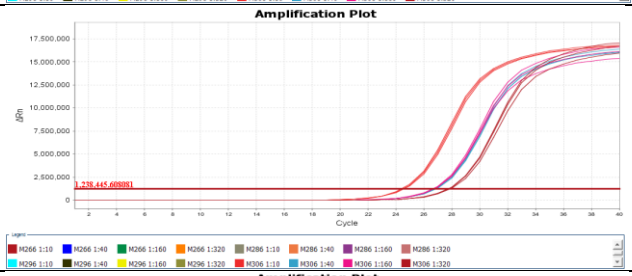
G175A (GBS-only control)	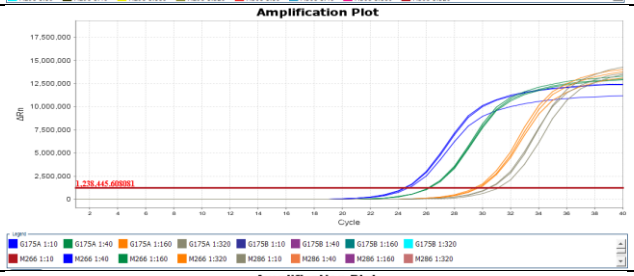
G175B (GBS-only control)	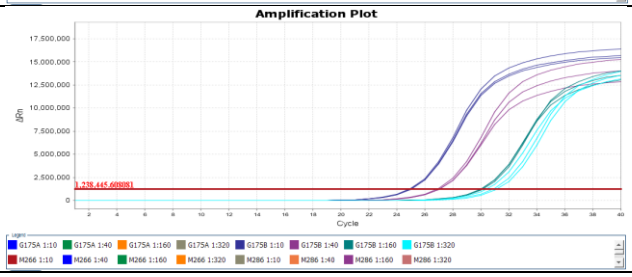

Even at 1:320 dilutions of cDNA, *ropB* was detected in under 31 RT-qPCR cycles for all samples. A decision was made to use 1:160 dilutions of cDNA instead of 1:320 in the subsequent gene expression study – to mitigate the possibility of excluding rarely expressed genes from detection and analysis.

4.3.4 RT-qPCR Gene Expression Analysis

4.3.4.1 Human Genes

The Results Summary generated by Quantstudio Real-Time PCR Software showing the amplification data for all human genes and all monocyte-derived samples can be found in Appendix 3, TABLE H.

For the human genes, over two independent attempts, 4 of the 12 genes tested (*IL1B*, *IL6*, *IL17A* and *CXCL1*) did not generate enough amplification data to contribute to the analysis. For *IL1A*, 4 of the 16 monocyte-only control wells failed to demonstrate amplification and for the purpose of analysis, were assumed to be amplifying after 45 cycles. Based on the differing absolute numbers, the reference genes appear to be amplifying inconsistently with each other (most starkly evidenced in *IL8*), though the overall expression pattern is reproduced for both reference genes.

TABLE 4.06: Statistical summary of gene expression change of infected U937 monocytes against the baseline control of uninfected U937 monocytes using the GAPDH housekeeping gene as the reference.

Reference Gene: *GAPDH*								
Gene	*IL8*	*IL1A*	*IL1B*	*TNF*	*LMO2*	*MCP-1*	*IL10*	*IL12A*
Number of values	4	4	4	4	4	4	4	4
Mean Fold-change	924.1	16.5	4.274	4.951	2.382	3.341	2.207	0.5974
Std. Error of Mean	92.11	3.942	0.4853	0.3985	0.3925	0.3765	0.2796	0.2112
t-test								
Significant?	Yes	Yes	Yes	Yes	Yes	Yes	Yes	No
Summary	**	*	**	**	*	**	*	ns
Adjusted P Value	0.0021	0.0295	0.0067	0.0022	0.0389	0.0084	0.0229	0.1527

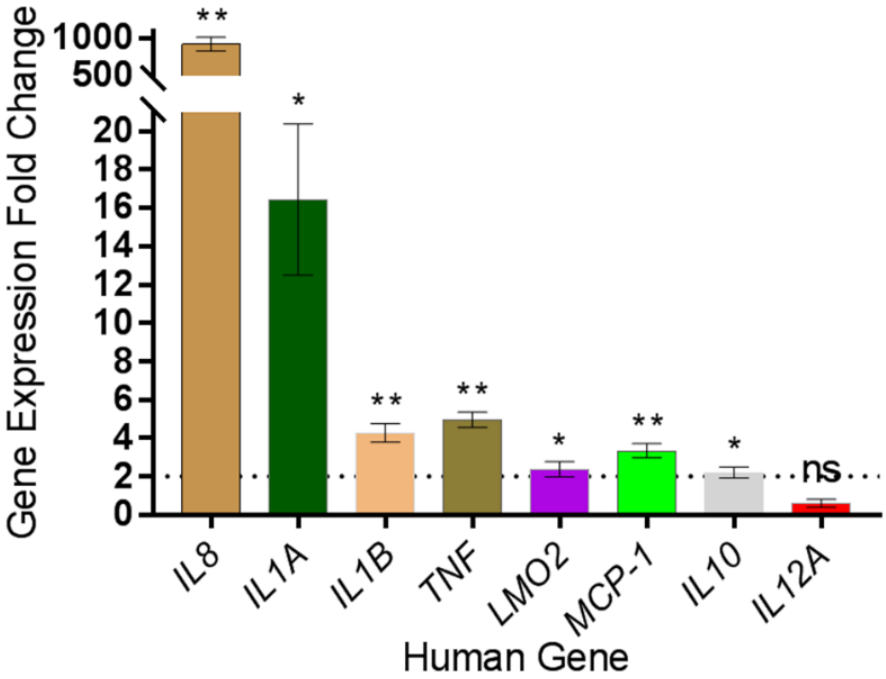

FIGURE 4.05: Fold gene expression change of the infected U937 monocytes against the baseline transcript control of uninfected U937 monocytes - with GAPDH as the reference gene.

Gene expression data generated by RT-qPCR using primers for 8 human genes on cDNA derived from infections – quantified against cDNA derived from the monocyte-only controls. Data based on 2 independent RT-qPCR runs per gene; 4 mixed and 4 control samples per RT-qPCR run; 4 technical replicates per sample. Human reference gene is GAPDH. Increases to gene expression over 2-fold were considered nominally significant (dotted line). Lines are SEM.

TABLE 4.07: Statistical summary of gene expression change of infected U937 monocytes against the baseline control of uninfected U937 monocytes using the ACTB housekeeping gene as the reference.

Reference Gene: *ACTB*								
Gene	*IL8*	*IL1A*	*IL1B*	*TNF*	*LMO2*	*MCP-1*	*IL10*	*IL12A*
Number of values	4	4	4	4	4	4	4	4
Mean Fold-change	4569	17.38	5.135	4.984	2.392	3.557	2.416	0.6916
Std. Error of Mean	314.6	4.442	0.7905	0.2045	0.3248	0.7247	0.2615	0.294
t-test								
Significant?	Yes	Yes	Yes	Yes	Yes	Yes	Yes	No
Summary	***	*	*	***	*	*	*	ns
P Value	0.0007	0.0346	0.0136	0.0003	0.0233	0.0387	0.0124	0.3713

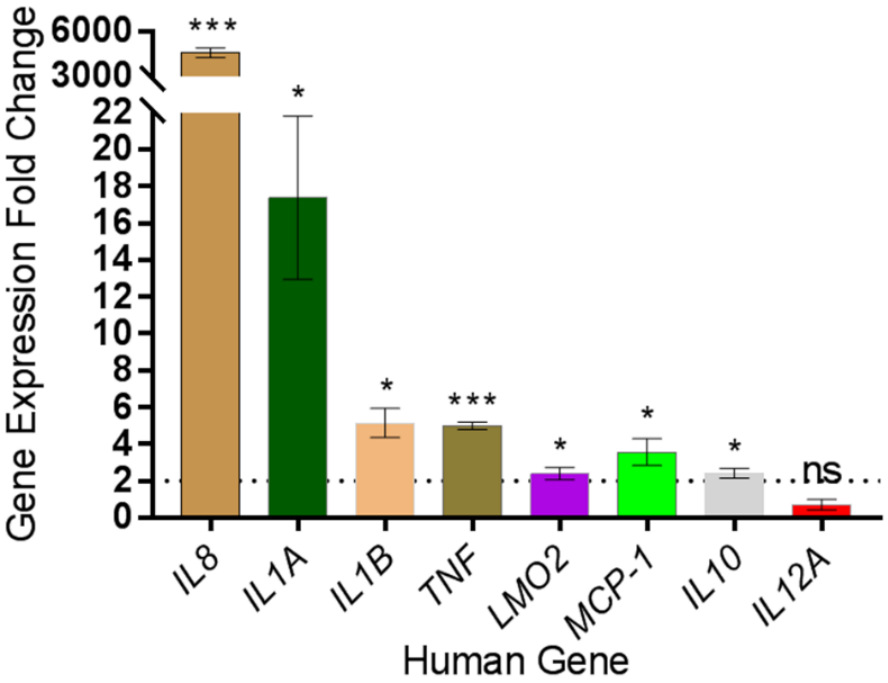

FIGURE 4.06: Fold gene expression change of the infected U937 monocytes against the baseline transcript control of uninfected U937 monocytes - with ACTB as the reference gene.
Gene expression data generated by RT-qPCR using primers for 8 human genes on cDNA derived from infections – quantified against cDNA derived from the monocyte-only controls. Data based on 2 independent RT-qPCR runs per gene; 4 mixed and 4 control samples per RT-qPCR run; 4 technical replicates per sample. Human reference gene is ACTB. Increases to gene expression over 2-fold were considered nominally significant (dotted line). Lines are SEM.

All reported increases in gene-fold expression were over two-fold, and statistically significant (α=0.05). *IL12A* demonstrated a two-fold decrease in expression against the *GAPDH* reference, but not against the *ACTB* reference, and neither was statistically significant (α=0.05). The increase in *IL8* expression in the infection samples is 2 to 3 orders of magnitude higher than reported for the other genes with increased expression.

4.3.4.2 Bacterial Genes

The Results Summary generated by Quantstudio Real-Time PCR Software showing the amplification data for all bacterial genes and all GBS-derived samples can be found in Appendix 3, TABLE I.

The differential expression patterns are generally repeated for both reference genes (FIGURES 4.09 and 4.10). Three of the 12 genes tested (*pil2B*, *cfb* and *copA*) did not demonstrate more than two-fold differential expression in the intracellular bacteria, when compared to the bacteria-only control samples. *CopA* approached a two-fold expression increase when using *rpoB* as the reference, but was not statistically significant for either reference (α=0.05). *MaeE* demonstrated a greater than two-fold, statistically significant increase in expression when using the *rpoB* as a reference, but differential expression was less than two-fold and not significant when using *dnaN* as the reference gene. *CpsE* reported a statistically significant, two-fold, decrease in expression using the *dnaN* reference gene, but not for the *rpoB* reference gene. In comparing the intracellular bacteria to the bacterial controls, *htp* revealed the most differential expression; followed by *czcD*, *scpB* and *hvgA* respectively.

TABLE 4.08: Statistical summary of gene expression change intracellular GBS 874391 against the baseline control of non-infection GBS 874391 using the rpoB gene as the reference.

Reference Gene: *rpoB*												
Gene	*rib*	*czcD*	*cylE*	*pil2B*	*cpsE*	*scpB*	*1010*	*htp*	*cfb*	*copA*	*hvgA*	*maeE*
Number of values	8	8	8	8	8	8	8	8	8	8	8	8
Mean Fold-change	3.505	7.272	2.509	1.779	0.8874	5.22	3.351	10.82	1.538	1.935	4.885	2.507
Std. Error of Mean	0.6491	1.231	0.4921	0.2248	0.09508	0.4223	0.2232	1.05	0.2008	0.4181	0.7306	0.4507
t-test												
Significant?	Yes	Yes	Yes	Yes	No	Yes	Yes	Yes	Yes	No	Yes	Yes
Summary	**	**	*	*	ns	****	****	****	*	ns	**	*
P Value	0.0062	0.0014	0.0181	0.0105	0.275	<0.0001	<0.0001	<0.0001	0.0315	0.0604	0.0011	0.0123

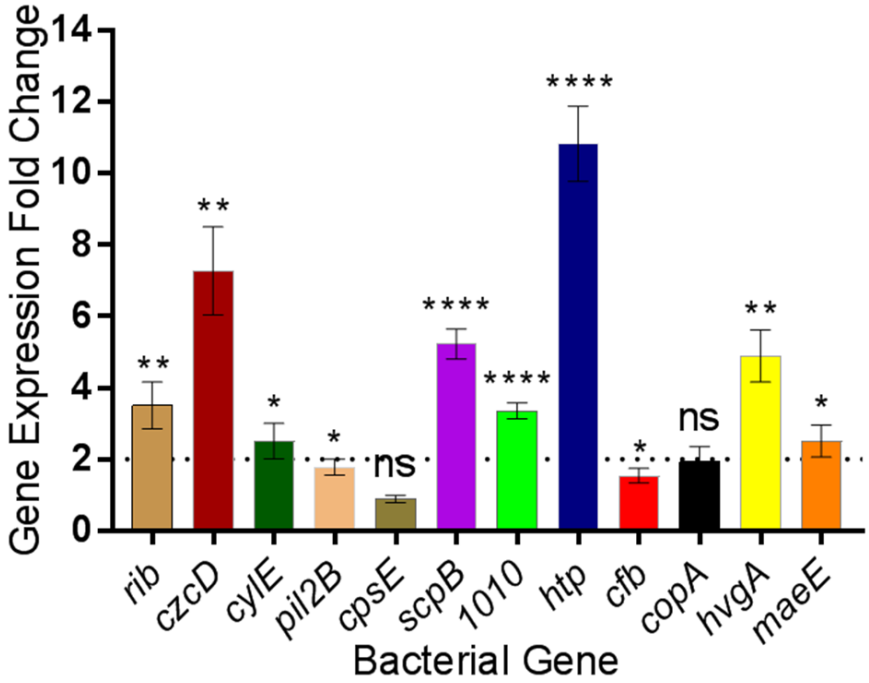

FIGURE 4.07: Fold change of bacterial genes in the GBS-infected U937 monocyte group compared to control GBS incubations without monocytes, using rpoB as the reference gene.

Gene expression data generated by RT-qPCR using primers for 12 GBS genes on cDNA derived from infections – quantified against cDNA derived from the GBS-only controls. Data based on 2 independent RT-qPCR runs per gene; 4 mixed and 4 control samples per RT-qPCR run; 4 technical replicates per sample. GBS reference gene was rpoB. Increases to gene expression over 2-fold were considered nominally significant (dotted line). Lines are SEM.

TABLE 4.09: Statistical summary of gene expression change intracellular GBS 874391 against the baseline control of non-infection GBS 874391 using the dnaN gene as the reference.

Reference Gene: *dnaN*												
Gene	*rib*	*czcD*	*cylE*	*pil2B*	*cpsE*	*scpB*	*1010*	*htp*	*cfb*	*copA*	*hvgA*	*maeE*
Number of values	8	8	8	8	8	8	8	8	8	8	8	8
Mean Fold-change	2.569	5.351	2.323	1.815	0.596	3.556	2.28	7.523	0.9639	1.252	3.057	1.585
Std. Error of Mean	0.4019	0.5753	0.8884	0.5432	0.05182	0.2894	0.1578	0.9443	0.1746	0.3425	0.5957	0.3625
t-test												
Significant?	Yes	Yes	No	No	Yes	Yes	Yes	Yes	No	No	Yes	No
Summary	**	****	ns	ns	****	****	****	***	ns	ns	*	ns
P Value	0.0059	0.0001	0.1802	0.1773	0.0001	<0.0001	<0.0001	0.0002	0.8419	0.4856	0.0106	0.1504

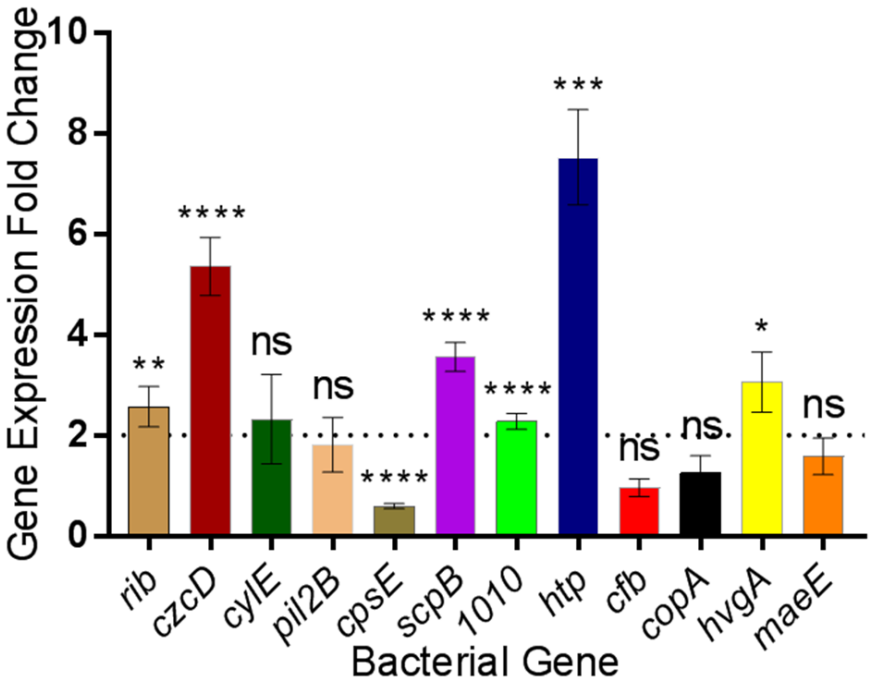

FIGURE 4.08: Fold change of bacterial genes in the GBS-infected U937 monocyte group compared to control GBS incubations without monocytes, using dnaN as the reference gene.

Gene expression data generated by RT-qPCR using primers for 12 GBS genes on cDNA derived from infections – quantified against cDNA derived from the GBS-only controls. Data based on 2 independent RT-qPCR runs per gene; 4 mixed and 4 control samples per RT-qPCR run; 4 technical replicates per sample. GBS reference gene was dnaN. Increases to gene expression over 2-fold were considered nominally significant (dotted line). Lines are SEM.

4.4 Discussion

In Chapter 3, an infection model was optimised to deliver an appropriate bacterial control condition yielding quality RNA at sufficient yields to be used in RT-qPCR. In this chapter, the protocol underwent minor refinements to ensure the bacterial RNA could be isolated from intracellular bacteria. Gene expression analysis by RT-qPCR was subsequently, successfully performed on 12 human genes and 12 bacterial genes. 7 of the 12 tested human genes were upregulated in the infected monocytes by more than two-fold (*IL8*, *IL1A*, *IL1B*, *IL10*, *TNF*, *LMO2* and *MCP-1*). The remaining 4 human genes (*IL6*, *IL12B*, *IL17*, *CXCL1*) did not produce enough amplification data to contribute to the analysis. Since this result was repeated over independent RT-qPCRs, it is likely that these genes were simply being expressed at very low levels. 7 of the 12 bacterial genes tested were found to be upregulated in GBS by more than two-fold. Of those 7, *cylE* was only statistically significant against the *rpoB* reference (p=0.0181), but not against the *dnaN* reference (p=0.1802). The *maeE* gene was both upregulated more than two-fold and significant against the *rpoB* reference gene (p=0.0123), but upregulated less than two-fold and not significant for the *dnaN* reference (p=0.1504). All bacterial genes tested produced enough amplification data to contribute to the analysis. None of the genes tested for either humans or bacteria were downregulated more than two-fold.

Gene expression data was calculated independently against two reference genes for each condition to increase the robustness of the results. There were differences in the gene-expression data between fold-change calculated using the reference gene *GAPDH* and fold-change calculated using the reference gene *ACTB*. This distinction was observed across independent RT-qPCR runs – indicating that these constituent genes are expressed at different levels. As demonstrated with *IL8*, the differences between these two housekeeping genes was amplified with the magnitude of expression change. Nevertheless, the overall patterns of differential expression were repeated for both reference genes.

In this study, interleukin 8 (*IL8*) was by far the most upregulated gene in the infected monocytes; reporting between 924-fold and 4570-fold upregulation (against references *GAPDH* and *ACTB* respectively). IL8 belongs to the CXC family of chemokines, and is primarily recognised for its role in the recruitment of neutrophils (Harada *et al.*, 1994). The C-X-C motif appears to be almost-exclusively specific to neutrophils (Kunkel *et al.*, 1995, Baggiolini *et al.*, 1994). IL8 was originally called monocyte-derived neutrophil chemotactic factor (MDNCF) in recognition of its abundant monocytic source and distinction from the previously characterised IL1 and TNF (Yoshimura *et al.*, 1987). Matsushima *et al.* (Matsushima *et al.*, 1988) showed that IL8 is induced by IL1 and TNF. Given the primary role of IL8 to chemoattract neutrophils to sites if infection, and given that in this study, both IL1 genes as well as TNF were upregulated, it is unsurprising that IL8 was so highly upregulated in U937 monocytes as a response to extended contact with GBS 874391 bacteria.

Interleukin 1 alpha (*IL1A*) was upregulated in the infected monocytes around 17-fold. IL1A is a pro-inflammatory cytokine from the interleukin 1 family containing 11 cytokines and 10 receptors (Di Paolo & Shayakhmetov, 2016, Dinarello, 2018). Isolated in 1974 from monocytes and neutrophils (Dinarello *et al.*, 1974), IL1A has since been found to be expressed in a wide variety of hematopoietic and non-hematopoieteic cell types (Bersudsky *et al.*, 2014, Cohen *et al.*, 2010). Both *IL1A* and Interleukin 1 beta (*IL1B*) are synthesised into large structures (precursors or pro-forms) before being cleaved into mature forms (Giri *et al.*, 1985). Unlike IL1B, which is only functional in its mature form, both the precursor and mature forms of IL1A are biologically active (Kim *et al.*, 2013). In most cell types, the IL1A remains constituently in the larger, pro-form state, and is therefore rarely secreted from the cells, however monocytes and macrophages only synthesise IL1A in response to stimuli (Cohen *et al.*, 2010). While isolating IL1A and IL1B, Dinarello *et al.* (Dinarello *et al.*, 1974) found that monocytes released nearly 20 times more interleukin 1 pyrogens than neutrophils when stimulated by heat-inactivated staphylococcal bacteria. Ulett *et al.* (Ulett *et al.*, 2010) reported GBS inducing *IL1A* in bladder epithelial cells. The current study adds support to the claim that IL1A is induced by

GBS; reporting a 16 to 18-fold upregulation of *IL1A* expression in U937 monocytes after a five hour incubation with internalised GBS 874391.

Interleukin 1 beta (IL1B) was also significantly upregulated in the infected monocytes, though *IL1A* was upregulated more than 3-fold more than *IL1B*; reporting 4.274 and 5.135-fold upregulation for *IL1B* (against references *GAPDH* and *ACTB* respectively). IL1B is more specifically associated with monocytes than IL1A (Hsi & Remick, 1995). The majority of IL1 secreted in humans is the beta form (Demczuk *et al.*, 1987, Lonnemann *et al.*, 1989). Unlike IL1A, the precursor molecular of IL1B does not to bind to IL1 receptors (Mosley *et al.*, 1987); though Jobling *et al.* (Jobling *et al.*, 1988) noted some biological activity for the IL1B precursor at high concentrations. In terms of pro-inflammatory activity, the Tumour Necrosis Factor (TNF) cytokine is considered largely indistinct from IL1 (Oppenheim *et al.*, 1989). The GBS cytotoxin β-hemolysin has been reported to induce TNF in the THP-1 cell line (Sagar *et al.*, 2013). In the current study, TNF was upregulated around 5-fold, roughly the same levels as IL1B.

Interleukin 10 (IL10) has been previously reported to be induced by GBS in mouse models (Cusumano *et al.*, 1996). IL10 is an anti-inflammatory, immuno-regulating, Type II cytokine (Pestka *et al.*, 2004, Commins *et al.*, 2008). IL10 was initially characterised as cytokine synthesis inhibitory factor (CSIF) for its observed capacity to mitigate the activity of several cytokines (Fiorentino *et al.*, 1989). Leukocytes appear to the major source if IL10 synthesis (Wolk *et al.*, 2002). The predominant function of IL10 is to mitigate the pro-inflammatory response by cells which can, in excess, cause tissue damage (Mege *et al.*, 2006, de Vries, 1995). IL10 has also been reported to ameliorate synthesis of IL1, IL8 and TNF (Fiorentino *et al.*, 1991, de Waal Malefyt *et al.*, 1991, Nicod *et al.*, 1995). Diminished IL10 has been associated with inflammatory diseases such as asthma (Lim *et al.*, 1998). In the current study *IL10* was upregulated just over two-fold. This may have been a response to increasing IL1, IL8 and TNF levels. Conversely, pathogens have been reported to exploit IL10 to mitigate the host defence response (Duell *et al.*, 2012, Sing *et al.*, 2002, Ghalib *et al.*, 1993).

LIM Domain Only Protein 2 (*LMO2*) is an oncogene that codes for the cysteine-rich, two LIM domain, rhombotin-like proteins that have been found to be a vital component of erythroid differentiation (Warren *et al.*, 1994, Bach, 2000). Aberrant expression of *LMO2* has been linked to leukaemia (Van Vlierberghe *et al.*, 2006, McCormack *et al.*, 2010); having been originally cloned from lymphoblastic leukaemia patient sample (Royer-Pokora *et al.*, 1991, Boehm *et al.*, 1991). In the current study, LMO2 was upregulated in infected monocytes a little over 2-fold. Monocyte Chemoattractant Protein-1 (*MCP-1*), also known as C-C Motif Ligand Chemokine 2 (CCL2) was upregulated in infected monocytes more than 3-fold. MCP-1 recruits monocytes, T lymphocytes and dendritic cells to sites of inflammation (Sozzani *et al.*, 1991, Carr *et al.*, 1994, Xu *et al.*, 1996). Given the antagonistic nature of infection, it is unsurprising that the infected monocytes would upregulate *MCP-1* in an attempt to recruit more leukocytes to the site of infection.

The increased expression of pro-inflammatory cytokines in this study from the host cells, in response to GBS infection, is consistent with the literature; with the exception of IL6 – which was not expressed at detectable levels in our study in either uninfected or infected monocytes). *In vitro*, peripheral blood mononuclear cells have demonstrated a rapid pro-inflammatory response to contact with GBS; including the increased generation of IL1, IL6, IL8 and TNF (Berner *et al.*, 2002, Williams *et al.*, 1993, Levy *et al.*, 2003). Aksu and Yanilmaz (Burak Aksu 2019) found a significant increase in IL8 production in Human cervical epithelial cancer cells (HeLa) when treated with heat-killed GBS (encapsulated COH1 and unencapsulated COH1-13 hypervirulent ST-17 strains); further finding that the GBS capsule itself did not significantly contribute to the IL-8 response in the host. This is consistent with an earlier study using *cylE* mutants of the above-mentioned strains (COH1 and COH1-13) to demonstrate that the GBS β-hemolysin/cytoysin (β-h/c) plays a more significant role in inducing an IL8 response in the A549 Lung epithelial cell line, than the GBS capsule (Doran *et al.*, 2002). Sagar *et al.* (Sagar *et al.*, 2013) used *cylE* mutations of GBS (strain BSU-6) to infect THP-1 macrophage-like cells, reporting that *TNF* is also highly upregulated in response to β-h/c; along with *IL8*. Stoner *et al.* (Stoner *et al.*, 2015) found that human foetal astrocyte cells (SVG-A) significantly

upregulated the expression of *IL1*, *IL6* and *IL8* in response to GBS COH1 infection; hypothesising that neutrophil recruitment (especially by IL8) and the release of other cytokines might compromise the integrity of the blood-brain-barrier - promoting the progression of GBS meningitis.

Mikamo *et al.* (Mikamo *et al.*, 2004) found that serotypes III strains of GBS (prevalent in disease in the US) induces a stronger TNF and IL10 response in A549 cells, than serotype VIII strains (commonly isolated from pregnant women in Japan); though the serotype VIII strains demonstrated a greater capacity for invasion. As an immunosuppressive cytokine, IL10 has been implicated as a regulator of the host inflammatory response (Moore *et al.*, 2001). IL10-deficient mice pups have demonstrated an increased survival capacity against GBS infection due to the uninhibited recruitment of neutrophils to the sites of infection (Madureira *et al.*, 2011). Madureira *et al.* (Madureira *et al.*, 2007) had previously found that GBS uses a bacterial GAPDH to stimulate IL10 production in the host, to subvert the host inflammatory response.

Of the bacterial genes tested in this study, Histidine Triad Protein (*htp*) was the most substantially upregulated from the infections; 10.82 and 7.523-fold against *rpoB* and *dnaN* references respectively. Sometimes referred to as Pneumococcal histidine triad (Pht), Htp is a cell surface-exposed protein, found in at least three species of human pathogenic streptococci, belonging to a family of proteins characterised by histidine triad motifs, and whose activities are still being explored (Adamou *et al.*, 2001, Shao *et al.*, 2013). The htp protein has been associated with zinc binding and complement opsonisation evasion in pneumococcus and GBS (Riboldi-Tunnicliffe *et al.*, 2005, Loisel *et al.*, 2011, Maruvada *et al.*, 2009, Ogunniyi *et al.*, 2009). The Cobalt-zinc-cadmium resistance protein (czcD) was also highly upregulated in the infected samples; 7.272 and 5.351-fold against *rpoB* and *dnaN* references respectively. In the CzcD-SczA system (which is highly conserved in streptococcal species), SczA regulates *czcD* expression, to either repress or induce *czcD* by binding to differing sites on the *czcD* promoter; dependant on the presence of absence of environmental zinc ions (Kloosterman *et al.*, 2007). Ong *et al.* (Ong *et al.*, 2014a, Ong *et al.*, 2015) has demonstrated that

deleting *czcD* in streptococcal pathogens reduces virulence and increases susceptibility to leukocyte destruction. Martin *et al.* (Martin *et al.*, 2017) showed that deleting either *czcD* or *sczA* inhibits the growth of *S. pneumoniae* in the presence of high concentrations of zinc. Since czcD is characterised as a zinc exporter (Ong *et al.*, 2014b, Anton *et al.*, 1999), the upregulation of both *czcD* with *htp* indicates the importance of zinc regulation to GBS survival in the context of infection. The CHF17_01108 iron ABC transporter permease (labelled *1010*) is another membrane transport protein that was upregulated between 2 and 4-fold; 2.28 and 3.351-fold against *dnaN* and *rpoB* respectively.

The cell surface, hypervirulent GBS adhesin (*HvgA*), which is a GBS ST17-specific virulence factor considered critical to GBS adhesion (Tazi *et al.*, 2010) was also upregulated in the infection between 3 and 5-fold. Teatero *et al.* (Teatero *et al.*, 2014) recently described an *hvgA*-carrying strain of GBS that did not belong to the CC17 clonal complex characteristic of ST17 strains – highlighting the importance of horizontal gene transfer in pathogenesis. The Rib protein (resistance to proteases, immunity, group B) is a large cell surface-anchored protein consisting of 12 identical tandem repeats (each 79 residues in length) – and is found predominantly in invasive serotype III strains of GBS (Stalhammar-Carlemalm *et al.*, 1993, Wastfelt *et al.*, 1996). Rib confers GBS with protease resistance (Stalhammar-Carlemalm *et al.*, 1993). In the current study, *rib* was upregulated in the infection bacteria 2.569 and 3.505-fold against *dnaN* and *rpoB* respectively.

Streptococcal C5a-Peptidase, Group B (*scpB*) was the third-most differentially regulated bacterial gene in the current study; with a 3.556 and 5.22-fold increase against *dnaN* and *rpoB* respectively. This protease cleaves the C5a compliment component involved in the chemotactic recruitment of neutrophils (Bohnsack *et al.*, 1991, Hill *et al.*, 1988). Studies have also demonstrated scpB to play an important role in adhesion and invasion of host cells (Hull *et al.*, 2008, Cheng *et al.*, 2002, Tamura *et al.*, 2006).

The current study confirmed that RNA samples derived from the dual-transcript model optimised in Chapter 3 could be used in downstream, RT-qPCR. In particular, we were able to successfully overcome the challenge, common to co-transcript studies, of generating sufficient quantity and quality bacterial RNA from the infection samples. All bacterial genes tested in this study yielded enough consistent amplification data, over independent RT-qPCRs, to contribute to expression analysis. Conversely, only 8 of the human genes tested yielded enough consistent amplification data to contribute to gene expression analysis. Since these results were confirmed over multiple RT-qPCRs, it is likely that these genes are transcribed at very low levels. As a neutrophil recruitment chemokine, *IL8* was predictably the highest differentially expressed human gene in the infected monocytes. Interestingly, *IL1A*, which has been previously described as being induced by GBS in human cells (Ulett *et al.*, 2010), was also significantly upregulated. The two highest differentially regulated bacterial gene in the infected samples were *htp* and *czcD* which have both been associated with zinc regulation. Genes for iron transport (*1010*), proteases (*scpB* and *rib*), and an adhesion gene (*hvgA*) were also upregulated in the infection samples more than 2-fold. In the future, infection samples could be tested with RNAseq technology to characterise the co-transcriptome of the optimised infection model. Our lab has also developed a probe for staining GBS 874391 which could be used to examine the dynamics of intracellular bacteria through microscopy (Sullivan & Ulett, 2018). Gene knockout assays could also be performed for those bacterial genes which were upregulated in the infections to assess their influence on GBS intracellular survival.

CHAPTER 5: The role of GBS *Htp* in intracellular survival in monocytes

5.1 Introduction

Histidine Triad Proteins (Htp) are a family of cell surface expressed proteins which are commonly found in pathogenic species of streptococcal bacteria (Ogunniyi *et al.*, 2009, Maruvada *et al.*, 2009, Kunitomo *et al.*, 2008). Although their sequence identity is variable across species, this family of proteins is named for sharing characteristic, repeated histidine triad (i.e. His-x-x-His-x-His) motifs (Adamou *et al.*, 2001). Htp were originally found in *Streptococcus pneumoniae* and named Pneumococcal Histidine Triads (Pht) (Adamou *et al.*, 2001). They have been alternatively labelled Streptococcal Histidine Triad proteins (Sht) (Moulin *et al.*, 2019), Pneumococcal Histidine Proteins (Php) (Zhang *et al.*, 2001) and Pneumococcal BVH Proteins (Hamel *et al.*, 2004). For simplicity, Htp or *htp* will be used henceforth.

Htp genes were previously thought to be restricted to *Streptococcus* (Rioux *et al.*, 2011). Testing this hypothesis using a Blastp search on more than 1800 bacterial genomes, Shao *et al.* (Shao *et al.*, 2013) were surprised to find *htp* genes in 9 species of non-streptococcal bacteria; 7 in the class Bacilli (shared with *Streptococcus*), and 2 in the class Clostridia. Shao *et al.* (Shao *et al.*, 2013) investigated 38 streptococcal genomes and found 25 containing *htp* genes. *S. pneumoniae* contained 4 *htp* copies (plus 1 *htp* pseudogene). Another 5 streptococcal species carried 3 *htp* copies (including GBS). The *htp* gene was further delineated into two subfamilies, *htp* I and *htp* II, based on their sequence locations (Shao *et al.*, 2013); both of these being present in strains of GBS.

The functional activity of Htp is not well understood, though it has been implicated in several behaviours related to virulence (Plumptre *et al.*, 2012). Proteins that fuse with leucine-rich-repeat (LRR) domains, such as Htp (Shao *et al.*, 2013, Reid *et al.*, 2003, Waldemarsson *et al.*, 2006) have been shown to bind to human Type I Collagen (Bober *et al.*, 2011); making chimeric Htp/LRR a

potential adhesion. Htp proteins are also suggested to play a role in host complement evasion through recruitment of complement factor H; thereby mitigating C3b deposition on bacterial cells (Maruvada *et al.*, 2009, Ogunniyi *et al.*, 2009). Moulin *et al.* (Moulin *et al.*, 2019) also found that Htp in GBS has a binding affinity to complement factor H, but the results of a human blood assay challenged the conclusion that this affinity between Htp and complement factor H significantly inhibits complement-mediated clearing.

Htp have an established affinity to the zinc cation (Zn^{2+}). Having previously characterised the structure of Pneumococcal Htp using x-ray diffraction, Riboldi-Tunnecliffe *et al.* (Riboldi-Tunnicliffe *et al.*, 2004, Riboldi-Tunnicliffe *et al.*, 2005) later revealed a zinc-binding ion region in some of the histidine triad repeats. This affinity of Htp to zinc was independently confirmed using metal-binding assays (Kunitomo *et al.*, 2008) and Induced Coupled Plasma – Mass Spectrography and Isothermal Titration Calorimetry (Loisel *et al.*, 2011). Using Nuclear Magnetic Resonance (NMR) Spectroscopy Bersch *et al.* (Bersch *et al.*, 2013) reported Htp proteins passing Zn^{2+} to transcription regulator (AdcR) proteins; namely AdcAII – a zinc-specific, homologue of the ATP Binding Cassette (ABC) transport system which is often encoded in the promoter region of *htp* (Panina *et al.*, 2003, Loisel *et al.*, 2008). Several studies have found that deleting the ABC zinc transporters associated with *htp* limit bacterial virulence and growth in various streptococcal species (Loo *et al.*, 2003, Bayle *et al.*, 2011, Tedde *et al.*, 2016).

In Streptococcal species, *htp* is also commonly found in the same operon, and downstream of the laminin binding protein (*lmb*) region; coding a cell-surface expressed adhesin (Zhang *et al.*, 2014). Laminin is one of several extracellular matrix (ECM) proteins found in host tissues utilised by microbial pathogens; mediating adherence to, and invasion of, host cells (Singh *et al.*, 2012). The Lmb protein was originally reported in *S. agalactiae* where it was found to bind to human laminin (Spellerberg *et al.*, 1999b). A BLASTn search revealed that the *lmb-htp* operon is found 98.6% of 187 searched human GBS isolates and 26.7% of 84 searched animal GBS isolates (Moulin *et al.*, 2016).

Moulin *et al.* (Moulin *et al.*, 2019, Moulin *et al.*, 2016) recently reported that GBS Htp proteins work in conjunction with Lmb proteins (and an ABC transporter) for the efficient acquisition of zinc ions from zinc-poor environments.

Using an intranasal infection model, Ogunniyi *et al.* reported that a single deletion Htp mutant significantly attenuates pneumococcal infection (Ogunniyi *et al.*, 2009). Rioux *et al.* reported impaired growth in Htp mutants in the absence of zinc supplementation (Rioux *et al.*, 2011). Htp have also been investigated as potential vaccine targets. Introducing Htp to mice has been shown to elicit humoral protection against *Streptococcus pneumoniae* and *Streptococcus suis* (Zhang *et al.*, 2001, Hamel *et al.*, 2004, Shao *et al.*, 2011). An Htp-based vaccine has been reported to confer protection to rhesus monkeys against pneumococcal disease – indicating a potential application of Htp vaccines for streptococcal protection in humans (Denoel *et al.*, 2011).

5.1.1 Aims of this study

RT-qPCR previously revealed that *htp* is highly upregulated in the GBS 874391 pathogen after being internalised in U937 monocytic host cells for at least 5 hours (CHAPTER 4). Since *htp* was the most highly upregulated GBS gene from the co-transcript study, and since the function of *htp* in GBS is yet to be well-characterised, *htp* was selected for further investigation as a potential gene of interest in GBS virulence. An *htp* knockout mutant of GBS 874391 was therefore constructed (FIGURE 5.01), and infection assays performed with both wild-type and mutant to determine if the upregulation of *htp* is reflected in differential survival of the internalised pathogen.

5.2 Materials and Methods

5.2.1 General Procedures

5.2.1.1 THY/Spec100 selective growth media

THY media was prepared in accordance with General Procedures 2.2.1.2. Shortly prior to use, a 50ml tube containing 10ml of THY media was supplemented with 10µl of 100mg/ml spectinomycin (to a final spectinomycin concentration of 100µg/ml).

5.2.1.2 THY/Spec100 selective growth agar gel plates

THY media was prepared in accordance with General Procedures 2.2.1.2 with the following modifications. 15g/L of Bacteriological Agar was stirred into the media prior to autoclaving. After autoclaving, the media was cooled while stirring. At 49°C, 1ml of 100mg/ml spectinomycin (to a final spectinomycin concentration of 100µg/ml) was stirred into 1L of the media before hand-pouring the media into petri dishes. Gel plates were set for roughly 1 hour and stored at 4°C.

5.2.1.3 THY/CM10 selective growth media

THY media was prepared in accordance with General Procedures 2.2.1.2. A 50ml tube containing 10ml of THY media was supplemented before use with 1.7µl of 60mg/ml chloramphenicol (to a final chloramphenicol concentration of 10µg/ml).

5.2.1.4 THY/CM10 selective growth agar gel plates

THY media was prepared in accordance with General Procedures 2.2.1.2 with the following modifications. 15g/L of Bacteriological Agar was stirred into the media prior to autoclaving. After autoclaving, the media was cooled while stirring. At 49°C, 167µl of 60mg/ml chloramphenicol (to a final chloramphenicol concentration of 10µg/ml) was stirred into 1L of the media before hand-

pouring the media into petri dishes. Gel plates were set for < 1 hour (to mitigate the ABX concentrating) and stored at 4°C.

5.2.2 Experimental Procedures

TABLE 5.01: Bacterial strains and plasmids used in this study.

Identifier	Description	Source
GBS 874391	Wild-type Group B Streptococcus, Serotype III, ST 17 hypervirulent strain, vaginal isolate	(Takahashi *et al.*, 1993)
E. coli DH5α	Cloning host	Bethesda Research Laboratories
GU2812	*E. coli* DH5α + *htp*-::Cm^R::pHY304aad9 (pGU2812), Cm^R, $Spec^R$, T^S	D Gosling
GU2824	GBS 874391 + pGU2812, Cm^R, $Spec^R$, T^S	D Gosling
GU2830	GBS 874391 + pHY304aad9 (empty vector control) $Spec^R$, T^S	Dr MJ Sullivan
GU2842	GBS 874391 + pGU2812 (GV6_177), *htp*- mutant, Cm^R, $Spec^R$, T^S	This study
GU2843	GBS 874391 + pGU2812 (GV12_8), *htp*- mutant, Cm^R, $Spec^R$, T^S	This study

5.2.2.1 Plasmid Construct for mutating *htp*

The Δ*htp* mutants of GBS 874391 were constructed by Dean Gosling (Research Assistant, Ulett Lab) up to the point of cross-over induction using a method described previously (Ipe *et al.*, 2015). Briefly, ~500bp regions upstream and downstream of the *htp* gene (locus tag CHF17_01323) of GBS 874391 were amplified using primers that also carried ~20 bp homology to the chloramphenicol cassette of pLZ12, which was also amplified by PCR. The three PCR products were fused in a subsequent PCR overlapping extension reaction and cloned into the spectinomycin resistant pHY304aad9 vector, which carries a temperature-sensitive origin of replication that has permissive replication at < 32°C. The resultant recombinant plasmid was then transformed into competent GBS 874391 cells by electroporation, and transformants were used to mutate *htp* using allelic exchange by homologous recombination (See FIGURE 5.01).

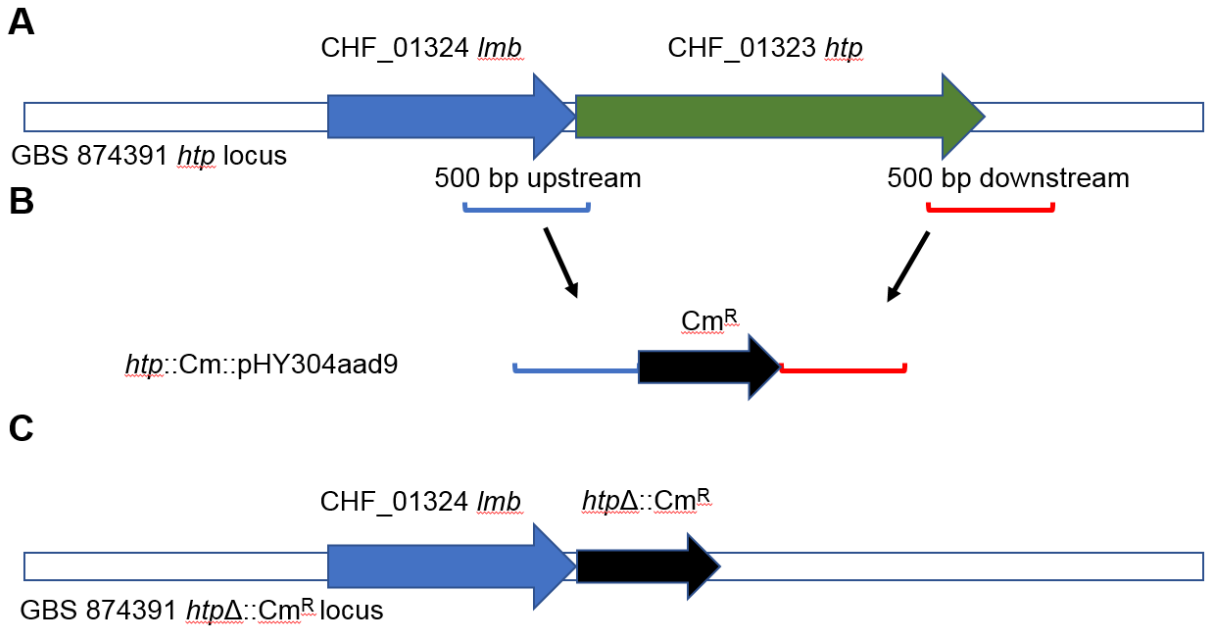

FIGURE 5.01: GBS 874391 htp mutation.
(A) In GBS 874391, htp is located downstream of lmb (for Laminin Binding Protein). (B) ~500bp upstream and downstream of htp was used to generate an htp mutant construct in pHY304aad9. (C) Following mutation by allelic exchange, ~98% of the coding sequence of htp was exchanged for the chloramphenicol resistance marker (Cm^R). Image constructed by Dr Matthew Sullivan.

5.2.2.2 Cross-over induction to generate Δ*htp* mutants

Five putative Δ*htp* transformants of GBS 874391 (designated GV, GVI, GVII, GVIII and GIX) and 1 negative control (GBS 874391 carrying empty vector pHY304aad9) were each inoculated into 10ml THY/Spec100 media). Inoculated cultures were incubated overnight at 28°C (shaking at 200rpm). 200µl of the overnight culture was inoculated into 10ml THY/Spec100 media (i.e. a 1:50 dilution) and incubated for 28°C for 2.5 hours (shaking at 200rpm), then incubated at 40°C for a further 2.5 hours (shaking at 200rpm).

Cultures were 10-fold serially diluted, in 500µl volumes, and 100µl of dilutions from neat (10^0) to 1E-3 were spread over THY/Spec100 gel plates (pre-warmed to 40°C); i.e. 4 THY/Spec100 plates per culture. Plates were incubated overnight at 40°C. This step induces integration of the *htp*::Cm::pHY304aad9 mutation construct into the GBS chromosome at either the upstream or downstream homologous regions to the target gene (*htp*). For controls to monitor success of integration, 5µl of dilutions from neat (10^0) to 1E-5 were aliquoted onto another THY/Spec100 plate

and incubated at 28°C to assess CFU/mL of Spec-resistant colonies at permissive temperature (28°C) versus CFU/mL Spec-resistant colonies arising at non-permissive temperature (40°C), to demonstrate loss of the plasmid upon selection using temperature. In addition, 5µl of dilutions from neat (10^0) to 1E-5 were aliquoted to a non-selective, TSA Blood agar plate (pre-warmed to 40°C). Insertion ratios were calculated on the basis of colony counts, comparing CFU/mL of $Spec^R$ colonies at 40°C divided by CFU/mL of $Spec^R$ colonies at 28°C to give the frequency of integration. Single cross-over mutants were passaged by streaking 6 separate colonies from the THY/Spec100 overnight plates grown at 40°C onto new THY/Spec100 plates and incubated overnight at 40°C. To induce a double-cross over mutation, and deletion of *htp* by allelic exchange with the Cm-resistance cassette, 1ml of THY media (without ABX) was inoculated with a single colony from each of the streaked samples and incubated at 28°C for 16 hours (shaking at 200rpm). 50µl of each culture was inoculated into 1ml of fresh THY media (without ABX) and incubated at 28°C for 6 hours (shaking at 200rpm), then at 40°C for a further 6 hours (shaking at 200rpm).

1:10 serial dilutions were performed on each transformant from 1E-1 to 1E-5; i.e. 20µl of culture into 180µl of PBS, pre-warmed to 40°C in 96-well plates. 100µl of each dilution from 1E-3 to 1E-5 was spread over THY/CM10 gel plates (pre-warmed to 40°C). 5µl of each dilution from 1E-1 to 1E-5 was aliquoted in triplicate onto THY/CM10 gel plates (pre-warmed to 40°C). All plates were incubated overnight at 40°C. After performing colony counts, 800 single colonies were selected and individually streaked, first onto THY/Spec100 agar, then (without returning to the colony) onto THY/CM10 agar. This was done to identify Cm-resistant, Spec-sensitive colonies that had lost the Spec-resistance marker encoded on pHY304aad9, and therefore likely underwent a double-cross over mutation. Patched plates were incubated overnight at 37°C. Of 800 colonies picked in this manner, some ~300 exhibited spectinomycin sensitivity and chloramphenicol resistance. Twelve independent single colony isolates were chosen for further analyses, by streaking to new agar plates (THY/CM10) and culturing in 10 mL THY/CM10 for genomic DNA isolation and subsequent PCR analysis.

5.2.2.3 Genomic Preparations of transformants

In 50ml tubes, 10ml of THY/CM10 media was inoculated with selected patches (X10) from the THY/CM10 plates (of those exhibiting both spectinomycin sensitivity and chloramphenicol resistance) and incubated overnight at 37°C. Each overnight culture was centrifuged at 7197g for 10 minutes, the pellet resuspended in 395µl Lysostaphin buffer (50mM Tris-HCL, 0.145M NaCl, pH 7.5) and transferred to a 1.5ml tube. 10µl of 10U/µl Mutanolysin was added before incubating at 37°C for 90 minutes. To each preparation, 154µl of Lysostaphin buffer, 30µl of 10% SDS, 6µl of 20mg/ml Proteinase K, and 10µl of RNase A was added before gently mixing then incubating at 37°C for 1 hour.

100µl of 5M NaCl was added to each preparation and pipette-mixed vigorously for 3 minutes. Then 80µl of CTAB/NaCl was added to each preparation and pipette-mixed vigorously for 3 minutes before incubating at 65°C for 10 minutes. 650µl of the digest was transferred to a pre-pelleted, Maxtract High Density 1.5ml Tube (QIAGEN). 650µl of Chloroform-isoamyl was added to the digest and pipette-mixed thoroughly before centrifuging at 15,000g for 5 minutes in 4°C. The upper aqueous phase (~600µl) was transferred to a new pre-pelleted Maxtract High Density 1.5ml Tube. 600µl of Phenol-Chloroform-isoamyl was thoroughly pipette-mixed into the sample before centrifuging at 15,000g for 5 minutes in 4°C. After transferring the aqueous phase to a new 1.5ml tube, 0.6 volumes of isopropanol were added to precipitate the DNA. And centrifuged at 15,000g for 5 minutes in 4°C. After removing the supernatant with a p200 pipette, the pellet was resuspended in 500µl of 70% Ethanol and centrifuged at 15,000g for 5 minutes in 4°C. After removing all supernatant with a p20 pipette, the pellet was re-centrifuged at 15,000g for 5 minutes in 4°C and the remaining supernatant removed with a p20 pipette. The pellet was air-dried at room temperature for 5 minutes before manually dissolving (with a pipette tip) in 200µl of nuclease-free Ultrapure Distilled Water. After resting the DNA for 5 minutes at room temperature, DNA quantification was performed on the Eppendorf Biospectrometer.

5.2.2.4 PCR confirmation of the Δ*htp* mutant

Standard PCR was performed using the Phusion High-Fidelity DNA polymerase (Thermo-Scientific) and following the manufacture's protocol. PCRs were performed on 10 putative transformants of GBS 874391, the GBS 874391 wild-type, and the DNA from 2 previous failed transformant attempts as additional positive controls.

The *htp* primers used in this PCR were;

Forward 5'-TTGCCTAAATAAAGGAGCAATC (Designation: *htp*_CHK_F1)

Reverse 5'-AAGCTTGGGCAAGGGATCTA (Designation: *htp*_CHK_R1)

- generating an amplicon of ~3740bp for the wild-type and ~2142bp for the *htp* mutant strain.

5.2.2.5 Gel Extraction for DNA sequencing

From the gel of the above-mentioned PCR, 2 mutant samples and the wild-type were selected for sequencing with AGRF. The QIAquick Gel Extraction Kit was used in accordance with the manufacturer's protocol to isolate the DNA from the agarose gel. Final elutions were performed in 55µl nuclease-free Ultrapure Distilled Water. DNA quantification was performed on the Eppendorf Biospectrometer. Between 70 and 80ng of the amplicon was sent to AGRF for both forward and reverse primer reactions for all three samples. The samples were sequenced using 2 primer sets amplifying either side of the *htp* region. The first primer set used was the *htp*_CHK primers used in the previous PCR (section 5.2.2.4). The second primer set was;

Forward 5'-GATCCCGGGATTATCCGCTCAATGTCTCGAA (Designation: 22up-1)

Reverse 5'-GATCTCGAGACTTTATGACCCACATACCTGGAC (Designation *Lmb* 1-6)

5.2.2.6 GBS Growth Assay

Wild-type and mutant GBS were tested for differential growth at stationary phase. 10ml of THY (50ml tube) was inoculated with a single colony of each strain and incubated at 37^{o}C, shaking at

200rpm for 17 hours. 3 independent replicates were inoculated for each strain. Each sample was serially diluted 10-fold and plated in triplicate onto TSA-blood agar plates. Colony counts were performed and CFU/ml calculated from the plates after they had been incubated overnight at 37^{o}C.

5.2.2.7 Infection Assays

The infection protocol optimised in Chapter 3 (section 3.3.1) was followed with the following modifications;

- To maintain a consistent MOI between 80 and 200, washed GBS cultures had to be resuspended in varying amounts of media to account for the variable growth rates between the wild-type and the mutant strain.
- The infection was scaled down to 4 technical replicates, each 1ml reactions, aliquoted into 24-well plates.
- The internalised bacteria were processed at 6, 12, 24 and 48 hour time-points post-infection.

5.2.2.8 Statistical Analysis

All statistical analysis was performed using Graphpad Prism version 7.02. Central tendency bars and error bars in figures represent the Mean and Standard Error of the Mean (SEM) unless otherwise stated. The means of 4 technical replicates for each treatment (WT and mutant for each time-point) across 4 independent infection assays were pooled. A two-tailed, unpaired t-test was performed on the calculated Area Under the Curve (AUC) to compare mutant against wild-type survival in monocytes from 6 to 48 hours of infection.

5.3 Results

5.3.1 Confirmation of *htp* mutant construct

Comparing GBS growth of the putative mutants on THY/Spec100 plates against growth on TSA Blood agar plates revealed the single crossover insertion ratio for each of the 5 putative mutant strains (TABLE 5.02). There were no insertions detected in the negative control (GBS 874391 with an empty vector pHY304aad9) as the Spectinomycin resistance carrying plasmid is lost after several replication generations at 40^{o}C.

TABLE 5.02: Chloramphenicol cassette Insertion ratio for each putative mutant strain of GBS.

Strain of putative *htp* mutant	**Growth on TSA-blood**	**Growth on THY/Spec100**	**Insertion Ratio**
GV	2.3E8	8E2	3.5E-6
GVI	3.3E8	8E2	2.4E-6
GVII	4.2E8	7E2	1.7E-6
GVIII	5.0E8	1E2	2.0E-7
GVIX	6.0E8	4E2	6.7E-7
GU2830	5.2E8	0	0

After confirming the single-crossover mutants for spectinomycin resistance, further incubations, without selection, were performed to promote double-crossover events (i.e. ejecting the spectinomycin resistance from the chromosome), and plated onto THY/CM10 plates. 800 colonies from these plates were each consecutively patched onto both THY/Spec100 and THY/CM10 plates. An estimated 60-70% of the patched colonies exhibited spectinomycin sensitivity and chloramphenicol resistance – indicating double crossover events. 16 patches from the GV strain were selected for further confirmation, and 10 were found to have retained their spectinomycin sensitivity and chloramphenicol resistance. Genomic preparations were performed on each strain yielding high quantity, good quality DNA for all 10 strains. PCR confirmed that at least 7 of the putative mutants contained the 2142bp amplicon for the inserted *htp* knockout cassette; with the three positive controls (including the wild-type) carrying the 3740bp *htp* gene (FIGURE 5.02).

TABLE 5.03: Eppendorf Biospectrometer (1mm) absorbance readings of DNA isolations from 10 putative htp mutants.

	GBS Strain	ng/µl	A260/280	A260/230	Total µg (200 µl)
1	**GV_1_1**	580.5	2.06	2.42	116.1
2	**GV_3_1**	482.8	2.08	2.32	96.4
3	**GV_4_1**	214.5	2.06	2.12	42.9
4	**GV_5_1**	335.3	1.99	2.15	67.1
5	**GV_5_152**	446.0	2.05	2.28	89.2
6	**GV_6_1**	248.5	2.04	2.27	49.7
7	**GV_6_104**	485.6	2.06	2.33	97.1
8	**GV_6_177**	248.5	2.06	2.21	49.7
9	**GV_12_8**	433.6	2.04	2.21	86.7
10	**GV_12_80**	257.1	2.05	2.21	51.4

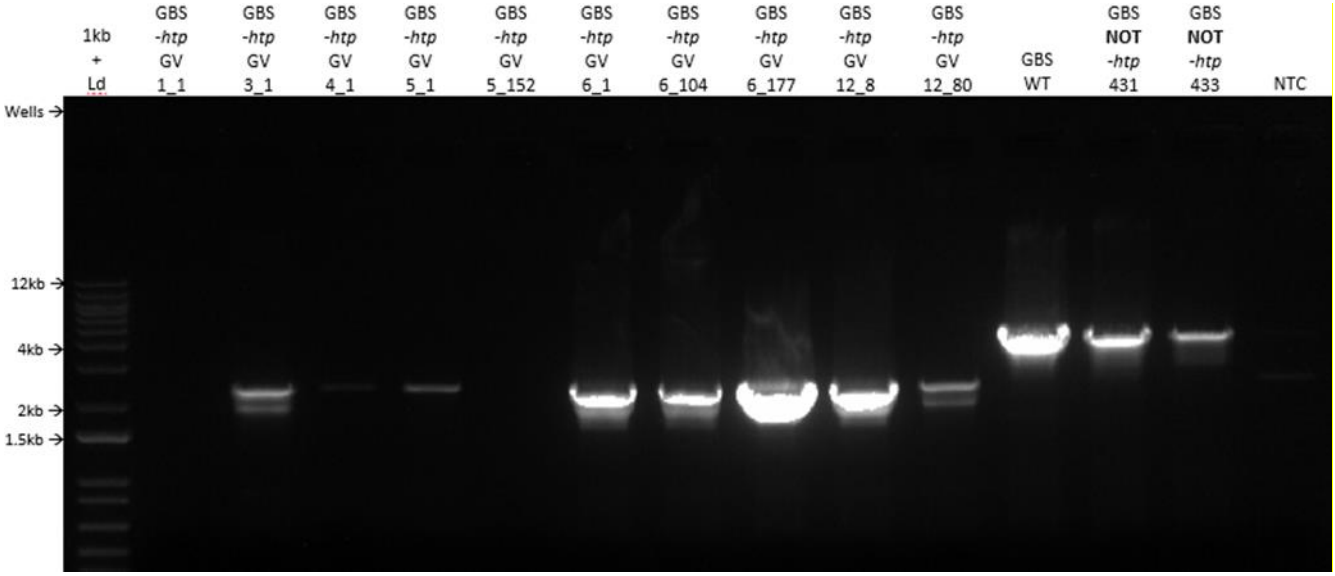

FIGURE 5.02: Agarose gel showing the PCR-generated amplicons of 10 putative mutants using the htp_CHK primers.

Templates were DNA isolations from 10 putative htp mutant strains of GBS. Templates for the positive controls were a single DNA isolation from the GBS 874391 wild-type (WT), and 2 DNA isolations from previously failed transformation attempts (431 and 433). Using the htp-CHK primers (section 5.2.2.4), the expected amplicon size is 2124bp for the transformants and 3740bp for non-transformants.

The amplicons from colony 6 - patch 177, colony 12 - patch 8 (both mutant strain GV), and the wild-type were gel extracted for sequencing. Assemblies based on the returned sequences, performed in Sequencher 5.3, generated single contigs for all 3 assemblies (see Appendix 3, TABLES J, K and L).

Two primer sets confirmed that both sequenced mutants contained the chloramphenicol cassette (pLZ12), and the wild-type contained *htp* (CHF17_01323) (FIGURES 5.03, 5.04 and 5.05).

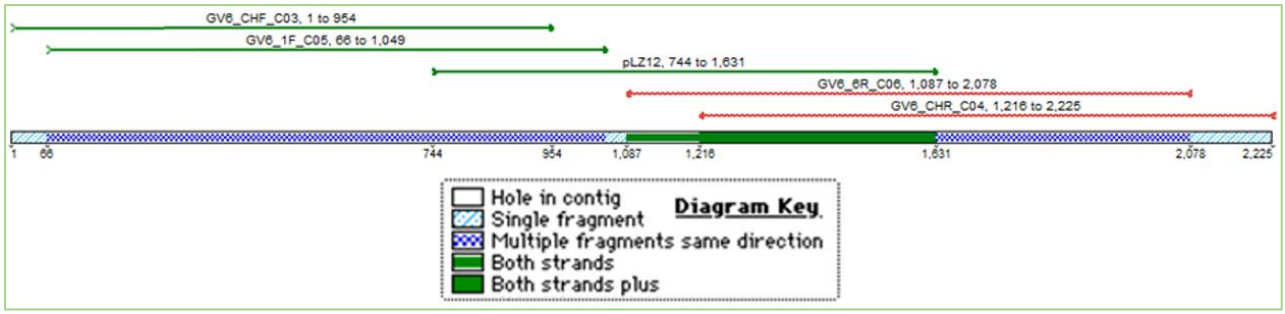

FIGURE 5.03: Sequence Assemblies generated using of 2 primer sets on the Δhtp strain GV_6_177 against the chloramphenicol cassette (pLZ12).

Figure generated in Sequencher 5.3. Arrow colours (red and green) and direction indicate the direction of sequences.

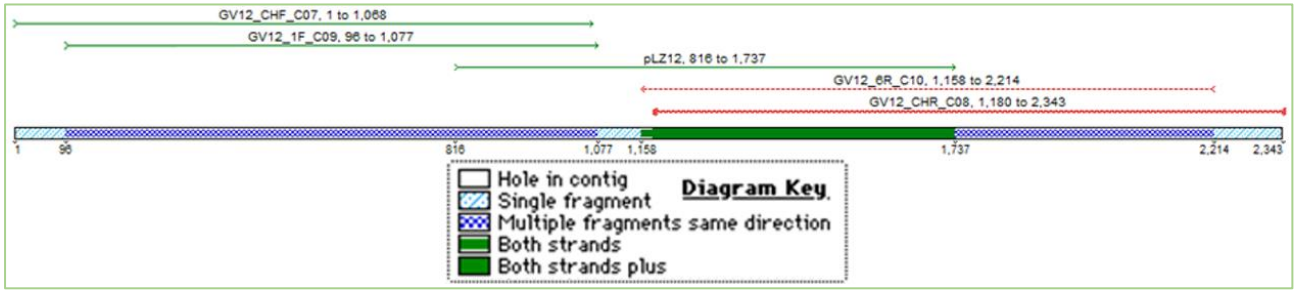

FIGURE 5.04: Sequence Assemblies generated using of 2 primer sets on the Δhtp strain GV_12_8 against the chloramphenicol cassette (pLZ12).

Figure generated in Sequencher 5.3. Arrow colours (red and green) and direction indicate the direction of sequences.

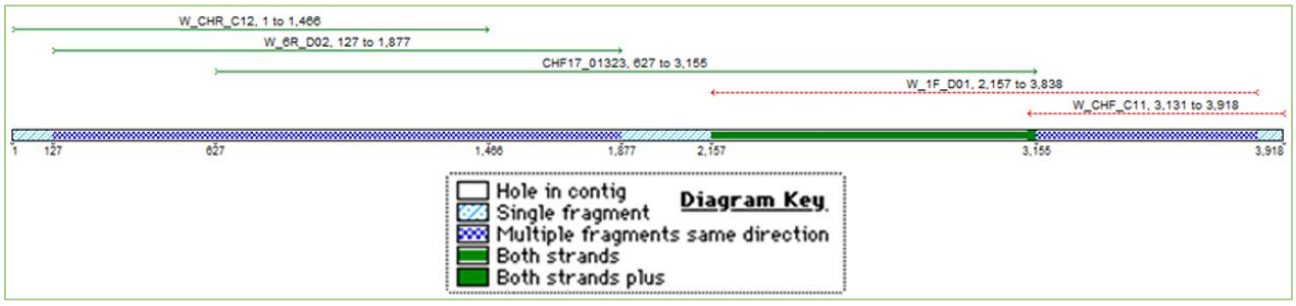

FIGURE 5.05: Sequence Assemblies generated using of 2 primer sets on the wild-type GBS 874391 against the htp gene (CHF17_01323).

Figure generated in Sequencher 5.3. Arrow colours (red and green) and direction indicate the direction of sequences.

5.3.2 Infection Assays

The 2 sequenced mutant strains were subjected to preliminary, overnight culturing experiments which revealed that the CFU/ml at stationary phase (after 17 hours incubation at 37°C) was reduced in both mutant strains compared to the wild-type (TABLE 5.04). Based on these results, Δ*htp* strain GV_12_8 was selected as the mutant strain to be used in the infection assays as the observed CFU/ml numbers were closer to the wild-type. In order to secure a comparable MOI between wild-type and mutant for the infection assays, final, post-wash resuspensions of GBS in bRPMI were adjusted – so that the same CFU for both WT and mutant strains were used in the infections.

TABLE 5.04: Comparative stationary-phase growth of GBS mutant and wild-type strains in THY after 17 hours of incubation.

GBS Strain	Replicate 1 CFU/ml	Replicate 2 CFU/ml	Replicate 3 CFU/ml	Average CFU/ml	Proportion of Wild-type (%)
Wild-type	1.53E9	1.33E9	1.73E9	1.53E9	100.0
GV_6_177	6.66E8	5.34E8	5.34E8	5.78E8	37.8
GV_12_8	1.00E9	8.66E8	6.66E8	8.44E8	55.1

Infection assay experiments were carried out in accordance with the protocol optimised in chapter 3 (section 3.3.1) with the modifications described above (section 5.2.2.7). Briefly, monocytes were infected with GBS (either WT or mutant strain) aiming for an MOI between 80 and 200, then incubated in 5% CO_2 at 37°C for 48 hours; ABX added after 1 hour of incubation. Internalised GBS were processed for counting at 6 hours, 12 hours, 24 hours and 48 hours.

TABLE 5.05: MOI calculations for each of the 4 independent infection assays.

Infection Assay	U937 monocytes cells/ml	GBS CFU/ml	Strain	MOI
1	1.21E6	1.87E8	Wild-type	154
		2.20E8	GV_12_8	181
2	2.06E6	2.68E8	Wild-type	130
		2.05E8	GV_12_8	100
3	2.28E6	1.74E8	Wild-type	76
		2.00E8	GV_12_8	88
4	2.30E6	2.62E8	Wild-type	117
		2.62E8	GV_12_8	117

With the single exception of the 6 hour time-point in Assay 1, there were significantly higher numbers of the *htp* mutant GBS recovered from the intracellular environment of monocytes than the wild-type GBS. In assay 1 (FIGURE 5.06A), the internalised *htp* mutant recovered to higher numbers than the wildtype subsequent to the 6 hour processing point – despite the lower initial numbers. In Assays 2 to 4 (FIGURES 5.06B, C and D), the survival differential between the 2 GBS strains was as high as $2\log_{10}$ – which was maintained throughout the infection; representing a major difference between the WT and *Δhtp* GBS.

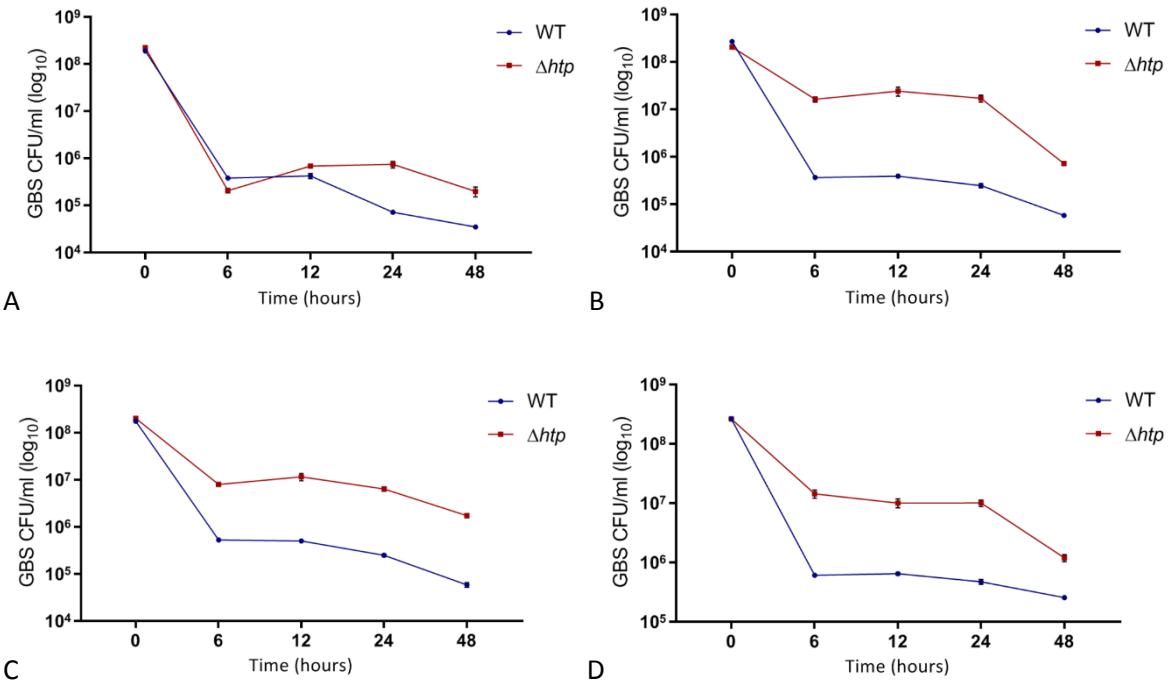

FIGURE 5.06: Four independent infection assays comparing monocyte-internalised GBS (both wild-type and Δhtp) over 48 hours of infection.

Figures compare GBS counts (mutant vs wild-type - CFU/ml) internalised in monocytes over the period of infection. Time 0 = time after infection and a 5 minute centrifuge. Error lines based on Mean and SEM (n=4 technical replicates).

The mean GBS CFU/ml recovered from 4 technical replicates at each time point over 4 independent assays were pooled into a single, time series data set (FIGURE 5.07). A t-test was performed on the Area Under the Curves (from 6 to 48 hours of infection) to reveal that the *Δhtp* GBS were recovered from the intracellular monocyte environment at significantly higher rates than the WT GBS (p=0.0005).

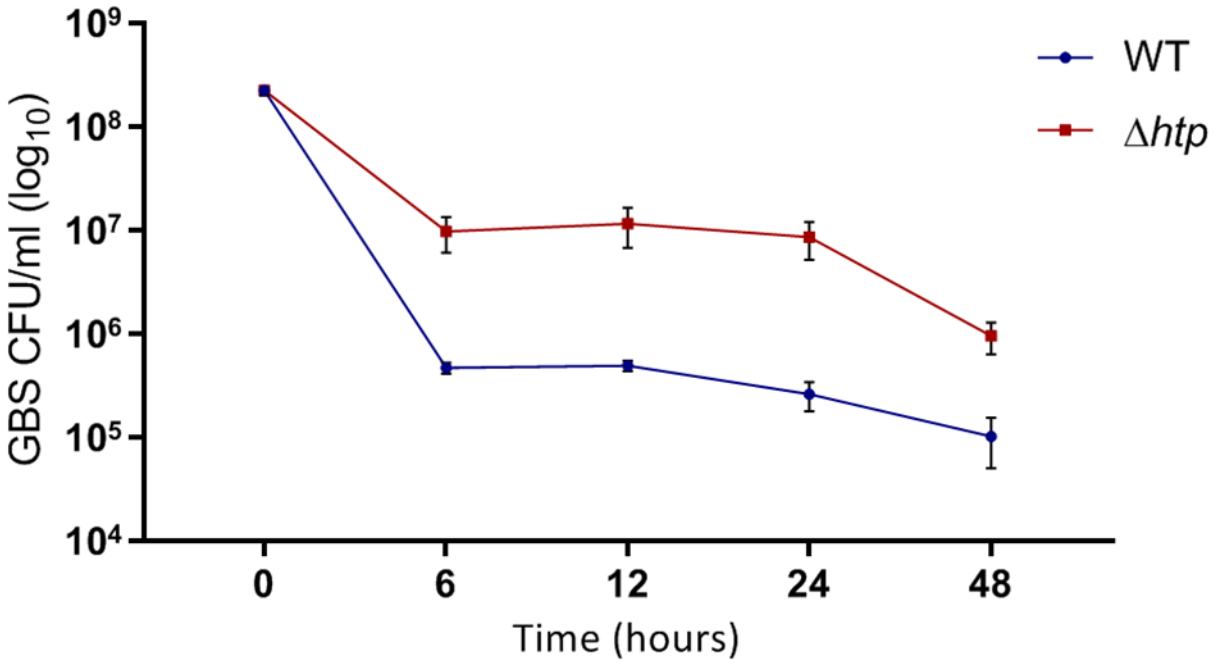

FIGURE 5.07: Pooled means from 4 independent infection assays comparing monocyte-internalised GBS (both wild-type and Δhtp) over 48 hours of infection.

Mean data from 4 infection assays (FIGURE 5.05). Area Under the Curve analysis from hours 6 to 48 infection were significant (p= 0.0005). Each point represents the pooled means from 4 independent assays. Error bars represent SEM.

5.4 Discussion

In chapter 3, a protocol was optimised to attain sufficient amounts of high quality host and pathogen RNA from a single reaction for co-transcription analysis. RT-qPCR performed on the RNA revealed that GBS 874391 which has been internalised in U937 monocytes upregulates the expression of *htp* 7 to 11-fold after 6 hours of infection. Here we constructed an *htp* knockout strain of GBS 874391 (Δ*htp*), which was subsequently used in assays to determine if Htp has any influence on growth and survival of internalised GBS in monocytes. The infection model optimised in chapter 3 was utilised; extending the infection time from 6 to 48 hours.

Given that *htp* was so highly upregulated in the pathogen after 5 to 6 hours inside the monocyte, it was assumed that Htp provided some protection against monocyte destruction. It was therefore expected that the *htp* knockout mutant strain would struggle to survive the internal environment of the monocyte more than the wild-type strain. Contrary to expectation, the *htp* knockout strain survived the internal environment of the monocytes at significantly higher numbers than the wild-type strain. This stark distinction between mutant and wild-type remained consistent throughout the 48 hours of infection. This counter-intuitive result indicates that the production of Htp hinders the survival capacity of internalised GBS. Whatever the perceived benefit of upregulating *htp*, this benefit is outweighed by some, as yet, unknown cost – which inhibits survival. It may simply be a matter that the energy cost associated with Htp production deprives other survival mechanisms of their required energy.

While the function of the Htp family of proteins is still being investigated, the potential role of these proteins in zinc acquisition has been recently elucidated (Bersch *et al.*, 2013). It has been estimated that around 5% of the bacterial proteome (across the bacterial domain) is comprised of zinc-binding proteins (Andreini *et al.*, 2006). Zinc is one of the most abundant transition metals in biological systems; functioning as transcription factors and serving proteins as structural cofactors, as well as in

other structural and catalytic roles (Hantke, 2005, Maret, 2013, Andreini & Bertini, 2012). Zinc is the most abundant, non-redox, transition metal found in enzymes (Andreini *et al.*, 2008).

Given the biological importance of zinc, it makes sense that both host and pathogen cells have a range of strategies allowing them to compete for, and regulate, this resource in the context of infection. There are 2 main zinc-based strategies employed by host cells to undermine pathogen proliferation; 1) host cells can recruit excess concentrations of zinc to levels which are toxic to the invading pathogen, or 2) host cells can starve the pathogenic cells of this biologically crucial micronutrient (Djoko *et al.*, 2015). In various streptococcal species, excess zinc has been reported to competitively bind to several cellular sites (including some which do not normally engage with metal ions) - limiting the uptake of other vital nutrients and inhibiting the functions of important enzymes (Eijkelkamp *et al.*, 2014, McDevitt *et al.*, 2011, Scheie & Pearce, 1994, Ong *et al.*, 2015). Human neutrophils infected with Group A Streptococcus were found to trigger the release of zinc as an antimicrobial strategy (Ong *et al.*, 2014b). Excess zinc was also recently reported to induce copper starvation in the gram-negative bacteria, *Acinetobacter baumannii* (Hassan *et al.*, 2017). Botella *etal*. (Botella *et al.*, 2011) reported that zinc is transferred to the phagosomes of macrophages with internalised *Mycobacterium tuberculosis*; facilitating zinc poisoning of the bacteria – along with the bacterial mechanisms of zinc export. Bacterial pathogens commonly employ metal efflux systems (such as the streptococcal CzcD zinc efflux system) to counter the effects of heavy metal toxicity (Nies, 2003, Ong *et al.*, 2014b).

The converse host strategy of depriving the pathogen of zinc is also reported. The calprotectin protein, for example, is abundant in neutrophils, and contains 2 high affinity zinc binding sites; chelating the zinc, thereby restricting access to the zinc by internalised bacteria (Gebhardt *et al.*, 2006, Corbin *et al.*, 2008, Kehl-Fie & Skaar, 2010). The Natural Resistance-Associated Macrophage Proteins (NRAMP) have a strong affinity for metal cations (including zinc), and after being recruited to phagosomal membranes where it is proposed they pump these metal cations out of the

phagosome; thus depriving the internalised pathogens of these essential nutrients (Gruenheid *et al.*, 1997, Jabado *et al.*, 2000). Pathogens counter this nutrient-deprivation strategy using high affinity zinc transporters to sequester zinc from low concentration environments. Examples of these zinc transport systems include the ZnuABC system found in Escherichia coli (with homologues of this system found in both gram positive and negative bacteria) (Hantke, 2005), MntA found in *Neisseria meningitides* (Lim *et al.*, 2008), and TroABC transports system found in Treponema pallidum (Lee *et al.*, 2002). Htp is also a putative family of high zinc-affinity transporters, conserved in Streptococcal bacteria, proposed to play a role in a zinc acquisition ABC transport system (Shao *et al.*, 2013, Bersch *et al.*, 2013).

This study focussed on survival of the GBS after being internalised by the monocytes. An alternative interpretation of the data is that the *htp* knockout mutant was compromised to the point that they succumbed to phagocytosis in larger numbers than the *htp*-expressing wild-type. So it is possible that upregulation of *htp* mitigates phagocytosis. The initial phagocytosis efficiency does not address the upregulation of *htp* by the internalised GBS 6 hours post infection (CHAPTER 4 - section 4.3.5.2 Bacterial Genes). That is, it would not explain why, after 6 hours of infection, the internalised GBS upregulate a gene that belies its own survival in that environment.

Future experiments may be designed to test for differential phagocytosis efficiency of the monocytes between the wildtype and *htp* mutant strains of GBS. Using the optimised protocol, RNA could be collected from the assays leading up to the 6 hour period and RT-qPCR performed to determine the progression of *htp* upregulation from the time of infection. The next step in the research progression is to construct a complemented strain of GBS by reinserting *htp* into the mutant, then repeating the assays to confirm that *htp* is the principle factor influencing the results. It would also be interesting to compare the wild-type and mutant responses to zinc survival/growth assays to further test the hypothesis that Htp plays a significant role in zinc acquisition.

Similar studies (infection assays with wild-type and complement strains, as well as the above-mentioned time-series experiments) should also be performed for both the upregulated host and GBS genes reported in Chapter 4. Generating mutant strains for the more complex, eukaryotic host cells may require using recently developed CRISPR gene-editing technology (Komor *et al.*, 2017). It would be particularly interesting to investigate the upregulation of the *czcD* gene with *htp* over time – given that *htp* is associated with zinc acquisition, and czcD is characterised as a zinc efflux protein. With the optimised protocol, it should also be possible to examine the transcript and survival of a variety of GBS strains (both pathogenic and non-pathogenic strains from different sites of infection) and a variety of phagocytic host cells (e.g. neutrophils and macrophages instead of monocytes). It would also be interesting to perform further co-transcript studies using the mutant strains.

The data in this study reveals that GBS 874391 upregulates *htp* in a manner that mitigates its own survival inside of the infected monocytes. A preliminary conclusion might therefore be that the monocytes are stimulating *htp* expression in the GBS (possibly via zinc deprivation) as a strategy to limit the survival and proliferation of the internalised pathogen. The functional mechanisms of this strategy are yet to be investigated.

CHAPTER 6: Conclusion

In the war against microbial disease, the development and discovery of medical treatments requires the identification of molecular targets against the pathogenic agents and/or knowledge of the immune response of host cells to each unique pathogen (Furman & Davis, 2015). To this end, transcript studies have been frequently employed for the purpose of revealing the pathogen's reaction to specific environmental conditions (e.g. (Ordas *et al.*, 2011, Xiang *et al.*, 2010, Xiu *et al.*, 2015)). However, this piecemeal approach fails to account for the complexity of a pathogen with multiple virulence factors interacting with the full immune response of the host (Furman & Davis, 2015). Increasingly, co-transcript methods are being employed to gauge the host/pathogen response to the broader context of infection (Ravasi *et al.*, 2016, Avraham *et al.*, 2016). That is, co-transcript studies allow us to analyse the pathogen's acute response to the presence of the host. Co-transcript studies also permit the analysis of the host's response to the pathogen. Co-transcript studies therefore provide the potential opportunity to reveal mechanisms to undermine pathogenic virulence and/or enhance host resistance to disease. A common limitation encountered by co-transcript projects is the scarcity of pathogenic RNA yield in the mixed RNA preparation. Infection models therefore have to be optimised to ensure sufficient host RNA is available for reliable downstream analysis.

Though GBS is reported in animal disease (Keefe, 1997, Plastridge, 1958, Lancefield, 1934), it is a significant, and increasingly reported, human pathogen (Dermer *et al.*, 2004, Eickhoff *et al.*, 1964, Harper, 1971, Farley *et al.*, 1993, Verghese *et al.*, 1986). The first chapter of this project reviewed the literature regarding the classification, virulence and disease outcomes associated with GBS infections. GBS are gram-positive, encapsulated, chain-forming, cocci-shaped bacteria that are responsible for the majority of globally reported neonatal disease and mortality (Dermer *et al.*, 2004). The DEVANI Europe project was instigated in 2008 for the purpose of generating solutions to specifically combat the rise in neonatal disease stemming from GBS infections (Afshar *et al.*, 2011).

Two distinct syndromes are recognised in GBS neonatal disease; 1) early onset disease – characterised by the appearance of GBS-associated pathology with 7 days of birth, and 2) late onset disease – characterised by the appearance of GBS disease between 7 and 90 post-birth (Anthony & Okada, 1977, Wu *et al.*, 2004). Over recent decades, GBS has also been increasingly reported as a significant adult pathogen; especially for the elderly and otherwise immunocompromised (Eickhoff *et al.*, 1964, Harper, 1971, Farley *et al.*, 1993, Verghese *et al.*, 1986). The rise in GBS disease has been attributed to the use of tetracycline in humans (Da Cunha *et al.*, 2014). It is proposed that prior to the use of tetracycline in humans, non-pathogenic GBS strains offered sufficient competition to pathogenic strains – such that GBS disease was rare in humans. Since many pathogenic GBS carry tetracycline-resistance, the use of this antibiotic eliminated the competition – leaving the pathogenic strains to thrive. Finding a solution to GBS disease is further complicated by the highly diverse nature of the GBS genome across the species; a problem which is amplified by the demonstrated capacity of GBS to acquire new genes via horizontal gene transfer (Teatero *et al.*, 2016, Campisi *et al.*, 2016, Brochet *et al.*, 2008). It is estimated that the roughly 20% of the genome of each GBS strain lies outside of the core GBS genome (Tettelin *et al.*, 2005). It was further predicted by Tettelin *et al.* (Tettelin *et al.*, 2005) that each strain of GBS adds more than 30 unique genes to the GBS pan genome. This genomic diversity complicates discovery of a universal vaccine against GBS infection.

GBS is being increasingly reported as the etiological agent of genitourinary tract infections (Dermer *et al.*, 2004, Eickhoff *et al.*, 1964, Harper, 1971, Farley *et al.*, 1993, Verghese *et al.*, 1986). In Chapter 2 of this project, the genomes of 8 diverse human GU isolates of GBS were prepared for PacBio sequencing. Due to the generation of longer read lengths, PacBio sequencing is the preferred sequencing method of bacterial genomes – as longer read lengths better account for the long repeat motifs often found in bacterial genomes. To gain high quality genomic preparations for all 8 strains of GBS, the DNA-extraction protocol required some optimisation. Sequencing was performed at the Doherty Institute (Melbourne University); returning high quality data permitting the complete assemblies of all 8 submitted strains. A Genome Announcement was reported for the pathogenic,

hypervirulent (ST17) GBS 874391 strain (Sullivan *et al.*, 2017a). This strain is a vaginal isolate used in several previous studies (Takahashi *et al.*, 1993, Seifert *et al.*, 2006). GBS 874391 was selected to be used throughout the subsequent chapters of this project.

As a causative agent of bacteraemia and sepsis, GBS has a demonstrated capacity to thrive in the human blood stream – giving the pathogen access to a variety of tissues throughout the body (Verghese *et al.*, 1986, Edwards *et al.*, 2016). Phagocytic cells (i.e. neutrophils and monocytes) represent the primary humoral defence mechanism against foreign agents in the blood (Dale *et al.*, 2008). Originally isolated from a histiocytic lymphoma patient, the U937 cell line is a common *in vitro* human monocyte/macrophage model (Sundstrom & Nilsson, 1976). Chapter 3 of this study developed a blood-infection model for the pathogen, GBS 874391, internalised in U937 monocytes. Given that co-transcript reactions are usually saturated with host RNA, the focus of this study was to generate a model producing enough high quality pathogen RNA from the single, infection reaction - for use in downstream co-transcript analysis. Extensive optimisation was required to generate a model that preserved both host and pathogen viability throughout the infection period. A 45 minute post-infection centrifuge suggested by the literature was found to increase bacterial yield, but reduce monocyte viability. Reducing the centrifuge to 5 minutes did not have a significant impact on the pathogen numbers, but increased host cell viability. An MOI above 200 was also found to weaken the host cells, resulting in likely cell rupture and pathogen release during the wash process. An infection media formulation was developed based on the growth-rate of the pathogen. The media promoted no detectable growth or stress in the non-infection, pathogen control. However, this media was too restrictive to yield enough RNA from the pathogen; regardless of how many cells contributed to the RNA preparation. In order to produce a viable pathogen transcript control, it was necessary to add nutrients to the optimised media – permitting the stimulation of sufficient pathogen transcription. Even though the antibiotics used in this study had been previously demonstrated effective against this strain of GBS, time-kill assays revealed that the pathogen survived and stabilized at low levels in the formulated media at the prescribed antibiotic

concentrations. Given the high internalised pathogen cell numbers (CFU/ml) derived from the host cells, the numbers of pathogenic cells surviving in the media (i.e. outside of the host cells) were considered so low as to have no significant impact on any transcript analysis – more-so since the host cells were pelleted and the media removed before extracting the RNA. Varying methods of cell collection and RNA extractions were tested. Mixed cells (host cells with internalised pathogen) were pelleted, quick frozen on dry ice and stored at -80^{o}C. Column extractions were found to be the most reliably consistent method of RNA extraction. New GAPDH primers were developed to test the mixed RNA preparations for eukaryotic genomic DNA contamination. After generating cDNA from the mixed RNA, RT-qPCR successfully amplified all 12 tested pathogenic genes from 1 in 60 dilutions of the cDNA. The optimised infection model is therefore viable for producing sufficient, high quality RNA for analysis by RT-qPCR.

For Chapter 4 of this study RT-qPCR was performed on RNA derived from the infection mix for 12 host and 12 pathogen genes. The co-transcript based on these 24 genes revealed that, after 6 hours of infection, 7 of the 12 host genes and 6 of the 12 pathogen genes were significantly upregulated more than 2-fold. Differential gene expression was calculated using a published formula that accounts for variations in amplification efficiencies (Pfaffl, 2001). Using *β-actin* as the host reference/housekeeping gene, the pro-inflammatory *IL8* was upregulated more than 4000-fold. A second pro-inflammatory gene (*IL1A*) was also significantly upregulated (>17-fold). Two other pro-inflammatory cytokines (*IL1B* and *TNF*) were upregulated around 5-fold. The oncogene (*LIM2*) and a monocyte chemokine (*MCP-1*) were upregulated around 2 to 3-fold. And *IL10* (which has anti-inflammatory properties) was upregulated a little over 2-fold. Of the pathogen genes tested, *htp* was the most significantly upregulated (>10-fold against the reference/housekeeping gene *rpoB*). Htp is reported to have various cellular functions, but is most thoroughly described as having a role in zinc acquisition. The second highest pathogen gene to be upregulated from the infection was *czcD*, which translates to a cellular, heavy metal (including zinc) exporter protein. This contrast between zinc acquisition and export point to the importance of zinc regulation in the pathogen cells – in the

context of survival inside phagocytes. The iron transporter *1010* was also upregulated 2 to 4-fold. Three virulence factors were also upregulated in the pathogen between 2 and 5-fold; *hvgA* (an adhesion), *scpB* (a protease) and *rib* (conferring protease resistance).

Histidine Triad Proteins (Htp) and their homologues have been reported across the Streptococcal genus (Ogunniyi *et al.*, 2009, Maruvada *et al.*, 2009, Kunitomo *et al.*, 2008). These proteins have been described in a variety of functions including adhesion (Bober *et al.*, 2011), immune evasion (Moulin *et al.*, 2019) and zinc acquisition (Riboldi-Tunnicliffe *et al.*, 2004, Riboldi-Tunnicliffe *et al.*, 2005). Since *htp* was so highly upregulated in the monocyte-internalised GBS, an *htp*-knockout mutant (*Δhtp*) was constructed, and comparative infection survival assays performed for the 5th Chapter of this study. Contrary to expectation, the *Δhtp* strain survived the internal environment of the monocyte in much higher numbers over a period of 6 to 48 hours of infection. The expression of *htp* therefore appears to provide a disadvantage to the survival of the internalised pathogen. The monocytes may be employing zinc starvation strategy against the pathogen in order to limit their survival. Alternatively, the expression of *htp* in the wild-type may be limiting the phagocytosis efficiency of the monocytes; with much fewer *Δhtp* cells being internalised during the infection. Several studies have identified Htp as a potential vaccine target; including one study in monkeys – with the associated implications for humans (Denoel *et al.*, 2011).

The findings of this study suggest a key role for metal ion (namely zinc) transport for GBS intracellular survival. Host cells may try to starve an intracellular pathogens of these essential nutrients, or alternatively flood the pathogen with toxic concentrations of these metals (Hood & Skaar, 2012, Djoko *et al.*, 2015). Pathogenic microbes have therefore accumulated a range of measures to acquire these trace nutrients during periods of starvation (often incorporating complex interactions between metal-binding proteins and trans-membrane transport proteins), or efflux systems to export excess nutrients out of the cell (Porcheron *et al.*, 2013, Waldron & Robinson, 2009). In gram-negative bacteria, many substrate-binding proteins are soluble; localised in the

periplasm, whereas in gram positive bacteria, these binding proteins tend to be tethered to the cell membrane (Gilson *et al.*, 1988, Tam & Saier, 1993, Sutcliffe & Russell, 1995). Andreini *et al.* (Andreini *et al.*, 2006) estimates that up to 6% of prokaryote proteomes consist of zinc-binding proteins (80% of which are enzymes); emphasising the importance of the cell's ability to acquire zinc from the environment. Zinc-binding transport systems, including the Adc transport system associated with htp, have been described for several streptococci species (Dintilhac *et al.*, 1997, Panina *et al.*, 2003).

To our knowledge, this study was the first to demonstrate the viability of optimising a host/pathogen infection model for internalised GBS in monocytes. The differential survival between the internalised *Δhtp* and wild-type strains of GBS is to be confirmed in the future using a complement strain. The remaining monocyte and GBS genes which were upregulated (Chapter 4) may also be investigated through infection assays with complement strains; possibly including time-series transcript assays to assess how and when each gene changes over the infection period. It would further be interesting to examine the co-transcript of monocytes and GBS using the mutant strains. Due to the high quality of the RNA from the infections, the RNA may also be submitted for full co-transcriptome sequencing on a next generation platform such as RNAseq. This has the potential to reveal many more potential vaccine targets against pathogenic GBS. It would also be interesting to consider more complex co-infection models incorporating multiple pathogen and/or multiple host cells to more closely mimic the complexity of these *in vivo* interactions. This study provides a scaffold by which future co-transcript models may be optimised for a range of host phagocytic cells against GBS infection, as well as for different pathogenic strains of GBS.

References

Aber, R.C., N. Allen, J.T. Howell, H.W. Wilkenson & R.R. Facklam, (1976) Nosocomial transmission of group B streptococci. *Pediatrics* **58**: 346-353.

Adamou, J.E., J.H. Heinrichs, A.L. Erwin, W. Walsh, T. Gayle, M. Dormitzer, R. Dagan, Y.A. Brewah, P. Barren, R. Lathigra, S. Langermann, S. Koenig & S. Johnson, (2001) Identification and characterization of a novel family of pneumococcal proteins that are protective against sepsis. *Infect. Immun.* **69**: 949-958.

Adamou, J.E., T.M. Wizemann, P. Barren & S. Langermann, (1998) Adherence of Streptococcus pneumoniae to human bronchial epithelial cells (BEAS-2B). *Infect. Immun.* **66**: 820-822.

Adams, J., (2008) Transcriptome: connecting the genome to gene function. *Nature Education* **1**: 195.

Afshar, B., K. Broughton, R. Creti, A. Decheva, M. Hufnagel, P. Kriz, L. Lambertsen, M. Lovgren, P. Melin, G. Orefici, C. Poyart, A. Radtke, J. Rodriguez-Granger, U.B. Sorensen, J. Telford, L. Valinsky, L. Zachariadou, D.S.G. Members of the & A. Efstratiou, (2011) International external quality assurance for laboratory identification and typing of Streptococcus agalactiae (Group B streptococci). *J. Clin. Microbiol.* **49**: 1475-1482.

Aisina, R.B. & L.I. Mukhametova, (2014) Structure and functions of plasminogen/plasmin system. *Bioorganicheskaya Khimiya* **40**: 642-657.

Al-Maani, A., L. Streitenberger, M. Clarke, Y.C. Yau, D. Kovach, R. Wray & A. Matlow, (2014) Nosocomial transmission of group B streptococci proven by positive environmental culture. *Oman Medical Journal* **29**: 376-379.

Amara, U., D. Rittirsch, M. Flierl, U. Bruckner, A. Klos, F. Gebhard, J.D. Lambris & M. Huber-Lang, (2008) Interaction between the coagulation and complement system. *Adv. Exp. Med. Biol.* **632**: 71-79.

Ancona, R.J., P. Ferrieri & P.P. Williams, (1980) Maternal factors that enhance the acquisition of group-B streptococci by newborn infants. *J. Med. Microbiol.* **13**: 273-280.

Anderson, C.L. & G.N. Abraham, (1980) Characterization of the Fc receptor for IgG on a human macrophage cell line, U937. *J. Immunol.* **125**: 2735-2741.

Andreini, C., L. Banci, I. Bertini & A. Rosato, (2006) Zinc through the three domains of life. *J. Proteome Res.* **5**: 3173-3178.

Andreini, C. & I. Bertini, (2012) A bioinformatics view of zinc enzymes. *J. Inorg. Biochem.* **111**: 150-156.

Andreini, C., I. Bertini, G. Cavallaro, G.L. Holliday & J.M. Thornton, (2008) Metal ions in biological catalysis: from enzyme databases to general principles. *J. Biol. Inorg. Chem.* **13**: 1205-1218.

Anthony, B.F., J.A. Carter, R. Eisenstadt & D.G. Rimer, (1983) Isolation of group B streptococci from the proximal small intestine of adults. *J. Infect. Dis.* **147**: 776.

Anthony, B.F. & D.M. Okada, (1977) The emergence of group B streptococci in infections of the newborn infant. *Annu. Rev. Med.* **28**: 355-369.

Anthony, B.F., D.M. Okada & C.J. Hobel, (1979) Epidemiology of the group B streptococcus: maternal and nosocomial sources for infant acquisitions. *J. Pediatr.* **95**: 431-436.

Anton, A., C. Grosse, J. Reissmann, T. Pribyl & D.H. Nies, (1999) CzcD is a heavy metal ion transporter involved in regulation of heavy metal resistance in *Ralstonia* sp. strain CH34. *J. Bacteriol.* **181**: 6876-6881.

Aprianto, R., J. Slager, S. Holsappel & J.W. Veening, (2016) Time-resolved dual RNA-seq reveals extensive rewiring of lung epithelial and pneumococcal transcriptomes during early infection. *Genome Biol.* **17**: 198.

Aprianto, R., J. Slager, S. Holsappel & J.W. Veening, (2018) High-resolution analysis of the pneumococcal transcriptome under a wide range of infection-relevant conditions. *Nucleic Acids Res.* **46**: 9990-10006.

Armakolas, N., A. Dimakakos, A. Armakolas, A. Antonopoulos & M. Koutsilieris, (2016) Possible role of the Ec peptide of IGF1Ec in cartilage repair. *Molecular Medicine Reports* **14**: 3066-3072.
Avraham, R., N. Haseley, A. Fan, Z. Bloom-Ackermann, J. Livny & D.T. Hung, (2016) A highly multiplexed and sensitive RNA-seq protocol for simultaneous analysis of host and pathogen transcriptomes. *Nat. Protoc.* **11**: 1477-1491.
Ayres, S.M., (1985) SCCM's new horizons conference on sepsis and septic shock. *Crit. Care Med.* **13**: 864-866.
Bach, I., (2000) The LIM domain: regulation by association. *Mech. Dev.* **91**: 5-17.
Baddal, B., A. Muzzi, S. Censini, R.A. Calogero, G. Torricelli, S. Guidotti, A.R. Taddei, A. Covacci, M. Pizza, R. Rappuoli, M. Soriani & A. Pezzicoli, (2015) Dual RNA-seq of Nontypeable Haemophilus influenzae and Host Cell Transcriptomes Reveals Novel Insights into Host-Pathogen Cross Talk. *MBio* **6**: e01765-01715.
Badri, M.S., S. Zawaneh, A.C. Cruz, G. Mantilla, H. Baer, W.N. Spellacy & E.M. Ayoub, (1977) Rectal colonization with group B streptococcus: relation to vaginal colonization of pregnant women. *J. Infect. Dis.* **135**: 308-312.
Badwey, J.A. & M.L. Karnovsky, (1980) Active oxygen species and the functions of phagocytic leukocytes. *Annu. Rev. Biochem.* **49**: 695-726.
Baggiolini, M., B. Dewald & B. Moser, (1994) Interleukin-8 and related chemotactic cytokines--CXC and CC chemokines. *Adv. Immunol.* **55**: 97-179.
Baker, C.J., (1977) Summary of the workshop on perinatal infections due to group B Streptococcus. *J. Infect. Dis.* **136**: 137-152.
Baker, C.J., (1980) Group B streptococcal infections. *Adv. Intern. Med.* **25**: 475-501.
Baker, C.J. & F.F. Barrett, (1973) Transmission of group B streptococci among parturient women and their neonates. *J. Pediatr.* **83**: 919-925.
Baker, C.J. & F.F. Barrett, (1974) Group B streptococcal infections in infants. The importance of the various serotypes. *Journal of the American Medical Association* **230**: 1158-1160.
Baker, C.J., D.K. Goroff, S. Alpert, V.A. Crockett, S.H. Zinner, J.R. Evrard, B. Rosner & W.M. McCormack, (1977) Vaginal colonization with group B streptococcus: a study in college women. *J. Infect. Dis.* **135**: 392-397.
Baker, C.J. & D.L. Kasper, (1976) Correlation of maternal antibody deficiency with susceptibility to neonatal group B streptococcal infection. *N. Engl. J. Med.* **294**: 753-756.
Bambini, S. & R. Rappuoli, (2009) The use of genomics in microbial vaccine development. *Drug Discov. Today* **14**: 252-260.
Banerjee, A., B.J. Kim, E.M. Carmona, A.S. Cutting, M.A. Gurney, C. Carlos, R. Feuer, N.V. Prasadarao & K.S. Doran, (2011) Bacterial Pili exploit integrin machinery to promote immune activation and efficient blood-brain barrier penetration. *Nat. Commun.* **2**: 462.
Barcaite, E., A. Bartusevicius, R. Tameliene, M. Kliucinskas, L. Maleckiene & R. Nadisauskiene, (2008) Prevalence of maternal group B streptococcal colonisation in European countries. *Acta Obstet. Gynecol. Scand.* **87**: 260-271.
Barendt, S.M., A.D. Land, L.T. Sham, W.L. Ng, H.C. Tsui, R.J. Arnold & M.E. Winkler, (2009) Influences of capsule on cell shape and chain formation of wild-type and pcsB mutants of serotype 2 Streptococcus pneumoniae. *J. Bacteriol.* **191**: 3024-3040.
Barnham, M., (1983) The gut as a source of the haemolytic streptococci causing infection in surgery of the intestinal and biliary tracts. *J. Infect.* **6**: 129-139.
Bartual, S.G., D. Straume, G.A. Stamsas, I.G. Munoz, C. Alfonso, M. Martinez-Ripoll, L.S. Havarstein & J.A. Hermoso, (2014) Structural basis of PcsB-mediated cell separation in Streptococcus pneumoniae. *Nat. Commun.* **5**: 3842.
Bas, A., G. Forsberg, S. Hammarstrom & M.L. Hammarstrom, (2004) Utility of the housekeeping genes 18S rRNA, beta-actin and glyceraldehyde-3-phosphate-dehydrogenase for normalization in real-time quantitative reverse transcriptase-polymerase chain reaction analysis of gene expression in human T lymphocytes. *Scand. J. Immunol.* **59**: 566-573.

Batchelor, M., J. Guignot, A. Patel, N. Cummings, J. Cleary, S. Knutton, D.W. Holden, I. Connerton & G. Frankel, (2004) Involvement of the intermediate filament protein cytokeratin-18 in actin pedestal formation during EPEC infection. *EMBO Rep.* **5**: 104-110.

Bayle, L., S. Chimalapati, G. Schoehn, J. Brown, T. Vernet & C. Durmort, (2011) Zinc uptake by *Streptococcus pneumoniae* depends on both AdcA and AdcAII and is essential for normal bacterial morphology and virulence. *Mol. Microbiol.* **82**: 904-916.

Beckmann, C., J.D. Waggoner, T.O. Harris, G.S. Tamura & C.E. Rubens, (2002) Identification of novel adhesins from Group B streptococci by use of phage display reveals that C5a peptidase mediates fibronectin binding. *Infect. Immun.* **70**: 2869-2876.

Bellais, S., A. Six, A. Fouet, M. Longo, N. Dmytruk, P. Glaser, P. Trieu-Cuot & C. Poyart, (2012) Capsular switching in group B Streptococcus CC17 hypervirulent clone: a future challenge for polysaccharide vaccine development. *J. Infect. Dis.* **206**: 1745-1752.

Benitz, W.E., J.B. Gould & M.L. Druzin, (1999) Risk factors for early-onset group B streptococcal sepsis: estimation of odds ratios by critical literature review. *Pediatrics* **103**: e77.

Bent, Z.W., M.B. Tran-Gyamfi, S.A. Langevin, D.M. Brazel, R.Y. Hamblin, S.S. Branda, K.D. Patel, T.W. Lane & V.A. VanderNoot, (2013) Enriching pathogen transcripts from infected samples: a capture-based approach to enhanced host-pathogen RNA sequencing. *Anals of Biochemistry* **438**: 90-96.

Bergseng, H., M. Rygg, L. Bevanger & K. Bergh, (2008) Invasive group B streptococcus (GBS) disease in Norway 1996-2006. *Eur. J. Clin. Microbiol. Infect. Dis.* **27**: 1193-1199.

Berner, R., P. Welter & M. Brandis, (2002) Cytokine expression of cord and adult blood mononuclear cells in response to Streptococcus agalactiae. *Pediatr. Res.* **51**: 304-309.

Berry, D.S., F. Lynn, C.H. Lee, C.E. Frasch & M.C. Bash, (2002) Effect of O acetylation of Neisseria meningitidis serogroup A capsular polysaccharide on development of functional immune responses. *Infect. Immun.* **70**: 3707-3713.

Bersch, B., C. Bougault, L. Roux, A. Favier, T. Vernet & C. Durmort, (2013) New insights into histidine triad proteins: solution structure of a *Streptococcus pneumoniae* PhtD domain and zinc transfer to AdcAII. *PLoS ONE* **8**: e81168.

Bersudsky, M., L. Luski, D. Fishman, R.M. White, N. Ziv-Sokolovskaya, S. Dotan, P. Rider, I. Kaplanov, T. Aychek, C.A. Dinarello, R.N. Apte & E. Voronov, (2014) Non-redundant properties of IL-1alpha and IL-1beta during acute colon inflammation in mice. *Gut* **63**: 598-609.

Bevilacqua, M.P., D. Amrani, M.W. Mosesson & C. Bianco, (1981) Receptors for cold-insoluble globulin (plasma fibronectin) on human monocytes. *J. Exp. Med.* **153**: 42-60.

Beyersmann, D., (2002) Homeostasis and Cellular Functions of Zinc. *Materialwissenschaft und Werkstofftechnik* **33**: 764-769.

Bierne, H. & S. Dramsi, (2012) Spatial positioning of cell wall-anchored virulence factors in Gram-positive bacteria. *Curr. Opin. Microbiol.* **15**: 715-723.

Billroth, T., (1874) *Untersuchungen über die Vegetationsformen von "Coccobacteria septica" und den Antheil welchen sie an der Entstehung und Verbreitung der accidentellen Wunderkrankheiten haben, Versuch einer Wissenschaftlichen Kritik der verschiedenen Methode antiseptischer Wundbehandlung, von Dr Theodor Billroth*. G. Reimer.

Bisharat, N., D.W. Crook, J. Leigh, R.M. Harding, P.N. Ward, T.J. Coffey, M.C. Maiden, T. Peto & N. Jones, (2004) Hyperinvasive neonatal group B streptococcus has arisen from a bovine ancestor. *J. Clin. Microbiol.* **42**: 2161-2167.

Bliss, S.J., S.D. Manning, P. Tallman, C.J. Baker, M.D. Pearlman, C.F. Marrs & B. Foxman, (2002) Group B Streptococcus colonization in male and nonpregnant female university students: a cross-sectional prevalence study. *Clin. Infect. Dis.* **34**: 184-190.

Blumberg, H.M., D.S. Stephens, M. Modansky, M. Erwin, J. Elliot, R.R. Facklam, A. Schuchat, W. Baughman & M.M. Farley, (1996) Invasive group B streptococcal disease: the emergence of serotype V. *J. Infect. Dis.* **173**: 365-373.

Bober, M., M. Morgelin, A.I. Olin, U. von Pawel-Rammingen & M. Collin, (2011) The membrane bound LRR lipoprotein Slr, and the cell wall-anchored M1 protein from *Streptococcus pyogenes* both interact with type I collagen. *PLoS ONE* **6**: e20345.

Boehm, T., L. Foroni, Y. Kaneko, M.F. Perutz & T.H. Rabbitts, (1991) The rhombotin family of cysteine-rich LIM-domain oncogenes: distinct members are involved in T-cell translocations to human chromosomes 11p15 and 11p13. *Proc. Natl. Acad. Sci. U. S. A.* **88**: 4367-4371.

Bohnsack, J.F., K.W. Mollison, A.M. Buko, J.C. Ashworth & H.R. Hill, (1991) Group B streptococci inactivate complement component C5a by enzymic cleavage at the C-terminus. *Biochem. J.* **273 (Pt 3)**: 635-640.

Bohnsack, J.F., A.A. Whiting, G. Martinez, N. Jones, E.E. Adderson, S. Detrick, A.J. Blaschke-Bonkowsky, N. Bisharat & M. Gottschalk, (2004) Serotype III *Streptococcus agalactiae* from bovine milk and human neonatal infections. *Emerg. Infect. Dis.* **10**: 1412-1419.

Bohnsack, J.F., K. Widjaja, S. Ghazizadeh, C.E. Rubens, D.R. Hillyard, C.J. Parker, K.H. Albertine & H.R. Hill, (1997) A role for C5 and C5a-ase in the acute neutrophil response to group B streptococcal infections. *J. Infect. Dis.* **175**: 847-855.

Bokil, N.J., M. Totsika, A.J. Carey, K.J. Stacey, V. Hancock, B.M. Saunders, T. Ravasi, G.C. Ulett, M.A. Schembri & M.J. Sweet, (2011) Intramacrophage survival of uropathogenic *Escherichia coli*: differences between diverse clinical isolates and between mouse and human macrophages. *Immunobiology* **216**: 1164-1171.

Bonadio, W.A., W. Jeruc, Y. Anderson & D. Smith, (1992) Systemic infection due to group B beta-hemolytic streptococcus in children. A review of 75 outpatient-evaluated cases during 13 years. *Clin. Pediatr. (Phila.)* **31**: 230-233.

Bone, R.C., (1991) Sepsis, the sepsis syndrome, multi-organ failure: a plea for comparable definitions. *Ann. Intern. Med.* **114**: 332-333.

Bonsor, D.A., N.A. Meenan & C. Kleanthous, (2008) Colicins exploit native disorder to gain cell entry: a hitchhiker's guide to translocation. *Biochem. Soc. Trans.* **36**: 1409-1413.

Boone, T.J., C.A. Burnham & G.J. Tyrrell, (2011) Binding of group B streptococcal phosphoglycerate kinase to plasminogen and actin. *Microb. Pathog.* **51**: 255-261.

Boone, T.J. & G.J. Tyrrell, (2012) Identification of the actin and plasminogen binding regions of group B streptococcal phosphoglycerate kinase. *J. Biol. Chem.* **287**: 29035-29044.

Botella, H., P. Peyron, F. Levillain, R. Poincloux, Y. Poquet, I. Brandli, C. Wang, L. Tailleux, S. Tilleul, G.M. Charriere, S.J. Waddell, M. Foti, G. Lugo-Villarino, Q. Gao, I. Maridonneau-Parini, P.D. Butcher, P.R. Castagnoli, B. Gicquel, C. de Chastellier & O. Neyrolles, (2011) Mycobacterial p(1)-type ATPases mediate resistance to zinc poisoning in human macrophages. *Cell Host Microbe* **10**: 248-259.

Boyer, K.M., C.A. Gadzala, L.I. Burd, D.E. Fisher, J.B. Paton & S.P. Gotoff, (1983a) Selective intrapartum chemoprophylaxis of neonatal group B streptococcal early-onset disease. I. Epidemiologic rationale. *J. Infect. Dis.* **148**: 795-801.

Boyer, K.M., C.A. Gadzala, P.D. Kelly, L.I. Burd & S.P. Gotoff, (1983b) Selective intrapartum chemoprophylaxis of neonatal group B streptococcal early-onset disease. II. Predictive value of prenatal cultures. *J. Infect. Dis.* **148**: 802-809.

Boyer, K.M. & S.P. Gotoff, (1985) Strategies for chemoprophylaxis of GBS early-onset infections. *Antibiot Chemother (1971)* **35**: 267-280.

Boyer, K.M., L.C. Vogel, S.P. Gotoff, C.A. Gadzala, J. Stringer & W.R. Maxted, (1980) Nosocomial transmission of bacteriophage type 7/11/12 group B streptococci in a special care nursery. *Am. J. Dis. Child.* **134**: 964-966.

Brinkmann, V., U. Reichard, C. Goosmann, B. Fauler, Y. Uhlemann, D.S. Weiss, Y. Weinrauch & A. Zychlinsky, (2004) Neutrophil extracellular traps kill bacteria. *Science* **303**: 1532-1535.

Brochet, M., E. Couve, R. Bercion, J.M. Sire & P. Glaser, (2009) Population structure of human isolates of Streptococcus agalactiae from Dakar and Bangui. *J. Clin. Microbiol.* **47**: 800-803.

Brochet, M., E. Couve, M. Zouine, T. Vallaeys, C. Rusniok, M.C. Lamy, C. Buchrieser, P. Trieu-Cuot, F. Kunst, C. Poyart & P. Glaser, (2006) Genomic diversity and evolution within the species *Streptococcus agalactiae*. *Microbes Infect.* **8**: 1227-1243.

Brochet, M., C. Rusniok, E. Couve, S. Dramsi, C. Poyart, P. Trieu-Cuot, F. Kunst & P. Glaser, (2008) Shaping a bacterial genome by large chromosomal replacements, the evolutionary history of Streptococcus agalactiae. *Proc. Natl. Acad. Sci. U. S. A.* **105**: 15961-15966.

Brown, J.H., (1919) *The Use of Blood Agar for the Study of Streptococci*. Rockefeller Institute for Medical Research.

Bryan, J.D., R. Liles, U. Cvek, M. Trutschl & D. Shelver, (2008) Global transcriptional profiling reveals Streptococcus agalactiae genes controlled by the MtaR transcription factor. *BMC Genomics* **9**: 607.

Buchanan, R.E., (1917) Studies on the Nomenclature and Classification of the Bacteria: IV. Subgroups and Genera of the Coccaceae. *J. Bacteriol.* **2**: 603-617.

Buermans, H.P. & J.T. den Dunnen, (2014) Next generation sequencing technology: Advances and applications. *Biochim. Biophys. Acta* **1842**: 1932-1941.

Burak Aksu , Ö.Y., (2019) Group B Streptococci Induce Interleukin 8 Production in Human Cervical Epithelial Cell Cultures: The Role of Capsule Polysaccharide. *Clinical and Experimental Health Sciences* **9**: 49-52.

Buscetta, M., S. Papasergi, A. Firon, G. Pietrocola, C. Biondo, G. Mancuso, A. Midiri, L. Romeo, G. Teti, P. Speziale, P. Trieu-Cuot & C. Beninati, (2014) FbsC, a Novel Fibrinogen-binding Protein, Promotes Streptococcus agalactiae-Host Cell Interactions. *J. Biol. Chem.* **289**: 21003-21015.

Caboche, S., C. Audebert & D. Hot, (2014) High-Throughput Sequencing, a VersatileWeapon to Support Genome-Based Diagnosis in Infectious Diseases: Applications to Clinical Bacteriology. *Pathogens* **3**: 258-279.

Caliot, E., S. Dramsi, M.P. Chapot-Chartier, P. Courtin, S. Kulakauskas, C. Pechoux, P. Trieu-Cuot & M.Y. Mistou, (2012) Role of the Group B antigen of *Streptococcus agalactiae*: a peptidoglycan-anchored polysaccharide involved in cell wall biogenesis. *PLoS Pathog.* **8**: e1002756.

Campbell, J.R., S.L. Hillier, M.A. Krohn, P. Ferrieri, D.F. Zaleznik & C.J. Baker, (2000) Group B streptococcal colonization and serotype-specific immunity in pregnant women at delivery. *Obstet. Gynecol.* **96**: 498-503.

Campisi, E., C.D. Rinaudo, C. Donati, M. Barucco, G. Torricelli, M.S. Edwards, C.J. Baker, I. Margarit & R. Rosini, (2016) Serotype IV Streptococcus agalactiae ST-452 has arisen from large genomic recombination events between CC23 and the hypervirulent CC17 lineages. *Scientific Reports* **6**: 29799.

Carey, A.J., C.K. Tan, S. Mirza, H. Irving-Rodgers, R.I. Webb, A. Lam & G.C. Ulett, (2014) Infection and cellular defense dynamics in a novel 17beta-estradiol murine model of chronic human group B streptococcus genital tract colonization reveal a role for hemolysin in persistence and neutrophil accumulation. *J. Immunol.* **192**: 1718-1731.

Carlin, A.F., S. Uchiyama, Y.C. Chang, A.L. Lewis, V. Nizet & A. Varki, (2009) Molecular mimicry of host sialylated glycans allows a bacterial pathogen to engage neutrophil Siglec-9 and dampen the innate immune response. *Blood* **113**: 3333-3336.

Carlson, S.A., M.B. Omary & B.D. Jones, (2002) Identification of cytokeratins as accessory mediators of Salmonella entry into eukaryotic cells. *Life Sci.* **70**: 1415-1426.

Carr, M.W., S.J. Roth, E. Luther, S.S. Rose & T.A. Springer, (1994) Monocyte chemoattractant protein 1 acts as a T-lymphocyte chemoattractant. *Proc. Natl. Acad. Sci. U. S. A.* **91**: 3652-3656.

Carter, J.A., B.G. Neville & C.R. Newton, (2003) Neuro-cognitive impairment following acquired central nervous system infections in childhood: a systematic review. *Brain Research Reviews* **43**: 57-69.

Castelruiz, Y., E. Larrea, P. Boya, M.P. Civeira & J. Prieto, (1999) Interferon alfa subtypes and levels of type I interferons in the liver and peripheral mononuclear cells in patients with chronic hepatitis C and controls. *Hepatology* **29**: 1900-1904.

Caudron, J.M., N. Ford, M. Henkens, C. Mace, R. Kiddle-Monroe & J. Pinel, (2008) Substandard medicines in resource-poor settings: a problem that can no longer be ignored. *Trop. Med. Int. Health* **13**: 1062-1072.

CDC, (2014) Active Bacterial Core Surveillance Report, Emerging Infections Program Network, Group B Streptococcus, 2014. . In.: Centers for Disease Control and Prevention, pp.

CG102, N., Bacterial meningitis and meningococcal septicaemia: Management of bacterial meningitis and meningococcal septicaemia in children and young people younger than 16 years in primary and secondary care. 2010. In., pp.

Chaffin, D.O., S.B. Beres, H.H. Yim & C.E. Rubens, (2000) The serotype of type Ia and III group B streptococci is determined by the polymerase gene within the polycistronic capsule operon. *J. Bacteriol.* **182**: 4466-4477.

Chan, Y.C., K.J. Boor & M. Wiedmann, (2007) SigmaB-dependent and sigmaB-independent mechanisms contribute to transcription of *Listeria monocytogenes* cold stress genes during cold shock and cold growth. *Appl. Environ. Microbiol.* **73**: 6019-6029.

Chandrangsu, P., C. Rensing & J.D. Helmann, (2017) Metal homeostasis and resistance in bacteria. *Nat. Rev. Microbiol.* **15**: 338-350.

Chanput, W., V. Peters & H. Wichers, (2015) THP-1 and U937 Cells. In: The Impact of Food Bioactives on Health: in vitro and ex vivo models. K. Verhoeckx, P. Cotter, I. Lopez-Exposito, C. Kleiveland, T. Lea, A. Mackie, T. Requena, D. Swiatecka & H. Wichers (eds). Cham (CH): Springer International Publishing, pp. 147-159.

Chaze, T., A. Guillot, B. Valot, O. Langella, J. Chamot-Rooke, A.M. Di Guilmi, P. Trieu-Cuot, S. Dramsi & M.Y. Mistou, (2014) O-Glycosylation of the N-terminal region of the serine-rich adhesin Srr1 of *Streptococcus agalactiae* explored by mass spectrometry. *Mol. Cell. Proteomics* **13**: 2168-2182.

Cheng, Q., D. Stafslien, S.S. Purushothaman & P. Cleary, (2002) The group B streptococcal C5a peptidase is both a specific protease and an invasin. *Infect. Immun.* **70**: 2408-2413.

Chia, J.S., L.Y. Chang, C.T. Shun, Y.Y. Chang, Y.G. Tsay & J.Y. Chen, (2001) A 60-kilodalton immunodominant glycoprotein is essential for cell wall integrity and the maintenance of cell shape in Streptococcus mutans. *Infect. Immun.* **69**: 6987-6998.

Chretien, J.H., C.G. McGinniss, J. Thompson, E. Delaha & V.F. Garagusi, (1979) Group B beta-hemolytic streptococci causing pharyngitis. *J. Clin. Microbiol.* **10**: 263-266.

Christensen, K.K., A.K. Dykes & P. Christensen, (1984) Relation between use of tampons and urogenital carriage of group B streptococci. *Br. Med. J.* **289**: 731-732.

Christiansen, H. & H. Leth, (2011) Breast milk as a cause of group B streptococcal sepsis. *Ugeskr. Laeger* **173**: 129-130.

Cieslewicz, M.J., D. Chaffin, G. Glusman, D. Kasper, A. Madan, S. Rodrigues, J. Fahey, M.R. Wessels & C.E. Rubens, (2005) Structural and genetic diversity of group B streptococcus capsular polysaccharides. *Infect. Immun.* **73**: 3096-3103.

Cieslewicz, M.J., D.L. Kasper, Y. Wang & M.R. Wessels, (2001) Functional analysis in type Ia group B Streptococcus of a cluster of genes involved in extracellular polysaccharide production by diverse species of streptococci. *J. Biol. Chem.* **276**: 139-146.

Cohen, I., P. Rider, Y. Carmi, A. Braiman, S. Dotan, M.R. White, E. Voronov, M.U. Martin, C.A. Dinarello & R.N. Apte, (2010) Differential release of chromatin-bound IL-1alpha discriminates between necrotic and apoptotic cell death by the ability to induce sterile inflammation. *Proc. Natl. Acad. Sci. U. S. A.* **107**: 2574-2579.

Colten, H.R., (1986) Molecular biology of complement. *Bioessays* **4**: 249-254.

Commins, S., J.W. Steinke & L. Borish, (2008) The extended IL-10 superfamily: IL-10, IL-19, IL-20, IL-22, IL-24, IL-26, IL-28, and IL-29. *J. Allergy Clin. Immunol.* **121**: 1108-1111.

Corbin, B.D., E.H. Seeley, A. Raab, J. Feldmann, M.R. Miller, V.J. Torres, K.L. Anderson, B.M. Dattilo, P.M. Dunman, R. Gerads, R.M. Caprioli, W. Nacken, W.J. Chazin & E.P. Skaar, (2008) Metal chelation and inhibition of bacterial growth in tissue abscesses. *Science* **319**: 962-965.

Cornacchione, P., L. Scaringi, K. Fettucciari, E. Rosati, R. Sabatini, G. Orefici, C. von Hunolstein, A. Modesti, A. Modica, F. Minelli & P. Marconi, (1998) Group B streptococci persist inside macrophages. *Immunology* **93**: 86-95.

Coulombe, P.A. & M.B. Omary, (2002) 'Hard' and 'soft' principles defining the structure, function and regulation of keratin intermediate filaments. *Curr. Opin. Cell Biol.* **14**: 110-122.

Creti, R., M. Imperi, M. Pataracchia, G. Alfarone, S. Recchia & L. Baldassarri, (2012) Identification and molecular characterization of a *S. agalactiae* strain lacking the capsular locus. *Eur. J. Clin. Microbiol. Infect. Dis.* **31**: 233-235.

Crick, F., (1970) Central dogma of molecular biology. *Nature* **227**: 561-563.

Crick, F.H., (1958) On protein synthesis. *Symp. Soc. Exp. Biol.* **12**: 138-163.

Croucher, N.J. & N.R. Thomson, (2010) Studying bacterial transcriptomes using RNA-seq. *Curr. Opin. Microbiol.* **13**: 619-624.

Cumley, N.J., L.M. Smith, M. Anthony & R.C. May, (2012) The CovS/CovR acid response regulator is required for intracellular survival of group B Streptococcus in macrophages. *Infect. Immun.* **80**: 1650-1661.

Cundell, D.R., J.N. Weiser, J. Shen, A. Young & E.I. Tuomanen, (1995) Relationship between colonial morphology and adherence of Streptococcus pneumoniae. *Infect. Immun.* **63**: 757-761.

Currie, A.J., S. Curtis, T. Strunk, K. Riley, K. Liyanage, S. Prescott, D. Doherty, K. Simmer, P. Richmond & D. Burgner, (2011) Preterm infants have deficient monocyte and lymphocyte cytokine responses to group B streptococcus. *Infect. Immun.* **79**: 1588-1596.

Cusumano, V., F. Genovese, G. Mancuso, M. Carbone, M.T. Fera & G. Teti, (1996) Interleukin-10 protects neonatal mice from lethal group B streptococcal infection. *Infect. Immun.* **64**: 2850-2852.

Da Cunha, V., M.R. Davies, P.E. Douarre, I. Rosinski-Chupin, I. Margarit, S. Spinali, T. Perkins, P. Lechat, N. Dmytruk, E. Sauvage, L. Ma, B. Romi, M. Tichit, M.J. Lopez-Sanchez, S. Descorps-Declere, E. Souche, C. Buchrieser, P. Trieu-Cuot, I. Moszer, D. Clermont, D. Maione, C. Bouchier, D.J. McMillan, J. Parkhill, J.L. Telford, G. Dougan, M.J. Walker, D. Consortium, M.T. Holden, C. Poyart & P. Glaser, (2014) *Streptococcus agalactiae* clones infecting humans were selected and fixed through the extensive use of tetracycline. *Nat. Commun.* **5**: 4544.

Dale, D.C., L. Boxer & W.C. Liles, (2008) The phagocytes: neutrophils and monocytes. *Blood* **112**: 935-945.

Dalia, A.B. & J.N. Weiser, (2011) Minimization of bacterial size allows for complement evasion and is overcome by the agglutinating effect of antibody. *Cell Host Microbe* **10**: 486-496.

Dando, S.J., A. Mackay-Sim, R. Norton, B.J. Currie, J.A. St John, J.A. Ekberg, M. Batzloff, G.C. Ulett & I.R. Beacham, (2014) Pathogens penetrating the central nervous system: infection pathways and the cellular and molecular mechanisms of invasion. *Clin. Microbiol. Rev.* **27**: 691-726.

Davies, H.D., N. Jones, T.S. Whittam, S. Elsayed, N. Bisharat & C.J. Baker, (2004) Multilocus sequence typing of serotype III group B streptococcus and correlation with pathogenic potential. *J. Infect. Dis.* **189**: 1097-1102.

de Aguiar, E.L., D.C. Mariano, M.V. Viana, J. Benevides Lde, F. de Souza Rocha, L. de Castro Oliveira, F.L. Pereira, F.A. Dorella, C.A. Leal, A.F. de Carvalho, G.S. Santos, A.L. Mattos-Guaraldi, P.E. Nagao, S. de Castro Soares, S.S. Hassan, A.C. Pinto, H.C. Figueiredo & V. Azevedo, (2016) Complete genome sequence of Streptococcus agalactiae strain GBS85147 serotype of type Ia isolated from human oropharynx. *Stand Genomic Sci* **11**: 39.

De Groot, A.S. & R. Rappuoli, (2004) Genome-derived vaccines. *Expert Rev. Vaccines* **3**: 59-76.

de Louvois, J., S. Halket & D. Harvey, (2005) Neonatal meningitis in England and Wales: sequelae at 5 years of age. *Eur. J. Pediatr.* **164**: 730-734.

de Louvois, J., S. Halket & D. Harvey, (2007) Effect of meningitis in infancy on school-leaving examination results. *Arch. Dis. Child.* **92**: 959-962.
de Oliveira, S., E.E. Rosowski & A. Huttenlocher, (2016) Neutrophil migration in infection and wound repair: going forward in reverse. *Nat. Rev. Immunol.* **16**: 378-391.
de Vries, J.E., (1995) Immunosuppressive and anti-inflammatory properties of interleukin 10. *Ann. Med.* **27**: 537-541.
de Waal Malefyt, R., J. Abrams, B. Bennett, C.G. Figdor & J.E. de Vries, (1991) Interleukin 10(IL-10) inhibits cytokine synthesis by human monocytes: an autoregulatory role of IL-10 produced by monocytes. *J. Exp. Med.* **174**: 1209-1220.
Delannoy, C.M., M. Crumlish, M.C. Fontaine, J. Pollock, G. Foster, M.P. Dagleish, J.F. Turnbull & R.N. Zadoks, (2013) Human *Streptococcus agalactiae* strains in aquatic mammals and fish. *BMC Microbiol.* **13**: 41.
Demczuk, S., C. Baumberger, B. Mach & J.M. Dayer, (1987) Expression of human IL 1 alpha and beta messenger RNAs and IL 1 activity in human peripheral blood mononuclear cells. *Cell. Mol. Immunol.* **3**: 255-265.
Denoel, P., M.T. Philipp, L. Doyle, D. Martin, G. Carletti & J.T. Poolman, (2011) A protein-based pneumococcal vaccine protects rhesus macaques from pneumonia after experimental infection with Streptococcus pneumoniae. *Vaccine* **29**: 5495-5501.
Dermer, P., C. Lee, J. Eggert & B. Few, (2004) A history of neonatal group B streptococcus with its related morbidity and mortality rates in the United States. *J. Pediatr. Nurs.* **19**: 357-363.
Derre-Bobillot, A., N.G. Cortes-Perez, Y. Yamamoto, P. Kharrat, E. Couve, V. Da Cunha, P. Decker, M.C. Boissier, F. Escartin, B. Cesselin, P. Langella, L.G. Bermudez-Humaran & P. Gaudu, (2013) Nuclease A (Gbs0661), an extracellular nuclease of Streptococcus agalactiae, attacks the neutrophil extracellular traps and is needed for full virulence. *Mol. Microbiol.* **89**: 518-531.
Di Paolo, N.C. & D.M. Shayakhmetov, (2016) Interleukin 1alpha and the inflammatory process. *Nat. Immunol.* **17**: 906-913.
Diedrick, M.J., A.E. Flores, S.L. Hillier, R. Creti & P. Ferrieri, (2010) Clonal analysis of colonizing group B Streptococcus, serotype IV, an emerging pathogen in the United States. *J. Clin. Microbiol.* **48**: 3100-3104.
Dillon, H.C., Jr., E. Gray, M.A. Pass & B.M. Gray, (1982) Anorectal and vaginal carriage of group B streptococci during pregnancy. *J. Infect. Dis.* **145**: 794-799.
Dillon, H.C., Jr., S. Khare & B.M. Gray, (1987) Group B streptococcal carriage and disease: a 6-year prospective study. *J. Pediatr.* **110**: 31-36.
Dillon, L.A., R. Suresh, K. Okrah, H. Corrada Bravo, D.M. Mosser & N.M. El-Sayed, (2015) Simultaneous transcriptional profiling of Leishmania major and its murine macrophage host cell reveals insights into host-pathogen interactions. *BMC Genomics* **16**: 1108.
Dinarello, C.A., (2018) Introduction to the interleukin-1 family of cytokines and receptors: Drivers of innate inflammation and acquired immunity. *Immunol. Rev.* **281**: 5-7.
Dinarello, C.A., N.P. Goldin & S.M. Wolff, (1974) Demonstration and characterization of two distinct human leukocytic pyrogens. *J. Exp. Med.* **139**: 1369-1381.
Dintilhac, A., G. Alloing, C. Granadel & J.P. Claverys, (1997) Competence and virulence of Streptococcus pneumoniae: Adc and PsaA mutants exhibit a requirement for Zn and Mn resulting from inactivation of putative ABC metal permeases. *Mol. Microbiol.* **25**: 727-739.
Djoko, K.Y., C.L. Ong, M.J. Walker & A.G. McEwan, (2015) The Role of Copper and Zinc Toxicity in Innate Immune Defense against Bacterial Pathogens. *J. Biol. Chem.* **290**: 18954-18961.
Doran, K.S., J.C. Chang, V.M. Benoit, L. Eckmann & V. Nizet, (2002) Group B streptococcal beta-hemolysin/cytolysin promotes invasion of human lung epithelial cells and the release of interleukin-8. *J. Infect. Dis.* **185**: 196-203.

Doran, K.S., G.Y. Liu & V. Nizet, (2003) Group B streptococcal beta-hemolysin/cytolysin activates neutrophil signaling pathways in brain endothelium and contributes to development of meningitis. *J. Clin. Invest.* **112**: 736-744.

Doran, K.S. & V. Nizet, (2004) Molecular pathogenesis of neonatal group B streptococcal infection: no longer in its infancy. *Mol. Microbiol.* **54**: 23-31.

Dramsi, S. & H. Bierne, (2016) Spatial Organization of Cell Wall-Anchored Proteins at the Surface of Gram-Positive Bacteria. *Curr. Top. Microbiol. Immunol.*

Dramsi, S., E. Caliot, I. Bonne, S. Guadagnini, M.C. Prevost, M. Kojadinovic, L. Lalioui, C. Poyart & P. Trieu-Cuot, (2006) Assembly and role of pili in group B streptococci. *Mol. Microbiol.* **60**: 1401-1413.

Dramsi, S., E. Morello, C. Poyart & P. Trieu-Cuot, (2012) Epidemiologically and clinically relevant Group B Streptococcus isolates do not bind collagen but display enhanced binding to human fibrinogen. *Microbes Infect.* **14**: 1044-1048.

Duell, B.L., C.K. Tan, A.J. Carey, F. Wu, A.W. Cripps & G.C. Ulett, (2012) Recent insights into microbial triggers of interleukin-10 production in the host and the impact on infectious disease pathogenesis. *FEMS Immunol. Med. Microbiol.* **64**: 295-313.

Dupre-Crochet, S., M. Erard & O. Nubetae, (2013) ROS production in phagocytes: why, when, and where? *J. Leukoc. Biol.* **94**: 657-670.

Dutra, V.G., V.M.N. Alves, A.N. Olendzki, C.A.G. Dias, A.F.A. de Bastos, G.O. Santos, E.L.T. de Amorin, M.Â. Sousa, R. Santos, P.C.S. Ribeiro, C.F. Fontes, M. Andrey, K. Magalhães, A.A. Araujo, L.F. Paffadore, C. Marconi, E.F.C. Murta, P.C. Fernandes Jr, M.S.G. Raddi, P.S. Marinho, R.B.G. Bornia, J.K. Palmeiro, L.M. Dalla-Costa, T.C.A. Pinto, A.C.N. Botelho, L.M. Teixeira & S.E.L. Fracalanzza, (2014) *Streptococcus agalactiae* in Brazil: serotype distribution, virulence determinants and antimicrobial susceptibility. *BMC Infect. Dis.* **14**: 323-323.

Easmon, C.S., (1986) The carrier state: group B streptococcus. *J. Antimicrob. Chemother.* **18 Suppl A**: 59-65.

Easmon, C.S., M.J. Hastings, A.J. Clare, B. Bloxham, R. Marwood, R.P. Rivers & J. Stringer, (1981) Nosocomial transmission of group B streptococci. *Br. Med. J.* **283**: 459-461.

Ebert, R. & H. Florey, (1939) The extravascular development of the monocyte observed in vivo. *Br. J. Exp. Pathol.* **20**: 342.

Edmond, K., A. Clark, V.S. Korczak, C. Sanderson, U.K. Griffiths & I. Rudan, (2010) Global and regional risk of disabling sequelae from bacterial meningitis: a systematic review and meta-analysis. *Lancet Infect. Dis.* **10**: 317-328.

Edmond, K.M., C. Kortsalioudaki, S. Scott, S.J. Schrag, A.K. Zaidi, S. Cousens & P.T. Heath, (2012) Group B streptococcal disease in infants aged younger than 3 months: systematic review and meta-analysis. *Lancet* **379**: 547-556.

Edwards, D.J. & K.E. Holt, (2013) Beginner's guide to comparative bacterial genome analysis using next-generation sequence data. *Microbial Informatics and Experimentation* **3**: 2.

Edwards, M.S., (2008) Group B streptococcal conjugate vaccine: a timely concept for which the time has come. *Hum. Vaccin.* **4**: 444-448.

Edwards, M.S. & C.J. Baker, (2005) Group B streptococcal infections in elderly adults. *Clin. Infect. Dis.* **41**: 839-847.

Edwards, M.S., D.L. Kasper, H.J. Jennings, C.J. Baker & A. Nicholson-Weller, (1982) Capsular sialic acid prevents activation of the alternative complement pathway by type III, group B streptococci. *J. Immunol.* **128**: 1278-1283.

Edwards, M.S., V. Nizet & C.J. Baker, (2011) CHAPTER 12 - Group B Streptococcal Infections. In: Infectious Diseases of the Fetus and Newborn (Seventh Edition). Philadelphia: W.B. Saunders, pp. 419-469.

Edwards, M.S., M.A. Rench, C.D. Rinaudo, M. Fabbrini, G. Tuscano, G. Buffi, E. Bartolini, S. Bonacci, C.J. Baker & I. Margarit, (2016) Immune Responses to Invasive Group B Streptococcal Disease in Adults. *Emerg. Infect. Dis.* **22**: 1877-1883.

Ehlenberger, A.G. & V. Nussenzweig, (1977) The role of membrane receptors for C3b and C3d in phagocytosis. *J. Exp. Med.* **145**: 357-371.
Eickhoff, T.C., J.O. Klein, A.K. Daly, D. Ingall & M. Finland, (1964) Neonatal Sepsis and Other Infections Due to Group B Beta-Hemolytic Streptococci. *N. Engl. J. Med.* **271**: 1221-1228.
Eijkelkamp, B.A., J.R. Morey, M.P. Ween, C.L. Ong, A.G. McEwan, J.C. Paton & C.A. McDevitt, (2014) Extracellular zinc competitively inhibits manganese uptake and compromises oxidative stress management in *Streptococcus pneumoniae*. *PLoS ONE* **9**: e89427.
Eisenberg, T., J. Rau, U. Westerhus, T. Knauf-Witzens, A. Fawzy, K. Schlez, M. Zschock, E. Prenger-Berninghoff, C. Heydel, R. Sting, S.P. Glaeser, D. Pulami, M. van der Linden & C. Ewers, (2017) *Streptococcus agalactiae* in elephants - A comparative study with isolates from human and zoo animal and livestock origin. *Vet. Microbiol.* **204**: 141-150.
el-Lati, S.G., C.A. Dahinden & M.K. Church, (1994) Complement peptides C3a- and C5a-induced mediator release from dissociated human skin mast cells. *J. Invest. Dermatol.* **102**: 803-806.
El Ghoroury, A.A., (1950) Comparative studies of group "B" streptococci of human and bovine origin. I. Cultural and biochemical characters. *American Journal of Public of Health* **40**: 1273-1277.
Esser, A.F., (1994) The membrane attack complex of complement. Assembly, structure and cytotoxic activity. *Toxicology* **87**: 229-247.
Evans, K., V. Stone, L. Chen, X. Ge & P. Xu, (2014) Systematic study of genes influencing cellular chain length in Streptococcus sanguinis. *Microbiology* **160**: 307-315.
Fang, F.C., (2004) Antimicrobial reactive oxygen and nitrogen species: concepts and controversies. *Nat. Rev. Microbiol.* **2**: 820-832.
Farley, M.M., (2001) Group B streptococcal disease in nonpregnant adults. *Clin. Infect. Dis.* **33**: 556-561.
Farley, M.M., R.C. Harvey, T. Stull, J.D. Smith, A. Schuchat, J.D. Wenger & D.S. Stephens, (1993) A population-based assessment of invasive disease due to group B Streptococcus in nonpregnant adults. *N. Engl. J. Med.* **328**: 1807-1811.
Fernandes, M.C., L.A. Dillon, A.T. Belew, H.C. Bravo, D.M. Mosser & N.M. El-Sayed, (2016) Dual Transcriptome Profiling of Leishmania-Infected Human Macrophages Reveals Distinct Reprogramming Signatures. *MBio* **7**.
Ferreira-Machado, A.B., M.C. Freitas, G.R. Saji, A.B. Rezende, P.E. Almeida, D.E. Cesar, J.A. Resende, M.F. Nicolas, V.L. Silva & C.G. Diniz, (2015) Integrity of prokaryotic mRNA isolated from complex samples for in vivo bacterial transcriptome analysis. *Genet. Mol. Res.* **14**: 14752-14759.
Ferretti, J. & W. Kohler, (2016) History of Streptococcal Research. In: Streptococcus pyogenes: Basic Biology to Clinical Manifestations. J.J. Ferretti, D.L. Stevens & V.A. Fischetti (eds). Oklahoma City (OK), pp.
Ferrieri, P. & L.L. Blair, (1977) Pharyngeal carriage of group B streptococci: detection by three methods. *J. Clin. Microbiol.* **6**: 136-139.
Ferrieri, P., E.D. Gray & L.W. Wannamaker, (1980) Biochemical and immunological characterization of the extracellular nucleases of group B streptococci. *J. Exp. Med.* **151**: 56-68.
Ferrieri, P., R. Lynfield, R. Creti & A.E. Flores, (2013) Serotype IV and invasive group B Streptococcus disease in neonates, Minnesota, USA, 2000-2010. *Emerg. Infect. Dis.* **19**: 551-558.
Fettucciari, K., F. Quotadamo, R. Noce, C. Palumbo, A. Modesti, E. Rosati, R. Mannucci, A. Bartoli & P. Marconi, (2011) Group B Streptococcus (GBS) disrupts by calpain activation the actin and microtubule cytoskeleton of macrophages. *Cell. Microbiol.* **13**: 859-884.
Finch, L.A. & D.R. Martin, (1984) Human and bovine group B streptococci: two distinct populations. *J. Appl. Bacteriol.* **57**: 273-278.
Finch, R.G., G.L. French & I. Phillips, (1976) Group B streptococci in the female genital tract. *Br. Med. J.* **1**: 1245-1247.

Fiorentino, D.F., M.W. Bond & T.R. Mosmann, (1989) Two types of mouse T helper cell. IV. Th2 clones secrete a factor that inhibits cytokine production by Th1 clones. *J. Exp. Med.* **170**: 2081-2095.

Fiorentino, D.F., A. Zlotnik, T.R. Mosmann, M. Howard & A. O'Garra, (1991) IL-10 inhibits cytokine production by activated macrophages. *J. Immunol.* **147**: 3815-3822.

Fischetti, V.A., V. Pancholi & O. Schneewind, (1990) Conservation of a hexapeptide sequence in the anchor region of surface proteins from gram-positive cocci. *Mol. Microbiol.* **4**: 1603-1605.

Fleischmann, R.D., M.D. Adams, O. White, R.A. Clayton, E.F. Kirkness, A.R. Kerlavage, C.J. Bult, J.F. Tomb, B.A. Dougherty, J.M. Merrick & et al., (1995) Whole-genome random sequencing and assembly of Haemophilus influenzae Rd. *Science* **269**: 496-512.

Flores, A.R., J. Galloway-Pena, P. Sahasrabhojane, M. Saldana, H. Yao, X. Su, N.J. Ajami, M.E. Holder, J.F. Petrosino, E. Thompson, Y.R.I. Margarit, R. Rosini, G. Grandi, N. Horstmann, S. Teatero, A. McGeer, N. Fittipaldi, R. Rappuoli, C.J. Baker & S.A. Shelburne, (2015) Sequence type 1 group B Streptococcus, an emerging cause of invasive disease in adults, evolves by small genetic changes. *Proc. Natl. Acad. Sci. U. S. A.* **112**: 6431-6436.

Fluegge, K., A. Siedler, B. Heinrich, J. Schulte-Moenting, M.J. Moennig, D.B. Bartels, O. Dammann, R. von Kries, R. Berner & G. German Pediatric Surveillance Unit Study, (2006) Incidence and clinical presentation of invasive neonatal group B streptococcal infections in Germany. *Pediatrics* **117**: e1139-1145.

Fortnum, H. & A. Davis, (1993) Hearing impairment in children after bacterial meningitis: incidence and resource implications. *Br. J. Audiol.* **27**: 43-52.

Fortnum, H.M., (1992) Hearing impairment after bacterial meningitis: a review. *Arch. Dis. Child.* **67**: 1128-1133.

Foxman, B., (2010) The epidemiology of urinary tract infection. *Nature Reviews. Urology* **7**: 653-660.

Foxman, B. & P. Brown, (2003) Epidemiology of urinary tract infections: transmission and risk factors, incidence, and costs. *Infect. Dis. Clin. North Am.* **17**: 227-241.

Foxman, B., B.W. Gillespie, S.D. Manning & C.F. Marrs, (2007) Risk factors for group B streptococcal colonization: potential for different transmission systems by capsular type. *Ann. Epidemiol.* **17**: 854-862.

Franciosi, R.A., J.D. Knostman & R.A. Zimmerman, (1973) Group B streptococcal neonatal and infant infections. *J. Pediatr.* **82**: 707-718.

Franken, C., G. Haase, C. Brandt, J. Weber-Heynemann, S. Martin, C. Lammler, A. Podbielski, R. Lutticken & B. Spellerberg, (2001) Horizontal gene transfer and host specificity of beta-haemolytic streptococci: the role of a putative composite transposon containing scpB and lmb. *Mol. Microbiol.* **41**: 925-935.

Freshney, R.I., (2000) *Culture of Animal Cells: A Manual of Basic Technique*. Wiley.

Fry, R.M., (1938) Fatal infections by haemolytic streptococcus Group B. *Lancet* **1**: 199-201.

Furman, D. & M.M. Davis, (2015) New approaches to understanding the immune response to vaccination and infection. *Vaccine* **33**: 5271-5281.

Gabay, C., (2006) Interleukin-6 and chronic inflammation. *Arthritis Res. Ther.* **8 Suppl 2**: S3.

Gardner, S.E., E.O. Mason, Jr. & M.D. Yow, (1980) Community acquisition of group B Streptococcus by infants of colonized mothers. *Pediatrics* **66**: 873-875.

Gebhardt, C., J. Nemeth, P. Angel & J. Hess, (2006) S100A8 and S100A9 in inflammation and cancer. *Biochem. Pharmacol.* **72**: 1622-1631.

Ghalib, H.W., M.R. Piuvezam, Y.A. Skeiky, M. Siddig, F.A. Hashim, A.M. el-Hassan, D.M. Russo & S.G. Reed, (1993) Interleukin 10 production correlates with pathology in human *Leishmania donovani* infections. *J. Clin. Invest.* **92**: 324-329.

Ghatak, S., R.B. Muthukumaran & S.K. Nachimuthu, (2013) A simple method of genomic DNA extraction from human samples for PCR-RFLP analysis. *J. Biomol. Tech.* **24**: 224-231.

Giannoukos, G., D.M. Ciulla, K. Huang, B.J. Haas, J. Izard, J.Z. Levin, J. Livny, A.M. Earl, D. Gevers, D.V. Ward, C. Nusbaum, B.W. Birren & A. Gnirke, (2012) Efficient and robust RNA-seq process for cultured bacteria and complex community transcriptomes. *Genome Biol.* **13**: R23.

Gibbs, R.S., S. Schrag & A. Schuchat, (2004) Perinatal infections due to group B streptococci. *Obstet. Gynecol.* **104**: 1062-1076.

Gibson, R.L., V. Nizet & C.E. Rubens, (1999) Group B streptococcal beta-hemolysin promotes injury of lung microvascular endothelial cells. *Pediatr. Res.* **45**: 626-634.

Gill, C., J.H. van de Wijgert, F. Blow & A.C. Darby, (2016) Evaluation of Lysis Methods for the Extraction of Bacterial DNA for Analysis of the Vaginal Microbiota. *PLoS ONE* **11**: e0163148.

Gilson, E., G. Alloing, T. Schmidt, J.P. Claverys, R. Dudler & M. Hofnung, (1988) Evidence for high affinity binding-protein dependent transport systems in gram-positive bacteria and in Mycoplasma. *EMBO J.* **7**: 3971-3974.

Giri, J.G., P.T. Lomedico & S.B. Mizel, (1985) Studies on the synthesis and secretion of interleukin 1. I. A 33,000 molecular weight precursor for interleukin 1. *J. Immunol.* **134**: 343-349.

Glaser, P., C. Rusniok, C. Buchrieser, F. Chevalier, L. Frangeul, T. Msadek, M. Zouine, E. Couve, L. Lalioui, C. Poyart, P. Trieu-Cuot & F. Kunst, (2002) Genome sequence of *Streptococcus agalactiae*, a pathogen causing invasive neonatal disease. *Mol. Microbiol.* **45**: 1499-1513.

Godambe, S., P.S. Shah & V. Shah, (2005) Breast milk as a source of late onset neonatal sepsis. *Pediatr. Infect. Dis. J.* **24**: 381-382.

Goodwin, S., J.D. McPherson & W.R. McCombie, (2016) Coming of age: ten years of next-generation sequencing technologies. *Nat. Rev. Genet.* **17**: 333-351.

Gordon, S. & P.R. Taylor, (2005) Monocyte and macrophage heterogeneity. *Nat. Rev. Immunol.* **5**: 953-964.

Gotoff, S.P., (1977) Emergence of group B streptococci as major perinatal pathogens. *Hosp. Pract.* **12**: 85-90.

Gottesman, S. & G. Storz, (2011) Bacterial small RNA regulators: versatile roles and rapidly evolving variations. *Cold Spring Harb. Perspect. Biol.* **3**.

Gruenheid, S., E. Pinner, M. Desjardins & P. Gros, (1997) Natural resistance to infection with intracellular pathogens: the Nramp1 protein is recruited to the membrane of the phagosome. *J. Exp. Med.* **185**: 717-730.

Guilbert, J., C. Levy, R. Cohen, g. Bacterial meningitis, C. Delacourt, S. Renolleau & C. Flamant, (2010) Late and ultra late onset Streptococcus B meningitis: clinical and bacteriological data over 6 years in France. *Acta Paediatr.* **99**: 47-51.

Guo, R.F. & P.A. Ward, (2005) Role of C5a in inflammatory responses. *Annu. Rev. Immunol.* **23**: 821-852.

Gutekunst, H., B.J. Eikmanns & D.J. Reinscheid, (2003) Analysis of RogB-controlled virulence mechanisms and gene repression in Streptococcus agalactiae. *Infect. Immun.* **71**: 5056-5064.

Hadders, M.A., D. Bubeck, P. Roversi, S. Hakobyan, F. Forneris, B.P. Morgan, M.K. Pangburn, O. Llorca, S.M. Lea & P. Gros, (2012) Assembly and regulation of the membrane attack complex based on structures of C5b6 and sC5b9. *Cell Reports* **1**: 200-207.

Halaas, O., N.B. Liabakk, R. Vik, C. Beninati, P. Henneke, A. Sundan & T. Espevik, (2004) Monocytes stimulated with group B streptococci or interferons release tumour necrosis factor-related apoptosis-inducing ligand. *Scand. J. Immunol.* **60**: 74-81.

Halket, S., J. de Louvois, D.E. Holt & D. Harvey, (2003) Long term follow up after meningitis in infancy: behaviour of teenagers. *Arch. Dis. Child.* **88**: 395-398.

Hamel, J., N. Charland, I. Pineau, C. Ouellet, S. Rioux, D. Martin & B.R. Brodeur, (2004) Prevention of pneumococcal disease in mice immunized with conserved surface-accessible proteins. *Infect. Immun.* **72**: 2659-2670.

Hammerschmidt, S., S. Wolff, A. Hocke, S. Rosseau, E. Muller & M. Rohde, (2005) Illustration of pneumococcal polysaccharide capsule during adherence and invasion of epithelial cells. *Infect. Immun.* **73**: 4653-4667.

Hanson, B.R., D.L. Runft, C. Streeter, A. Kumar, T.W. Carion & M.N. Neely, (2012) Functional analysis of the CpsA protein of *Streptococcus agalactiae*. *J. Bacteriol.* **194**: 1668-1678.
Hantke, K., (2005) Bacterial zinc uptake and regulators. *Curr. Opin. Microbiol.* **8**: 196-202.
Harada, A., N. Sekido, T. Akahoshi, T. Wada, N. Mukaida & K. Matsushima, (1994) Essential involvement of interleukin-8 (IL-8) in acute inflammation. *J. Leukoc. Biol.* **56**: 559-564.
Harper, I.A., (1971) The importance of group B streptococci as human pathogens in the British Isles. *J. Clin. Pathol.* **24**: 438-441.
Hass, R., H. Bartels, N. Topley, M. Hadam, L. Kohler, M. Goppelt-Strube & K. Resch, (1989) TPA-induced differentiation and adhesion of U937 cells: changes in ultrastructure, cytoskeletal organization and expression of cell surface antigens. *Eur. J. Cell Biol.* **48**: 282-293.
Hassan, K.A., V.G. Pederick, L.D. Elbourne, I.T. Paulsen, J.C. Paton, C.A. McDevitt & B.A. Eijkelkamp, (2017) Zinc stress induces copper depletion in *Acinetobacter baumannii*. *BMC Microbiol.* **17**: 59.
Hauge, M., C. Jespersgaard, K. Poulsen & M. Kilian, (1996) Population structure of *Streptococcus agalactiae* reveals an association between specific evolutionary lineages and putative virulence factors but not disease. *Infect. Immun.* **64**: 919-925.
Hawiger, J., (2001) Innate immunity and inflammation: a transcriptional paradigm. *Immunol. Res.* **23**: 99-109.
Hawlisch, H., M. Wills-Karp, C.L. Karp & J. Kohl, (2004) The anaphylatoxins bridge innate and adaptive immune responses in allergic asthma. *Mol. Immunol.* **41**: 123-131.
Hayrinen, J., S. Pelkonen & J. Finne, (1989) Structural similarity of the type-specific group B streptococcal polysaccharides and the carbohydrate units of tissue glycoproteins: evaluation of possible cross-reactivity. *Vaccine* **7**: 217-224.
Heath, C.J., M. del Mar Cendra, A. Watson, J.P. Auger, A. Pandey, P. Tighe & M. Christodoulides, (2015) Co-Transcriptomes of Initial Interactions In Vitro between *Streptococcus pneumoniae* and Human Pleural Mesothelial Cells. *PLoS ONE* **10**: e0142773.
Helmig, R., N. Uldbjerg, J. Boris & M. Kilian, (1993) Clonal analysis of *Streptococcus agalactiae* isolated from infants with neonatal sepsis or meningitis and their mothers and from healthy pregnant women. *J. Infect. Dis.* **168**: 904-909.
Hemming, V.G., D.W. McCloskey & H.R. Hill, (1976) Pneumonia in the neonate associated with group B streptococcal septicemia. *Am. J. Dis. Child.* **130**: 1231-1233.
Henrichsen, J., P. Ferrieri, J. Jelinkova, W. Koehler & W. Maxted, (1984) Nomenclature of antigens of group B streptococci. *Int. J. Syst. Evol. Microbiol.* **34**: 500-500.
Hensler, M.E., S. Miyamoto & V. Nizet, (2008) Group B streptococcal beta-hemolysin/cytolysin directly impairs cardiomyocyte viability and function. *PLoS ONE* **3**: e2446.
Herbert, M.A., C.J. Beveridge, D. McCormick, E. Aten, N. Jones, L.A. Snyder & N.J. Saunders, (2005) Genetic islands of Streptococcus agalactiae strains NEM316 and 2603VR and their presence in other Group B streptococcal strains. *BMC Microbiol.* **5**: 31.
Heumann, D., C. Barras, A. Severin, M.P. Glauser & A. Tomasz, (1994) Gram-positive cell walls stimulate synthesis of tumor necrosis factor alpha and interleukin-6 by human monocytes. *Infect. Immun.* **62**: 2715-2721.
Hickman, M.E., M.A. Rench, P. Ferrieri & C.J. Baker, (1999) Changing epidemiology of group B streptococcal colonization. *Pediatrics* **104**: 203-209.
Hill, H.R., J.F. Bohnsack, E.Z. Morris, N.H. Augustine, C.J. Parker, P.P. Cleary & J.T. Wu, (1988) Group B streptococci inhibit the chemotactic activity of the fifth component of complement. *J. Immunol.* **141**: 3551-3556.
Holtje, J.V. & E.I. Tuomanen, (1991) The murein hydrolases of *Escherichia coli*: properties, functions and impact on the course of infections in vivo. *J. Gen. Microbiol.* **137**: 441-454.
Hood, M.I. & E.P. Skaar, (2012) Nutritional immunity: transition metals at the pathogen-host interface. *Nat. Rev. Microbiol.* **10**: 525-537.

Hooven, T.A., T.M. Randis, S.C. Daugherty, A. Narechania, P.J. Planet, H. Tettelin & A.J. Ratner, (2014) Complete Genome Sequence of Streptococcus agalactiae CNCTC 10/84, a Hypervirulent Sequence Type 26 Strain. *Genome Announcements* **2**.

Hosein, B. & C. Bianco, (1985) Monocyte receptors for fibronectin characterized by a monoclonal antibody that interferes with receptor activity. *J. Exp. Med.* **162**: 157-170.

Hsi, E.D. & D.G. Remick, (1995) Monocytes are the major producers of interleukin-1 beta in an ex vivo model of local cytokine production. *J. Interferon Cytokine Res.* **15**: 89-94.

Hu, R., Z.F. Chen, J. Yan, Q.F. Li, Y. Huang, H. Xu, X.P. Zhang & H. Jiang, (2015) Endoplasmic Reticulum Stress of Neutrophils Is Required for Ischemia/Reperfusion-Induced Acute Lung Injury. *J. Immunol.* **195**: 4802-4809.

Hull, J.R., G.S. Tamura & D.G. Castner, (2008) Interactions of the streptococcal C5a peptidase with human fibronectin. *Acta Biomaterials* **4**: 504-513.

Hulse, M.L., S. Smith, E.Y. Chi, A. Pham & C.E. Rubens, (1993) Effect of type III group B streptococcal capsular polysaccharide on invasion of respiratory epithelial cells. *Infect. Immun.* **61**: 4835-4841.

Humphrys, M.S., T. Creasy, Y. Sun, A.C. Shetty, M.C. Chibucos, E.F. Drabek, C.M. Fraser, U. Farooq, N. Sengamalay, S. Ott, H. Shou, P.M. Bavoil, A. Mahurkar & G.S. Myers, (2013) Simultaneous transcriptional profiling of bacteria and their host cells. *PLoS ONE* **8**: e80597.

Inoue, K., Y. Akiyama, T. Kinoshita, Y. Higashi & T. Amano, (1976) Evidence for a one-hit theory in the immune bactericidal reaction and demonstration of a multi-hit response for hemolysis by streptolysin O and *Clostridium perfringens* theta-toxin. *Infect. Immun.* **13**: 337-344.

Ipe, D.S., N.L. Ben Zakour, M.J. Sullivan, S.A. Beatson, K.B. Ulett, W.H.J. Benjamin, M.R. Davies, S.J. Dando, N.P. King, A.W. Cripps, M.A. Schembri, G. Dougan & G.C. Ulett, (2015) Discovery and Characterization of Human-Urine Utilization by Asymptomatic-Bacteriuria-Causing *Streptococcus agalactiae*. *Infect. Immun.* **84**: 307-319.

Jabado, N., A. Jankowski, S. Dougaparsad, V. Picard, S. Grinstein & P. Gros, (2000) Natural resistance to intracellular infections: natural resistance-associated macrophage protein 1 (Nramp1) functions as a pH-dependent manganese transporter at the phagosomal membrane. *J. Exp. Med.* **192**: 1237-1248.

Jackson, L.A., R. Hilsdon, M.M. Farley, L.H. Harrison, A.L. Reingold, B.D. Plikaytis, J.D. Wenger & A. Schuchat, (1995) Risk factors for group B streptococcal disease in adults. *Ann. Intern. Med.* **123**: 415-420.

Jacob, J., D. Edwards & L. Gluck, (1980) Early-onset sepsis and pneumonia observed as respiratory distress syndrome: assessment of lung maturity. *Am. J. Dis. Child.* **134**: 766-768.

Jaishankar, J. & P. Srivastava, (2017) Molecular Basis of Stationary Phase Survival and Applications. *Front Microbiol* **8**: 2000.

Jelinkova, J. & J. Motlova, (1985) Worldwide distribution of two new serotypes of group B streptococci: type IV and provisional type V. *J. Clin. Microbiol.* **21**: 361-362.

Jiang, S., S.E. Park, P. Yadav, L.C. Paoletti & M.R. Wessels, (2012) Regulation and function of pilus island 1 in group B streptococcus. *J. Bacteriol.* **194**: 2479-2490.

Jiang, S.M., M.J. Cieslewicz, D.L. Kasper & M.R. Wessels, (2005) Regulation of virulence by a two-component system in group B streptococcus. *J. Bacteriol.* **187**: 1105-1113.

Jiang, S.M., N. Ishmael, J. Dunning Hotopp, M. Puliti, L. Tissi, N. Kumar, M.J. Cieslewicz, H. Tettelin & M.R. Wessels, (2008) Variation in the group B Streptococcus CsrRS regulon and effects on pathogenicity. *J. Bacteriol.* **190**: 1956-1965.

Jobling, S.A., P.E. Auron, G. Gurka, A.C. Webb, B. McDonald, L.J. Rosenwasser & L. Gehrke, (1988) Biological activity and receptor binding of human prointerleukin-1 beta and subpeptides. *J. Biol. Chem.* **263**: 16372-16378.

Johri, A.K., L.C. Paoletti, P. Glaser, M. Dua, P.K. Sharma, G. Grandi & R. Rappuoli, (2006) Group B Streptococcus: global incidence and vaccine development. *Nat. Rev. Microbiol.* **4**: 932-942.

Joiner, K., E. Brown, C. Hammer, K. Warren & M. Frank, (1983) Studies on the mechanism of bacterial resistance to complement-mediated killing. III. C5b-9 deposits stably on rough and type 7 S. pneumoniae without causing bacterial killing. *J. Immunol.* **130**: 845-849.

Jones, N., J.F. Bohnsack, S. Takahashi, K.A. Oliver, M.S. Chan, F. Kunst, P. Glaser, C. Rusniok, D.W. Crook, R.M. Harding, N. Bisharat & B.G. Spratt, (2003) Multilocus sequence typing system for group B streptococcus. *J. Clin. Microbiol.* **41**: 2530-2536.

Jones, N., K.A. Oliver, J. Barry, R.M. Harding, N. Bisharat, B.G. Spratt, T. Peto, D.W. Crook & B.S.C. Oxford Group, (2006) Enhanced invasiveness of bovine-derived neonatal sequence type 17 group B streptococcus is independent of capsular serotype. *Clin. Infect. Dis.* **42**: 915-924.

Jordan, H.T., M.M. Farley, A. Craig, J. Mohle-Boetani, L.H. Harrison, S. Petit, R. Lynfield, A. Thomas, S. Zansky, K. Gershman, B.A. Albanese, W. Schaffner, S.J. Schrag & C.D.C. Active Bacterial Core Surveillance /Emerging Infections Program Network, (2008) Revisiting the need for vaccine prevention of late-onset neonatal group B streptococcal disease: a multistate, population-based analysis. *Pediatr. Infect. Dis. J.* **27**: 1057-1064.

Kaseman, J.A., N.M. Myers, J.E. Miracle & J.P. Myers, (2013) Group B streptococcal bacteremia in adults in the 21st century: review of 132 episodes over a 10-year period in a large community teaching hospital. *Infectious Diseases in Clinical Practice* **21**: 105-110.

Kasper, D.L., (1986) Bacterial capsule--old dogmas and new tricks. *J. Infect. Dis.* **153**: 407-415.

Katz, V.L., M.K. Moos, R.C. Cefalo, J.M. Thorp, Jr., W.A. Bowes, Jr. & S.D. Wells, (1994) Group B streptococci: results of a protocol of antepartum screening and intrapartum treatment. *Am. J. Obstet. Gynecol.* **170**: 521-526.

Kaushik, D.K. & D. Sehgal, (2008) Developing antibacterial vaccines in genomics and proteomics era. *Scandanavian Journal of Immunology* **67**: 544-552.

Kawahara, Y., Y. Oono, H. Kanamori, T. Matsumoto, T. Itoh & E. Minami, (2012) Simultaneous RNA-seq analysis of a mixed transcriptome of rice and blast fungus interaction. *PLoS ONE* **7**: e49423.

Keefe, G.P., (1997) *Streptococcus agalactiae* mastitis: a review. *Can. Vet. J.* **38**: 429-437.

Kehl-Fie, T.E. & E.P. Skaar, (2010) Nutritional immunity beyond iron: a role for manganese and zinc. *Curr. Opin. Chem. Biol.* **14**: 218-224.

Kerr, M.A., (1981) The complement system. *Biochemical Education* **9**: 82-88.

Kethiri, A.R., S. Basu, S. Shukla, V.S. Sangwan & V. Singh, (2017) Optimizing the role of limbal explant size and source in determining the outcomes of limbal transplantation: An in vitro study. *PLoS ONE* **12**: e0185623.

Kim, B., Y. Lee, E. Kim, A. Kwak, S. Ryoo, S.H. Bae, T. Azam, S. Kim & C.A. Dinarello, (2013) The Interleukin-1alpha Precursor is Biologically Active and is Likely a Key Alarmin in the IL-1 Family of Cytokines. *Frontiers in Immunology* **4**: 391.

Kinoshita, T., (1991) Biology of complement: the overture. *Immunol. Today* **12**: 291-295.

Klein, J.S. & O. Lewinson, (2011) Bacterial ATP-driven transporters of transition metals: physiological roles, mechanisms of action, and roles in bacterial virulence. *Metallomics* **3**: 1098-1108.

Kloosterman, T.G., M.M. van der Kooi-Pol, J.J. Bijlsma & O.P. Kuipers, (2007) The novel transcriptional regulator SczA mediates protection against Zn2+ stress by activation of the Zn2+-resistance gene czcD in Streptococcus pneumoniae. *Mol. Microbiol.* **65**: 1049-1063.

Kolaczkowska, E. & P. Kubes, (2013) Neutrophil recruitment and function in health and inflammation. *Nat. Rev. Immunol.* **13**: 159-175.

Kolter, R., D.A. Siegele & A. Tormo, (1993) The stationary phase of the bacterial life cycle. *Annu. Rev. Microbiol.* **47**: 855-874.

Komor, A.C., A.H. Badran & D.R. Liu, (2017) CRISPR-Based Technologies for the Manipulation of Eukaryotic Genomes. *Cell* **169**: 559.

Kong, F., L.M. Lambertsen, H.C. Slotved, D. Ko, H. Wang & G.L. Gilbert, (2008) Use of phenotypic and molecular serotype identification methods to characterize previously nonserotypeable group B streptococci. *J. Clin. Microbiol.* **46**: 2745-2750.

Konto-Ghiorghi, Y., E. Mairey, A. Mallet, G. Dumenil, E. Caliot, P. Trieu-Cuot & S. Dramsi, (2009) Dual role for pilus in adherence to epithelial cells and biofilm formation in *Streptococcus agalactiae*. *PLoS Pathog.* **5**: e1000422.

Koonin, E.V., (2012) Does the central dogma still stand? *Biol. Direct* **7**: 27.

Koren, S., G.P. Harhay, T.P. Smith, J.L. Bono, D.M. Harhay, S.D. McVey, D. Radune, N.H. Bergman & A.M. Phillippy, (2013) Reducing assembly complexity of microbial genomes with single-molecule sequencing. *Genome Biol.* **14**: R101.

Krishnan, V., A.H. Gaspar, N. Ye, A. Mandlik, H. Ton-That & S.V. Narayana, (2007) An IgG-like domain in the minor pilin GBS52 of *Streptococcus agalactiae* mediates lung epithelial cell adhesion. *Structure* **15**: 893-903.

Kunitomo, E., Y. Terao, S. Okamoto, T. Rikimaru, S. Hamada & S. Kawabata, (2008) Molecular and biological characterization of histidine triad protein in group A streptococci. *Microbes Infect.* **10**: 414-423.

Kunkel, S.L., N. Lukacs & R.M. Strieter, (1995) Expression and biology of neutrophil and endothelial cell-derived chemokines. *Semin. Cell Biol.* **6**: 327-336.

Lagunoff, D., T.W. Martin & G. Read, (1983) Agents that release histamine from mast cells. *Annu. Rev. Pharmacol. Toxicol.* **23**: 331-351.

Lambris, J.D., D. Ricklin & B.V. Geisbrecht, (2008) Complement evasion by human pathogens. *Nat. Rev. Microbiol.* **6**: 132-142.

Lamy, M.C., S. Dramsi, A. Billoet, H. Reglier-Poupet, A. Tazi, J. Raymond, F. Guerin, E. Couve, F. Kunst, P. Glaser, P. Trieu-Cuot & C. Poyart, (2006) Rapid detection of the "highly virulent" group B Streptococcus ST-17 clone. *Microbes Infect.* **8**: 1714-1722.

Lamy, M.C., M. Zouine, J. Fert, M. Vergassola, E. Couve, E. Pellegrini, P. Glaser, F. Kunst, T. Msadek, P. Trieu-Cuot & C. Poyart, (2004) CovS/CovR of group B streptococcus: a two-component global regulatory system involved in virulence. *Mol. Microbiol.* **54**: 1250-1268.

Lanari, M., L. Serra, F. Cavrini, G. Liguori & V. Sambri, (2007) Late-onset group B streptococcal disease by infected mother's milk detected by polymerase chain reaction. *New Microbiology* **30**: 253-254.

Lancefield, R.C., (1928) The Antigenic Complex of Streptococcus Haemolyticus : Iii. Chemical and Immunological Properties of the Species-Specific Substance. *J. Exp. Med.* **47**: 481-491.

Lancefield, R.C., (1933) A Serological Differentiation of Human and Other Groups of Hemolytic Streptococci. *J. Exp. Med.* **57**: 571-595.

Lancefield, R.C., (1934) A Serological Differentiation of Specific Types of Bovine Hemolytic Streptococci (Group B). *J. Exp. Med.* **59**: 441-458.

Lancefield, R.C., (1938) Two Serological Types of Group B Hemolytic Streptococci with Related, but Not Identical, Type-Specific Substances. *J. Exp. Med.* **67**: 25-40.

Lancefield, R.C., M. McCarty & W.N. Everly, (1975) Multiple mouse-protective antibodies directed against group B streptococci. Special reference to antibodies effective against protein antigens. *J. Exp. Med.* **142**: 165-179.

Land, M., L. Hauser, S.R. Jun, I. Nookaew, M.R. Leuze, T.H. Ahn, T. Karpinets, O. Lund, G. Kora, T. Wassenaar, S. Poudel & D.W. Ussery, (2015) Insights from 20 years of bacterial genome sequencing. *Funct. Integr. Genomics* **15**: 141-161.

Lauer, P., C.D. Rinaudo, M. Soriani, I. Margarit, D. Maione, R. Rosini, A.R. Taddei, M. Mora, R. Rappuoli, G. Grandi & J.L. Telford, (2005) Genome analysis reveals pili in Group B Streptococcus. *Science* **309**: 105.

Leclercq, S.Y., M.J. Sullivan, D.S. Ipe, J.P. Smith, A.W. Cripps & G.C. Ulett, (2016) Pathogenesis of *Streptococcus* urinary tract infection depends on bacterial strain and beta-hemolysin/cytolysin that mediates cytotoxicity, cytokine synthesis, inflammation and virulence. *Scientific Reports* **6**: 29000.

Lee, Y.H., M.R. Dorwart, K.R. Hazlett, R.K. Deka, M.V. Norgard, J.D. Radolf & C.A. Hasemann, (2002) The crystal structure of Zn(II)-free *Treponema pallidum* TroA, a periplasmic metal-binding protein, reveals a closed conformation. *J. Bacteriol.* **184**: 2300-2304.

Lehmann, M.H., (1998) Recombinant human granulocyte-macrophage colony-stimulating factor triggers interleukin-10 expression in the monocytic cell line U937. *Mol. Immunol.* **35**: 479-485.

Levene, M.J., J. Korlach, S.W. Turner, M. Foquet, H.G. Craighead & W.W. Webb, (2003) Zero-mode waveguides for single-molecule analysis at high concentrations. *Science* **299**: 682-686.

Levy, O., R.M. Jean-Jacques, C. Cywes, R.B. Sisson, K.A. Zarember, P.J. Godowski, J.L. Christianson, H.K. Guttormsen, M.C. Carroll, A. Nicholson-Weller & M.R. Wessels, (2003) Critical role of the complement system in group B streptococcus-induced tumor necrosis factor alpha release. *Infect. Immun.* **71**: 6344-6353.

Lewis, A.L., H. Cao, S.K. Patel, S. Diaz, W. Ryan, A.F. Carlin, V. Thon, W.G. Lewis, A. Varki, X. Chen & V. Nizet, (2007) NeuA sialic acid O-acetylesterase activity modulates O-acetylation of capsular polysaccharide in group B Streptococcus. *J. Biol. Chem.* **282**: 27562-27571.

Lewis, A.L., V. Nizet & A. Varki, (2004) Discovery and characterization of sialic acid O-acetylation in group B Streptococcus. *Proc. Natl. Acad. Sci. U. S. A.* **101**: 11123-11128.

Lim, K.H., C.E. Jones, R.N. vanden Hoven, J.L. Edwards, M.L. Falsetta, M.A. Apicella, M.P. Jennings & A.G. McEwan, (2008) Metal binding specificity of the MntABC permease of *Neisseria gonorrhoeae* and its influence on bacterial growth and interaction with cervical epithelial cells. *Infect. Immun.* **76**: 3569-3576.

Lim, S., E. Crawley, P. Woo & P.J. Barnes, (1998) Haplotype associated with low interleukin-10 production in patients with severe asthma. *Lancet* **352**: 113.

Lin, A.E., C.A. Autran, A. Szyszka, T. Escajadillo, M. Huang, K. Godula, A.R. Prudden, G.J. Boons, A.L. Lewis, K.S. Doran, V. Nizet & L. Bode, (2017) Human milk oligosaccharides inhibit growth of group B Streptococcus. *J. Biol. Chem.* **292**: 11243-11249.

Lin, F.Y., L.E. Weisman, J. Troendle & K. Adams, (2003) Prematurity is the major risk factor for late-onset group B streptococcus disease. *J. Infect. Dis.* **188**: 267-271.

Lin, W.J., D. Walthers, J.E. Connelly, K. Burnside, K.A. Jewell, L.J. Kenney & L. Rajagopal, (2009) Threonine phosphorylation prevents promoter DNA binding of the Group B Streptococcus response regulator CovR. *Mol. Microbiol.* **71**: 1477-1495.

Lipsitch, M., (2001) The rise and fall of antimicrobial resistance. *Trends Microbiol.* **9**: 438-444.

Liu, G., W. Zhang & C. Lu, (2012) Complete genome sequence of Streptococcus agalactiae GD201008-001, isolated in China from tilapia with meningoencephalitis. *J. Bacteriol.* **194**: 6653.

Liu, G.Y., K.S. Doran, T. Lawrence, N. Turkson, M. Puliti, L. Tissi & V. Nizet, (2004) Sword and shield: linked group B streptococcal beta-hemolysin/cytolysin and carotenoid pigment function to subvert host phagocyte defense. *Proc. Natl. Acad. Sci. U. S. A.* **101**: 14491-14496.

Liu, G.Y. & V. Nizet, (2004) Extracellular virulence factors of group B Streptococci. *Front. Biosci.* **9**: 1794-1802.

Liu, G.Y. & V. Nizet, (2006) *The group B streptococcal beta-hemolysin/cytolysin,* p. 737-747. Elsevier, Boston.

Lizcano, A., C.J. Sanchez & C.J. Orihuela, (2012) A role for glycosylated serine-rich repeat proteins in gram-positive bacterial pathogenesis. *Molecular Oral Microbiology* **27**: 257-269.

Llorens, F., M. Hummel, X. Pastor, A. Ferrer, R. Pluvinet, A. Vivancos, E. Castillo, S. Iraola, A.M. Mosquera, E. Gonzalez, J. Lozano, M. Ingham, J.C. Dohm, M. Noguera, R. Kofler, J.A. del Rio, M. Bayes, H. Himmelbauer & L. Sumoy, (2011) Multiple platform assessment of the EGF dependent transcriptome by microarray and deep tag sequencing analysis. *BMC Genomics* **12**: 326.

Loisel, E., S. Chimalapati, C. Bougault, A. Imberty, B. Gallet, A.M. Di Guilmi, J. Brown, T. Vernet & C. Durmort, (2011) Biochemical characterization of the histidine triad protein PhtD as a cell surface zinc-binding protein of pneumococcus. *Biochemistry (Mosc.)* **50**: 3551-3558.

Loisel, E., L. Jacquamet, L. Serre, C. Bauvois, J.L. Ferrer, T. Vernet, A.M. Di Guilmi & C. Durmort, (2008) AdcAII, a new pneumococcal Zn-binding protein homologous with ABC transporters: biochemical and structural analysis. *J. Mol. Biol.* **381**: 594-606.

Loman, N.J., C. Constantinidou, J.Z. Chan, M. Halachev, M. Sergeant, C.W. Penn, E.R. Robinson & M.J. Pallen, (2012) High-throughput bacterial genome sequencing: an embarrassment of choice, a world of opportunity. *Nat. Rev. Microbiol.* **10**: 599-606.

Loman, N.J. & M.J. Pallen, (2015) Twenty years of bacterial genome sequencing. *Nat. Rev. Microbiol.* **13**: 787-794.

Lonnemann, G., S. Endres, J.W. Van der Meer, J.G. Cannon, K.M. Koch & C.A. Dinarello, (1989) Differences in the synthesis and kinetics of release of interleukin 1 alpha, interleukin 1 beta and tumor necrosis factor from human mononuclear cells. *Eur. J. Immunol.* **19**: 1531-1536.

Loo, C.Y., K. Mitrakul, I.B. Voss, C.V. Hughes & N. Ganeshkumar, (2003) Involvement of the *adc* operon and manganese homeostasis in *Streptococcus gordonii* biofilm formation. *J. Bacteriol.* **185**: 2887-2900.

Luan, S.L., M. Granlund, M. Sellin, T. Lagergard, B.G. Spratt & M. Norgren, (2005) Multilocus sequence typing of Swedish invasive group B streptococcus isolates indicates a neonatally associated genetic lineage and capsule switching. *J. Clin. Microbiol.* **43**: 3727-3733.

Lundquist, P.M., C.F. Zhong, P. Zhao, A.B. Tomaney, P.S. Peluso, J. Dixon, B. Bettman, Y. Lacroix, D.P. Kwo, E. McCullough, M. Maxham, K. Hester, P. McNitt, D.M. Grey, C. Henriquez, M. Foquet, S.W. Turner & D. Zaccarin, (2008) Parallel confocal detection of single molecules in real time. *Opt. Lett.* **33**: 1026-1028.

Ma, Z., F.E. Jacobsen & D.P. Giedroc, (2009) Coordination chemistry of bacterial metal transport and sensing. *Chem. Rev.* **109**: 4644-4681.

MacFarquhar, J.K., T.F. Jones, A.M. Woron, M.A. Kainer, C.G. Whitney, B. Beall, S.J. Schrag & W. Schaffner, (2010) Outbreak of late-onset group B Streptococcus in a neonatal intensive care unit. *Am. J. Infect. Control* **38**: 283-288.

Madureira, P., E.B. Andrade, B. Gama, L. Oliveira, S. Moreira, A. Ribeiro, M. Correia-Neves, P. Trieu-Cuot, M. Vilanova & P. Ferreira, (2011) Inhibition of IL-10 production by maternal antibodies against Group B Streptococcus GAPDH confers immunity to offspring by favoring neutrophil recruitment. *PLoS Pathog.* **7**: e1002363.

Madureira, P., M. Baptista, M. Vieira, V. Magalhaes, A. Camelo, L. Oliveira, A. Ribeiro, D. Tavares, P. Trieu-Cuot, M. Vilanova & P. Ferreira, (2007) *Streptococcus agalactiae* GAPDH is a virulence-associated immunomodulatory protein. *J. Immunol.* **178**: 1379-1387.

Magalhaes, V., E.B. Andrade, J. Alves, A. Ribeiro, K.S. Kim, M. Lima, P. Trieu-Cuot & P. Ferreira, (2013) Group B Streptococcus hijacks the host plasminogen system to promote brain endothelial cell invasion. *PLoS ONE* **8**: e63244.

Magalhaes, V., I. Veiga-Malta, M.R. Almeida, M. Baptista, A. Ribeiro, P. Trieu-Cuot & P. Ferreira, (2007) Interaction with human plasminogen system turns on proteolytic activity in *Streptococcus agalactiae* and enhances its virulence in a mouse model. *Microbes Infect.* **9**: 1276-1284.

Maisey, H.C., M. Hensler, V. Nizet & K.S. Doran, (2007) Group B streptococcal pilus proteins contribute to adherence to and invasion of brain microvascular endothelial cells. *J. Bacteriol.* **189**: 1464-1467.

Maisey, H.C., D. Quach, M.E. Hensler, G.Y. Liu, R.L. Gallo, V. Nizet & K.S. Doran, (2008) A group B streptococcal pilus protein promotes phagocyte resistance and systemic virulence. *FASEB J.* **22**: 1715-1724.

Malek, B.A.E., N.D. Embleton & A.D. Loughney, (2005) Group B streptococcal disease: screening and treatment in pregnancy. *The Obstetrician & Gynaecologist* **7**: 34-39.

Mangan, D.F., S.E. Mergenhagen & S.M. Wahl, (1993) Apoptosis in human monocytes: possible role in chronic inflammatory diseases. *J. Periodontol.* **64**: 461-466.
Manning, S.D., K. Neighbors, P.A. Tallman, B. Gillespie, C.F. Marrs, S.M. Borchardt, C.J. Baker, M.D. Pearlman & B. Foxman, (2004) Prevalence of group B streptococcus colonization and potential for transmission by casual contact in healthy young men and women. *Clin. Infect. Dis.* **39**: 380-388.
Manthey, H.D., T.M. Woodruff, S.M. Taylor & P.N. Monk, (2009) Complement component 5a (C5a). *Int. J. Biochem. Cell Biol.* **41**: 2114-2117.
Marchlewicz, B.A. & J.L. Duncan, (1981) Lysis of erythrocytes by a hemolysin produced by a group B Streptococcus sp. *Infect. Immun.* **34**: 787-794.
Marder, S.R., D.E. Chenoweth, I.M. Goldstein & H.D. Perez, (1985) Chemotactic responses of human peripheral blood monocytes to the complement-derived peptides C5a and C5a des Arg. *J. Immunol.* **134**: 3325-3331.
Mardis, E.R., (2011) A decade's perspective on DNA sequencing technology. *Nature* **470**: 198-203.
Mardis, E.R., (2013) Next-generation sequencing platforms. *Annu. Rev. Anal. Chem.* **6**: 287-303.
Maret, W., (2013) Zinc biochemistry: from a single zinc enzyme to a key element of life. *Advances in Nutrition* **4**: 82-91.
Marques, M.B., D.L. Kasper, M.K. Pangburn & M.R. Wessels, (1992) Prevention of C3 deposition by capsular polysaccharide is a virulence mechanism of type III group B streptococci. *Infect. Immun.* **60**: 3986-3993.
Marques, M.B., D.L. Kasper, A. Shroff, F. Michon, H.J. Jennings & M.R. Wessels, (1994) Functional activity of antibodies to the group B polysaccharide of group B streptococci elicited by a polysaccharide-protein conjugate vaccine. *Infect. Immun.* **62**: 1593-1599.
Martin, J.A. & Z. Wang, (2011) Next-generation transcriptome assembly. *Nat. Rev. Genet.* **12**: 671-682.
Martin, J.E., K.A. Edmonds, K.E. Bruce, G.C. Campanello, B.A. Eijkelkamp, E.B. Brazel, C.A. McDevitt, M.E. Winkler & D.P. Giedroc, (2017) The zinc efflux activator SczA protects Streptococcus pneumoniae serotype 2 D39 from intracellular zinc toxicity. *Mol. Microbiol.* **104**: 636-651.
Martin, T.R., J.T. Ruzinski, C.E. Rubens, E.Y. Chi & C.B. Wilson, (1992) The effect of type-specific polysaccharide capsule on the clearance of group B streptococci from the lungs of infant and adult rats. *J. Infect. Dis.* **165**: 306-314.
Maruvada, R., N.V. Prasadarao & C.E. Rubens, (2009) Acquisition of factor H by a novel surface protein on group B Streptococcus promotes complement degradation. *FASEB J.* **23**: 3967-3977.
Matsushima, K., K. Morishita, T. Yoshimura, S. Lavu, Y. Kobayashi, W. Lew, E. Appella, H.F. Kung, E.J. Leonard & J.J. Oppenheim, (1988) Molecular cloning of a human monocyte-derived neutrophil chemotactic factor (MDNCF) and the induction of MDNCF mRNA by interleukin 1 and tumor necrosis factor. *J. Exp. Med.* **167**: 1883-1893.
Mavromatis, C.H., N.J. Bokil, M. Totsika, A. Kakkanat, K. Schaale, C.V. Cannistraci, T. Ryu, S.A. Beatson, G.C. Ulett, M.A. Schembri, M.J. Sweet & T. Ravasi, (2015) The co-transcriptome of uropathogenic *Escherichia coli*-infected mouse macrophages reveals new insights into host-pathogen interactions. *Cell. Microbiol.* **17**: 730-746.
McCormack, M.P., L.F. Young, S. Vasudevan, C.A. de Graaf, R. Codrington, T.H. Rabbitts, S.M. Jane & D.J. Curtis, (2010) The Lmo2 oncogene initiates leukemia in mice by inducing thymocyte self-renewal. *Science* **327**: 879-883.
McDevitt, C.A., A.D. Ogunniyi, E. Valkov, M.C. Lawrence, B. Kobe, A.G. McEwan & J.C. Paton, (2011) A molecular mechanism for bacterial susceptibility to zinc. *PLoS Pathog.* **7**: e1002357.
McNeely, T.B., J.M. Staub, C.M. Rusk, M.J. Blum & J.J. Donnelly, (1998) Antibody responses to capsular polysaccharide backbone and O-acetate side groups of Streptococcus pneumoniae type 9V in humans and rhesus macaques. *Infect. Immun.* **66**: 3705-3710.
Medzhitov, R. & C. Janeway, Jr., (2000) Innate immunity. *N. Engl. J. Med.* **343**: 338-344.

Meehan, M., R. Cunney & M. Cafferkey, (2014) Molecular epidemiology of group B streptococci in Ireland reveals a diverse population with evidence of capsular switching. *Eur. J. Clin. Microbiol. Infect. Dis.* **33**: 1155-1162.

Mege, J.L., S. Meghari, A. Honstettre, C. Capo & D. Raoult, (2006) The two faces of interleukin 10 in human infectious diseases. *Lancet Infect. Dis.* **6**: 557-569.

Melchers, W.J., J.M. Bakkers, M. Toonen, F.J. van Kuppeveld, M. Trijbels & J.A. Hoogkamp-Korstanje, (2003) Genetic analysis of Streptococcus agalactiae strains isolated from neonates and their mothers. *FEMS Immunol. Med. Microbiol.* **36**: 111-113.

Mereghetti, L., I. Sitkiewicz, N.M. Green & J.M. Musser, (2008) Extensive adaptive changes occur in the transcriptome of Streptococcus agalactiae (group B streptococcus) in response to incubation with human blood. *PLoS ONE* **3**: e3143.

Metzker, M.L., (2010) Sequencing technologies - the next generation. *Nat. Rev. Genet.* **11**: 31-46.

Meyn, L.A., D.M. Moore, S.L. Hillier & M.A. Krohn, (2002) Association of sexual activity with colonization and vaginal acquisition of group B Streptococcus in nonpregnant women. *Am. J. Epidemiol.* **155**: 949-957.

Mikamo, H., A.K. Johri, L.C. Paoletti, L.C. Madoff & A.B. Onderdonk, (2004) Adherence to, invasion by, and cytokine production in response to serotype VIII group B Streptococci. *Infect. Immun.* **72**: 4716-4722.

Miller, J.D. & M.N. Neely, (2005) Large-scale screen highlights the importance of capsule for virulence in the zoonotic pathogen Streptococcus iniae. *Infect. Immun.* **73**: 921-934.

Minta, J.O. & L. Pambrun, (1985) In vitro induction of cytologic and functional differentiation of the immature human monocytelike cell line U-937 with phorbol myristate acetate. *Am. J. Pathol.* **119**: 111-126.

Monk, P.N., A.M. Scola, P. Madala & D.P. Fairlie, (2007) Function, structure and therapeutic potential of complement C5a receptors. *Br. J. Pharmacol.* **152**: 429-448.

Moore, K.W., R. de Waal Malefyt, R.L. Coffman & A. O'Garra, (2001) Interleukin-10 and the interleukin-10 receptor. *Annu. Rev. Immunol.* **19**: 683-765.

Morange, M., (2008) What history tells us XIII. Fifty years of the Central Dogma. *Journal of Biosciences* **33**: 171-175.

Morgan, B.P., (1999) Regulation of the complement membrane attack pathway. *Crit. Rev. Immunol.* **19**: 173-198.

Morozova, O. & M.A. Marra, (2008) Applications of next-generation sequencing technologies in functional genomics. *Genomics* **92**: 255-264.

Mosley, B., D.L. Urdal, K.S. Prickett, A. Larsen, D. Cosman, P.J. Conlon, S. Gillis & S.K. Dower, (1987) The interleukin-1 receptor binds the human interleukin-1 alpha precursor but not the interleukin-1 beta precursor. *J. Biol. Chem.* **262**: 2941-2944.

Moulin, P., K. Patron, C. Cano, M.A. Zorgani, E. Camiade, E. Borezee-Durant, A. Rosenau, L. Mereghetti & A. Hiron, (2016) The Adc/Lmb System Mediates Zinc Acquisition in *Streptococcus agalactiae* and Contributes to Bacterial Growth and Survival. *J. Bacteriol.* **198**: 3265-3277.

Moulin, P., V. Rong, E.S.A. Ribeiro, V.G. Pederick, E. Camiade, L. Mereghetti, C.A. McDevitt & A. Hiron, (2019) Defining the Role of the *Streptococcus agalactiae* Sht-Family Proteins in Zinc Acquisition and Complement Evasion. *J. Bacteriol.* **201**.

Munoz, P., T. Coque, M. Rodriguez Creixems, J.C. Bernaldo de Quiros, S. Moreno & E. Bouza, (1992) Group B Streptococcus: a cause of urinary tract infection in nonpregnant adults. *Clin. Infect. Dis.* **14**: 492-496.

Nagano, Y., N. Nagano, S. Takahashi, K. Murono, K. Fujita, F. Taguchi & Y. Okuwaki, (1991) Restriction endonuclease digest patterns of chromosomal DNA from group B beta-haemolytic streptococci. *J. Med. Microbiol.* **35**: 297-303.

Nelson, M.L. & S.B. Levy, (2011) The history of the tetracyclines. *Annals of the New York Academy of Science* **1241**: 17-32.

Neubert, M.J., E.A. Dahlmann, A. Ambrose & M.D.L. Johnson, (2017) Copper Chaperone CupA and Zinc Control CopY Regulation of the Pneumococcal cop Operon. *mSphere* **2**.

Newton, E.R., M.C. Butler & R.N. Shain, (1996) Sexual behavior and vaginal colonization by group B streptococcus among minority women. *Obstet. Gynecol.* **88**: 577-582.

Ng, W.L., K.M. Kazmierczak & M.E. Winkler, (2004) Defective cell wall synthesis in Streptococcus pneumoniae R6 depleted for the essential PcsB putative murein hydrolase or the VicR (YycF) response regulator. *Mol. Microbiol.* **53**: 1161-1175.

Ng, W.L., G.T. Robertson, K.M. Kazmierczak, J. Zhao, R. Gilmour & M.E. Winkler, (2003) Constitutive expression of PcsB suppresses the requirement for the essential VicR (YycF) response regulator in Streptococcus pneumoniae R6. *Mol. Microbiol.* **50**: 1647-1663.

Nicod, L.P., F. el Habre, J.M. Dayer & N. Boehringer, (1995) Interleukin-10 decreases tumor necrosis factor alpha and beta in alloreactions induced by human lung dendritic cells and macrophages. *Am. J. Respir. Cell Mol. Biol.* **13**: 83-90.

Nies, D.H., (2003) Efflux-mediated heavy metal resistance in prokaryotes. *FEMS Microbiol. Rev.* **27**: 313-339.

Nizet, V., (2002) Streptococcal beta-hemolysins: genetics and role in disease pathogenesis. *Trends Microbiol.* **10**: 575-580.

Nizet, V., R.L. Gibson, E.Y. Chi, P.E. Framson, M. Hulse & C.E. Rubens, (1996) Group B streptococcal beta-hemolysin expression is associated with injury of lung epithelial cells. *Infect. Immun.* **64**: 3818-3826.

Nizet, V., K.S. Kim, M. Stins, M. Jonas, E.Y. Chi, D. Nguyen & C.E. Rubens, (1997) Invasion of brain microvascular endothelial cells by group B streptococci. *Infect. Immun.* **65**: 5074-5081.

O'Brien, L.M., E.J. Walsh, R.C. Massey, S.J. Peacock & T.J. Foster, (2002) Staphylococcus aureus clumping factor B (ClfB) promotes adherence to human type I cytokeratin 10: implications for nasal colonization. *Cell. Microbiol.* **4**: 759-770.

Ogunniyi, A.D., M. Grabowicz, L.K. Mahdi, J. Cook, D.L. Gordon, T.A. Sadlon & J.C. Paton, (2009) Pneumococcal histidine triad proteins are regulated by the Zn2+-dependent repressor AdcR and inhibit complement deposition through the recruitment of complement factor H. *FASEB J.* **23**: 731-738.

Olsson, I., U. Gullberg, I. Ivhed & K. Nilsson, (1983) Induction of differentiation of the human histiocytic lymphoma cell line U-937 by 1 alpha,25-dihydroxycholecalciferol. *Cancer Res.* **43**: 5862-5867.

Ong, C.L., C.M. Gillen, T.C. Barnett, M.J. Walker & A.G. McEwan, (2014a) An antimicrobial role for zinc in innate immune defense against group A streptococcus. *J. Infect. Dis.* **209**: 1500-1508.

Ong, C.L., C.M. Gillen, T.C. Barnett, M.J. Walker & A.G. McEwan, (2014b) An antimicrobial role for zinc in innate immune defense against group A streptococcus. *J. Infect. Dis.* **209**: 1500-1508.

Ong, C.L., M.J. Walker & A.G. McEwan, (2015) Zinc disrupts central carbon metabolism and capsule biosynthesis in *Streptococcus pyogenes*. *Scientific Reports* **5**: 10799.

Oppenheim, J.J., K. Matsushima, T. Yoshimura, E.J. Leonard & R. Neta, (1989) Relationship between interleukin 1 (IL1), tumor necrosis factor (TNF) and a neutrophil attracting peptide (NAP-1). *Agents Actions* **26**: 134-140.

Ordas, A., Z. Hegedus, C.V. Henkel, O.W. Stockhammer, D. Butler, H.J. Jansen, P. Racz, M. Mink, H.P. Spaink & A.H. Meijer, (2011) Deep sequencing of the innate immune transcriptomic response of zebrafish embryos to *Salmonella* infection. *Fish & Shellfish Immunology* **31**: 716-724.

Palmeiro, J.K., L.M. Dalla-Costa, S.E. Fracalanzza, A.C. Botelho, K. da Silva Nogueira, M.C. Scheffer, R.S. de Almeida Torres, N.S. de Carvalho, L.L. Cogo & H.M. Madeira, (2010) Phenotypic and genotypic characterization of group B streptococcal isolates in southern Brazil. *J. Clin. Microbiol.* **48**: 4397-4403.

Panina, E.M., A.A. Mironov & M.S. Gelfand, (2003) Comparative genomics of bacterial zinc regulons: enhanced ion transport, pathogenesis, and rearrangement of ribosomal proteins. *Proc. Natl. Acad. Sci. U. S. A.* **100**: 9912-9917.

Paoletti, L.C. & D.L. Kasper, (2003) Glycoconjugate vaccines to prevent group B streptococcal infections. *Expert Opin. Biol. Ther.* **3**: 975-984.

Paredes, A., P. Wong, E.O. Mason, Jr., L.H. Taber & F.F. Barrett, (1977) Nosocomial transmission of group B Streptococci in a newborn nursery. *Pediatrics* **59**: 679-682.

Patterson, M.J., (1996) Streptococcus. In: Medical Microbiology. S. Baron (ed). Galveston (TX), pp.

Pattison, I.H., P.R. Matthews & D.G. Howell, (1955a) The type classification of group-B streptococci, with special reference to bovine strains apparently lacking in type polysaccharide. *The Journal of Pathology and Bacteriology* **69**: 51-60.

Pattison, I.H., P.R. Matthews & W.R. Maxted, (1955b) Type classification by Lancefield's precipitin method of human and bovine group-B streptococci isolated in Britain. *The Journal of Pathology and Bacteriology* **69**: 43-50.

Payne, N.R., B.A. Burke, D.L. Day, P.D. Christenson, T.R. Thompson & P. Ferrieri, (1988) Correlation of clinical and pathologic findings in early onset neonatal group B streptococcal infection with disease severity and prediction of outcome. *Pediatr. Infect. Dis. J.* **7**: 836-847.

Peotta, V.A., F.L. Gomes, A.C. Arnholdt & P.E. Nagao, (2001) Human monocytes and monocyte-derived macrophage phagocytosis of serotype III group B streptococci strains. *Curr. Microbiol.* **43**: 64-68.

Pestka, S., C.D. Krause, D. Sarkar, M.R. Walter, Y. Shi & P.B. Fisher, (2004) Interleukin-10 and related cytokines and receptors. *Annu. Rev. Immunol.* **22**: 929-979.

Pezzicoli, A., I. Santi, P. Lauer, R. Rosini, D. Rinaudo, G. Grandi, J.L. Telford & M. Soriani, (2008) Pilus backbone contributes to group B Streptococcus paracellular translocation through epithelial cells. *J. Infect. Dis.* **198**: 890-898.

Pfaffl, M.W., (2001) A new mathematical model for relative quantification in real-time RT-PCR. *Nucleic Acids Res.* **29**: e45.

Phares, C.R., R. Lynfield, M.M. Farley, J. Mohle-Boetani, L.H. Harrison, S. Petit, A.S. Craig, W. Schaffner, S.M. Zansky, K. Gershman, K.R. Stefonek, B.A. Albanese, E.R. Zell, A. Schuchat & S.J. Schrag, (2008) Epidemiology of invasive group B streptococcal disease in the United States, 1999-2005. *Journal of the American Medical Association* **299**: 2056-2065.

Pinho, M.G., M. Kjos & J.W. Veening, (2013) How to get (a)round: mechanisms controlling growth and division of coccoid bacteria. *Nat. Rev. Microbiol.* **11**: 601-614.

Plastridge, W.N., (1958) Bovine Mastitis - a Review. *J. Dairy Sci.* **41**: 1141-1181.

Platt, M.W., (1995) In vivo hemolytic activity of group B streptococcus is dependent on erythrocyte-bacteria contact and independent of a carrier molecule. *Curr. Microbiol.* **31**: 5-9.

Plumptre, C.D., A.D. Ogunniyi & J.C. Paton, (2012) Polyhistidine triad proteins of pathogenic streptococci. *Trends Microbiol.* **20**: 485-493.

Podack, E.R., (1984) Molecular composition of the tubular structure of the membrane attack complex of complement. *J. Biol. Chem.* **259**: 8641-8647.

Ponnuraj, K., M.G. Bowden, S. Davis, S. Gurusiddappa, D. Moore, D. Choe, Y. Xu, M. Hook & S.V.L. Narayana, (2003) A "dock, lock, and latch" structural model for a staphylococcal adhesin binding to fibrinogen. *Cell* **115**: 217-228.

Porcheron, G., A. Garenaux, J. Proulx, M. Sabri & C.M. Dozois, (2013) Iron, copper, zinc, and manganese transport and regulation in pathogenic Enterobacteria: correlations between strains, site of infection and the relative importance of the different metal transport systems for virulence. *Front Cell Infect Microbiol* **3**: 90.

Poyart, C., H. Reglier-Poupet, A. Tazi, A. Billoet, N. Dmytruk, P. Bidet, E. Bingen, J. Raymond & P. Trieu-Cuot, (2008) Invasive group B streptococcal infections in infants, France. *Emerg. Infect. Dis.* **14**: 1647-1649.

Poyart, C., A. Tazi, H. Reglier-Poupet, A. Billoet, N. Tavares, J. Raymond & P. Trieu-Cuot, (2007) Multiplex PCR assay for rapid and accurate capsular typing of group B streptococci. *J. Clin. Microbiol.* **45**: 1985-1988.

Pritzlaff, C.A., J.C. Chang, S.P. Kuo, G.S. Tamura, C.E. Rubens & V. Nizet, (2001) Genetic basis for the beta-haemolytic/cytolytic activity of group B Streptococcus. *Mol. Microbiol.* **39**: 236-247.

Raghavan, R., E.A. Groisman & H. Ochman, (2011a) Genome-wide detection of novel regulatory RNAs in E. coli. *Genome Res.* **21**: 1487-1497.

Raghavan, R., A. Sage & H. Ochman, (2011b) Genome-wide identification of transcription start sites yields a novel thermosensing RNA and new cyclic AMP receptor protein-regulated genes in Escherichia coli. *J. Bacteriol.* **193**: 2871-2874.

Rajagopal, L., (2009) Understanding the regulation of Group B Streptococcal virulence factors. *Future Microbiol.* **4**: 201-221.

Rajagopal, L., A. Vo, A. Silvestroni & C.E. Rubens, (2006) Regulation of cytotoxin expression by converging eukaryotic-type and two-component signalling mechanisms in *Streptococcus agalactiae*. *Mol. Microbiol.* **62**: 941-957.

Ramakrishnan, M., A.J. Ulland, L.C. Steinhardt, J.C. Moisi, F. Were & O.S. Levine, (2009) Sequelae due to bacterial meningitis among African children: a systematic literature review. *BMC Med.* **7**: 47.

Ramaswamy, S.V., P. Ferrieri, A.E. Flores & L.C. Paoletti, (2006) Molecular characterization of nontypeable group B streptococcus. *J. Clin. Microbiol.* **44**: 2398-2403.

Ravasi, T., C.H. Mavromatis, N.J. Bokil, M.A. Schembri & M.J. Sweet, (2016) Co-transcriptomic Analysis by RNA Sequencing to Simultaneously Measure Regulated Gene Expression in Host and Bacterial Pathogen. *Toll-Like Receptors*: 145.

Reid, S.D., A.G. Montgomery, J.M. Voyich, F.R. DeLeo, B. Lei, R.M. Ireland, N.M. Green, M. Liu, S. Lukomski & J.M. Musser, (2003) Characterization of an extracellular virulence factor made by group A Streptococcus with homology to the *Listeria monocytogenes* internalin family of proteins. *Infect. Immun.* **71**: 7043-7052.

Reinscheid, D.J., B. Gottschalk, A. Schubert, B.J. Eikmanns & G.S. Chhatwal, (2001) Identification and molecular analysis of PcsB, a protein required for cell wall separation of group B streptococcus. *J. Bacteriol.* **183**: 1175-1183.

Rhoads, A. & K.F. Au, (2015) PacBio Sequencing and Its Applications. *Genomics Proteomics Bioinformatics* **13**: 278-289.

Riboldi-Tunnicliffe, A., C.J. Bent, N.W. Isaacs & T.J. Mitchell, (2004) Expression, purification and X-ray characterization of residues 18-230 from the pneumococcal histidine triad protein A (PhtA) from Streptococcus pneumoniae. *Acta Crystallogr. D Biol. Crystallogr.* **60**: 926-928.

Riboldi-Tunnicliffe, A., N.W. Isaacs & T.J. Mitchell, (2005) 1.2 Angstroms crystal structure of the *S. pneumoniae* PhtA histidine triad domain a novel zinc binding fold. *FEBS Lett.* **579**: 5353-5360.

Richards, V.P., S.C. Choi, P.D. Pavinski Bitar, A.A. Gurjar & M.J. Stanhope, (2013) Transcriptomic and genomic evidence for *Streptococcus agalactiae* adaptation to the bovine environment. *BMC Genomics* **14**: 920.

Rienksma, R.A., M. Suarez-Diez, H.J. Mollenkopf, G.M. Dolganov, A. Dorhoi, G.K. Schoolnik, V.A. Martins Dos Santos, S.H. Kaufmann, P.J. Schaap & M. Gengenbacher, (2015) Comprehensive insights into transcriptional adaptation of intracellular *Mycobacteria* by microbe-enriched dual RNA sequencing. *BMC Genomics* **16**: 34.

Ring, A., J.S. Braun, V. Nizet, W. Stremmel & J.L. Shenep, (2000) Group B streptococcal beta-hemolysin induces nitric oxide production in murine macrophages. *J. Infect. Dis.* **182**: 150-157.

Rioux, S., C. Neyt, E. Di Paolo, L. Turpin, N. Charland, S. Labbe, M.C. Mortier, T.J. Mitchell, C. Feron, D. Martin & J.T. Poolman, (2011) Transcriptional regulation, occurrence and putative role of the Pht family of Streptococcus pneumoniae. *Microbiology* **157**: 336-348.

Rocha, L.A., M.A. Bernal, M.R. Gaither & M.E. Alfaro, (2013) Massively parallel DNA sequencing: the new frontier in biogeography. *Frontiers of Biogeography* **5**.

Rodriguez, J.L., A.B. Dalia & J.N. Weiser, (2012) Increased chain length promotes pneumococcal adherence and colonization. *Infect. Immun.* **80**: 3454-3459.

Rooijakkers, S.H. & J.A. van Strijp, (2007) Bacterial complement evasion. *Mol. Immunol.* **44**: 23-32.

Rosa-Fraile, M., S. Dramsi & B. Spellerberg, (2014) Group B streptococcal haemolysin and pigment, a tale of twins. *FEMS Microbiol. Rev.* **38**: 932-946.

Rosenbach, F.J., (1884) *Microorganisms in the wound infectious diseases,* p. 160. Wiesbaden JF Bergmann.

Rosini, R., E. Campisi, M. De Chiara, H. Tettelin, D. Rinaudo, C. Toniolo, M. Metruccio, S. Guidotti, U.B. Sorensen, M. Kilian, D. Consortium, M. Ramirez, R. Janulczyk, C. Donati, G. Grandi & I. Margarit, (2015) Genomic analysis reveals the molecular basis for capsule loss in the group B Streptococcus population. *PLoS ONE* **10**: e0125985.

Rosini, R., C.D. Rinaudo, M. Soriani, P. Lauer, M. Mora, D. Maione, A. Taddei, I. Santi, C. Ghezzo, C. Brettoni, S. Buccato, I. Margarit, G. Grandi & J.L. Telford, (2006) Identification of novel genomic islands coding for antigenic pilus-like structures in *Streptococcus agalactiae*. *Mol. Microbiol.* **61**: 126-141.

Rosinski-Chupin, I., E. Sauvage, O. Sismeiro, A. Villain, V. Da Cunha, M.E. Caliot, M.A. Dillies, P. Trieu-Cuot, P. Bouloc, M.F. Lartigue & P. Glaser, (2015) Single nucleotide resolution RNA-seq uncovers new regulatory mechanisms in the opportunistic pathogen Streptococcus agalactiae. *BMC Genomics* **16**: 419.

Royer-Pokora, B., U. Loos & W.D. Ludwig, (1991) TTG-2, a new gene encoding a cysteine-rich protein with the LIM motif, is overexpressed in acute T-cell leukaemia with the t(11;14)(p13;q11). *Oncogene* **6**: 1887-1893.

Rubens, C.E., M.R. Wessels, L.M. Heggen & D.L. Kasper, (1987) Transposon mutagenesis of type III group B Streptococcus: correlation of capsule expression with virulence. *Proc. Natl. Acad. Sci. U. S. A.* **84**: 7208-7212.

Sabath, L.D., (1969) Current Concepts: Drug Resistance of Bacteria. *N. Engl. J. Med.* **280**: 91-94.

Sagar, A., C. Klemm, L. Hartjes, S. Mauerer, G. van Zandbergen & B. Spellerberg, (2013) The beta-hemolysin and intracellular survival of Streptococcus agalactiae in human macrophages. *PLoS ONE* **8**: e60160.

Sajjan, U.S., F.A. Sylvester & J.F. Forstner, (2000) Cable-piliated Burkholderia cepacia binds to cytokeratin 13 of epithelial cells. *Infect. Immun.* **68**: 1787-1795.

Salton, M.R.J. & K.S. Kim, (1996) Structure. In: Medical Microbiology. th & S. Baron (eds). Galveston (TX), pp.

Samen, U., B.J. Eikmanns, D.J. Reinscheid & F. Borges, (2007) The surface protein Srr-1 of *Streptococcus agalactiae* binds human keratin 4 and promotes adherence to epithelial HEp-2 cells. *Infect. Immun.* **75**: 5405-5414.

Samen, U., B. Heinz, H. Boisvert, B.J. Eikmanns, D.J. Reinscheid & F. Borges, (2011) Rga is a regulator of adherence and pilus formation in Streptococcus agalactiae. *Microbiology* **157**: 2319-2327.

Samen, U.M., B.J. Eikmanns & D.J. Reinscheid, (2006) The transcriptional regulator RovS controls the attachment of Streptococcus agalactiae to human epithelial cells and the expression of virulence genes. *Infect. Immun.* **74**: 5625-5635.

Santi, I., M. Scarselli, M. Mariani, A. Pezzicoli, V. Masignani, A. Taddei, G. Grandi, J.L. Telford & M. Soriani, (2007) BibA: a novel immunogenic bacterial adhesin contributing to group B Streptococcus survival in human blood. *Mol. Microbiol.* **63**: 754-767.

Sarma, J.V. & P.A. Ward, (2011) The complement system. *Cell Tissue Res.* **343**: 227-235.

Sarobe, P., J.J. Lasarte, N. Casares, A. Lopez-Diaz de Cerio, E. Baixeras, P. Labarga, N. Garcia, F. Borras-Cuesta & J. Prieto, (2002) Abnormal priming of CD4(+) T cells by dendritic cells expressing hepatitis C virus core and E1 proteins. *J. Virol.* **76**: 5062-5070.

Scheie, A.A. & E.I. Pearce, (1994) The effect of mineral-derived zinc ions on in vitro glucose metabolism of *Streptococcus mutans* NCTC 10449. *Caries Res.* **28**: 329-334.
Scheller, J., A. Chalaris, D. Schmidt-Arras & S. Rose-John, (2011) The pro- and anti-inflammatory properties of the cytokine interleukin-6. *Biochim. Biophys. Acta* **1813**: 878-888.
Schuchat, A., (1998) Epidemiology of group B streptococcal disease in the United States: shifting paradigms. *Clin. Microbiol. Rev.* **11**: 497-513.
Schuchat, A. & J.D. Wenger, (1994) Epidemiology of group B streptococcal disease. Risk factors, prevention strategies, and vaccine development. *Epidemiol. Rev.* **16**: 374-402.
Schuchat, A., C. Whitney & K.M. Zangwill, (1996) Prevention of perinatal group B streptococcal disease: a public health perspective. Centers for Disease Control and Prevention. *MMWR Recomm. Rep.* **45**: 1-24.
Schuchat, A., S.S. Zywicki, M.J. Dinsmoor, B. Mercer, J. Romaguera, M.J. O'Sullivan, D. Patel, M.T. Peters, B. Stoll & O.S. Levine, (2000) Risk factors and opportunities for prevention of early-onset neonatal sepsis: a multicenter case-control study. *Pediatrics* **105**: 21-26.
Schultze, T., R. Hilker, G.K. Mannala, K. Gentil, M. Weigel, N. Farmani, A.C. Windhorst, A. Goesmann, T. Chakraborty & T. Hain, (2015) A detailed view of the intracellular transcriptome of Listeria monocytogenes in murine macrophages using RNA-seq. *Frontiers in Microbiology* **6**: 1199.
Schumacher, W.A., J.C. Fantone, S.E. Kunkel, R.C. Webb & B.R. Lucchesi, (1991) The anaphylatoxins C3a and C5a are vasodilators in the canine coronary vasculature in vitro and in vivo. *Agents Actions* **34**: 345-349.
Schwartz, B., A. Schuchat, M.J. Oxtoby, S.L. Cochi, A. Hightower & C.V. Broome, (1991) Invasive group B streptococcal disease in adults. A population-based study in metropolitan Atlanta. *Journal of the American Medical Association* **266**: 1112-1114.
Seaward, P.G., M.E. Hannah, T.L. Myhr, D. Farine, A. Ohlsson, E.E. Wang, E. Hodnett, K. Haque, J.A. Weston & G. Ohel, (1998) International multicenter term PROM study: evaluation of predictors of neonatal infection in infants born to patients with premature rupture of membranes at term. Premature Rupture of the Membranes. *Am. J. Obstet. Gynecol.* **179**: 635-639.
Seifert, K.N., E.E. Adderson, A.A. Whiting, J.F. Bohnsack, P.J. Crowley & L.J. Brady, (2006) A unique serine-rich repeat protein (Srr-2) and novel surface antigen (epsilon) associated with a virulent lineage of serotype III *Streptococcus agalactiae*. *Microbiology* **152**: 1029-1040.
Seo, H.S., G. Minasov, R. Seepersaud, K.S. Doran, I. Dubrovska, L. Shuvalova, W.F. Anderson, T.M. Iverson & P.M. Sullam, (2013) Characterization of fibrinogen binding by glycoproteins Srr1 and Srr2 of Streptococcus agalactiae. *J. Biol. Chem.* **288**: 35982-35996.
Seo, H.S., R. Mu, B.J. Kim, K.S. Doran & P.M. Sullam, (2012) Binding of glycoprotein Srr1 of Streptococcus agalactiae to fibrinogen promotes attachment to brain endothelium and the development of meningitis. *PLoS Pathog.* **8**: e1002947.
Serna, M., J.L. Giles, B.P. Morgan & D. Bubeck, (2016) Structural basis of complement membrane attack complex formation. *Nat. Commun.* **7**: 10587.
Shao, Z., X. Pan, X. Li, W. Liu, M. Han, C. Wang, J. Wang, F. Zheng, M. Cao & J. Tang, (2011) HtpS, a novel immunogenic cell surface-exposed protein of *Streptococcus suis*, confers protection in mice. *FEMS Microbiol. Lett.* **314**: 174-182.
Shao, Z.Q., Y.M. Zhang, X.Z. Pan, B. Wang & J.Q. Chen, (2013) Insight into the evolution of the histidine triad protein (HTP) family in *Streptococcus*. *PLoS ONE* **8**: e60116.
Shapiro, J.A., (2009) Revisiting the central dogma in the 21st century. *Ann. N. Y. Acad. Sci.* **1178**: 6-28.
Sharma, C.M., S. Hoffmann, F. Darfeuille, J. Reignier, S. Findeiss, A. Sittka, S. Chabas, K. Reiche, J. Hackermuller, R. Reinhardt, P.F. Stadler & J. Vogel, (2010) The primary transcriptome of the major human pathogen Helicobacter pylori. *Nature* **464**: 250-255.
Sharma, C.M. & J. Vogel, (2014) Differential RNA-seq: the approach behind and the biological insight gained. *Curr. Opin. Microbiol.* **19**: 97-105.

Sharma, P., H. Lata, D.K. Arya, A.K. Kashyap, H. Kumar, M. Dua, A. Ali & A.K. Johri, (2013) Role of pilus proteins in adherence and invasion of *Streptococcus agalactiae* to the lung and cervical epithelial cells. *J. Biol. Chem.* **288**: 4023-4034.

Shendure, J. & H. Ji, (2008) Next-generation DNA sequencing. *Nat. Biotechnol.* **26**: 1135-1145.

Sheppard, A.E., A. Vaughan, N. Jones, P. Turner, C. Turner, A. Efstratiou, D. Patel, G. Modernising Medical Microbiology Informatics, A.S. Walker, J.A. Berkley, D.W. Crook & A.C. Seale, (2016) Capsular Typing Method for Streptococcus agalactiae Using Whole-Genome Sequence Data. *J. Clin. Microbiol.* **54**: 1388-1390.

Shockman, G.D., L. Daneo-Moore, R. Kariyama & O. Massidda, (1996) Bacterial walls, peptidoglycan hydrolases, autolysins, and autolysis. *Microbial Drug Resistance* **2**: 95-98.

Siboo, I.R., H.F. Chambers & P.M. Sullam, (2005) Role of SraP, a Serine-Rich Surface Protein of Staphylococcus aureus, in binding to human platelets. *Infect. Immun.* **73**: 2273-2280.

Sing, A., D. Rost, N. Tvardovskaia, A. Roggenkamp, A. Wiedemann, C.J. Kirschning, M. Aepfelbacher & J. Heesemann, (2002) Yersinia V-antigen exploits toll-like receptor 2 and CD14 for interleukin 10-mediated immunosuppression. *J. Exp. Med.* **196**: 1017-1024.

Singer, M., C.S. Deutschman, C.W. Seymour, M. Shankar-Hari, D. Annane, M. Bauer, R. Bellomo, G.R. Bernard, J.D. Chiche, C.M. Coopersmith, R.S. Hotchkiss, M.M. Levy, J.C. Marshall, G.S. Martin, S.M. Opal, G.D. Rubenfeld, T. van der Poll, J.L. Vincent & D.C. Angus, (2016) The Third International Consensus Definitions for Sepsis and Septic Shock (Sepsis-3). *Journal of the American Medical Association* **315**: 801-810.

Singh, B., C. Fleury, F. Jalalvand & K. Riesbeck, (2012) Human pathogens utilize host extracellular matrix proteins laminin and collagen for adhesion and invasion of the host. *FEMS Microbiol. Rev.* **36**: 1122-1180.

Sitkiewicz, I., N.M. Green, N. Guo, A.M. Bongiovanni, S.S. Witkin & J.M. Musser, (2009) Transcriptome adaptation of group B Streptococcus to growth in human amniotic fluid. *PLoS ONE* **4**: e6114.

Sitkiewicz, I. & J.M. Musser, (2009) Analysis of growth-phase regulated genes in Streptococcus agalactiae by global transcript profiling. *BMC Microbiol.* **9**: 32.

Six, A., S. Bellais, A. Bouaboud, A. Fouet, C. Gabriel, A. Tazi, S. Dramsi, P. Trieu-Cuot & C. Poyart, (2015) Srr2, a multifaceted adhesin expressed by ST-17 hypervirulent Group B Streptococcus involved in binding to both fibrinogen and plasminogen. *Mol. Microbiol.* **97**: 1209-1222.

Skoff, T.H., M.M. Farley, S. Petit, A.S. Craig, W. Schaffner, K. Gershman, L.H. Harrison, R. Lynfield, J. Mohle-Boetani, S. Zansky, B.A. Albanese, K. Stefonek, E.R. Zell, D. Jackson, T. Thompson & S.J. Schrag, (2009) Increasing burden of invasive group B streptococcal disease in nonpregnant adults, 1990-2007. *Clin. Infect. Dis.* **49**: 85-92.

Slotved, H.C., F. Kong, L. Lambertsen, S. Sauer & G.L. Gilbert, (2007) Serotype IX, a Proposed New *Streptococcus agalactiae* Serotype. *J. Clin. Microbiol.* **45**: 2929-2936.

Smith, T.J., S.A. Blackman & S.J. Foster, (2000) Autolysins of Bacillus subtilis: multiple enzymes with multiple functions. *Microbiology* **146 (Pt 2)**: 249-262.

Snyderman, R., M.C. Pike, D. McCarley & L. Lang, (1975) Quantification of mouse macrophage chemotaxis in vitro: role of C5 for the production of chemotactic activity. *Infect. Immun.* **11**: 488-492.

Sojar, H.T., A. Sharma & R.J. Genco, (2002) Porphyromonas gingivalis fimbriae bind to cytokeratin of epithelial cells. *Infect. Immun.* **70**: 96-101.

Sonomoto, K. & A. Yokota, (2011) *Lactic acid bacteria and bifidobacteria : current progress in advanced research,* p. viii, 286 p. Caister Academic Press, Norfolk, UK.

Sorensen, U.B., K. Poulsen, C. Ghezzo, I. Margarit & M. Kilian, (2010) Emergence and global dissemination of host-specific *Streptococcus agalactiae* clones. *MBio* **1**: e00178-00110.

Soruri, A., Z. Kiafard, C. Dettmer, J. Riggert, J. Kohl & J. Zwirner, (2003) IL-4 down-regulates anaphylatoxin receptors in monocytes and dendritic cells and impairs anaphylatoxin-induced migration in vivo. *J. Immunol.* **170**: 3306-3314.

Sozzani, S., W. Luini, M. Molino, P. Jilek, B. Bottazzi, C. Cerletti, K. Matsushima & A. Mantovani, (1991) The signal transduction pathway involved in the migration induced by a monocyte chemotactic cytokine. *J. Immunol.* **147**: 2215-2221.

Spellerberg, B., S. Martin, C. Brandt & R. Lutticken, (2000) The cyl genes of *Streptococcus agalactiae* are involved in the production of pigment. *FEMS Microbiol. Lett.* **188**: 125-128.

Spellerberg, B., B. Pohl, G. Haase, S. Martin, J. Weber-Heynemann & R. Lütticken, (1999a) Identification of Genetic Determinants for the Hemolytic Activity of *Streptococcus agalactiae* by ISS1Transposition. *J. Bacteriol.* **181**: 3212-3219.

Spellerberg, B., E. Rozdzinski, S. Martin, J. Weber-Heynemann, N. Schnitzler, R. Lutticken & A. Podbielski, (1999b) Lmb, a protein with similarities to the LraI adhesin family, mediates attachment of *Streptococcus agalactiae* to human laminin. *Infect. Immun.* **67**: 871-878.

Stableforth, A., (1938) The incidence of the various serological types of Str. agalactiæ in herds of cows in Great Britain. *The Journal of Pathology and Bacteriology* **46**: 21-29.

Stalhammar-Carlemalm, M., L. Stenberg & G. Lindahl, (1993) Protein rib: a novel group B streptococcal cell surface protein that confers protective immunity and is expressed by most strains causing invasive infections. *J. Exp. Med.* **177**: 1593-1603.

Stamm, W.E., (2002) Scientific and clinical challenges in the management of urinary tract infections. *Am. J. Med.* **113 Suppl 1A**: 1S-4S.

Steere, A.C., R.C. Aber, L.R. Warford, K.E. Murphy, J.C. Feeley, P.S. Hayes, H.W. Wilkinson & R.R. Facklam, (1975) Possible nosocomial transmission of group B streptococci in a newborn nursery. *J. Pediatr.* **87**: 784-787.

Stephenson, A.E., H. Wu, J. Novak, M. Tomana, K. Mintz & P. Fives-Taylor, (2002) The Fap1 fimbrial adhesin is a glycoprotein: antibodies specific for the glycan moiety block the adhesion of Streptococcus parasanguis in an in vitro tooth model. *Mol. Microbiol.* **43**: 147-157.

Stevens, J.P., M. Eames, A. Kent, S. Halket, D. Holt & D. Harvey, (2003) Long term outcome of neonatal meningitis. *Arch. Dis. Child. Fetal Neonatal Ed.* **88**: F179-184.

Stimler, N.P., M.K. Bach, C.M. Bloor & T.E. Hugli, (1982) Release of leukotrienes from guinea pig lung stimulated by C5ades Arg anaphylatoxin. *J. Immunol.* **128**: 2247-2252.

Stoll, B.J. & A. Schuchat, (1998) Maternal carriage of group B streptococci in developing countries. *Pediatr. Infect. Dis. J.* **17**: 499-503.

Stoner, T.D., T.A. Weston, J. Trejo & K.S. Doran, (2015) Group B streptococcal infection and activation of human astrocytes. *PLoS ONE* **10**: e0128431.

Stoppelli, M.P., (2013) The Plasminogen Activation System in Cell Invasion.

Sullivan, M.J., B.M. Forde, D.W. Prince, D.S. Ipe, N.L. Ben Zakour, M.R. Davies, G. Dougan, S.A. Beatson & G.C. Ulett, (2017a) Complete Genome Sequence of Serotype III *Streptococcus agalactiae* Sequence Type 17 Strain 874391. *Genome Announcements* **5**.

Sullivan, M.J., S.Y. Leclercq, D.S. Ipe, A.J. Carey, J.P. Smith, N. Voller, A.W. Cripps & G.C. Ulett, (2017b) Effect of the *Streptococcus agalactiae* Virulence Regulator CovR on the Pathogenesis of Urinary Tract Infection. *J. Infect. Dis.* **215**: 475-483.

Sullivan, M.J. & G.C. Ulett, (2018) Stable Expression of Modified Green Fluorescent Protein in Group B Streptococci To Enable Visualization in Experimental Systems. *Appl. Environ. Microbiol.* **84**.

Sundstrom, C. & K. Nilsson, (1976) Establishment and characterization of a human histiocytic lymphoma cell line (U-937). *Int. J. Cancer* **17**: 565-577.

Sutcliffe, I.C. & R.R. Russell, (1995) Lipoproteins of gram-positive bacteria. *J. Bacteriol.* **177**: 1123-1128.

Suzuki, T., P.J. Higgins & D.R. Crawford, (2000) Control selection for RNA quantitation. *Biotechniques* **29**: 332-337.

t Hoen, P.A., Y. Ariyurek, H.H. Thygesen, E. Vreugdenhil, R.H. Vossen, R.X. de Menezes, J.M. Boer, G.J. van Ommen & J.T. den Dunnen, (2008) Deep sequencing-based expression analysis shows major advances in robustness, resolution and inter-lab portability over five microarray platforms. *Nucleic Acids Res.* **36**: e141.

Takafuji, S., A. Ishida, Y. Miyakuni & T. Nakagawa, (2003) Matrix metalloproteinase-9 release from human leukocytes. *The Journal of Investigational Allergology and Clinical Immunology* **13**: 50-55.

Takahashi, S., E.E. Adderson, Y. Nagano, N. Nagano, M.R. Briesacher & J.F. Bohnsack, (1998) Identification of a highly encapsulated, genetically related group of invasive type III group B streptococci. *J. Infect. Dis.* **177**: 1116-1119.

Takahashi, S., Y. Nagano, N. Nagano, K. Fujita, F. Taguchi & Y. Okuwaki, (1993) Opsonisation of group B streptococci and restriction endonuclease digestion patterns of their chromosomal DNA. *J. Med. Microbiol.* **38**: 191-196.

Takahashi, S., Y. Nagano, N. Nagano, O. Hayashi, F. Taguchi & Y. Okuwaki, (1995) Role of C5a-ase in group B streptococcal resistance to opsonophagocytic killing. *Infect. Immun.* **63**: 4764-4769.

Takamatsu, D., B.A. Bensing, H. Cheng, G.A. Jarvis, I.R. Siboo, J.A. Lopez, J.M. Griffiss & P.M. Sullam, (2005) Binding of the Streptococcus gordonii surface glycoproteins GspB and Hsa to specific carbohydrate structures on platelet membrane glycoprotein Ibalpha. *Mol. Microbiol.* **58**: 380-392.

Talbot, U.M., A.W. Paton & J.C. Paton, (1996) Uptake of Streptococcus pneumoniae by respiratory epithelial cells. *Infect. Immun.* **64**: 3772-3777.

Tam, R. & M.H. Saier, Jr., (1993) Structural, functional, and evolutionary relationships among extracellular solute-binding receptors of bacteria. *Microbiol. Rev.* **57**: 320-346.

Tamura, G.S., J.R. Hull, M.D. Oberg & D.G. Castner, (2006) High-affinity interaction between fibronectin and the group B streptococcal C5a peptidase is unaffected by a naturally occurring four-amino-acid deletion that eliminates peptidase activity. *Infect. Immun.* **74**: 5739-5746.

Tamura, G.S., J.M. Kuypers, S. Smith, H. Raff & C.E. Rubens, (1994) Adherence of group B streptococci to cultured epithelial cells: roles of environmental factors and bacterial surface components. *Infect. Immun.* **62**: 2450-2458.

Tamura, G.S. & A. Nittayajarn, (2000) Group B streptococci and other gram-positive cocci bind to cytokeratin 8. *Infect. Immun.* **68**: 2129-2134.

Tan, S.C. & B.C. Yiap, (2009) DNA, RNA, and protein extraction: the past and the present. *J Biomed Biotechnol* **2009**: 574398.

Tapsall, J.W., (1986) Pigment production by Lancefield-group-B streptococci (*Streptococcus agalactiae*). *J. Med. Microbiol.* **21**: 75-81.

Tapsall, J.W. & E.A. Phillips, (1991) The hemolytic and cytolytic activity of group B streptococcal hemolysin and its possible role in early onset group B streptococcal disease. *Pathology (Phila.)* **23**: 139-144.

Tatusov, R.L., D.A. Natale, I.V. Garkavtsev, T.A. Tatusova, U.T. Shankavaram, B.S. Rao, B. Kiryutin, M.Y. Galperin, N.D. Fedorova & E.V. Koonin, (2001) The COG database: new developments in phylogenetic classification of proteins from complete genomes. *Nucleic Acids Res.* **29**: 22-28.

Taylor, J.K., R.W. Hall & A.R. Dupre, (2002) The incidence of group B streptococcus in the vaginal tracts of pregnant women in central Alabama. *Clin. Lab. Sci.* **15**: 16-17.

Tazi, A., S. Bellais, I. Tardieux, S. Dramsi, P. Trieu-Cuot & C. Poyart, (2012) Group B Streptococcus surface proteins as major determinants for meningeal tropism. *Curr. Opin. Microbiol.* **15**: 44-49.

Tazi, A., O. Disson, S. Bellais, A. Bouaboud, N. Dmytruk, S. Dramsi, M.Y. Mistou, H. Khun, C. Mechler, I. Tardieux, P. Trieu-Cuot, M. Lecuit & C. Poyart, (2010) The surface protein HvgA mediates group B streptococcus hypervirulence and meningeal tropism in neonates. *J. Exp. Med.* **207**: 2313-2322.

Teatero, S., T.B. Athey, P. Van Caeseele, G. Horsman, D.C. Alexander, R.G. Melano, A. Li, A.R. Flores, S.A. Shelburne, 3rd, A. McGeer, W. Demczuk, I. Martin & N. Fittipaldi, (2015) Emergence of Serotype IV Group B Streptococcus Adult Invasive Disease in Manitoba and Saskatchewan, Canada, Is Driven by Clonal Sequence Type 459 Strains. *J. Clin. Microbiol.* **53**: 2919-2926.

Teatero, S., A. McGeer, D.E. Low, A. Li, W. Demczuk, I. Martin & N. Fittipaldi, (2014) Characterization of invasive group B streptococcus strains from the greater Toronto area, Canada. *J. Clin. Microbiol.* **52**: 1441-1447.

Teatero, S., E. Ramoutar, A. McGeer, A. Li, R.G. Melano, J. Wasserscheid, K. Dewar & N. Fittipaldi, (2016) Clonal Complex 17 Group B Streptococcus strains causing invasive disease in neonates and adults originate from the same genetic pool. *Scientific Reports* **6**: 20047.

Tedde, V., R. Rosini & C.L. Galeotti, (2016) Zn2+ Uptake in *Streptococcus pyogenes*: Characterization of *adcA* and *lmb* Null Mutants. *PLoS ONE* **11**: e0152835.

Tettelin, H., V. Masignani, M.J. Cieslewicz, C. Donati, D. Medini, N.L. Ward, S.V. Angiuoli, J. Crabtree, A.L. Jones, A.S. Durkin, R.T. Deboy, T.M. Davidsen, M. Mora, M. Scarselli, I. Margarit y Ros, J.D. Peterson, C.R. Hauser, J.P. Sundaram, W.C. Nelson, R. Madupu, L.M. Brinkac, R.J. Dodson, M.J. Rosovitz, S.A. Sullivan, S.C. Daugherty, D.H. Haft, J. Selengut, M.L. Gwinn, L. Zhou, N. Zafar, H. Khouri, D. Radune, G. Dimitrov, K. Watkins, K.J. O'Connor, S. Smith, T.R. Utterback, O. White, C.E. Rubens, G. Grandi, L.C. Madoff, D.L. Kasper, J.L. Telford, M.R. Wessels, R. Rappuoli & C.M. Fraser, (2005) Genome analysis of multiple pathogenic isolates of *Streptococcus agalactiae*: implications for the microbial "pan-genome". *Proc. Natl. Acad. Sci. U. S. A.* **102**: 13950-13955.

Tettelin, H., V. Masignani, M.J. Cieslewicz, J.A. Eisen, S. Peterson, M.R. Wessels, I.T. Paulsen, K.E. Nelson, I. Margarit, T.D. Read, L.C. Madoff, A.M. Wolf, M.J. Beanan, L.M. Brinkac, S.C. Daugherty, R.T. DeBoy, A.S. Durkin, J.F. Kolonay, R. Madupu, M.R. Lewis, D. Radune, N.B. Fedorova, D. Scanlan, H. Khouri, S. Mulligan, H.A. Carty, R.T. Cline, S.E. Van Aken, J. Gill, M. Scarselli, M. Mora, E.T. Iacobini, C. Brettoni, G. Galli, M. Mariani, F. Vegni, D. Maione, D. Rinaudo, R. Rappuoli, J.L. Telford, D.L. Kasper, G. Grandi & C.M. Fraser, (2002) Complete genome sequence and comparative genomic analysis of an emerging human pathogen, serotype V *Streptococcus agalactiae*. *Proc. Natl. Acad. Sci. U. S. A.* **99**: 12391-12396.

Tettelin, H., D. Medini, C. Donati & V. Masignani, (2006) Towards a universal group B Streptococcus vaccine using multistrain genome analysis. *Expert Rev. Vaccines* **5**: 687-694.

Thigpen, M.C., C.G. Whitney, N.E. Messonnier, E.R. Zell, R. Lynfield, J.L. Hadler, L.H. Harrison, M.M. Farley, A. Reingold, N.M. Bennett, A.S. Craig, W. Schaffner, A. Thomas, M.M. Lewis, E. Scallan, A. Schuchat & N. Emerging Infections Programs, (2011) Bacterial meningitis in the United States, 1998-2007. *N. Engl. J. Med.* **364**: 2016-2025.

Tierney, L., J. Linde, S. Muller, S. Brunke, J.C. Molina, B. Hube, U. Schock, R. Guthke & K. Kuchler, (2012) An Interspecies Regulatory Network Inferred from Simultaneous RNA-seq of Candida albicans Invading Innate Immune Cells. *Frontiers in Microbiology* **3**: 85.

Tjaden, B., (2015) De novo assembly of bacterial transcriptomes from RNA-seq data. *Genome Biol.* **16**: 1.

Todd, E., (1934) A comparative serological study of streptolysins derived from human and from animal infections, with notes on pneumococcal haemolysin, tetanolysin and staphylococcus toxin. *The Journal of Pathology and Bacteriology* **39**: 299-321.

Tristan, C., N. Shahani, T.W. Sedlak & A. Sawa, (2011) The diverse functions of GAPDH: views from different subcellular compartments. *Cell. Signal.* **23**: 317-323.

Tseng, P.I. & S.R. Kandall, (1974) Group B streptococcal disease. In neonates and infants. *N. Y. State J. Med.* **74**: 2169-2173.

Tyrrell, G.J., L.D. Senzilet, J.S. Spika, D.A. Kertesz, M. Alagaratnam, M. Lovgren & J.A. Talbot, (2000) Invasive disease due to group B streptococcal infection in adults: results from a Canadian, population-based, active laboratory surveillance study--1996. Sentinel Health Unit Surveillance System Site Coordinators. *J. Infect. Dis.* **182**: 168-173.

Ulett, G.C. & E.E. Adderson, (2005) Nitric oxide is a key determinant of group B streptococcus-induced murine macrophage apoptosis. *J. Infect. Dis.* **191**: 1761-1770.

Ulett, G.C., J.F. Bohnsack, J. Armstrong & E.E. Adderson, (2003) Beta-hemolysin-independent induction of apoptosis of macrophages infected with serotype III group B streptococcus. *J. Infect. Dis.* **188**: 1049-1053.

Ulett, G.C., R.I. Webb, K.B. Ulett, X. Cui, W.H. Benjamin, M. Crowley & M.A. Schembri, (2010) Group B Streptococcus (GBS) urinary tract infection involves binding of GBS to bladder uroepithelium and potent but GBS-specific induction of interleukin 1alpha. *J. Infect. Dis.* **201**: 866-870.

Ulett, K.B., W.H. Benjamin, Jr., F. Zhuo, M. Xiao, F. Kong, G.L. Gilbert, M.A. Schembri & G.C. Ulett, (2009) Diversity of group B streptococcus serotypes causing urinary tract infection in adults. *J. Clin. Microbiol.* **47**: 2055-2060.

Untergasser, A., I. Cutcutache, T. Koressaar, J. Ye, B.C. Faircloth, M. Remm & S.G. Rozen, (2012) Primer3--new capabilities and interfaces. *Nucleic Acids Res.* **40**: e115.

Valenti-Weigand, P., P. Benkel, M. Rohde & G.S. Chhatwal, (1996) Entry and intracellular survival of group B streptococci in J774 macrophages. *Infect. Immun.* **64**: 2467-2473.

Vallejo, J.G., C.J. Baker & M.S. Edwards, (1996) Interleukin-6 production by human neonatal monocytes stimulated by type III group B streptococci. *J. Infect. Dis.* **174**: 332-337.

van Sorge, N.M., D. Quach, M.A. Gurney, P.M. Sullam, V. Nizet & K.S. Doran, (2009) The group B streptococcal serine-rich repeat 1 glycoprotein mediates penetration of the blood-brain barrier. *J. Infect. Dis.* **199**: 1479-1487.

Van Vlierberghe, P., M. van Grotel, H.B. Beverloo, C. Lee, T. Helgason, J. Buijs-Gladdines, M. Passier, E.R. van Wering, A.J. Veerman, W.A. Kamps, J.P. Meijerink & R. Pieters, (2006) The cryptic chromosomal deletion del(11)(p12p13) as a new activation mechanism of LMO2 in pediatric T-cell acute lymphoblastic leukemia. *Blood* **108**: 3520-3529.

Varki, A., (2008) Sialic acids in human health and disease. *Trends Mol. Med.* **14**: 351-360.

Verghese, A., K. Mireault & R.D. Arbeit, (1986) Group B streptococcal bacteremia in men. *Reviews in Infectious Diseases* **8**: 912-917.

Victora, C.G., A. Wagstaff, J.A. Schellenberg, D. Gwatkin, M. Claeson & J.P. Habicht, (2003) Applying an equity lens to child health and mortality: more of the same is not enough. *Lancet* **362**: 233-241.

Virok, D., A. Loboda, L. Kari, M. Nebozhyn, C. Chang, C. Nichols, V. Endresz, E. Gonczol, K. Berencsi, M.K. Showe & L.C. Showe, (2003) Infection of U937 monocytic cells with *Chlamydia pneumoniae* induces extensive changes in host cell gene expression. *J. Infect. Dis.* **188**: 1310-1321.

Visintin, C., M.A. Mugglestone, E.J. Fields, P. Jacklin, M.S. Murphy & A.J. Pollard, (2010) Management of bacterial meningitis and meningococcal septicaemia in children and young people: summary of NICE guidance. *Br. Med. J.* **340**: c3209.

Viswanathan, V.K., S. Lukic, A. Koutsouris, R. Miao, M.M. Muza & G. Hecht, (2004) Cytokeratin 18 interacts with the enteropathogenic Escherichia coli secreted protein F (EspF) and is redistributed after infection. *Cell. Microbiol.* **6**: 987-997.

Volkman, A. & J.L. Gowans, (1965) The Origin of Macrophages from Bone Marrow in the Rat. *Br. J. Exp. Pathol.* **46**: 62-70.

Vollman, J.H., W.L. Smith, E.T. Ballard & I.J. Light, (1976) Early onset group B streptococcal disease: clinical, roentgenographic, and pathologic features. *J. Pediatr.* **89**: 199-203.

Vollmer, W., B. Joris, P. Charlier & S. Foster, (2008) Bacterial peptidoglycan (murein) hydrolases. *FEMS Microbiol. Rev.* **32**: 259-286.

Vos, P., G. Garrity, D. Jones, N.R. Krieg, W. Ludwig, F.A. Rainey, K.-H. Schleifer & W. Whitman, (2011) *Bergey's Manual of Systematic Bacteriology: Volume 3: The Firmicutes*. Springer Science & Business Media.

Waldemarsson, J., T. Areschoug, G. Lindahl & E. Johnsson, (2006) The streptococcal Blr and Slr proteins define a family of surface proteins with leucine-rich repeats: camouflaging by other surface structures. *J. Bacteriol.* **188**: 378-388.

Waldron, K.J. & N.J. Robinson, (2009) How do bacterial cells ensure that metalloproteins get the correct metal? *Nat. Rev. Microbiol.* **7**: 25-35.
Walsh, E.J., L.M. O'Brien, X. Liang, M. Hook & T.J. Foster, (2004) Clumping factor B, a fibrinogen-binding MSCRAMM (microbial surface components recognizing adhesive matrix molecules) adhesin of Staphylococcus aureus, also binds to the tail region of type I cytokeratin 10. *J. Biol. Chem.* **279**: 50691-50699.
Wang, L., P. Liu, Z.Y. Wan, S.Q. Huang, Y.F. Wen, G. Lin & G.H. Yue, (2016) RNA-Seq revealed the impairment of immune defence of tilapia against the infection of Streptococcus agalactiae with simulated climate warming. *Fish & Shellfish Immunology* **55**: 679-689.
Wang, N.Y., K.A. Patras, H.S. Seo, C.K. Cavaco, B. Rosler, M.N. Neely, P.M. Sullam & K.S. Doran, (2014) Group B streptococcal serine-rich repeat proteins promote interaction with fibrinogen and vaginal colonization. *J. Infect. Dis.* **210**: 982-991.
Wang, Z., M. Gerstein & M. Snyder, (2009) RNA-Seq: a revolutionary tool for transcriptomics. *Nat. Rev. Genet.* **10**: 57-63.
Warren, A.J., W.H. Colledge, M.B. Carlton, M.J. Evans, A.J. Smith & T.H. Rabbitts, (1994) The oncogenic cysteine-rich LIM domain protein rbtn2 is essential for erythroid development. *Cell* **78**: 45-57.
Wastfelt, M., M. Stalhammar-Carlemalm, A.M. Delisse, T. Cabezon & G. Lindahl, (1996) Identification of a family of streptococcal surface proteins with extremely repetitive structure. *J. Biol. Chem.* **271**: 18892-18897.
Watanabe, T., (1963) Infective heredity of multiple drug resistance in bacteria. *Bacteriology Reviews* **27**: 87-115.
Watson, J.D., (1965) *Molecular biology of the gene,* p. xxii, 494 p. W. A. Benjamin, New York,.
Weems Jr, J.J., W.R. Jarvis & G. Colman, (1986) A cluster of late onset group B streptococcal infections in low birth weight premature infants: no evidence for horizontal transmission. *Pediatr. Infect. Dis. J.* **5**: 715-716.
Weiser, J.N., D. Bae, C. Fasching, R.W. Scamurra, A.J. Ratner & E.N. Janoff, (2003) Antibody-enhanced pneumococcal adherence requires IgA1 protease. *Proc. Natl. Acad. Sci. U. S. A.* **100**: 4215-4220.
Wellman, M.B., D.D. Sommer & J. McKenna, (2003) Sensorineural hearing loss in postmeningitic children. *Otol. Neurotol.* **24**: 907-912.
Wenger, J.D., A.W. Hightower, R.R. Facklam, S. Gaventa & C.V. Broome, (1990) Bacterial meningitis in the United States, 1986: report of a multistate surveillance study. The Bacterial Meningitis Study Group. *J. Infect. Dis.* **162**: 1316-1323.
Wessels, M.R., R.F. Haft, L.M. Heggen & C.E. Rubens, (1992) Identification of a genetic locus essential for capsule sialylation in type III group B streptococci. *Infect. Immun.* **60**: 392-400.
Wessels, M.R., C.E. Rubens, V.J. Benedi & D.L. Kasper, (1989) Definition of a bacterial virulence factor: sialylation of the group B streptococcal capsule. *Proc. Natl. Acad. Sci. U. S. A.* **86**: 8983-8987.
Westermann, A.J., S.A. Gorski & J. Vogel, (2012) Dual RNA-seq of pathogen and host. *Nat. Rev. Microbiol.* **10**: 618-630.
Wibawan, I.W. & C. Lammler, (1990) Properties of group B streptococci with protein surface antigens X and R. *J. Clin. Microbiol.* **28**: 2834-2836.
Widger, J., N.H. O'Connell & T. Stack, (2010) Breast milk causing neonatal sepsis and death. *Clin. Microbiol. Infect.* **16**: 1796-1798.
Wiles, K.G., P. Panizzi, H.K. Kroh & P.E. Bock, (2010) Skizzle is a novel plasminogen- and plasmin-binding protein from Streptococcus agalactiae that targets proteins of human fibrinolysis to promote plasmin generation. *J. Biol. Chem.* **285**: 21153-21164.
Wiley, S.R., K. Schooley, P.J. Smolak, W.S. Din, C.P. Huang, J.K. Nicholl, G.R. Sutherland, T.D. Smith, C. Rauch, C.A. Smith & et al., (1995) Identification and characterization of a new member of the TNF family that induces apoptosis. *Immunity* **3**: 673-682.

Wilkinson, H.W., (1977) Nontypable group B streptococci isolated from human sources. *J. Clin. Microbiol.* **6**: 183-184.

Williams, P.A., J.F. Bohnsack, N.H. Augustine, W.K. Drummond, C.E. Rubens & H.R. Hill, (1993) Production of tumor necrosis factor by human cells in vitro and in vivo, induced by group B streptococci. *J. Pediatr.* **123**: 292-300.

Wilson, L.G., (1987) The early recognition of streptococci as causes of disease. *Med. Hist.* **31**: 403-414.

Wolk, K., S. Kunz, K. Asadullah & R. Sabat, (2002) Cutting edge: immune cells as sources and targets of the IL-10 family members? *J. Immunol.* **168**: 5397-5402.

Wu, C.S., S.M. Wang, W.C. Ko, J.J. Wu, Y.J. Yang & C.C. Liu, (2004) Group B streptococcal infections in children in a tertiary care hospital in southern Taiwan. *Journal of Microbiology, Immunology and Infection* **37**: 169-175.

Wu, H., K.P. Mintz, M. Ladha & P.M. Fives-Taylor, (1998) Isolation and characterization of Fap1, a fimbriae-associated adhesin of *Streptococcus parasanguis* FW213. *Mol. Microbiol.* **28**: 487-500.

Xiang, L.X., D. He, W.R. Dong, Y.W. Zhang & J.Z. Shao, (2010) Deep sequencing-based transcriptome profiling analysis of bacteria-challenged Lateolabrax japonicus reveals insight into the immune-relevant genes in marine fish. *BMC Genomics* **11**: 472.

Xiu, L., Y.B. Fu, Y. Deng, X.J. Shi, Z.Y. Bian, A. Ruhan & X. Wang, (2015) Deep sequencing-based analysis of gene expression in bovine mammary epithelial cells after Staphylococcus aureus, Escherichia coli, and Klebsiella pneumoniae infection. *Genet. Mol. Res.* **14**: 16948-16965.

Xu, G., M.J. Strong, M.R. Lacey, C. Baribault, E.K. Flemington & C.M. Taylor, (2014) RNA CoMPASS: a dual approach for pathogen and host transcriptome analysis of RNA-seq datasets. *PLoS ONE* **9**: e89445.

Xu, L.L., M.K. Warren, W.L. Rose, W. Gong & J.M. Wang, (1996) Human recombinant monocyte chemotactic protein and other C-C chemokines bind and induce directional migration of dendritic cells in vitro. *J. Leukoc. Biol.* **60**: 365-371.

Xue, V.W., S.S.M. Ng, W.W. Leung, B.B.Y. Ma, W.C.S. Cho, T.C.C. Au, A.C.S. Yu, H.F.A. Tsang & S.C.C. Wong, (2018) The Effect of Centrifugal Force in Quantification of Colorectal Cancer-Related mRNA in Plasma Using Targeted Sequencing. *Frontiers in Genetics* **9**: 165.

Yachie, A., N. Takano, K. Ohta, T. Uehara, S. Fujita, T. Miyawaki & N. Taniguchi, (1992) Defective production of interleukin-6 in very small premature infants in response to bacterial pathogens. *Infect. Immun.* **60**: 749-753.

Yang, W., (2011) Nucleases: diversity of structure, function and mechanism. *Q. Rev. Biophys.* **44**: 1-93.

Yona, S. & S. Jung, (2010) Monocytes: subsets, origins, fates and functions. *Curr. Opin. Hematol.* **17**: 53-59.

Yoshimura, T., K. Matsushima, S. Tanaka, E.A. Robinson, E. Appella, J.J. Oppenheim & E.J. Leonard, (1987) Purification of a human monocyte-derived neutrophil chemotactic factor that has peptide sequence similarity to other host defense cytokines. *Proc. Natl. Acad. Sci. U. S. A.* **84**: 9233-9237.

Zangwill, K.M., A. Schuchat & J.D. Wenger, (1992) Group B streptococcal disease in the United States, 1990: report from a multistate active surveillance system. *MMWR CDC Surveill. Summ.* **41**: 25-32.

Zapun, A., T. Vernet & M.G. Pinho, (2008) The different shapes of cocci. *FEMS Microbiol. Rev.* **32**: 345-360.

Zhang, M.A., D. Rego, M. Moshkova, H. Kebir, A. Chruscinski, H. Nguyen, R. Akkermann, F.Z. Stanczyk, A. Prat, L. Steinman & S.E. Dunn, (2012) Peroxisome proliferator-activated receptor (PPAR)alpha and -gamma regulate IFNgamma and IL-17A production by human T cells in a sex-specific way. *Proc. Natl. Acad. Sci. U. S. A.* **109**: 9505-9510.

Zhang, Y., A.W. Masi, V. Barniak, K. Mountzouros, M.K. Hostetter & B.A. Green, (2001) Recombinant PhpA protein, a unique histidine motif-containing protein from *Streptococcus pneumoniae*, protects mice against intranasal pneumococcal challenge. *Infect. Immun.* **69**: 3827-3836.

Zhang, Y.M., Z.Q. Shao, J. Wang, L. Wang, X. Li, C. Wang, J. Tang & X. Pan, (2014) Prevalent distribution and conservation of *Streptococcus suis* Lmb protein and its protective capacity against the Chinese highly virulent strain infection. *Microbiol. Res.* **169**: 395-401.

Zhou, Y., Z. Xu, C. Duan, Y. Chen, Q. Meng, J. Wu, Z. Hao, Z. Wang, M. Li, H. Yong, D. Zhang, S. Zhang, J. Weng & X. Li, (2016) Dual transcriptome analysis reveals insights into the response to Rice black-streaked dwarf virus in maize. *Journal of Experimental Botany* **67**: 4593-4609.

Zipfel, P.F., R. Wurzner & C. Skerka, (2007) Complement evasion of pathogens: common strategies are shared by diverse organisms. *Mol. Immunol.* **44**: 3850-3857.

Appendix 1 – Genomic Preparation Optimisations

Each of the experiments in this methodological optimisation unit (along with Appendix 2) are delineated into 4 sections; 1) a preamble (defining the reason and purpose of each experiment), 2) a description of the experiment performed, 3) an "Observations" section displaying the experimental outcomes, and 4) an "Interpretation" section discussing the implications of the observations.

Experiment 1: Quantify bacterial growth from overnight THY cultures of GBS

Each bacterial strain used in this study was cultured and bacterial counts performed to ensure their viability for the study. An overnight incubation in nutrient rich broth is expected to promote GBS growth to stationary phase; i.e. yielding at least 1E8 CFU/ml GBS. The initial goal was to generate quality, high yields of genomic DNA from eight strains of GBS for PacBio sequencing. The sequence of one of these strains was intended for use as the scaffold in later transcript research. Strains were selected for their variety of pathology, epidemiological sources, availability, and appearance in the literature (see TABLE 2.01). This number and variety was intended to provide a measure of redundancy in case of poor sequence outcomes.

Bacterial Culture

To mitigate the possibility of cross contamination between bacterial strains, genomic preparations were performed separately for each strain. 10ml THY in a 50ml tube was inoculated with a single bacterial colony growing on a TSA blood agar plate. This was replicated for all 8 strains being used in this study and repeated for each strain (i.e. a total of 20ml inoculate per strain). All samples were incubated at 37^{o}C for 16 hours.

The two 10ml samples for each strain were pooled into a single, 50ml tube. 200µl from each strain was taken for serial dilutions and bacterial counts. Then each strain was divided into eight 2ml tubes, each containing 1.8ml culture (discarding any remaining culture). All 64 samples were centrifuged

for 30 seconds at 10,000g. After carefully removing most of the supernatant, the centrifuge was repeated and the remaining supernatant discarded. Pellets were stored at -20°C.

Observations

GBS cell density in THY liquid cultures after 16 hours incubation in THY ranged from 3.6E8 CFU/ml (GBS 0247) to 2.6E9 CFU/ml (GBS 0729). At 3.6E8 CFU/ml, GBS 0247 yield was substantially lower than the next lowest of 1.4E9 CFU/ml (GBS 0714). Clear pellets were visible in all centrifuged tubes. Some of the post-centrifuge bacterial pellets were less dense, causing the possible loss of some cells with the discarded supernatants.

TABLE AP1.01: CFU/ml of 8 GBS strains after 16 hours incubation at 37°C in THY media.

GBS Strain	CFU/ml
GBS 0058	1.86E9
GBS 0247	3.6E8
GBS 0714	1.4E9
GBS 0729	2.6E9
GBS 0807	2.4E9
GBS 0834	1.54E9
GBS 1014	2.06E9
GBS 874391	1.6E9

Interpretation

All selected GBS strains demonstrated sufficient growth in THY media to proceed to the DNA extraction experiments. However, the centrifuge stage should use a higher spin rate (i.e. > 10,000g) in order to improve pellet integrity.

Experiment 2: Pilot DNA extraction from GBS strain 0058

A gDNA extraction was attempted for GBS strain 058 to determine the quality and quantity of gDNA which could be prepared using a laboratory Standard Operating Procedure (SOP) combined with the UltraClean Microbial DNA Isolation Kit (MO BIO Laboratories). The approach was to perform gDNA

preparations on one bacterial strain at a time to mitigate the possibility of genomic cross-contamination between strains.

DNA Isolation

The UltraClean Microbial DNA Isolation Kit instructions were generally followed to extract DNA from the eight pellets of GBS 0058 collected in experiment 1. Namely;

Bacterial pellets were thawed on ice. 300µl of Microbead Solution was added to each thawed pellet and mixed gently by vortex (10 sec). 10µl of Mutanolysin (100 units @ 10units/µl) was added to each mix and vortexed for 5 seconds. The mixes were then incubated for 1hr at 37^{o}C before being transferred to the Microbead Tubes where 50µl of Solution MD1 was added to each mix. The mixes were then horizontally bead-beat for 10 minutes at 30 beats per second using the TissueLyser II.

The lysates were then centrifuged for 30 seconds at 10,000g. After carefully transferring the supernatants to 2ml collection tubes, 100µl of Solution MD2 was added to each supernatant, and the mix vortexed for 5 seconds before incubating in ice for 5 minutes. Following a further 1 minute centrifuge at 10,000g, the supernatants were transferred to clean 2ml collection tubes and 900µl of Solution MD3 added to each supernatant and vortexed for 5 seconds.

700µl of each supernatant mix was aliquoted into the spin filter and centrifuged for 30 seconds at 10,000g. After discarding the flowthrough, the remaining supernatant mix was loaded (700µl or less at a time) into the spin filter and centrifuged as above. 300µl of Solution MD4 was then loaded into each membrane and centrifuged for 30 seconds at 10,000g. After discarding the flowthrough, the tubes were re-centrifuged for 1 minute at 10,000g to remove residual MD4 Solution from the tube.

50µl of nuclease-free Ultrapure Distilled Water (Invitrogen) was added to each membrane and rested at room temperature for 2-5 minutes. DNA was then eluted from the membrane by centrifuge for 30 seconds at 10,000g. Quantification was performed on a Nanodrop Spectrophotometer. The genomic DNA preparations of GBS 0058 were then pooled, re-quantified, and the volume measured with a pipette before storing at -20^{o}C.

Observations

The gDNA concentrations of each preparation ranged from 22.1ng/µl to 62.9ng/µl; with an average concentration of 40.5ng/µl. The 260/280 absorbance ratios were within, or close to the ideal range (1.8-2.0); indicating low levels of protein contamination. However, the 260/230 absorbance ratio was inconsistent, and well above the ideal range (2.0-2.2); indicating higher than desired levels of residual contaminants from the purification reagents.

TABLE AP1.02: Nanodrop absorbance quantification of each gDNA preparation from 8 pellets of GBS 0058.

Pellet	gDNA ng/µl	gDNA ng per 50µl elution	$A_{260/280}$	$A_{260/230}$
1	32.2	1610	1.88	7.65
2	62.9	3145	1.87	4.30
3	22.1	1105	1.71	-21.09
4	42.8	2140	1.87	5.23
5	35.4	1770	1.79	6.64
6	46.1	2305	1.89	2.48
7	42.6	2130	1.91	5.83
8	40.1	2005	1.66	9.38
Total ng		16,210		
Total µg		16.2		

The 41.4ng/µl gDNA concentration of the pooled sample reflects the average of the individual preparations. The 260/230 absorbance ratio remains higher than desired.

TABLE AP1.03: Nanodrop absorbance quantification of pooled gDNA from 8 preparations of GBS 0058.

Sample	gDNA ng/µl	gDNA ng in 345µl	$A_{260/280}$	$A_{260/230}$
Pooled	41.4	14,283	1.87	4.21
Total µg		14.3		

Interpretation

The procedure successfully extracts gDNA from the GBS cell pellets. However the gDNA concentrations are lower than desired and the 260/230 absorbance ratios are higher than desired. Refinements to the extraction method were therefore required for subsequent preparations to increase gDNA yield per preparation.

Experiment 3: DNA extraction from GBS strain 0247

A gDNA extraction was performed on 8 pellets of GBS 0247 collected in experiment 1. The protocol was modified in an attempt to increase both yield and quality compared to the previous extraction experiment.

DNA Isolation (ii)

The procedure followed in experiment 2 was repeated with the following modifications;

- 15mg/ml Lysosyme was added to the MIcrobead Solution prior to use in order to assist bacterial cell wall digestion.

- Multiple (2-4) pellets were combined from the same strain into a single reaction; i.e. using the same 300µl of the Microbead/Lysosyme Solution across multiple pellets. This increased the cell count per genomic prep.

- Microbead tubes were briefly vortexed inverted to dislodge the beads in the tube prior to use.

- Elution centrifuge time was increased from 30 seconds to 1 minute.

Observations

The gDNA concentrations of each preparation ranged from 85ng/µl to 147ng/µl; with an average concentration of 104.45ng/µl. The 260/280 absorbance ratios were within, or close to the ideal range; indicating low levels of protein contamination. The 260/230 absorbance ratios were consistent; though slightly higher than ideal.

TABLE AP1.04: Nanodrop absorbance quantification of 4 gDNA preparations from GBS 0247.

Pellet	**gDNA ng/µl**	**gDNA ng per 50µl elution**	**$A_{260/280}$**	**$A_{260/230}$**
1	85.8	4290	2.01	3.75
2	100.0	5000	1.98	3.16
3	147.0	7350	1.96	3.19
4	85.0	4250	1.97	2.97
Total ng		20,890		
Total µg		20.9		

Pooling the 4 samples resulted in an increased measured yield, and a better 260/230 absorbance ratio (possibly due to the pooled sample being more thoroughly mixed).

TABLE AP1.05: Nanodrop absorbance quantification of pooled gDNA from 4 preparations of GBS 0247.

Sample	**gDNA ng/µl**	**gDNA ng in 200µl**	**$A_{260/280}$**	**$A_{260/230}$**
Pooled	111.1	22,220	1.91	2.22
Total µg		22.22		

Interpretation

The modified extraction protocol improved both quantity and quality of the gDNA preparations. The overall amount of gDNA in the preparation increased by over 50% compared against the original protocol. The improvement in the 260/230 absorbance ratio may be stem from user familiarity with the protocol, and/or be reflective of the increased gDNA yield. This extraction protocol was therefore determined to be suitable for use with the remaining GBS strains.

Supplemental observations for all GBS strains

TABLE AP1.06: Absorbance quantifications of pooled gDNA from multiple preparations of GBS.

Strain	**gDNA ng/µl**	**Total gDNA ng**	**Total gDNA µg**	**$A_{260/280}$**	**$A_{260/230}$**
GBS 0058	41.4	14,283	14.3	1.87	4.21
GBS 0247	111.1	22.220	22.2	1.91	2.22
GBS 0714	106.5	18,105	18.1	1.97	2.14
GBS 0729	58.4	11,388	11.4	2.04	2.15
GBS 0807	68.6	13,720	13.7	1.96	2.10
GBS 0834	94.3	17,445.5	17.4	2.03	2.21
GBS 1014*	158.2	15,815	15.8	1.93	1.93
GBS 874391*	101.2	10,120	10.1	1.91	1.95

** Average readings of 2 preparations (not pooled) – quantified on the Eppendorf Biospectrometer*

Experiment 4: gDNA extractions from larger pellets of GBS strains

Larger bacterial cell pellets were collected to test the efficiency of using more cells. It was anticipated that a higher yield of gDNA could be extracted from a larger pellet of cells.

DNA Isolation (iii)

Pellet collection

Overnight cultures of GBS in 10ml of THY were prepared for each GBS strain used in this study. 1.5ml of the culture was aliquoted into three 1.5ml tubes per culture. Tubes were centrifuged at 15,000g for 2 minutes. After discarding the supernatant, a further 1.5ml was added to the existing pellets from the same culture and re-centrifuged. The large pellets (3 per strain) were stored at -20^{o}C for later gDNA extraction.

gDNA Prep

The optimised protocol (Experiment 3) was performed using the 3 larger pellets. Preparations for each strain were pooled, absorbance quantified, and tested for genomic integrity by gel electrophoresis (i.e. 1µg of each preparation was run for 60 minutes at 100V on a 0.6% gel).

Observations

This approach yielded higher concentrations of good quality gDNA. However the overall yield of gDNA for most of the preparations was lower than the >20µg required for PacificBio sequencing. These preparations were therefore pooled with previous preparations for the same strains and quantified.

TABLE AP1.07: Averaged data for the gDNA extracted from 3 pellets of each GBS strain – quantified by absorption on the Eppendorf Biospectrometer.

Strain	gDNA ng/µl	Total gDNA ng	Total gDNA µg	$A_{260/280}$	$A_{260/230}$
GBS 0058	72.13	10,820	10.8	2.01	1.85
GBS 0714	112.1	11,210	11.2	1.93	2.05
GBS 0729	94.7	4,753	4.8	1.96	2.05
GBS 0807	71.15	7,115	7.1	1.93	1.88
GBS 0834	138.8	13,880	13.9	1.92	1.91
GBS 1014	150.06	22,515	22.2	1.93	2.15
GBS 874391	65.1	9,765	9.8	1.87	1.88

Note: Since enough gDNA was extracted in the initial preparation, no subsequent preparation was performed for GBS 0247.

After pooling, with the exception of 3 strains (GBS 0729, GBS 0807, GBS 874391) all preparations were greater than the required 20µg mark (TABLE 2.09). Further preparations for those strains were required.

TABLE AP1.08: Pooled preparations of GBS strains (extracted from both original & large pellets) absorbance quantified on the Eppendorf Biospectrometer.

Strain	gDNA ng/µl	$A_{260/280}$	$A_{260/230}$	Volume µl	Total ng	Total µg
GBS 0058	52.9	1.91	1.96	480	25,392	25.4
GBS 0247	111.1	1.84	1.84	200	22,220	22.2
GBS 0714	109.8	1.91	2.09	250	27,450	27.4
GBS 0729	56.1	1.95	1.99	280	15,708	15.7
GBS 0807	68.8	1.89	1.97	290	19,952	20.0
GBS 0834	111.6	1.93	2.09	270	30,132	30.1
GBS 1014	151.2	1.92	1.96	240	36,288	36.3
GBS 874391	78.6	1.87	1.89	240	18,864	18.9

1µg of the existing preparations were examined for genomic integrity by gel electrophoresis (FIGURE 2.01). The genomic preparations for all strains (except GBS 0058) showed generally good integrity (>12kb).

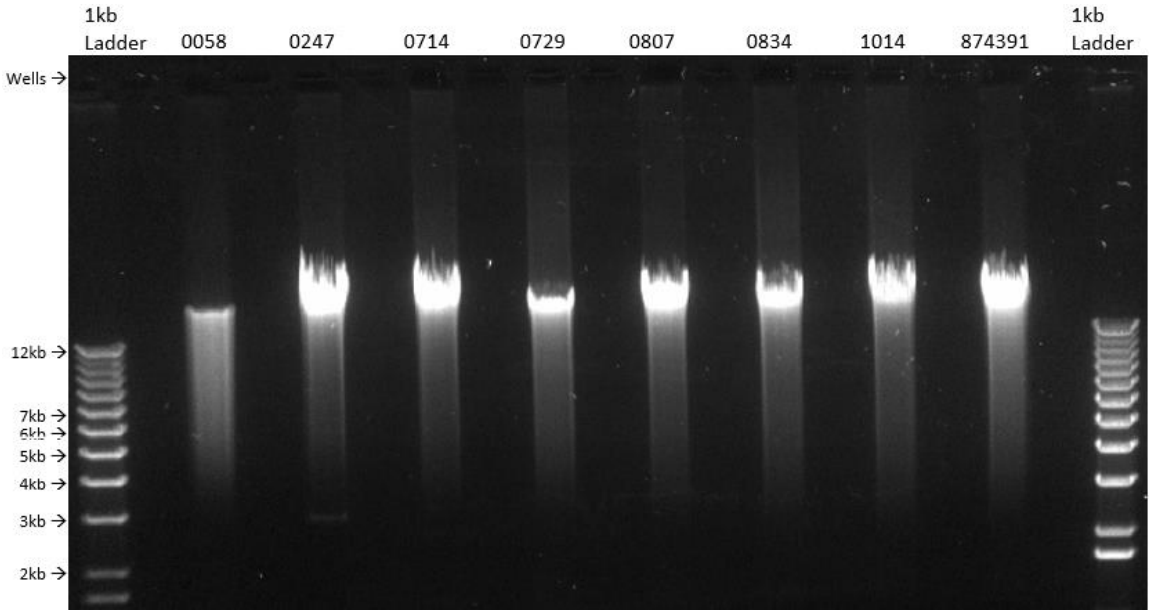

FIGURE AP1.01: Agarose gel showing 1µg gDNA from 8 GBS strains as indicated.
The ladder used was 1kb Plus DNA ladder (Invitrogen) with relevant sizes as indicated in kilobases (kb).

Interpretation

With the exception of GBS strain 0058, sufficient yield and good quality genomic preparations were attained using multiple applications of the optimised protocol. Nonetheless, additional modifications to the protocol were considered in order to improve genomic yield and quality.

Experiment 5: Genomic preparations using bacterial cells isolated during the mid-log phase of growth

Prior experiments utilised GBS cells at the stationary phase of growth. Collecting cells during the stationary phase can have deleterious effects on the quality of the genomic preparation because dead and dying cells will result in degraded DNA. It was therefore determined that genomic preparations should be performed using cells collected during the mid-log growth phase, rather than stationary phase.

DNA Isolation (iv)

Two conical flasks of 50ml THY (pre-warmed at 37°C) were each inoculated with 50µl of a 10ml overnight culture. The new, diluted culture was incubated at 37°C, shaking. Samples were tested every hour on a Thermo-Scientific Spectronic 200 – aiming for a reading OD_{600} between 0.4 and 0.8. The two cultures were pooled and stored on ice until use (total 100ml).

The culture was divided into 10ml aliquots (15ml tubes) and centrifuged for 10 minutes at 7,197g. After discarding supernatant, pellets were resuspended in 10ml PBS to wash the cells from the THY media and re-centrifuged. All-but 0.5ml of the supernatant was discarded, and the remaining PBS used to resuspend the pellets. Cells were transferred to clean 1.5ml tubes and centrifuged at 15,000g for 1 minute. Supernatants were removed by pipette and the pellets stored at -20°C.

The optimised protocol from Experiment 3 was used for the genomic preparations; with the following refinements;

- 40mg (2µl from 20mg/ml) RNaseA was added to the digest prior to the incubation (after the Mutanolysin).

- The digest incubation was increased from 1hour to 90 minutes.

- A second elution was performed through the same column in an attempt to increase the gDNA yield from each column.

Observations

The protocol produced good quality DNA preparations, but the concentrations were variable (TABLE 2.10). Further preparations were required to increase the genomic DNA to >20µg.

TABLE AP1.09: Genomic preparations of GBS using cells collected during the mid-log growth phase.

Strain	OD600	GBS CFU/ml	Total cells in 100 ml THY (10x10ml)	gDNA ng/µl	$A_{260/280}$	$A_{260/230}$	Total gDNA µg
GBS 0058	0.444	1.86E7	1.86E8	119.5	1.84	2.17	12
GBS 0247	0.564	1.74E6	1.74E8	227.0	1.83	1.98	11.4
GBS 0714	0.535	2.40E6	2.40E7	152.3	1.86	2.06	15.2
GBS 0729	0.475	3.46E7	3.46E8	53.3	1.87	1.86	5.3
GBS 0807	0.464	1.66E7	1.66E8	135.2	1.86	2.22	13.5
GBS 0834	0.769	2.54E7	2.54E8	229.3	1.82	2.26	22.9
GBS 1014	1.118	3.92E7	3.92E8	673.4	1.82	2.37	33.7
GBS 874391	0.456	4.72E7	4.72E8	254.1	1.83	2.31	25.4

TABLE AP1.10: Pooled and Absorbance measured genomic preparations of GBS using mid-log growth cells.

Strain	Volume µl	gDNA ng/µl	Total ng	$A_{260/280}$	$A_{260/230}$	Total gDNA µg
GBS 0058	280	95.2	26656.0	1.85	2.16	26.7
GBS 0247	133	166.1	22091.3	1.84	1.95	22.1
GBS 0714	189	147.6	27896.4	1.84	2.16	27.9
GBS 0729	190	162.2	30818.0	1.85	2.10	30.8
GBS 0807	189	133.5	25231.5	1.86	2.21	25.2
GBS 0834	95	232.2	22059.0	1.85	1.99	22.1
GBS 1014	42	670.5	28161.0	1.82	2.34	28.1
GBS 874391	85	256.2	21777.0	1.83	2.26	21.8

Once there was >20µg of pooled gDNA for each strain, 1µg of each was examined for genomic integrity by gel electrophoresis (FIGURE 2.02).

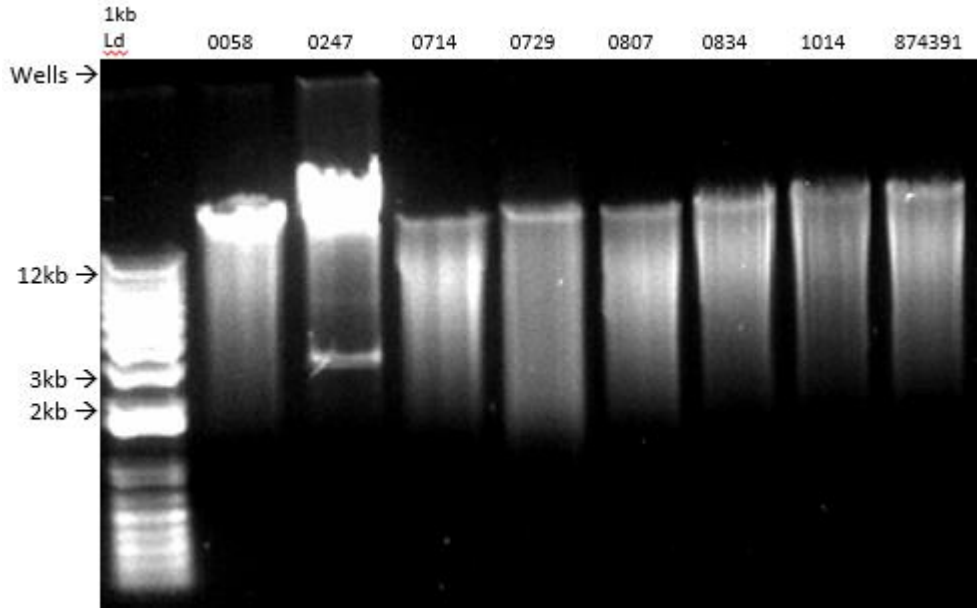

FIGURE AP1.02: Agarose gel showing separation of 1µg gDNA from 8 GBS strains as indicated, isolated from cells in mid-exponential (mid-log) growth phase.
The ladder used was 1kb Plus DNA ladder (Invitrogen) with relevant sizes as indicated in kilobases (kb).

Significant smearing was evident in all preparations except for GBS 0247. Genomic integrity >12kb was only evident in GBS 0058 and GBS 0247. To ensure this result wasn't due to absorbance calculation imprecision, each preparation was re-quantified using Qubit Fluorescence reagents (Qubit dsDNA BR Assay Kit) on the Eppendorf Biospectrometer.

TABLE AP1.11: Comparison of DNA quantity measurements using absorbance and fluorescence (Qubit) based methods, from experiment 5 (mid-exponential growth phase).

Strain	Absorbance gDNA ng/µl	Fluorescence gDNA ng/µl
GBS 0058	95.2	61.5
GBS 0247	166.1	99.6
GBS 0714	147.6	111.9
GBS 0729	162.2	120.4
GBS 0807	133.5	99.5
GBS 0834	232.2	179.2
GBS 1014	670.5	Too High
GBS 874391	256.2	212.1

Note: The measurement for GBS 1014 was more than 5% outside of the range of the range of the standard concentrations.

Fluorescence measurements were lower for all preparations than the absorbance measurements - indicating that the absorbance measurements may have been influenced by non-DNA molecules in the preparations. Based on the fluorescence readings, 1µg of each preparation was examined by gel electrophoresis (FIGURE 2.03). As GBS 1014 was outside the range of the fluorescence standards, the 1µg was based on the next highest reading (i.e. GBS 874391 212.1ng/µl).

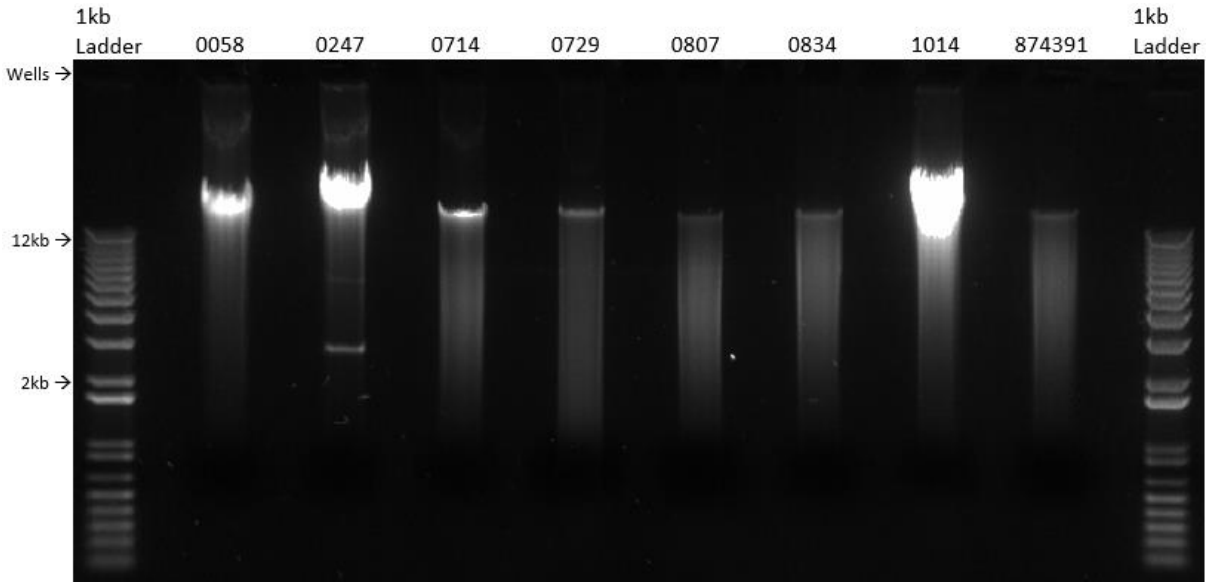

FIGURE AP1.03: Agarose gel showing separation of 1µg gDNA (fluorescence quantified) from 8 GBS strains as indicated.
The ladder used was 1kb Plus DNA ladder (Invitrogen) with relevant sizes as indicated in kilobases (kb).

Based on the relative intensity of the band and the previous absorbance measures, it was estimated that approximately 3µg of GBS 1014 was loaded. The rest of the gel mirrored the observations of the absorbance-quantified gel – i.e. quality genomic integrity for GBS 0058 and GBS 0247, but poor genomic integrity for the other strains.

Interpretation

Genomic preparations generated using the optimised protocol on GBS cells isolated during mid-log growth are less robust than the preparations from stationary phase cells. Whilst the DNA quality is generally good (i.e. contamination free when quantified by absorbance), the yields were low and the genomic integrity compromised. Further refinements to the protocol were therefore required to improve yield and genomic integrity.

Experiment 6: Protocol refinements for genomic preparations using bacterial cells isolated during the mid-log phase of growth

Previous gDNA preparations from mid-log growth GBS cells demonstrated poor integrity – as evidenced by extensive genomic smearing in the gels. The UltraClean Microbial DNA Isolation Kit (MO BIO Laboratories) protocol suggested replacing the bead-beating step with a heat/vortex step to reduce genomic degradation. Reducing the bead-beating time was also tested.

DNA Isolation (v)

To examine the effect of replacing the bead-beating step with the heat/vortex method, gDNA preparations were made from pellets of two strains of GBS (0834 and 874391). For each strain, two treatments were applied. The first treatment followed the established protocol (including a 10 minute bead-beating step). The alternative treatment for each strain replaced the bead-beating with a 10 minute incubation at 65^{o}C interspersed with a pulse-vortex every 2 minutes.

Using GBS strains 0807 and 1014, reducing the bead-beating time from 10 minutes, to 5 and 1 minutes respectively was also tested.

To test if DNA is released preferentially in differing amounts per elution, samples were eluted twice, each into separate tubes (50µl H_2O per tube).

Observations

The heat/vortex method preserved better genomic integrity than the 10 minute bead beaten treatment, however the concentrations of gDNA derived from the heat/vortex treatment were too low to be useful. The 1 minute bead-beating method yielded lower concentrations of gDNA than the 5 minute Bead-beaten treatment, but not so low as to be impractical. The gDNA concentrations from the second elutions were consistently lower than the initial elutions for all treatments however, in both 1 minute bead-beaten treatments, the second elution yielded several µg of gDNA.

TABLE AP1.12: BioSpec absorbance quantification of gDNA preparations for 4 GBS strains, 2 treatments per strain, and 2 elutions per treatment.

Strain	Treatment	Elution	ng/µl	$A_{260/280}$	$A_{260/230}$	Total µg
GBS 0834	**10 min bead-beat**	1	397.1	1.84	2.44	19.9
		2	167.2	1.85	2.44	8.4
	Heat/vortex	1	80.0	1.94	2.12	4.0
		2	58.2	1.83	2.42	2.9
GBS 874391	**10 min bead-beat**	1	196.3	1.84	2.19	9.8
		2	54.1	1.84	2.20	2.7
	Heat/vortex	1	25.7	1.81	1.31	1.3
		2	22.0	1.79	1.41	1.1
GBS 0807	**5 min bead-beat**	1	151.3	1.86	2.47	7.6
		2	39.7	1.88	2.28	2.0
	1 min bead-beat	1	137.4	1.85	2.41	6.9
		2	51.7	1.83	2.09	2.3
GBS 1014	**5 min bead-beat**	1	391.0	1.83	2.37	19.6
		2	103.3	1.85	2.04	5.2
	1 min bead-beat	1	231.8	1.84	2.34	11.6
		2	87.8	1.85	1.99	4.4

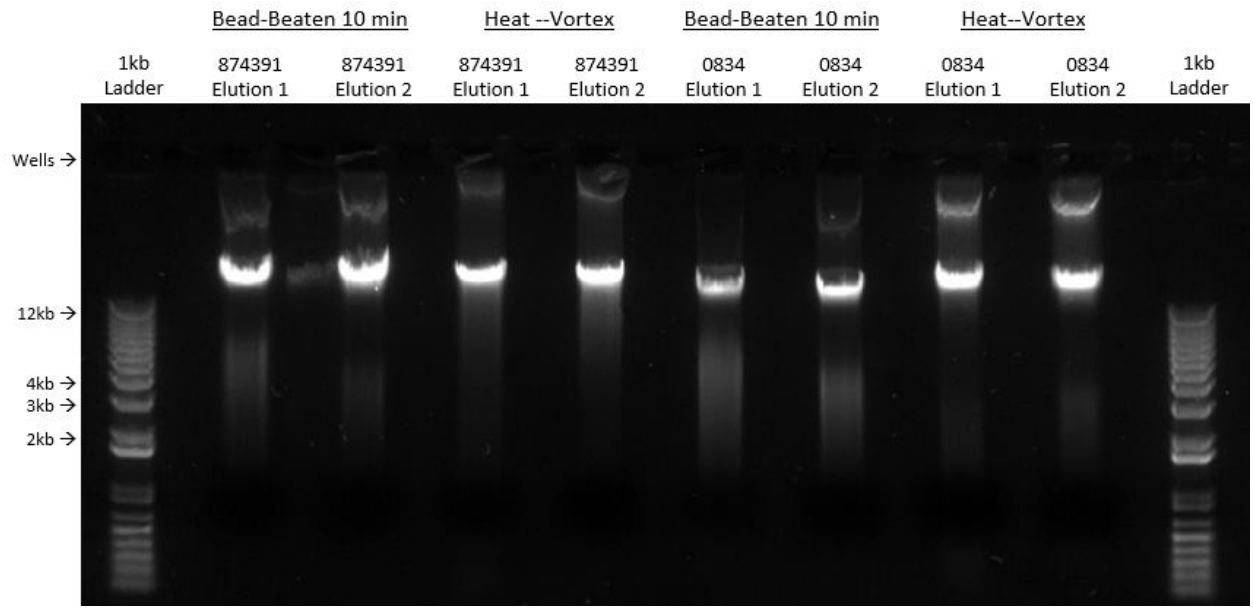

FIGURE AP1.04: Agarose gel showing separation of 1µg gDNA from GBS strains 874391 and 0834 as indicated, isolated from cells in mid-exponential growth phase, comparing 2 elutions of preparations derived from heat/vortexing vs bead-beating methods.

The ladder used was 1kb Plus DNA ladder (Invitrogen) with relevant sizes as indicated in kilobases (kb).

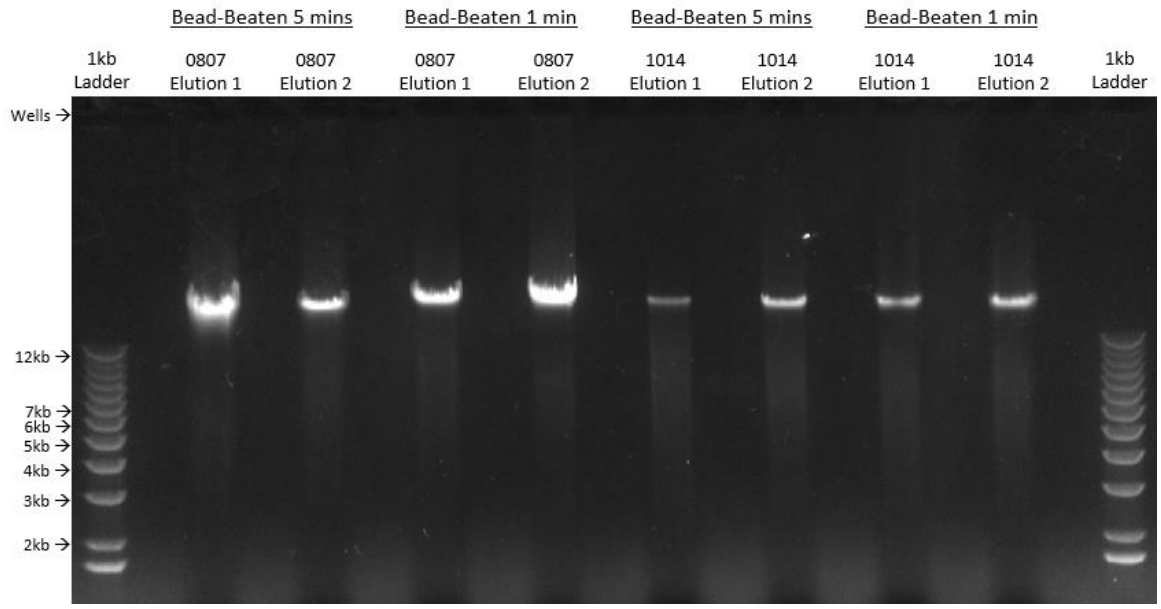

FIGURE AP1.05: Agarose gel showing separation of 1µg gDNA from GBS strains 874391 and 0843 as indicated, isolated from cells in mid-exponential growth phase, comparing 2 elutions of preparations derived from 1 minute vs 5 minutes bead-beating methods.

The ladder used was 1kb Plus DNA ladder (Invitrogen) with relevant sizes as indicated in kilobases (kb).

Interpretation

There is a gDNA smearing effect on the preparations which is contingent on the amount of bead-beating time. Replacing bead-beating with a softer, heat/vortex protocol resulted in impractically low concentrations of gDNA. However, only 1 minute of bead-beating was required to produce usable concentrations of gDNA without any notable degradation to the preparation. Therefore, future preparations will use a 1 minute bead-beat rather than the prescribed 10 minute bead-beat.

A second elution through the column can produce several µg of gDNA. Future preparations will therefore incorporate two 50µl elutions for each preparation.

Appendix 2 – Infection Assay Optimisations

Experiment 1: Infection 1. Pilot Infection Experiment – Adhesion and Invasion assays

To our knowledge, there have been no co-transcript studies to-date investigating GBS as the pathogen. A range of experiments are therefore required to optimise an infection protocol that will ultimately permit the extraction of high quality RNA from three distinct conditions; 1) The infection condition – i.e. U937 monocytes infected with GBS, 2) a GBS-only control used to compare against the transcripts of intracellular GBS, and 3) a monocyte-only control used to compare against the transcripts of infected monocytes.

Initial experiments were designed to generate baseline information for GBS and U937 cell survival and viability, considering the requirement to extract sufficient host and pathogen RNA from a single reaction for use in downstream applications. It was estimated that the minimum useable bacterial yield would be 1E4 CFU/ml based on RNA requirements. Initial experiments were therefore performed on a small scale to quantify the capacity of GBS to survive inside the monocytes in the proposed model. The goal of this experiment was to determine the general suitability of the proposed approach.

Adhesion and Uptake Assay

GBS 874391 was cultured overnight in 10ml THY in accordance with the General Procedures (Bacterial growth in THY - CHAPTER 2, section 2.2.1.4). GBS were washed from the overnight culture media in PBS and resuspended in bRPMI for the infection challenge. Specifically, the overnight culture was centrifuged for 15 minutes at 7197g, the pellet resuspended in 10ml PBS and centrifuged at 7197g for 10 minutes, the resulting pellet was again resuspended in 10ml PBS and centrifuged at 7197g for 10 minutes before resuspending the pellet in 10ml bRPMI and storing in ice prior to the infection. 20µl of washed GBS was processed in accordance with the General Procedures (Serial Dilutions of bacterial cultures and bacterial colony counts – CHAPTER 2, section 2.2.1.5).

U937 monocytes between passage 3 and 25 were cultured to attain 25ml of cells in bRPMI at >1E5 cells/ml. The monocytes were washed in PBS before being resuspended in bRPMI. Specifically, 25ml of cells were centrifuged for 5 minutes at 500g and the pellet resuspended in 25ml PBS. The centrifuge and PBS resuspension was repeated. After a third centrifuge, the cell pellet was resuspended in bRPMI and stored in ice until the infection.

For the infectious challenge, 1:10 volume ratios of GBS to monocyte cultures were used for these infections. For the infection, 1.6ml washed GBS cells in bRPMI were added to 14.4ml of washed monocytes in bRPMI. For the monocyte control, 1.2ml bRPMI was added to 10.8ml washed monocytes in bRPMI. For the GBS control, 1.2ml washed GBS cells in bRPMI was added to 10.8ml bRPMI. For the first time-point (T=0), four infection replicates of 1ml each were transferred directly into 1.5ml tubes for immediate processing. For the remaining time-points, four technical replicates of 1ml for each condition were aliquoted into separate wells of 24-well plates. The treatment plates were then incubated at 37^{o}C in 5% CO_2 until collection and processing. Processing entailed transferring the contents of each well to a 1.5ml tube and centrifuging for 5 minutes at 500g; repeated 5 times. The first 4 pellet resuspensions were in 1ml PBS. The final resuspension for each sample was in 900µl of PBS and 100µl of 1% Triton (i.e. final volume 0.1% Triton). Ten-fold serial dilutions in PBS were performed on each sample before plating in triplicates of 5µl on TSA-Blood Agar plates. Plates were incubated overnight at 37^{o}C and colony counts recorded.

Seven conditions were tested as follows - After a 1 hour incubation (T=1), GBS and monocytes, as well as the infection/adhesion treatments were collected for processing. At this time, antibiotics (ABX) (50µg/ml Gentamicin with 2.5X Pen/Strep) were added to the remaining treatments - except the GBS control. After a 2 hour incubation (T=2) (1 hour with ABX), the first infection/invasion treatment was collected and processed. After a 5 hour infection (T=5), GBS and monocyte controls as well as the infection/invasion treatments were collected for processing.

Observations

For each experiment, the number of monocytes and GBS were determined to calculate the multiplicity of infection (MOI) ratio. The concentration of viable washed monocytes was 1.24E6 cells/ml. 90% of these cells were used in the experiments (i.e. 1.12E6 cells/ml in each treatment). After overnight incubation and colony counts (TSA-Blood agar plates), the concentration of washed GBS prepared was determined to be 3.93E8 CFU/ml. 10% of this concentration was used for the experiment (i.e. 3.93E7 CFU/ml).

Henceforth this information will be summarised according to the following format - Infection 1; Prepared monocytes: 1.24E6 cells/ml, Used monocytes: 1.12E6 cells/ml, Prepared GBS: 3.93E8 CFU/ml, Used GBS: 3.93E7 CFU/ml. Therefore the MOI ratio was 35.

At T=0, the GBS counts for the GBS-only control were similar to the counts from the infection treatment (5.46E7 and 6.95E7 CFU/ml respectively). At T=1, the GBS adhesion count was 4.46E7 CFU/ml. At T=2, the GBS counts from the invasion assay (after 1 hour ABX) had dropped to 5.6E3 CFU/ml - i.e. a roughly 99.99% ($4\log_{10}$) reduction in GBS numbers. The colonies on this plate ranged in size from large to pinpoint, but all displayed clear haemolysis; indicative of pure GBS colonies. The survival numbers of GBS in the infection treatment reduced by approximately ten-fold over the subsequent 3 hours.

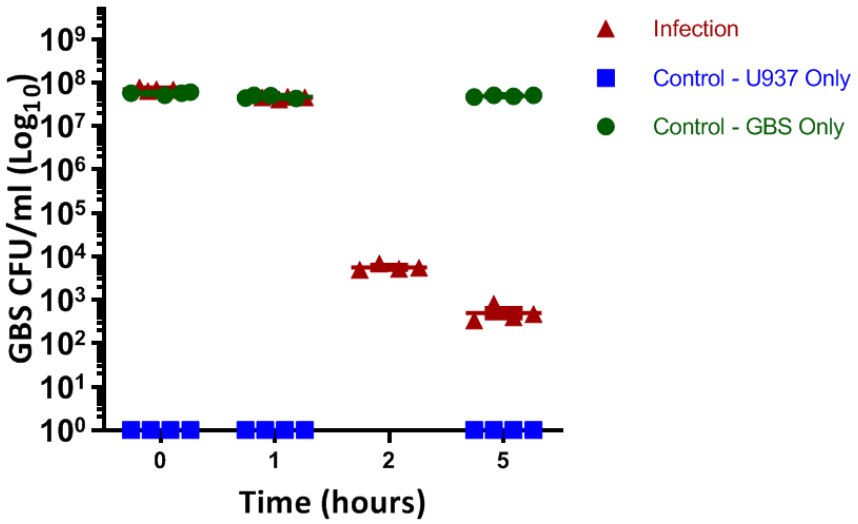

FIGURE AP2.01: Infection 1 – U937 Monocytes infected with GBS 874391 at an MOI of 35.
The monocyte control was comprised of bRPMI added to washed monocytes. The GBS control was comprised of washed GBS added to bRPMI. CFU/ml counts of GBS were performed at each time point after washing the cells with PBS and lysing the monocytes with Triton. Time 0 is the time of infection. ABX were added 1 hour after infection (after processing samples for that time point). Lines show mean and SEM from 4 technical replicates. The actual number of GBS in the monocyte control was zero throughout the assay. No CFU/ml data was available for time point 2 for the GBS control.

Interpretation

The numbers of GBS recovered from the invasion assay were higher than expected which may be due to the MOI (35), inefficient washing of the monocytes prior to processing, or damaged monocytes releasing intracellular GBS during the washing process. The latter two options cast some doubt on the reliability of the invasion assay. The post infection GBS counts were considered too low to yield a useful amount of RNA for downstream use. However, the experiment demonstrated theoretical suitability of a model of infection using U937 monocytes as the host cells and GBS 874391 as the pathogen.

Experiment 2: Infection 2. Centrifugation to Enhance the Host-Pathogen Interaction

A previous study utilised a pre-incubation centrifuge to more efficiently associate the chlamydial bacteria in their study to the U937 cells they were using as host cells (Virok *et al.*, 2003). By forcing the different cell types to associate with each other, it was assumed that the likelihood of bacteria becoming internalised in the host cells increases. Given the assumption of intracellular bacterial survival, the addition of an initial centrifugation step was expected to increase the bacterial yield from infected monocytes. The goal of this experiment was to determine if adding a pre-incubation centrifuge to the infection would increase GBS numbers recovered from the monocytes.

Infection with Centrifugation

The protocol from Experiment 1 was generally followed with the following modifications;

There were two primary treatments. The centrifuge treatment incorporated centrifuging the plated infection for 45 minutes at 600g at room temperature. The control infection treatment was incubated at 37^{o}C in 5% CO_2 while the first treatment was being centrifuged. T=0 was the time point after the initial centrifugation/incubation – at which time the ABX was added. Time points were processed at T=0, and 1, 3 and 5 hours post ABX (T=1, T=3 and T=5 respectively).

Observations

Infection 2; Prepared monocytes: 7.64E5 cells/ml, Used monocytes: 6.88E5 cells/ml, Prepared GBS: 5.46E8 CFU/ml, Used GBS: 5.46E7 CFU/ml. Therefore the MOI ratio was 79.

At T=0, GBS counts were equivalent from both non-centrifuged and centrifuged treatments (5.20E7 and 5.16E7 CFU/ml respectively). Contrary to expectation, the non-centrifuged treatment yielded more intracellular GBS after 1 hour of ABX (3.94E4) than the centrifuged treatment (1.04E4). By T=3, the GBS yield from both treatments was equivalent (3.24E3 from the non-centrifuged treatment and 2.98E3 from the centrifuged treatment).

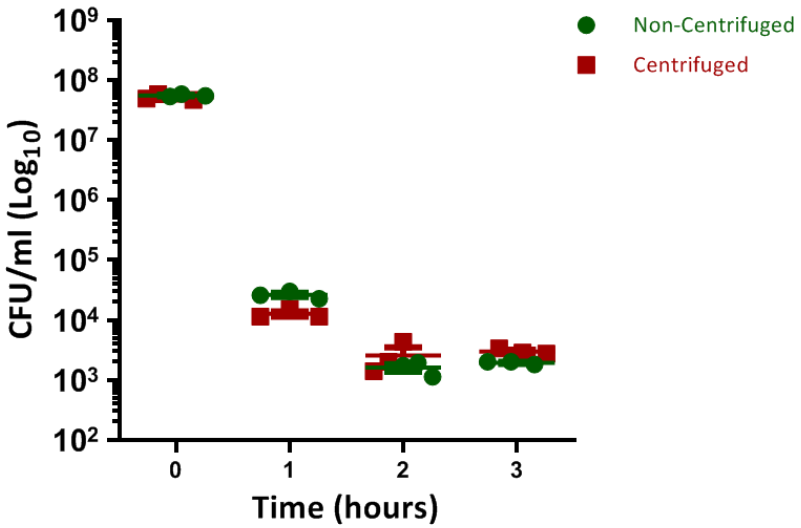

FIGURE AP2.02: Infection 2 - GBS recovered from centrifuged vs non-centrifuged monocytes infected with GBS 874391 at an MOI of 79.

CFU/ml counts of GBS were performed at each time point after washing the cells with PBS and lysing the monocytes with Triton. Time 0 is post centrifuge/incubation (i.e. 45 minutes after the infection). ABX were also added at time 0 (after processing samples for that time point). Lines show mean and SEM from 4 technical replicates.

Interpretation

The centrifugation protocol, as applied in this experiment, does not increase the GBS yield from the infection model. The non-centrifuged control treatment may be biased by phagocytosis that may occur during the 45 minute incubation – representing additional time for internalising the GBS. It is possible that the 600g centrifuge speed was insufficient to bring the GBS to the monocytes. Increasing the centrifuge speed is likely to be detrimental to the monocytes.

Experiment 3: Infection 3. Centrifugation to Enhance the Host-Pathogen Interaction (ii)

In Experiment 2, phagocytosis during the 45 minutes of incubation of the non-centrifuged treatment may have biased the results. Therefore, the experimental design was modified to include a more representative control treatment. The goal of this experiment was to compare the GBS numbers recovered from monocytes in a centrifuged treatment versus those recovered from a non-centrifuged treatment that included equivalent times of incubation.

Infection with Centrifugation (ii)

The protocol from Experiment 1 was generally followed with the following modifications;

To increase the bacterial load in the infection ten-fold, GBS was initially inoculated into a 100ml THY for the overnight culture, and after washing, was resuspended in 10ml bRPMI.

There were two primary treatments. The centrifuge treatment incorporated centrifuging the plated infection at 600g for 50 minutes at room temperature. The control infection treatment was incubated at room temperature on a bench while the first treatment was being centrifuged. T=0 was the time point after the initial centrifugation/incubation. After a 1 hour incubation at 37^{o}C in 5% CO_2, the ABX was added to all treatments. Three technical replicates were plated for each treatment for every time point. Time points were processed at T=0, and 1, 2 and 5 hours post ABX (T=1, T=2 and T=5 respectively).

Observations

Infection 3; Prepared monocytes: 1.19E6 cells/ml, Used monocytes: 1.07E6 cells/ml, Prepared GBS: 3.06E9 CFU/ml, Used GBS: 3.06E8 CFU/ml. Therefore the MOI ratio was 285.

At T=0 and T=1 (i.e. prior to the addition of ABX), the GBS numbers associated with the cells were equivalent for both treatments (For non-centrifuged and centrifuged treatments respectively; 3.02E8 and 2.88E8 CFU/ml at T=0, and 4.32E9 and 4.48E9 CFU/ml at T=1). After 1 hour of incubation with ABX, GBS numbers were reduced by more than 1$\log_{10}$; with 15% more GBS being recovered from the centrifuged sample (7.94E7 and 1.00E8 CFU/ml for non-centrifuged and centrifuged treatments respectively). The number of CFU/ml recovered from the centrifuged treatment remained constant over the next 3 hours of incubation. The GBS number recovered from the non-centrifuged treatment decreased to 4.84E7 CFU/ml.

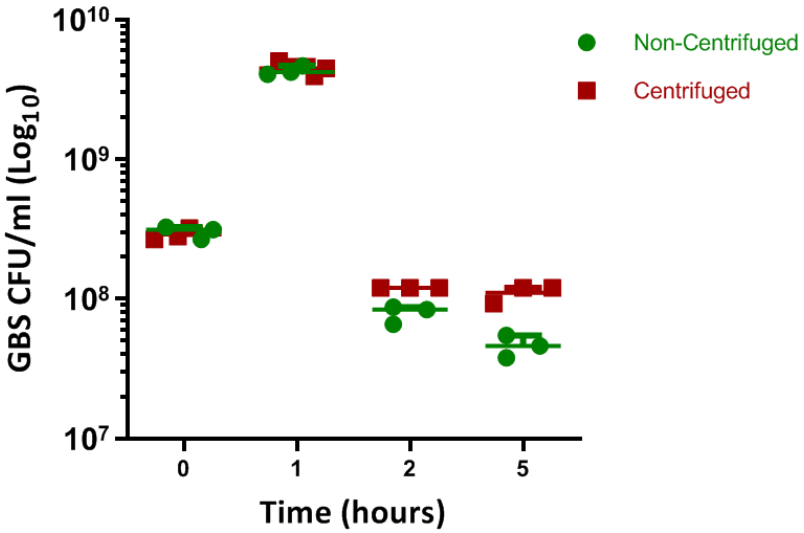

FIGURE AP2.03: Infection 3 - GBS recovered from centrifuged vs non-centrifuged monocytes infected with GBS 874391 at an MOI of 285.

CFU/ml counts of GBS were performed at each time point after washing the cells with PBS and lysing the monocytes with Triton. Time 0 is post centrifuge/incubation (i.e. 50 minutes after the infection). After both treatments underwent 1 hour of incubation in 5% CO_2 at 37°C, ABX were added at time point 1 (after processing samples for that time point). Lines show mean and SEM from 3 technical replicates.

Interpretation

The increase of GBS numbers recovered before the addition of ABX likely reflects GBS proliferation in the infection media. High numbers of internalised GBS were recovered from both treatments, which may reflect the higher MOI. The high GBS numbers recovered from the infection raises questions about the efficiency of the pre-processing washes, and/or the ABX activity. Centrifugation increases the GBS recovery rate from the infection – thus centrifuging prior to incubation increases the association frequency between GBS and monocytes.

Experiment 4: Infection 4. Centrifugation to Enhance the Host-Pathogen Interaction (iii)

Experiment 3 was repeated to verify the hypothesis that a pre-incubation centrifugation procedure enhances GBS recovery from the infection. A post-infection wash efficiency test was also performed. The goal of this experiment was 1) to verify the results of Experiment 3, and 2) to analyse the effects of pre-processing washes on recovered GBS numbers.

Infection with Centrifugation (iii)

The protocol from Experiment 1 was generally followed with the following additions;

At T=2 (after 1 hour of ABX), 20µl of supernatants from the first PBS wash and 20µl of supernatants from the final PBS wash were processed in accordance with the General Procedures (Serial Dilutions of bacterial cultures and bacterial colony counts – CHAPTER 2, section 2.2.1.5), to determine wash efficiency.

Observations

Infection 4; Prepared monocytes: 8.63E5 cells/ml, Used monocytes: 7.77E5 cells/ml, Prepared GBS: 3.86E9 CFU/ml, Used GBS: 3.86E8 CFU/ml. Therefore the MOI ratio was 497.

At T=5 (i.e. after 4 hours of antibiotic treatment), 73-fold more GBS were recovered from the centrifuged infection treatment than the non-centrifuged treatment (8.58E7 and 1.17E6 CFU/ml respectively).

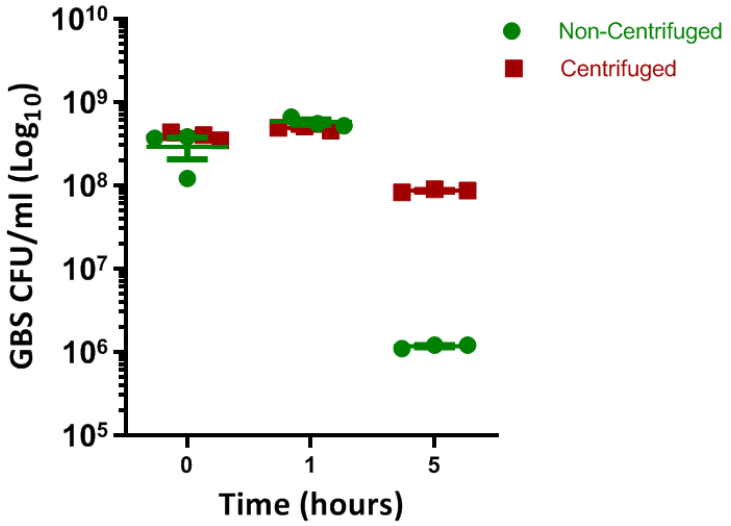

FIGURE AP2.04: Infection 4 - GBS recovered from centrifuged vs non-centrifuged monocytes infected with GBS 874391 at an MOI of 285.

CFU/ml counts of GBS were performed at each time point after washing the cells with PBS and lysing the monocytes with Triton. Time 0 is post centrifuge/incubation (i.e. 50 minutes after the infection). After both treatments underwent 1 hour of incubation in 5% CO_2 at 37°C, ABX were added at time point 1 (after processing samples for that time point). Lines show mean and SEM from 3 technical replicates.

Contrary to expectation, the final post-infection wash at T=2 yielded more GBS than the earlier wash (6.04E6 and 1.28E5 CFU/ml respectively).

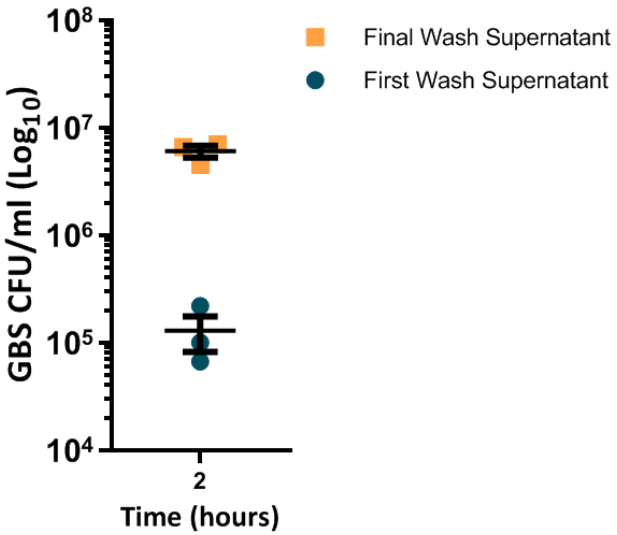

FIGURE AP2.05: Infection 3 - GBS recovered from first and final wash supernatants.
After 1 hour of ABX, infection samples were washed five times by centrifuge (pelleting the monocytes) and resuspension in PBS. Supernatants were taken from the first and final pelleted samples and processed for GBS CFU/ml counts of extracellular GBS. Lines show mean and SEM from 3 technical replicates.

Interpretation

Confirming the observations of Experiment 3, a pre-incubation centrifuge step enhances the association between GBS and monocytes – resulting in greater GBS recovery from the infection.

The post-infection washes are expected to yield progressively lower GBS numbers; ideally, reducing the supernatant bacterial load to near zero. Instead, the GBS numbers increased between the first and final washes. This result is unexplained, but may reflect GBS survival of the ABX treatment and remaining in the media in high numbers, or monocyte stress and release of GBS into the wash during centrifugation or pellet resuspension. Monocytes may be stressed by the high MOI (497) used in this experiment.

Experiment 5: Effectiveness of Antibiotics against GBS 874391

An antibiotic mix of 50µg/ml Gentamicin with 2.5X Pen/Strep has been previously shown to be effective in eliminating GBS from RPMI media in infection assays spanning 2 to 24 hours (Leclercq *et al.*, 2016) (Sullivan *et al.*, 2017b). Due to the possibility of GBS survival in this antibiotic mix (Experiment 4), experiments were conducted to confirm the killing efficiency of these antibiotics for GBS 874391; a genome-sequenced strain used in this thesis.

Bacterial Time-kill Assays

Overnight cell cultures of GBS 874391 were prepared in 100ml THY in accordance with the General Procedures (Bacterial growth in THY - CHAPTER 2, section 2.2.1.4). After PBS washing (Adhesion and Uptake Assay – Experiment 1), the pellet was resuspended in 10ml bRPMI and placed in ice. The GBS cells were then inoculated into fresh bRPMI at a 1:10 ratio into a 50ml tube and gently mixed by inverting the tube. For the first time-point (T=0.0), 1ml of the ABX-free inoculum was aliquoted in triplicate directly into 1.5ml tubes for immediate processing. Then ABX (50µg/ml Gentamicin with 2.5X Pen/Strep) was added to the remaining inoculate.

1ml of the remaining inoculum (with ABX) was aliquoted into 18 wells of a 24-well cell culture plate and incubated at 37^{o}C in 5% CO_2 to reflect the conditions of infection experiments. Every half hour thereafter, the contents of 3 wells was transferred into 3, 1.5ml tubes for processing.

This procedure was performed independently twice.

Observations

In the first assay, GBS numbers dropped from 6.27E8 CFU/ml at T=0.0 to non-detectable after 1.5 hours of antibiotic treatment. In the second assay, GBS numbers dropped from 6.8E8 CFU/ml at T=0.0 to non-detectable after 2 hours of antibiotic treatment.

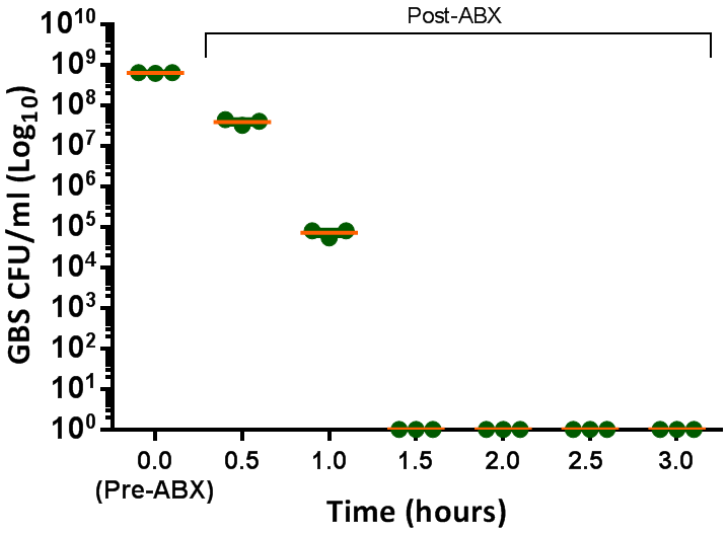

FIGURE AP2.06: GBS Time Kill Assay 1.

6.27E8 CFU/ml of GBS were exposed to a cocktail of Gentamycin and Pen/Step antibiotics for 3 hours. Surviving bacteria were enumerated by CFU/ml counts every 30 minutes. The lines show means of 3 technical replicates.

For all post ABX treatments in assay 2 (FIGURE AP2.07), by 2 hours, no colonies were observed on any of the processed colony count plates, indicating ≥ 99.99% killing of GBS 874391 in those conditions after 2 hours. However, no colonies were observed on the plates at dilution factors 0 and 1 – indicating continued activity of the ABX at these lower dilutions. Assuming 0.3 colonies as the lowest possible average detection from 3 technical replicates (i.e. 1 colony in 3 replicates), being detected in 5µl droplets only at a dilution factor of 2 (i.e. 10E-2), the actual limit of detection sensitivity was calculated to be 6E3 CFU/ml. Without the influence of ABX, the expected limit of detection sensitivity is 6E1 CFU/ml.

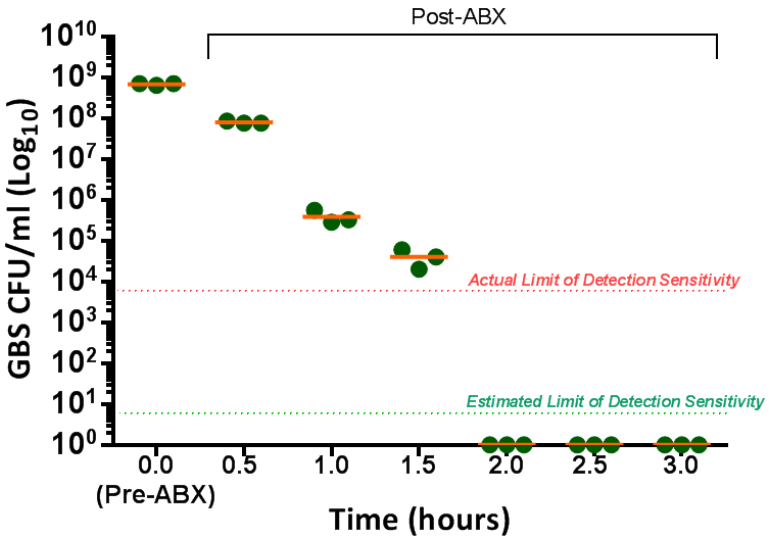

FIGURE AP2.07: GBS Time Kill Assay 2.

Around 1E9 CFU/ml of GBS were exposed to a cocktail of Gentamycin and Pen/Step antibiotics for 3 hours. Surviving bacteria were enumerated by CFU/ml counts every 30 minutes. The orange lines show means of 3 technical replicates. Calculated Detection limit (red) vs Expected Detection limit (green) are shown with dotted lines.

Interpretation

The ABX treatments appear are highly effective; reducing the bacterial load 8log_{10} over 2 hours of incubation. The sensitivity limit for detection was estimated to be 60 CFU/ml, but carry-over of antibiotic into colony counts likely means the detection sensitivity limit of this procedure was closer to 6.0E3 CFU/ml.

Experiment 6: Effectiveness of Antibiotics against GBS 874391 (ii)

The previous experiment suggested antibiotic carry-over to low dilutions in colony counts; increasing the limit of detection from 1E2 to 1E3 CFU/ml. To reduce the detection sensitivity limit of the assay, a modified protocol was used. The goal of this experiment was to achieve a lower detection limit.

Bacterial Time-kill Assays (ii)

The procedure from Experiment 5 was generally followed for two independent assays; with the following modifications;

A single PBS wash was utilised for each replicate in assay 1. Samples were centrifuged for 5 minutes at 15,000g before pellets were resuspended in 1ml PBS.

In assay 2, the samples were PBS-washed (as above) twice before processing. A further 200µl of time points T=2.0 to T=3.0 were spread over a single TSA-Blood agar plate (in triplicate) to improve the detection limit of sensitivity to 1.5 CFU/ml.

Observations

In the first assay (FIGURE AP2.08), GBS persisted in the assay at 1.6E3 CFU/ml after 3 hours of antibiotic treatment (T=3.0). At T=0.5, there were confluent colonies at the 1E2 dilution factor, but still no colonies at the lower dilution factors. Even though some colonies appeared in these lower dilution factors for later time points, they were not meaningful when related to higher dilutions at the same time point.

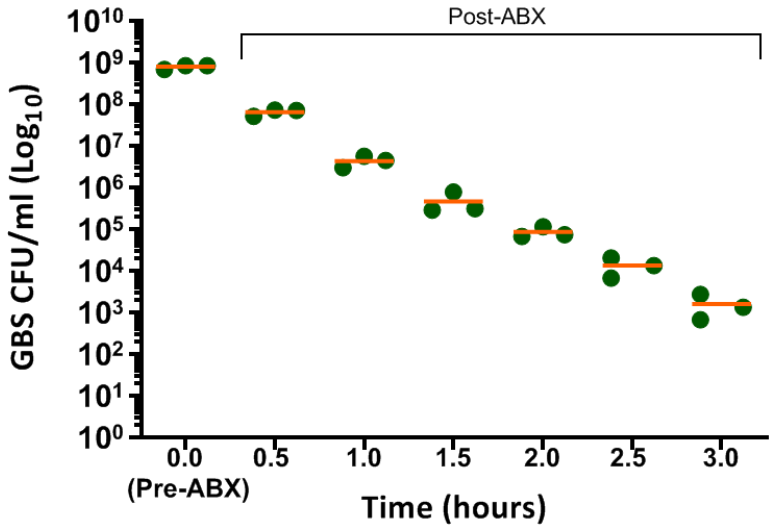

FIGURE AP2.08: GBS Time Kill Assay 3.
Around 1E9 CFU/ml of GBS were exposed to a cocktail of Gentamycin and Pen/Step antibiotics for 3 hours. Surviving bacteria were enumerated by CFU/ml counts every 30 minutes. The lines show means of 3 technical replicates.

In the second assay (FIGURE AP2.09) GBS numbers remained in the assay at 1.9E3 CFU/ml after 3 hours of antibiotic treatment (T=3.0). At T=0.5, there were confluent colonies at the 1E-2 dilution factor, but still no colonies at the lower dilution factors (1E-1 and 1E-0). There were also no colonies present for these dilution factors on the T=1.0 plate. However, there were confluent colonies at both these dilution factors on the T=1.5 plate. The T=2.0 to T=3 plates produced meaningful numbers at these dilution factors when related to the higher dilutions.

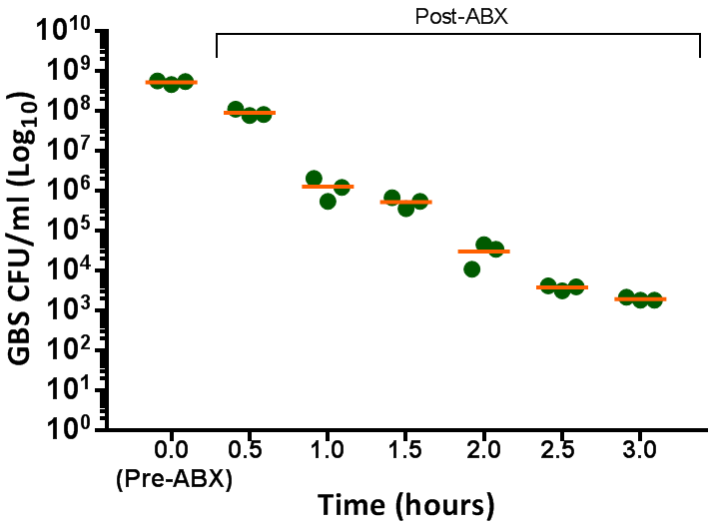

FIGURE AP2.09: GBS Time Kill Assay 4.

Around 1E9 CFU/ml of GBS were exposed to a cocktail of Gentamycin and Pen/Step antibiotics for 3 hours. Surviving bacteria were enumerated by CFU/ml counts every 30 minutes. The lines show means of 3 technical replicates.

Interpretation

A single PBS wash was insufficient mitigate the influence of ABX to a point where the outcome could be trusted. The antibiotic activity was still influencing the colony counts after two PBS washes, however, not at levels that impact the informative data. These assays revealed that while the numbers of GBS 874391 decrease roughly $5\log_{10}$, this strain of GBS can persist with the proposed ABX mix for at least 3 hours.

Experiment 7: Effectiveness of Antibiotics against GBS 874391 (iii)

Since GBS 874391 survive in the prescribed ABX (Gentamicin and Pen/Strep) for at least 3 hours, 6 hour assays were performed to determine the duration and rate of GBS persistence in ABX.

Bacterial Time-kill Assays (iii)

The procedure from Experiment 5 was generally followed for two independent assays; with the following modifications;

The assay incubation was extended from 3 hours to 6 hours (T=0 to T=6). Processing was performed hourly instead of every 30 minutes. Samples were washed in PBS twice before processing (Experiment 7).

Observations

For the first 6 hour time kill assay (FIGURE AP2.10), after 3 hours of antibiotics (T=3), the GBS numbers fell below the previous detection sensitivity limit of Experiment 5 (6.0E3 CFU/ml). After 5 hours of antibiotic treatment (T=5), the GBS counts fell below 10E3 CFU/ml. And after 6 hours of antibiotic treatment (T=6), the GBS numbers remained in the assay at 5.3E2 CFU/ml.

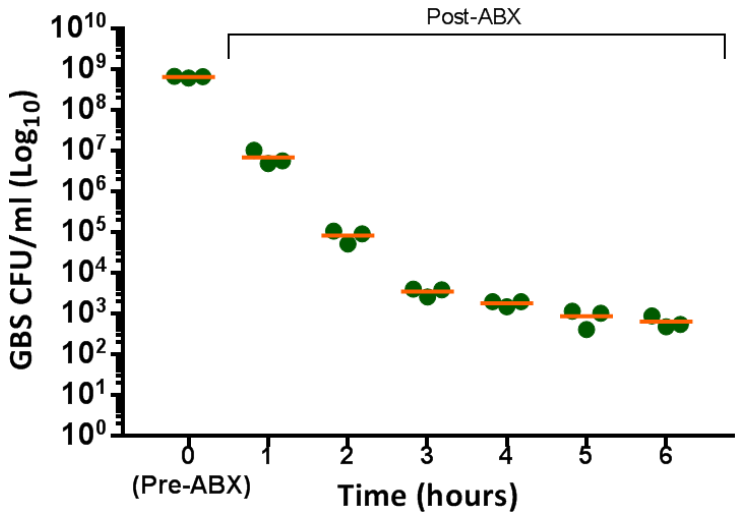

FIGURE AP2.10: GBS Time Kill – Six Hour Assay 1.
Around 1E9 CFU/ml of GBS were exposed to a cocktail of Gentamycin and Pen/Step antibiotics for 6 hours. Surviving bacteria were enumerated by CFU/ml counts every hour. The lines show means of 3 technical replicates.

For the second 6 hour time kill assay (FIGURE AP2.11), after 2 hours of antibiotics (T=2), the GBS numbers fell below the previous detection sensitivity limit of Experiment 5 (6.0E3 CFU/ml). At T=4, the GBS counts fell to 10E3 CFU/ml. And after 6 hours of antibiotic treatment (T=6), the GBS numbers remained in the assay at 4.2E2 CFU/ml; having increased from 4.0E2 at T=5.

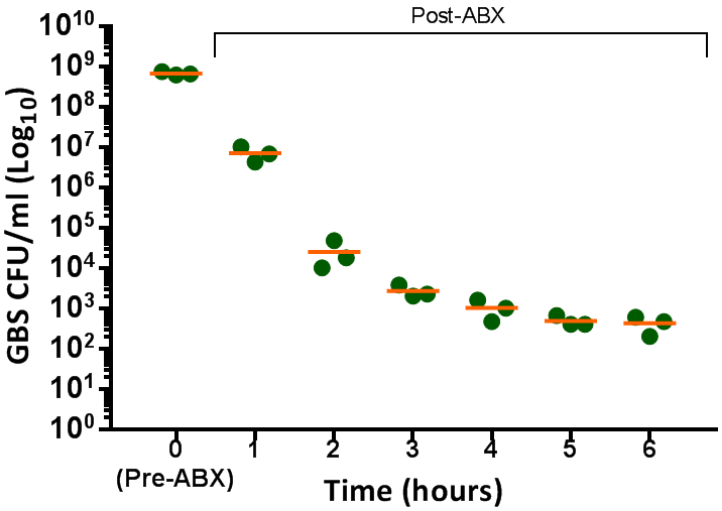

FIGURE AP2.11: GBS Time Kill – Six Hour Assay 2.
Around 1E9 CFU/ml of GBS were exposed to a cocktail of Gentamycin and Pen/Step antibiotics for 6 hours. Surviving bacteria were enumerated by CFU/ml counts every hour. The lines show means of 3 technical replicates.

For both assays, GBS colonies were noticeably stressed at T=1 to T=3 (i.e. varying sized colonies (ranging from pinpoint to typical sizes) with little to no haemolysis evident on the TSA-Blood agar plates). However from T=3 onwards, the colonies appeared healthy (i.e. consistently sized, larger colonies demonstrating clear haemolysis clearing around each colony on the plate).

Interpretation

GBS 874391 persists in the ABX for at least six hours. The numbers appear to stabilize between hours 4 and 6 of antibiotic treatment. This, coupled with the observed healthy colonies at later time periods may indicate a mutation promoting persistence.

After 3 to 4 hours of antibiotic treatment, the GBS numbers appear to stabilize under 10E3 CFU/ml. Given that the previous Invasion experiments are yielding between 10E7 and 10E8 CFU/ml of GBS, and given that the infection media is diluted by five PBS washes in the infection protocol, the low numbers of persistent GBS in this experiment are not considered significant enough to influence any downstream applications.

Since the GBS numbers appear to have reduced to stable levels after five hours of antibiotic treatment, it is unnecessary to further stress the monocytes by pushing the infection challenge to a

higher time point. Therefore, it was determined to limit the infections to five hours of antibiotic treatment.

Experiment 8: Infections 5 and 6. Centrifugation to Enhance the Host-Pathogen Interaction (iv)

Previous infection experiments had utilised a variety of time points. This experiment was performed to provide a final confirmation that the pre-incubation centrifuge step increases GBS yield from the monocytes in the context of five hours of antibiotic treatment.

Infection with Centrifugation (iv)

The procedure from Experiment 4 was generally repeated; with the following modifications;

The infections included five hours of antibiotic treatment. Supernatants from the final, pre-processing washes were taken for analysis of their GBS content.

Observations

Infection 5; Prepared monocytes: 5.55E5 cells/ml, Used monocytes: 5.00E5 cells/ml, Prepared GBS: 6.54E9 CFU/ml, Used GBS: 6.54E8 CFU/ml. Therefore the MOI ratio was 1308.

After five hours of antibiotic treatment, over 25 times more GBS were recovered from the centrifuged treatment than the non-centrifuged treatment (2.5E8 and 9.8E6 CFU/ml respectively).The GBS recovered from the final pre-wash supernatant remained much higher than desired; 3.87E7 CFU/ml at T=4 and 2.6E6 CFU/ml at T=6.

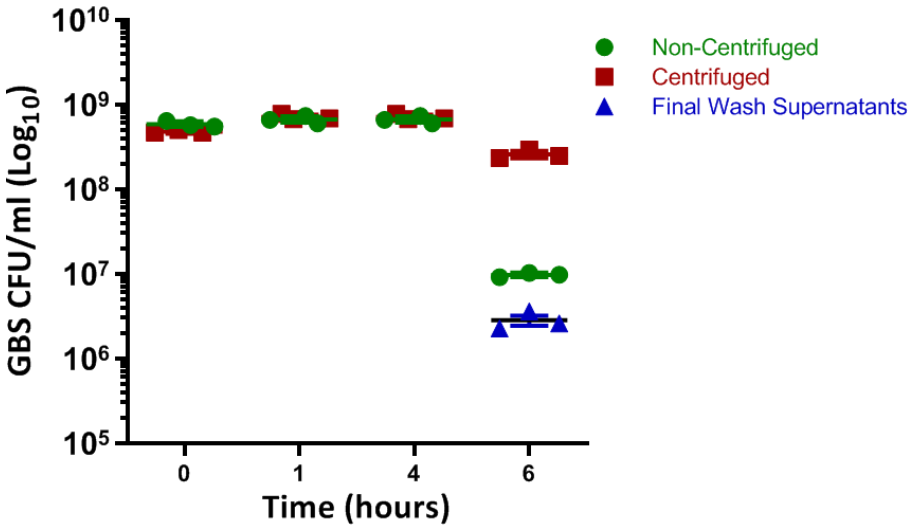

FIGURE AP2.12: Infection 5. GBS recovered from centrifuged vs non-centrifuged monocytes infected with GBS 874391 at an MOI of 1308; including the final wash supernatant at time point 6. *CFU/ml counts of GBS were performed at each time point after washing the cells with PBS and lysing the monocytes with Triton. After both treatments underwent 1 hour of incubation in 5% CO_2 at 37°C, ABX were added at time point 1 (after processing samples for that time point).After 5 hours of ABX, the supernatant from the final PBS wash was also processed for GBS CFU/ml counts. Time 0 is post centrifuge/incubation (i.e. 50 minutes after the infection). Lines show mean and SEM from 3 technical replicates.*

Infection 6; Prepared monocytes: 5.81E5 cells/ml, Used monocytes: 5.23E5 cells/ml, Prepared GBS: 7.14E9 CFU/ml, Used GBS: 7.14E8 CFU/ml. Therefore the MOI ratio was 285.

After five hours antibiotic treatment (T=6), 3.42E8 CFU/ml GBS were recovered from the infected cells. The number of GBS in the pre-processing supernatants increased between the first and final washes (5.8E5 to 9.7E6 CFU/ml respectively).

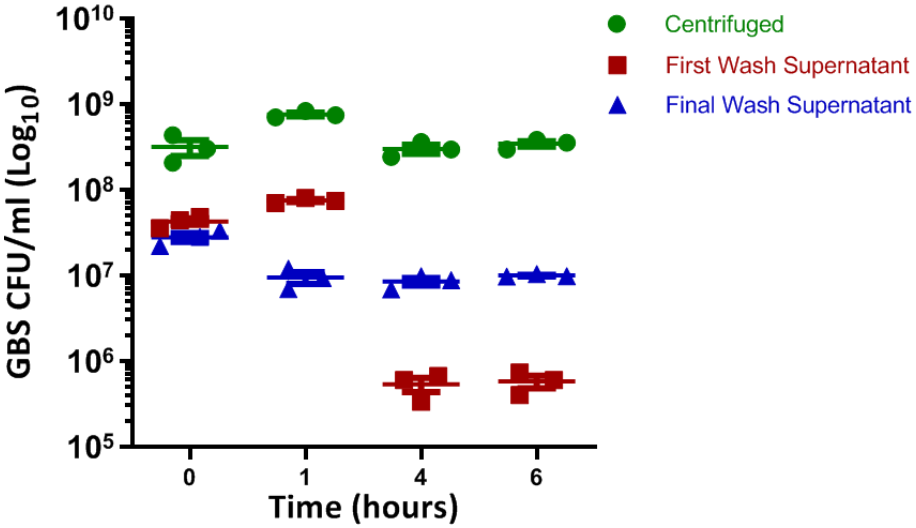

FIGURE AP2.13: Infection 6. GBS recovered from centrifuged monocytes infected at an MOI of 285; and including the first and final pre-processing wash supernatants.

CFU/ml counts of GBS were performed at each time point after washing the cells with PBS and lysing the monocytes with Triton. At each time point, the supernatant from both the first and final PBS washes were also processed for GBS CFU/ml counts. Time 0 is post centrifuge (i.e. 50 minutes after the infection). ABX was added after 1 hour of incubation in 5% CO_2 at 37°C (i.e. at time point 1 - after processing samples for that time point). Lines show mean and SEM from 3 technical replicates.

Interpretation

Higher GBS cell counts observed in subsequent wash supernatants indicates that fragile monocytes are releasing GBS back into the media during the washing process. Infection is naturally antagonistic and therefore stressful environment for the monocytes. So the infection context itself may contribute to the fragility of the monocytes after six hours of infection. It is also possible that subjecting the monocytes to a 50 minute centrifuge prior to the incubation may damage the monocytes in the infection. The MOI was high during both these infections. Therefore, the high bacterial loads likely contributed to stress resulting in damage to the monocytes.

Experiment 9: Infections 7 to 11. Assess Monocyte Viability

Experiments were performed to test the impact of protecting the monocytes from unnecessary damage during the infection in an attempt to mitigate release of GBS into the media during the pre-processing washes. The goal of these experiments was to optimise the infection protocol so that monocyte viability is preserved over the infection period.

Infection Assessing Monocyte Viability

The procedure used in Experiment 8 was generally repeated for four infections - with the following modifications;

In Infections 7 and 8, washed GBS cells were resuspended in 20ml bRPMI instead of 10ml in an attempt to reign in the MOI to <200 (ideally between 50 and 150). The pre-processing wash centrifuges were reduced from 500g to 300g to mitigate monocyte damage as much as possible. On top of these modifications, Infection 9 further diluted the washed GBS cells in 30ml bRPMI instead of 20ml. Also, the second pre-processing wash supernatant was processed instead of the first, to mitigate the effect of ABX in the media influencing the GBS counts. Additionally, Infection 10 utilised the NucleoCounter NC-200 to measure viable monocyte counts (employing the acridine orange fluorescent stain for all cells, less DAPI stained dead cells). For Infection 11, the pre-incubation centrifuge was reduced to 5 minutes from 50 minutes.

Observations

Infection 7; Prepared monocytes: 3.07E6 cells/ml, Used monocytes: 2.76E6 cells/ml, Prepared GBS: 5.86E9 CFU/ml, Used GBS: 5.86E8 CFU/ml. Therefore the MOI ratio was 212.

After 3 hours of antibiotic treatment (T=4), 7.26E5 GBS were recovered from the infection (Note: no GBS were counted for T=6 due to a gel failure). No GBS colonies were recorded in the first pre-processing wash supernatants at T=6. Only 2.6E4 colonies were recorded in the final wash supernatant.

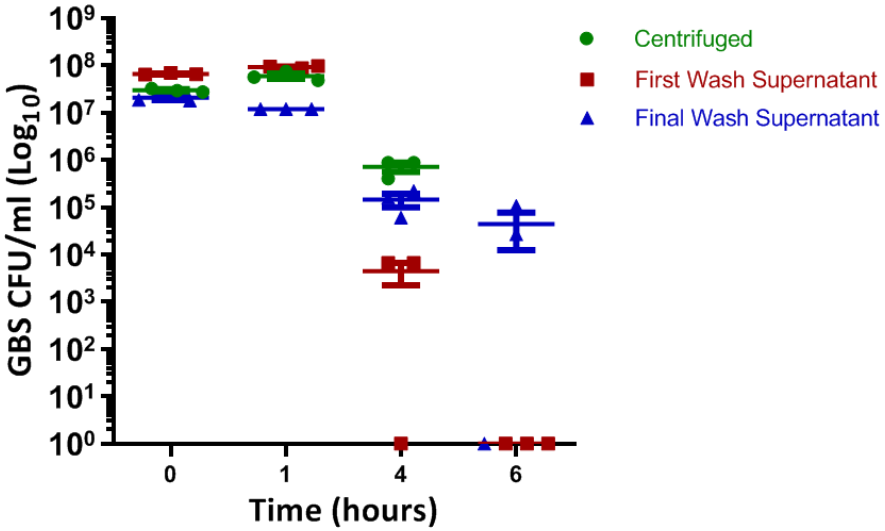

FIGURE AP2.14: Infection 7. GBS recovered from centrifuged monocytes infected at an MOI of 212; and including the first and final pre-processing wash supernatants.

CFU/ml counts of GBS were performed at each time point after washing the cells with PBS and lysing the monocytes with Triton. At each time point, the supernatant from both the first and final PBS washes were also processed for GBS CFU/ml counts. Time 0 is post centrifuge (i.e. 50 minutes after the infection). ABX was added after 1 hour of incubation in 5% CO_2 at 37°C (i.e. at time point 1 - after processing samples for that time point). Lines show mean and SEM from 3 technical replicates.

Infection 8; Prepared monocytes: 3.07E6 cells/ml, Used monocytes: 2.76E6 cells/ml, Prepared GBS: 4.66E9 CFU/ml, Used GBS: 4.66E8 CFU/ml. Therefore the MOI ratio was 168.

After 5 hours of antibiotic treatment (T=6), 2.84E6 CFU/ml of GBS was recovered from the infected monocytes. 1.92E5 CFU/ml GBS were recovered from the final wash supernatant.

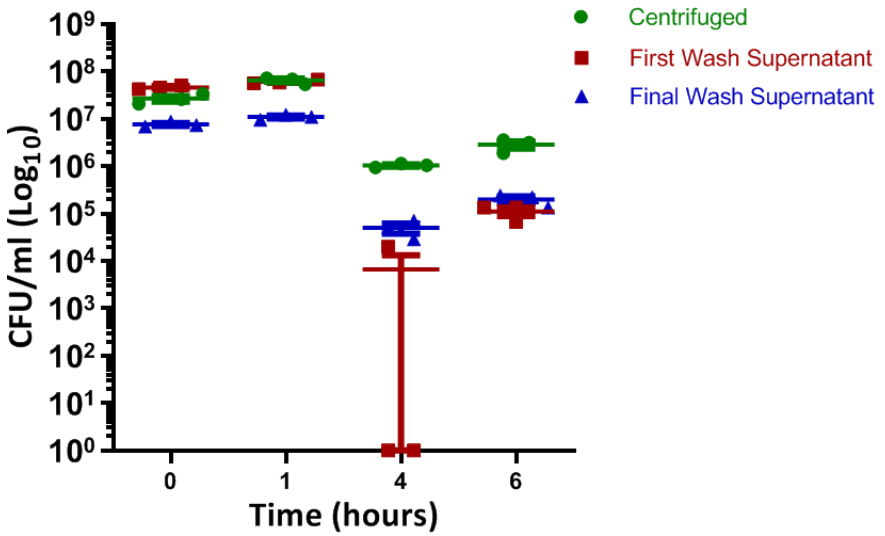

FIGURE AP2.15: Infection 8. GBS recovered from centrifuged monocytes infected at an MOI of 168; and including the first and final pre-processing wash supernatants.

CFU/ml counts of GBS were performed at each time point after washing the cells with PBS and lysing the monocytes with Triton. At each time point, the supernatant from both the first and final PBS washes were also processed for GBS CFU/ml counts. Time 0 is post centrifuge (i.e. 50 minutes after the infection). ABX was added

after 1 hour of incubation in 5% CO_2 at 37°C (i.e. at time point 1 - after processing samples for that time point). Lines show mean and SEM from 3 technical replicates.

Infection 9; Prepared monocytes: 2.94E6 cells/ml, Used monocytes: 2.65E6 cells/ml, Prepared GBS: 3.14E9 CFU/ml, Used GBS: 3.14E8 CFU/ml. Therefore the MOI ratio was 118.

After five hours of antibiotic treatment (T=6), 8.38E5 CFU/ml of GBS was recovered from the infected monocytes. The final wash supernatant yielded 2.09E4 CFU/ml of GBS. The second and final wash supernatants yielded close to the same amount of GBS.

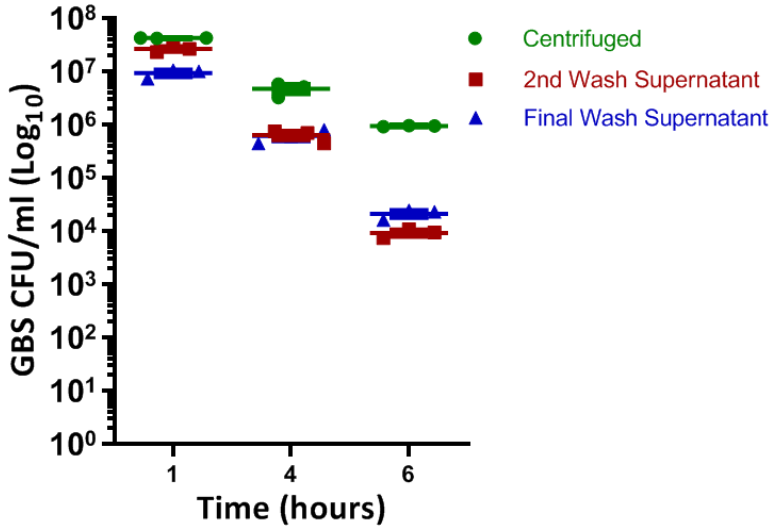

FIGURE AP2.16: Infection 9. GBS recovered from centrifuged monocytes infected at an MOI of 168; and including the second and final pre-processing wash supernatants.
CFU/ml counts of GBS were performed at each time point after washing the cells with PBS and lysing the monocytes with Triton. At each time point, the supernatant from both the second and final PBS washes were also processed for GBS CFU/ml counts. Time 0 is post centrifuge (i.e. 50 minutes after the infection). ABX was added after 1 hour of incubation in 5% CO_2 at 37°C (i.e. at time point 1 - after processing samples for that time point). Lines show mean and SEM from 3 technical replicates.

Infection 10; Prepared monocytes: 2.90E6 cells/ml, Used monocytes: 2.61E6 cells/ml, Prepared GBS: 2.64E9 CFU/ml, Used GBS: 2.64E8 CFU/ml. Therefore the MOI ratio was 101.

After five hours of antibiotic treatment (T=6), 1.56E6 CFU/ml of GBS was recovered from the infected monocytes. The final wash supernatant yielded 1.73E4 CFU/ml of GBS. The second and final wash supernatants yielded close to the same amount of GBS.

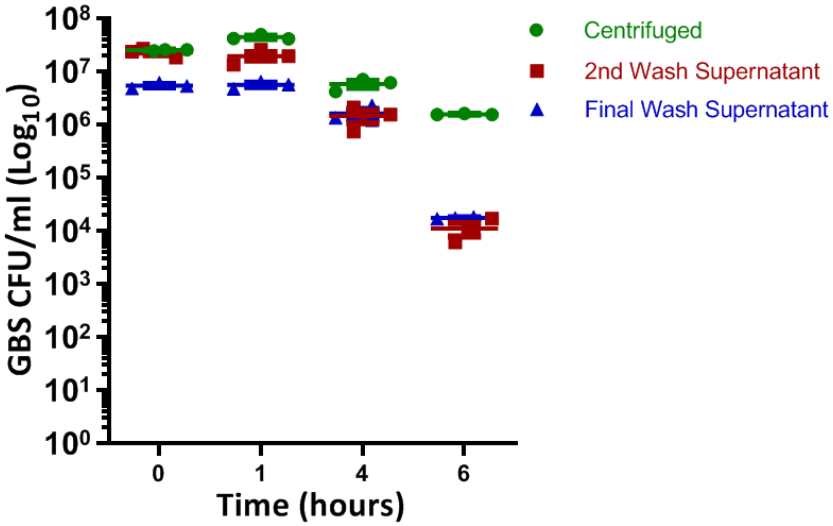

FIGURE AP2.17: Infection 10. GBS recovered from monocytes infected with GBS 874391 at an MOI of 101; and including the second and final pre-processing wash supernatants.

CFU/ml counts of GBS were performed at each time point after washing the cells with PBS and lysing the monocytes with Triton. At each time point, the supernatant from both the second and final PBS washes were also processed for GBS CFU/ml counts. Time 0 is post centrifuge (i.e. 50 minutes after the infection). ABX was added after 1 hour of incubation in 5% CO_2 at 37°C (i.e. at time point 1 - after processing samples for that time point). Lines show mean and SEM from 3 technical replicates.

At T=6, 1.04E6 viable cells/ml of monocytes were recorded from a total of 1.57E6 cells/ml (i.e. 66.1% cell viability). Monocyte viability underwent a significant decline from 83% viability at T=4 (1.26E6 viable monocytes/ml).

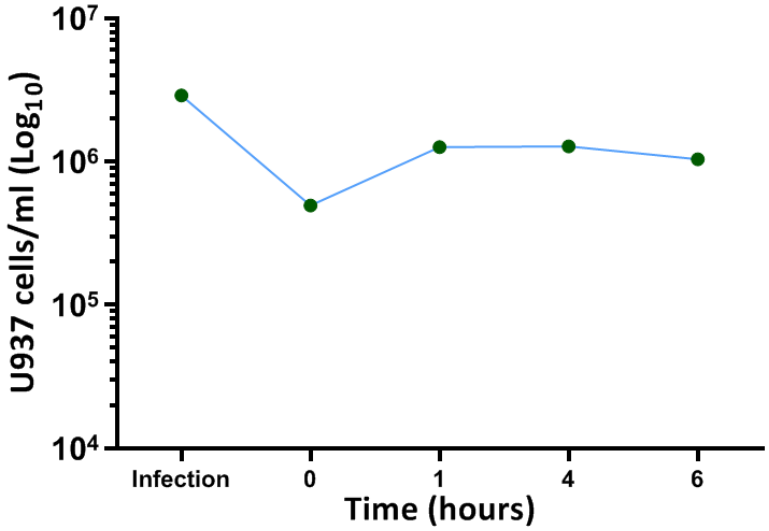

FIGURE AP2.18: Infection 10. Counts of viable infected monocytes over the infection period.

Single viable cells/ml counts of monocytes over 6 hours of infection with GBS. Cell count enumerated from the final wash pellet resuspensions using the Nucleocounter NC-200. Time 0 is post centrifuge (i.e. 50 minutes after the infection).

Infection 11; Prepared monocytes: 3.37E6 cells/ml, Used monocytes: 3.03E6 cells/ml, Prepared GBS: 2.66E9 CFU/ml, Used GBS: 2.66E8 CFU/ml. Therefore the MOI ratio was 79.

When reducing the infection centrifuge to 5 minutes from 50 minutes, after five hours of antibiotic treatment (T=6), 6.56E5 CFU/ml of GBS was recovered from the infected monocytes. The final wash supernatant yielded 7.29E3 CFU/ml of GBS. The second and final wash supernatants yielded close to the same amount of GBS.

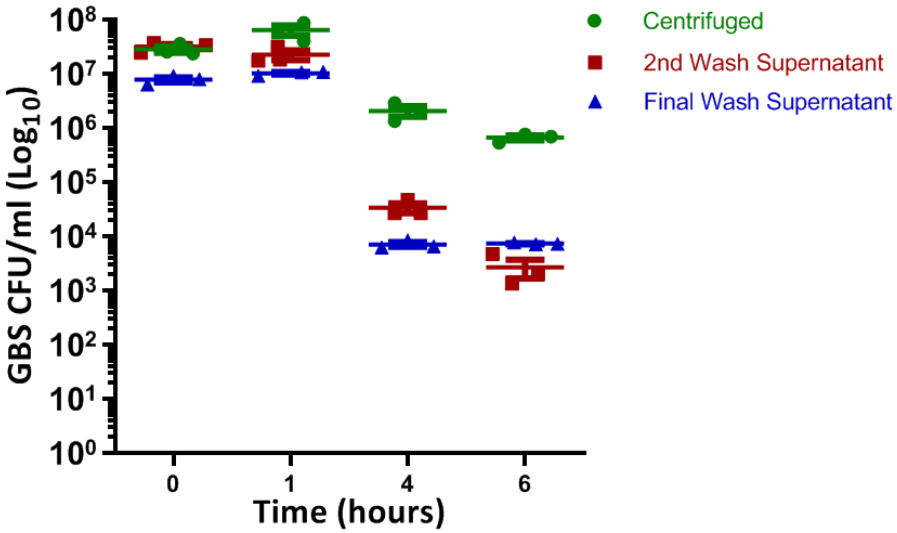

FIGURE AP2.19: Infection 11. GBS recovered from monocytes infected with GBS 874391 at an MOI of 79; and including the second and final pre-processing wash supernatants.
Infection centrifuge reduced from 50 to 5 minutes. CFU/ml counts of GBS were performed at each time point after washing the cells with PBS and lysing the monocytes with Triton. At each time point, the supernatant from both the second and final PBS washes were also processed for GBS CFU/ml counts. Time 0 is post centrifuge (i.e. 5 minutes after the infection). ABX was added after 1 hour of incubation in 5% CO_2 at 37°C (i.e. at time point 1 - after processing samples for that time point). Lines show mean and SEM from 3 technical replicates.

At T=6, 1.41E6 viable cells/ml of monocytes were recorded from a total of 1.70E6 cells/ml (i.e. 83.1% cell viability). This represented a moderate decline from T=4 where the recorded monocyte cell viability was 89.2%.

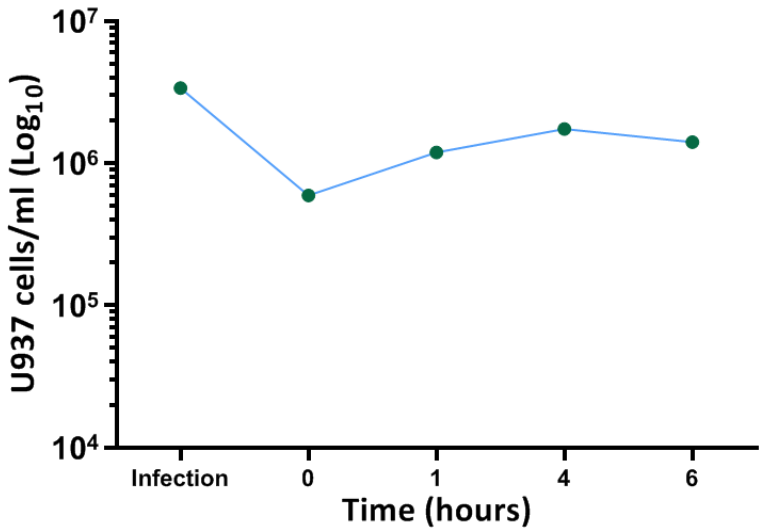

FIGURE AP2.20: Infection 11. Counts of viable infected monocytes over the infection period.
Single viable cells/ml counts of monocytes over 6 hours of infection with GBS 874391. Cell counts were enumerated from the final wash pellet resuspensions using the Nucleocounter NC-200. Time 0 is post centrifuge (i.e. 5 minutes after the infection).

Interpretation

Low GBS numbers recovered from the first wash supernatants were likely influenced by ABX remaining active in the media. Using the second wash (PBS) produced more consistent, reliable GBS counts for early wash analysis – indicating that the ABX had been effectively diluted out of the media.

Reducing the MOI to around 100 reduced the amount of GBS being released by damaged monocytes into the media during washing, however, the numbers of GBS recovered from the infected monocytes also declined as a result of this measure - to between 5.0E5 and 1.5E6 CFU/ml. This equates to roughly 1 GBS internalised for every two viable monocytes. Nevertheless, this is considered sufficient GBS for downstream RNA extractions as the infections can be scaled up.

Even though reducing the MOI also reduced monocyte stress, monocyte viability after five hours of antibiotic treatment was low – potentially having an undue influence on downstream applications. A roughly 3-fold drop between monocyte numbers at infection, and monocyte numbers after the centrifuge (FIGURE: 3.19) indicated that the pre-incubation centrifuge may also be contributing stress to the monocytes. Given the improvement on monocyte viability, reducing the pre-incubation

centrifuge to 5 minutes from 50 minutes appears to have reduced monocyte stress to the point where monocyte RNA can be considered reliable – though the roughly 3-fold reduction between infection and incubation remains (FIGURE: 3.20).

Experiment 10: Infections 12 to 14. Centrifugation to Preserve Monocyte Viability

Three independent infections were conducted to confirm the most ideal conditions for recovering the highest number of GBS from infected monocytes, while at the same time preserving monocyte integrity.

Infection with Centrifugation (v)

The protocol and optimisations applied in Experiment 9 were generally followed for three primary treatments over three independent infections. The three treatments were; 1) a 50 minute pre-incubation infection rested on a bench, 2) a 50 minute pre-incubation centrifuge, and 3) a 5 minute pre-incubation centrifuge. All pre-incubation conditions were performed at room temperature.

Observations

Infection 12; Prepared monocytes: 3.26E6 cells/ml, Used monocytes: 2.93E6 cells/ml, Prepared GBS: 4.54E9 CFU/ml, Used GBS: 4.54E8 CFU/ml. Therefore the MOI ratio was 155.

The highest amount of GBS recovered from the final, pre-processing wash supernatant was 4.5E5 (mean) from the 50-minute-centrifuge treatment. The least amount of GBS recovered from the final, pre-processing wash supernatant was 2.7E3 CFU/ml (mean) from the 50-minute-non-centrifuged treatment.

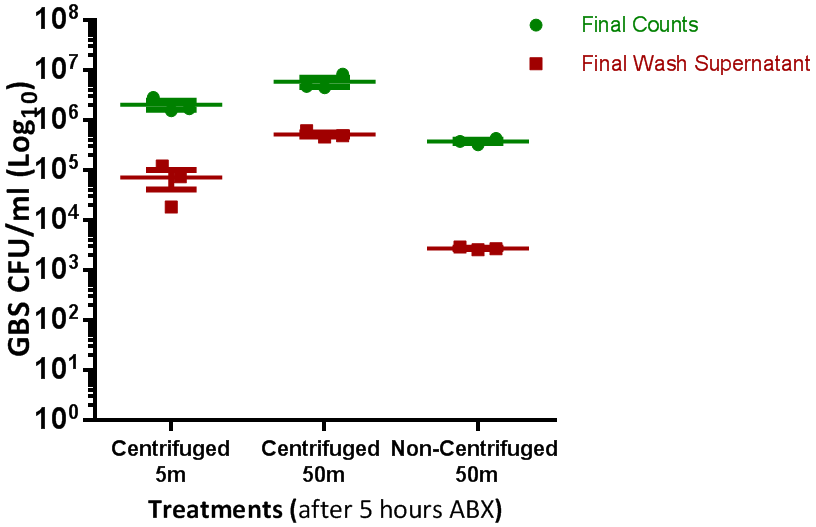

FIGURE AP2.21: Infection 12. GBS recovered from infected monocytes and final wash supernatants for three, pre-incubation conditions; no-centrifuge, 5 minute centrifuge and 50 minute centrifuge.
Monocytes were infected with GBS 874391 at an MOI of 155. The non-centrifuged treatment was left at room temperature for 50 minutes. The 5 minute centrifuge treatment was left at room temperature for 45 minutes, then centrifuged for 5 minutes. And the 50 minute centrifuge treatment was centrifuged for 50 minutes. All centrifuges were at room temperature. After the 50 minute treatment, infections were incubated in 5% CO_2 at 37°C for 6 hours (ABX added after 1 hour of incubation). GBS CFU/ml counts were enumerated after 6 hours of infection (5 hours of ABX treatment). Lines show mean and SEM from 3 technical replicates.

After six hours of infection, including five hours of ABX, the monocyte viability of the 5-minute-centrifuge, the 50-minute-centrifuge and 50-minute-non-centrifuged treatments were 84.1%, 62.2% and 63.7% respectively.

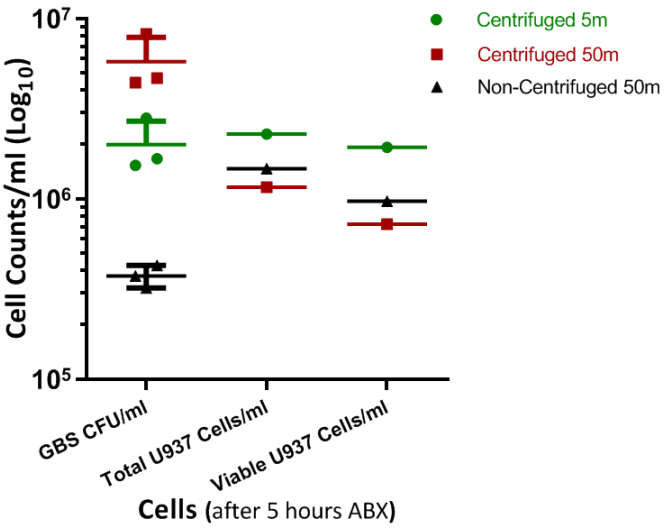

FIGURE AP2.22: Infection 12. Monocyte and GBS cell count/ml after 5 hours of antibiotic treatment.
Comparison of GBS CFU/ml, total monocyte cells/ml and viable monocyte cells/ml after 6 hours of infection (including 5 hours of ABX) for 3, pre-incubation conditions; no-centrifuge, 5 minute centrifuge and 50 minute centrifuge. Single viable monocyte counts and 3 technical replicates for GBS counts (Mean and SEM).

Infection 13; Prepared monocytes: 3.14E6 cells/ml, Used monocytes: 2.83E6 cells/ml, Prepared GBS: 3.80E9 CFU/ml, Used GBS: 3.80E8 CFU/ml. Therefore the MOI ratio was 134.

The highest amount of GBS recovered from the final, pre-processing wash supernatant was 1.9E4 (mean) from the 50-minute-centrifuge treatment. The least amount of GBS recovered from the final, pre-processing wash supernatant was 1.1E3 (mean) from the 50-minute-non-centrifuged treatment.

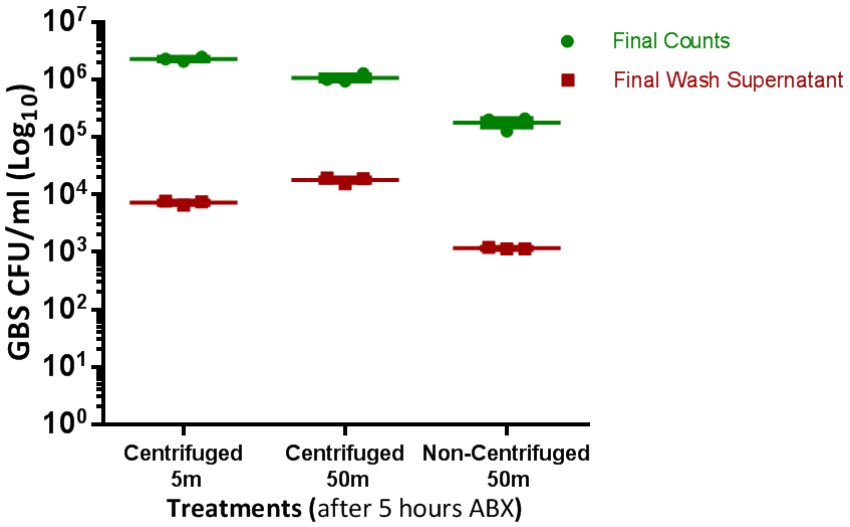

FIGURE AP2.23: Infection 13. GBS recovered from infected monocytes and final wash supernatants for three, pre-incubation conditions; no-centrifuge, 5 minute centrifuge and 50 minute centrifuge. *Monocytes were infected with GBS 874391 at an MOI of 134. The non-centrifuged treatment was left at room temperature for 50 minutes. The 5 minute centrifuge treatment was left at room temperature for 45 minutes, then centrifuged for 5 minutes. And the 50 minute centrifuge treatment was centrifuged for 50 minutes. All centrifuges were at room temperature. After the 50 minute treatment, infections were incubated in 5% CO_2 at 37°C for 6 hours (ABX added after 1 hour of incubation). GBS CFU/ml counts were enumerated after 6 hours of infection (5 hours of ABX treatment). Lines show mean and SEM from 3 technical replicates.*

After six hours of infection, including five hours of ABX, the monocyte viability of the 5-minute-centrifuge, the 50-minute-centrifuge and 50-minute-non-centrifuged treatments were 75.6%, 57.4% and 60.4% respectively.

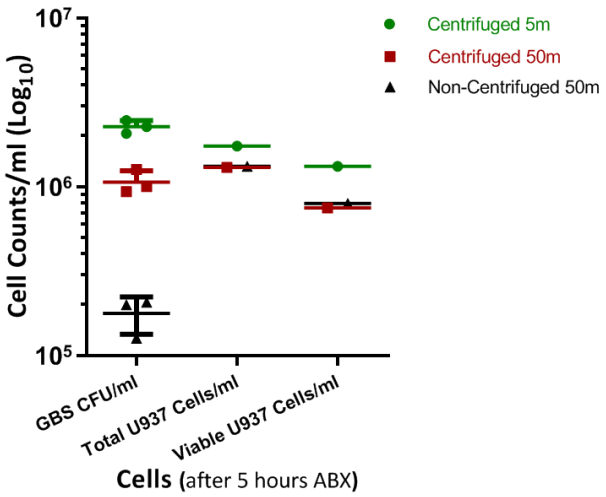

FIGURE AP2.24: Infection 13. Monocyte and GBS cell count/ml after 5 hours of antibiotic treatment.

Comparison of GBS CFU/ml, total monocyte cells/ml and viable monocyte cells/ml after 6 hours of infection (including 5 hours of ABX) for 3, pre-incubation conditions; no-centrifuge, 5 minute centrifuge and 50 minute centrifuge. Single viable monocyte counts and 3 technical replicates for GBS counts (Mean and SEM).

Infection 14; Prepared monocytes: 3.28E6 cells/ml, Used monocytes: 2.95E6 cells/ml, Prepared GBS: 3.60E9 CFU/ml, Used GBS: 3.60E8 CFU/ml. Therefore the MOI ratio was 122.

The highest amount of GBS recovered from the final, pre-processing wash supernatant was 1.5E4 (mean) from the 50-minute-centrifuge treatment. The least amount of GBS recovered from the final, pre-processing wash supernatant was 1.6E3 (mean) from the 50-minute-non-centrifuged treatment.

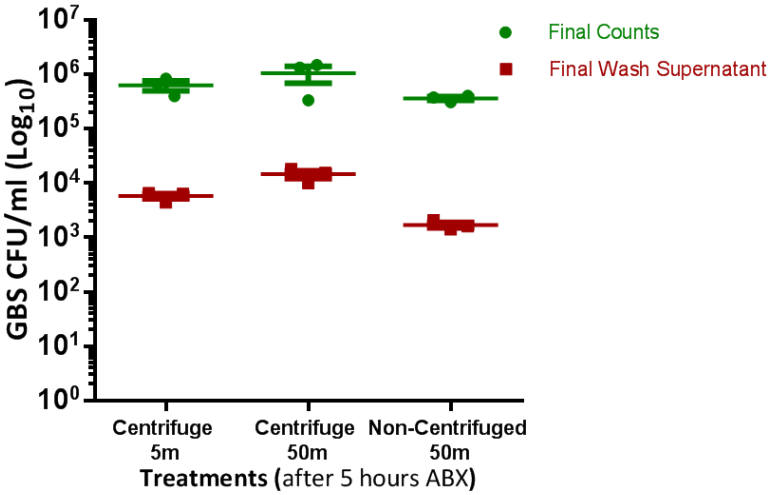

FIGURE AP2.25: Infection 14. GBS recovered from infected monocytes and final wash supernatants for three, pre-incubation conditions; no-centrifuge, 5 minute centrifuge and 50 minute centrifuge.

Monocytes were infected with GBS 874391 at an MOI of 122. The non-centrifuged treatment was left at room temperature for 50 minutes. The 5 minute centrifuge treatment was left at room temperature for 45 minutes, then centrifuged for 5 minutes. And the 50 minute centrifuge treatment was centrifuged for 50 minutes. All centrifuges were at room temperature. After the 50 minute treatment, infections were incubated in 5% CO_2 at

37°C for 6 hours (ABX added after 1 hour of incubation). GBS CFU/ml counts were enumerated after 6 hours of infection (5 hours of ABX treatment). Lines show mean and SEM from 3 technical replicates.

After six hours of infection, including five hours of ABX, the monocyte viability of the 5-minute-centrifuge, the 50-minute-centrifuge and 50-minute-non-centrifuged treatments were 80.6%, 83.1% and 62.3% respectively.

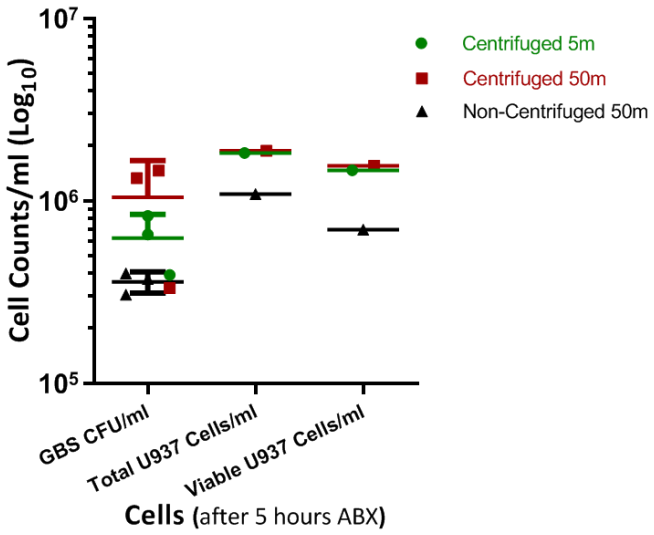

FIGURE AP2.26: Infection 14. Monocyte and GBS cell count/ml after 5 hours of antibiotic treatment.

Comparison of GBS CFU/ml, total monocyte cells/ml and viable monocyte cells/ml after 6 hours of infection (including 5 hours of ABX) for 3, pre-incubation conditions; no-centrifuge, 5 minute centrifuge and 50 minute centrifuge. Single viable monocyte counts and 3 technical replicates for GBS counts (Mean and SEM).

An initial One-way-ANOVA of the data reported no significant differences between the three treatments for GBS counts, monocyte counts or monocyte viability. This appears inconsistent with the biological and graphical data so it was decided to increase the resolution of the individual comparisons using t-tests. No significance was reported for GBS counts between the 50 and 5 minute centrifuge treatments. However GBS counts for the non-centrifuged treatment were significantly lower than both the 5 minute centrifuge treatment (P=0.0144) and the 50 minute centrifuge treatment (P=0.0194). With regards to monocyte counts and viability, no significance was reported between the 50 minute centrifuge treatment and either of the other treatments – possibly due to the broad spread of the 50 minute Centrifuge data (SEM = 7.9 compared to 2.4 for the 5 minute centrifuge treatment and 1.0 for the non-centrifuged treatment). The 5 minute centrifuge

treatment was significantly higher than the non-centrifuged treatment for both monocyte counts (P=0.0061) and the monocyte viability (P=0.012).

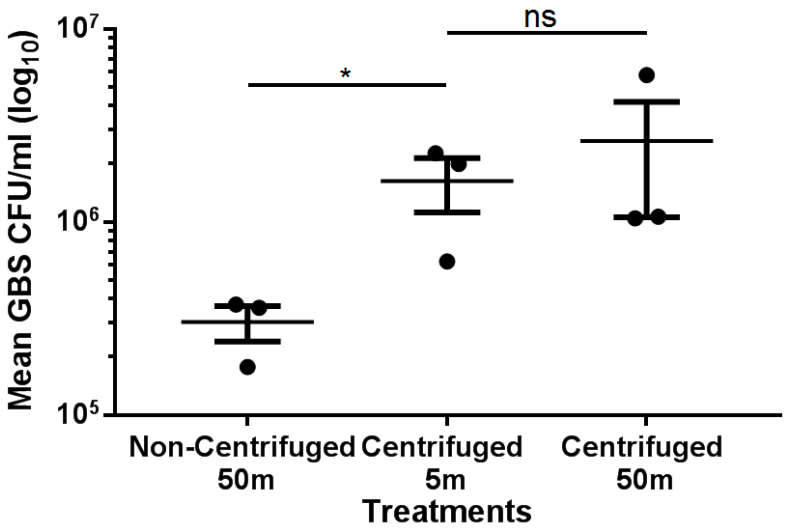

FIGURE AP2.27: The effect of varying pre-incubation centrifuging times on the GBS CFU/ml recovered from monocytes after 5hrs antibiotic treatments.

Data represents values derived from three independent infections. Lines are Mean and SEM. Based on the t-test analysis, GBS counts for the non-Centrifuged treatment were significantly lower than for both the 5 minute centrifuge treatment (p=0.0144) and the 50 minute centrifuge treatment (p=0.0194). No statistical significance is reported for GBS counts between the 5 minute and 50 minute centrifuge treatments.

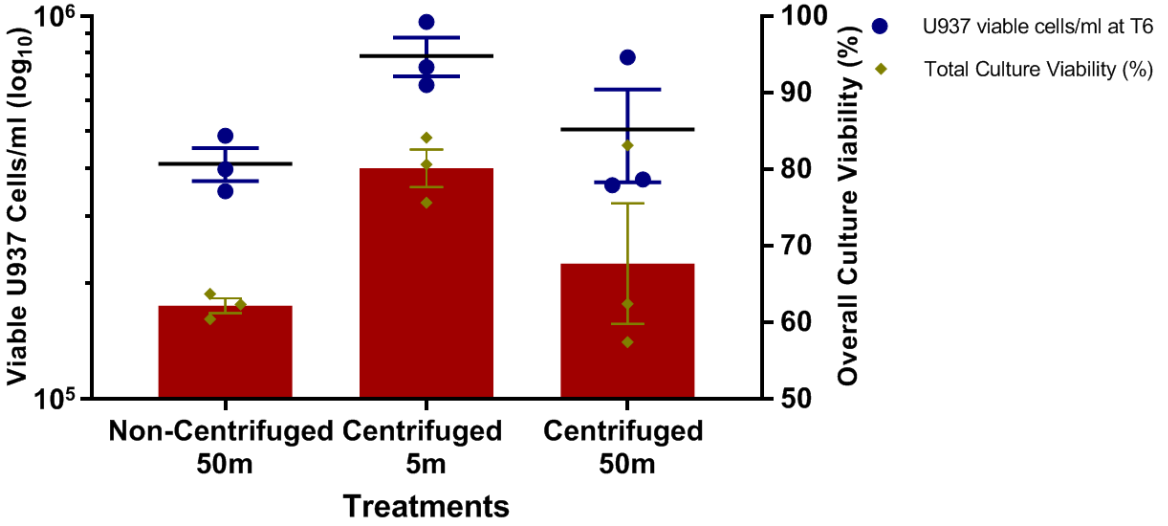

FIGURE AP2.28: The effect of varying pre-incubation centrifuging times on monocyte survival (cells/ml) and viability (%) after 5hrs antibiotic treatments.

Data represents values derived from three independent infections. Data in blue represents the viable monocyte counts (Mean and SEM). Red bars represents the viable monocytes as a percentage of the total monocytes (cells/ml). T6 = 6 hours of infection (5 hours of ABX). Notably, the 5 minute centrifuge treatment was significantly higher than the non-centrifuge in both monocyte counts (p= 0.0061) and percentage viability (p= 0.012). No statistical significance was reported between the 50 minute centrifuge treatment and either of the other treatments.

Interpretation

A 50 minute pre-incubation centrifuge treatment was found to increase the yield of recovered GBS from the monocytes by a factor of 1 to $3\log_{10}$. However monocyte viability suffered as a consequence; with damaged cells releasing GBS into the supernatant during washes. Reducing the centrifuge to 5 minutes results in higher viability of monocytes over the period of the experiment whilst maintaining high GBS yields. The 5 minute, pre-incubation centrifuge therefore provides the most optimal conditions for both consistently high levels of monocyte viability, and high yields of GBS recovered from the monocytes. With a five minute pre-incubation centrifuge, around 1.0E6 CFU/ml of GBS are consistently recovered from challenged U937 monocytes (i.e. total count around 3.0E6 CFU/3ml) after a 1 hour incubation followed by five hours of ABX – which is a theoretically sufficient survival rate to retrieve enough RNA to detect differential expression from the GBS after scaling up the infection model.

Experiment 11: Infections 15 to 17. Scaling Up the Infection Protocol

To secure enough bacterial RNA from the infection, the established protocol was scaled up so that more GBS could be recovered from each infection.

24ml Infection

The 5 minute pre-incubation protocol (Experiment 10) was generally followed – with the following modifications;

The infection was increased from 3ml to 24ml. 4mls per well of infected monocytes were aliquoted into all 6 wells of a Costar 6-well cell culture plate (Corning) before centrifuging and incubation. 1ml from each of the six wells was processed separately to attain GBS counts (i.e. 6 technical replicates, each plated in triplicate), then the remaining 3ml in each well was combined before performing monocyte counts and viability measures.

Observations

The MOI for infections 15, 16 and 17 were determined to be 80, 179 and 106 respectively. After six hours incubation (five hours ABX), the mean GBS recovered from the infection was 7.1E5, 9.8E5 and 9.6E5 CFU/ml respectively; with the mean total GBS recovered in 24 ml being 1.7E7, 2.4E7 and 2.30E7 CFU/24ml respectively. The mean GBS recovered from the final wash supernatants was 9.7E3, 1.9E4 and 9.9E3 CFU/ml respectively. Viable monocytes recovered from the infection were 3.10E6, 2.27E6 and 2.46E6 cells/ml respectively, and monocyte viability was 90.1%, 89.4% and 91.2% respectively.

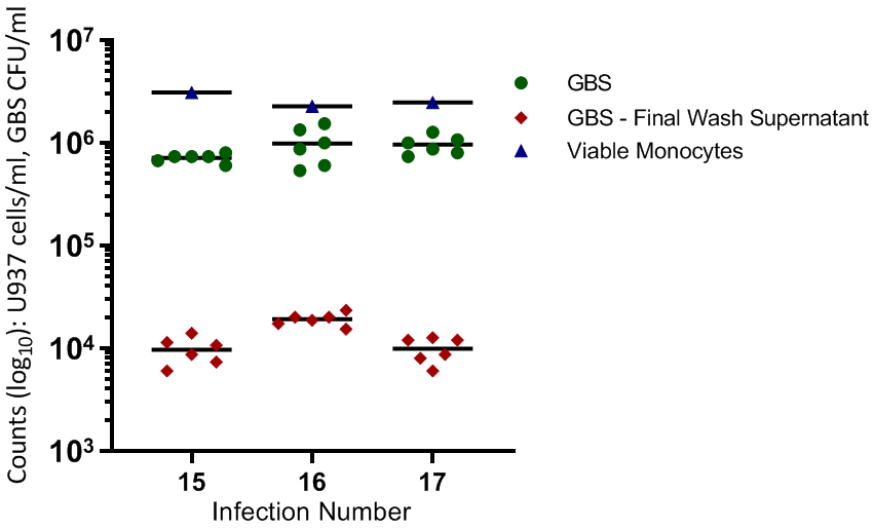

FIGURE AP2.29: GBS counts (CFU/ml) and Monocyte counts (cells/ml) from three, 24ml infections. *Lines are the means from 6 technical replicates for GBS and single viable monocyte count for each infection. For infections 15, 16 and 17, monocytes were infected with GBS 874391 at an MOI of 80, 179 and 106 respectively over 6 hours (5 hours ABX).*

Interpretation

After upscaling the infection model to 24ml over three independent infections, the concentration of GBS in the final wash supernatants was roughly $2log_{10}$ less than the concentration of GBS derived from infected monocytes. Furthermore, the monocyte integrity remained consistent – at around 90% cell viability. Scaling up the infection 8-fold increased the GBS recovered the infections more than 6-fold (roughly 3.0E6 to roughly 2.0E7). Therefore, upscaling the infections successfully increased GBS yield without compromising monocyte integrity.

Experiment 12: Pilot Testing the Optimised Protocol with a GBS-only control

Having established an infection protocol yielding sufficient GBS from U937 monocytes, the protocol was tested without monocytes to establish its suitability as a control against which to compare the infections.

Mock Infection – Diluted Media

The scaled up protocol from Experiment 11 was generally followed with the following modifications;

Given that GBS have been observed to proliferate in bRPMI media (Lin *et al.*, 2017, Lamy *et al.*, 2004), a 10% bRPMI media used in this infection (diluted 90% in autoclaved double-distilled water) to limit GBS growth. 1% of the washed GBS was added to the mock-infection media to reflect GBS numbers recovered from the previous infections. That is, 260µl of washed GBS cells in bRPMI were inoculated into 26ml (less 260µl) of diluted bRPMI. No ABX were used in the mock-infection.

Note: From this time, in addition to the mock infections (GBS 874391 in media), true infections were also performed (i.e. monocytes infected with GBS 874391). At T=6, after removing 1ml for processing, the infection mix was centrifuged at 4816g for 10 minutes and the pellets resuspended in 0.5ml TRIzol before freezing at -80^{o}C – to be used for later RNA preparations.

Observations

After overnight incubation and colony counts (TSA-Blood agar plates), the concentration of washed GBS was determined to be 3.66E9 CFU/ml. 1% of this concentration contributed to the mock-infection (3.66E7 CFU/ml). After six hours incubation, 1.28E7 CFU/ml of GBS was recovered from the mock-infection.

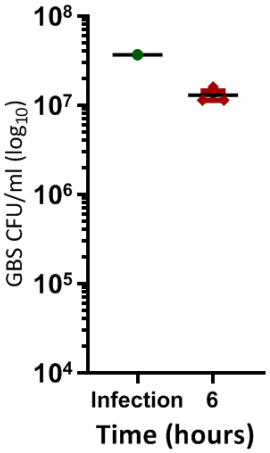

FIGURE AP2.30: Mock-infection 1. GBS-only control in 10% bRPMI diluted in water.
Diluted bRPMI media infected with 3.66E7 CFU/ml GBS 874391. GBS counts from 6 technical replicates after 6 hours of infection (no ABX).

Interpretation

Over the period of incubation, GBS numbers fell to 35% of the original inoculation levels. This indicates that the GBS were undergoing stress. The transcript of GBS is likely to be adversely influenced by cell stress. Therefore, this mock infection model does not provide a suitable control for the established infection model.

Experiment 13: GBS-only Mock-Infection

Experiments were conducted to find a suitable media formulation for the GBS control treatment. That is, a media formulation that can be used across the three treatments (infection, GBS-only, monocyte-only), that will generate a sufficient yield of quality RNA to provide neutral transcript controls (from GBS-only and monocyte-only treatments) to compare against the transcripts generated by the GBS and monocytes from infected samples. Both conditions causing GBS stress and conditions for optimal growth could be assumed to impact the transcriptome in ways that deviate from the conditions of the infection treatment. The goal of this experiment was therefore to develop a suitable media formulation; based on variations of basal, supplemented and complete RPMI (bRPMI, sRPMI and cRPMI) with FBS - empirically demonstrating neither GBS stress nor growth over the 6 hour incubation period. The correct media formulation will allow for similar numbers of GBS to

be incubated in parallel, in the absence of monocytes, such that differences in bacterial growth would not cloud the observations of GBS responding to the monocyte cells.

Mock-Infection (ii) - Media Formulations

The procedures from Experiment 12 were generally followed for varying formulations of infection media. The following media formulations were tested;

Mock-infection 2 – 10%, 20%, 50% and 100% (1X) bRPMI diluted in PBS (incubated for one hour: T=1).

Mock-infection 3 – 1X bRPMI, bRPMI with supplements (sRPMI) - i.e. cRPMI without ABX, Beta-Mercaptoethanol or FBS, and sRPMI with 10% FBS (incubated for one hour).

Mock-infection 4 – 0.5%, 1%, 2%, 2.5%, 5% and 10% FBS in sRPMI (incubated for one hour).

Mock-infection 5 – Repeat Mock-infection 4 with two additional conditions; sRPMI and bRPMI without any FBS (incubated for six hours).

Mock infection 6 – 0.01%, 0.05%, 0.1%, 0.5% FBS for both full sRPMI and 10% dilution of sRPMI in PBS (incubated for six hours).

Mock-infection 7 – 0.0000001%, 0.000001%, 0.00001%, 0.0001%, 0.001%, 0.01%, 0.1%, 0.5% FBS in sRPMI (incubated for six hours).

Mock-infection 8 – Repeat Mock-infection 7

Roughly 3.0E6 CFU/ml of washed GBS (in bRPMI) were added to the treatment media of each mock-infection to reflect the GBS numbers derived from earlier experiments (slightly higher to account for a range of possible experimental outcomes).

Observations

For Mock-infection 2 (FIGURE AP2.31), after just 1 hour of incubation, GBS numbers recovered from the media dropped by roughly $1\log_{10}$ – indicating that the GBS are undergoing stress, even in 1X bRPMI.

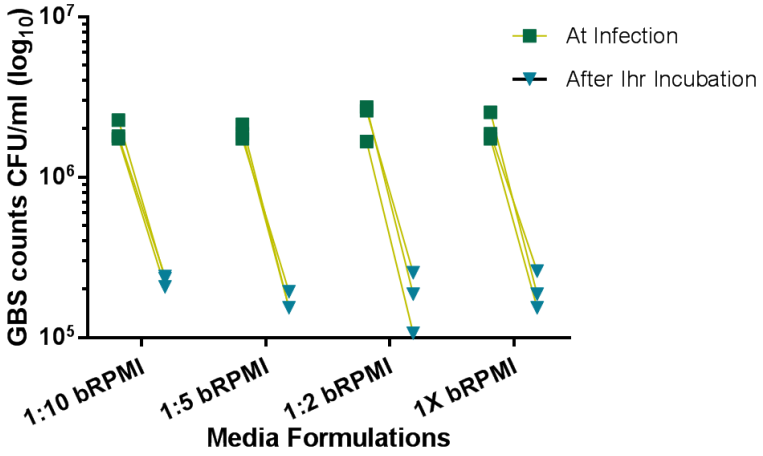

FIGURE AP2.31: Mock-infection 2. Testing GBS survival and proliferation in bRPMI diluted in PBS.
GBS survival in bRPMI (1X) and 3 dilutions of bRPMI - 10% (1:10), 20% (1:5) and 50% (1:2); diluted in PBS. GBS counts derived from 3 technical replicates processed both before and after a 1 hour incubation in 5% CO_2 at 37°C.

For Mock-infection 3 (FIGURE AP2.32), after 1 hour of incubation, GBS number recovered from the bRPMI and sRPMI media decreased by roughly $1\log_{10}$. However, cells in the media containing 10% FBS more than doubled over that same period – indicating that the conditional factor is in the FBS.

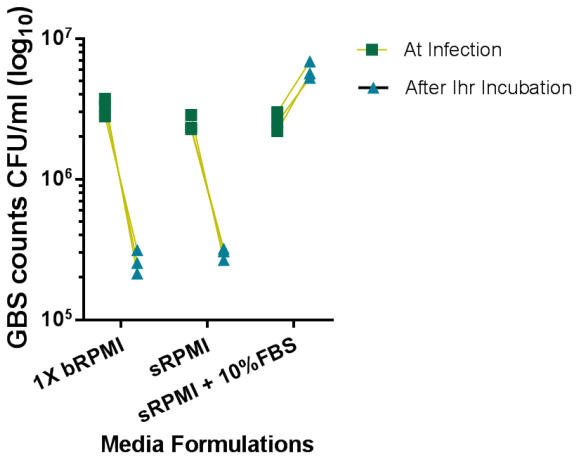

FIGURE AP2.32: Mock-infection 3. Testing GBS survival and proliferation in 1X bRPMI, sRPMI, and sRPMI with 10% FBS.
GBS survival in bRPMI (1X), supplemented RPMI (sRPMI) and sRPMI further supplemented with 10% FBS. GBS counts derived from 3 technical replicates processed both before and after a 1 hour incubation in 5% CO_2 at 37°C.

For Mock-infection 4 (FIGURE AP2.33), after 1 hour of incubation, GBS appeared to stabilize for the media containing between 0.5% and 5% FBS. However, the assay was inconclusive with regards to a lower optimal range of FBS.

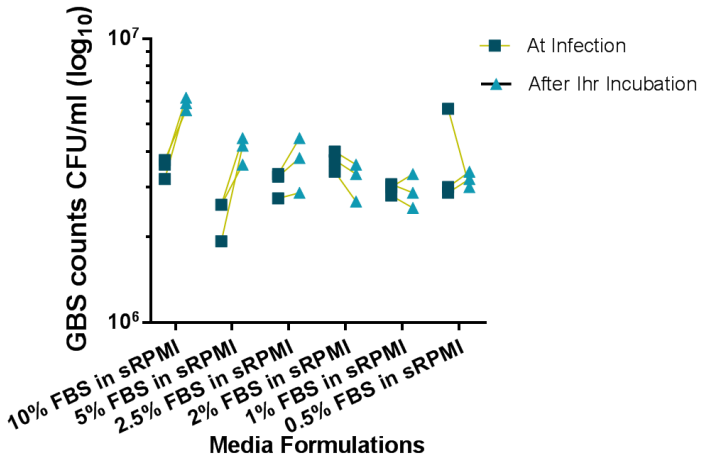

FIGURE AP2.33: Mock-infection 4. Testing GBS survival and proliferation in sRPMI containing various dilutions of FBS.

GBS survival in sRPMI containing 6 different concentrations of FBS (%). GBS counts derived from 3 technical replicates processed both before and after a 1 hour incubation in 5% CO_2 at 37°C.

In Mock-infection 5 (FIGURE AP2.34), extending the incubation time to six hours failed to resolve a lower range of FBS concentration using the given dilutions. bRPMI and sRPMI conditions confirmed earlier experiments that neither media formulation contains sufficient nutrients to maintain GBS numbers.

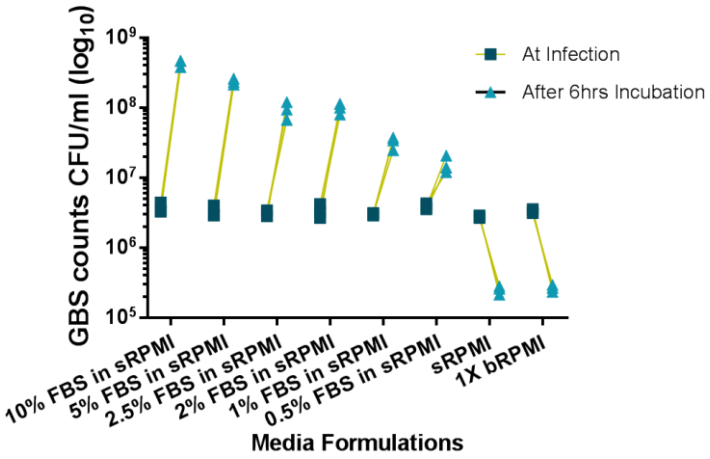

FIGURE AP2.34: Mock-infection 5. Testing GBS survival and proliferation in sRPMI containing various dilutions of FBS over six hours – with the addition a bRPMI and sRPMI treatment.

GBS survival in sRPMI containing 7 different concentrations of FBS (%), including sRPMI without any FBS, and 1X bRPMI. GBS counts derived from 3 technical replicates processed both before and after a 6 hour incubation in 5% CO_2 at 37°C.

For Mock-infection 6 (FIGURE AP2.35), after six hours of incubation, the sRPMI media containing 0.5% FBS revealed cell growth over the period. GBS numbers stabilised in the sRPMI media containing between 0.01% and 0.1% FBS. All 1:10 diluted sRPMI demonstrated cell death over the period; regardless of the concentration of FBS.

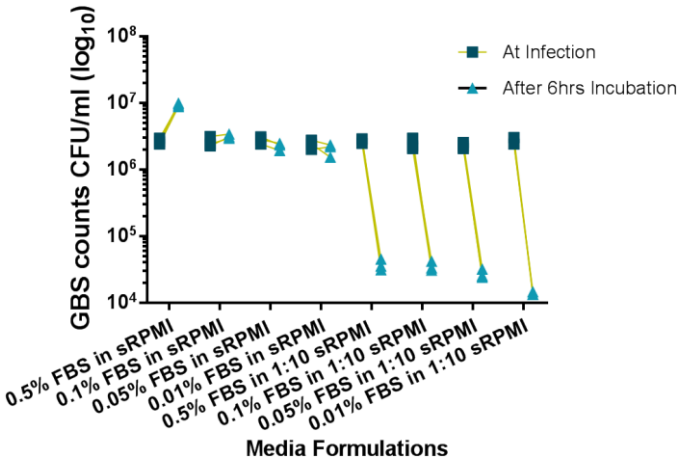

FIGURE AP2.35: Mock-infection 6. Testing GBS survival and proliferation in sRPMI containing heavier dilutions of FBS and additionally, the same concentrations of FBS in 1:10 dilutions of sRPMI.

GBS survival in 1X sRPMI and 10% (1:10) dilutions of sRPMI - each with 4 different concentrations of FBS (%). GBS counts derived from 3 technical replicates processed both before and after a 6 hour incubation in 5% CO_2 at 37^{o}C.

For Mock-infection 7 (FIGURE AP2.36), after six hours incubation, GBS numbers stabilised in the media formulations containing 0.01% and 0.1% FBS.

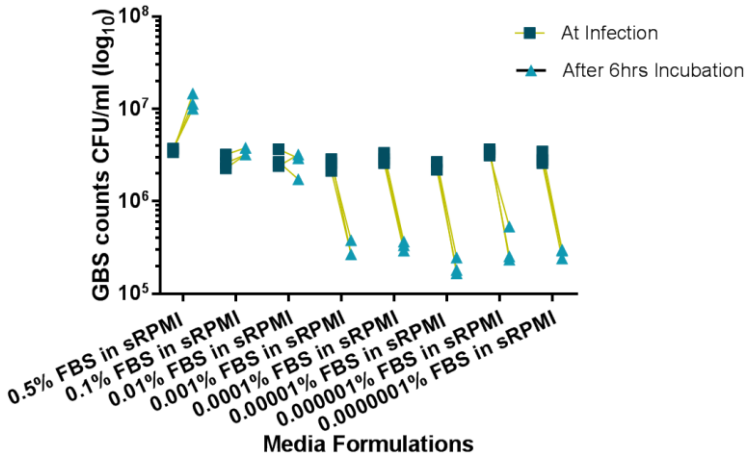

FIGURE AP2.36: Mock-infection 7. Testing GBS survival and proliferation in sRPMI containing heavier dilutions of FBS.

GBS survival in sRPMI containing 8 different concentrations of FBS (%). GBS counts derived from 3 technical replicates processed both before and after a 6 hour incubation in 5% CO_2 at 37°C.

For Mock-infection 8 (FIGURE AP2.37), after six hours incubation, GBS numbers stabilised in the sRPMI containing 0.1% FBS. Unlike the previous two experiments, the treatment containing 0.01% FBS yielded a clear reduction in cell numbers over the period.

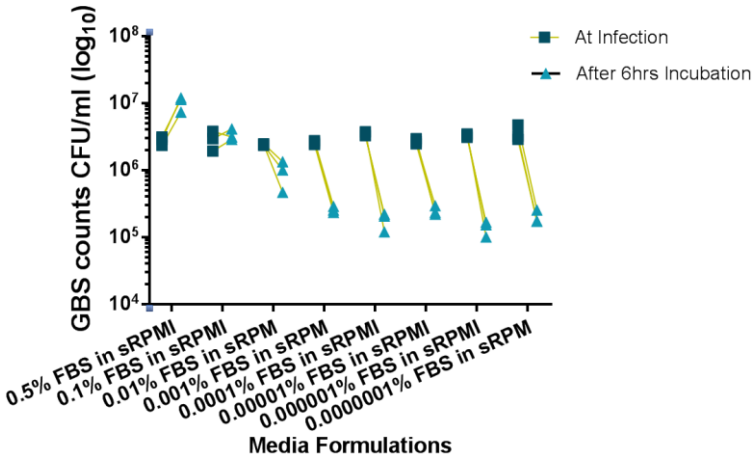

FIGURE AP2.37: Mock-infection 8. Testing GBS survival and proliferation in sRPMI containing heavier dilutions of FBS.

GBS survival in sRPMI containing 8 different concentrations of FBS (%). GBS counts derived from 3 technical replicates processed both before and after a 6 hour incubation in 5% CO_2 at 37°C.

Interpretation

Neither bRPMI nor sRPMI contained sufficient nutrients to facilitate maintenance of GBS numbers. Whilst FBS was determined to be the primary conditional factor, diluting the sRPMI also resulted in GBS stress regardless of the FBS concentration. Therefore both sRPMI and an empirically determined concentration of FBS are required to enable survival of GBS 874391 over the six hour incubation

period. The reduction in cells for the 0.01% FBS media in Mock-infection 8 indicates that the GBS in this condition are on the cusp of stress.

After eight independent experiments were performed (including Experiment 12) over varying time frames testing various media conditions, three independent experiments demonstrated that bRPMI media supplemented with 5ml 100mM Na Pyruvate, 5ml 100X non-essential Amino Acids, 5ml 100X GlutaMAX (Gibco), 5ml 100X Pen/Strep antibiotics, 12.5ml 1M HEPES (i.e. sRPMI) with added 0.1% heat-inactivated FBS, maintained consistent numbers of GBS 874391 under the incubation conditions required for the infections (i.e. no GBS growth or death indicated in the colony counts). This therefore represents an appropriate media formulation for both the infections and GBS-only control treatment.

Experiment 14: Extracting RNA from cells stored in TRIzol

Having optimised the experimental conditions required to produce sufficient, viable monocytes and GBS for downstream processing, these infected cells now had to be collected in a manner to facilitate RNA extraction and analysis. In order to optimise the RNA extraction process, a stock of mixed/infection samples and GBS controls were required. Gene expression levels of both GBS and monocytes derived from internalised infection will later be examined by Real-Time quantitative Polymerase Chain Reaction (RT-qPCR). Good quality and sufficient quantities of RNA therefore needs to be isolated from both cell types derived from the infections.

Excessive DNA in an RNA sample can interfere with downstream signalling of RNA expression. Nucleotide absorbance measured on the Biospetrometer only generally distinguishes between DNA and RNA. A poor RNA sample may be saturated with DNA, whereas a sample of reasonable quality should only reveal ribosomal RNA bands on a gel.

The goal of this experiment was to generate RNA from mixed and GBS-only samples collected through applying the protocol optimisations developed in previous experiments.

RNA Isolation

Following the optimised protocol (including the media formulation from Experiment 13), 18 infections and 4 GBS-only controls were performed. After 1ml of each was taken for processing, the remaining 23ml was centrifuged at 500g for 10 minutes before resuspending the pellet in 0.5ml TRIzol reagent and storing at -80°C.

The Thermo Fisher/Invitrogen TRIzol Reagent User Guide for RNA isolation was generally followed; namely, chloroform was added to the TRIzol suspension, then centrifuged before precipitation of the RNA from the aqueous phase, then washing, eluting and quantification. Elutions were performed with nuclease-free Ultrapure Distilled Water (Invitrogen). Samples were quantified by absorbance on an Eppendorf Biospetrometer (1mm) and stored at -80°C. 2µg of RNA for selected samples were run on electrophoretic gel (1%) for 60 minutes at 100V.

Observations

With three exceptions, the amount of RNA isolated from the infections using the phenol-chloroform method was >100µg. Less than 1µg of RNA was recovered from each of the GBS-only controls.

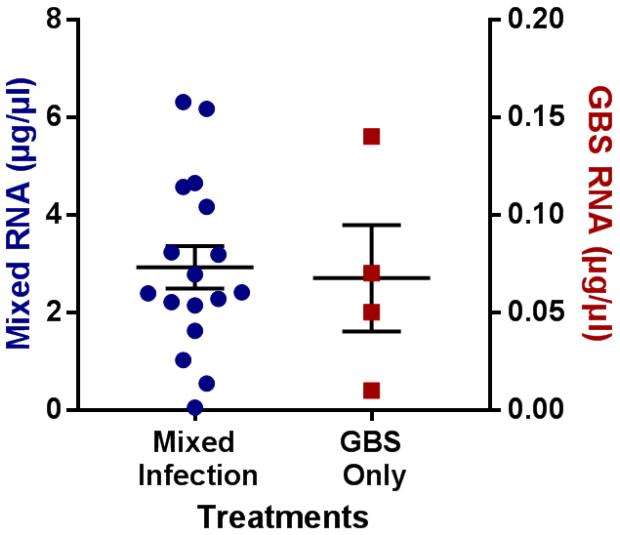

FIGURE AP2.38: Quantified RNA Extractions from TRIzol Reagent; Mixed (blue) and GBS-only (red) samples.

Absorbance-based quantifications from 17 mixed RNA samples and 4 GBS-only samples (Mean and SEM).

TABLE AP2.01: GBS counts from infections and Eppendorf Biospectrometer (1mm) absorbance readings from individual RNA isolations.

Sample	CFU/ml	ng/µl	A260/A280	A260/230	Total µg	Notes:
1	9.80E5	6306.2	1.73	2.32	315.3	Infection
2	1.08E6	2205.1	1.70	2.13	132.3	Infection
3	1.62E6	6173.9	1.84	2.21	370.4	Infection
4	1.38E6	3230.3	1.64	2.00	193.8	Infection
5	9.60E5	49.5	1.77	2.70	2.9	Infection
6	1.14E6	2142.2	1.73	2.36	128.5	Infection
7	1.86E6	4156.6	1.81	1.92	249.4	Infection
8	1.06E6	2407.2	1.71	2.25	144.4	Infection
9	8.20E5	2385.2	1.73	2.36	143.1	Infection
10	1.34E6	2834.9	1.79	1.73	166.8	Infection
11	1.06E6	2276.8	1.75	2.56	136.6	Infection
12	5.40E3	537.1	1.67	1.66	32.2	Infection
13	2.24E4	4645.4	1.75	2.24	278.2	Infection
14	1.72E5	1623.6	1.68	2.33	97.4	Infection
15	1.74E5	1017.4	1.69	2.19	101.7	Infection
16	1.66E6					Irrecoverable phase inversion
17	1.48E6	3181.7	1.95	2.39	190.9	Infection
18	6.20E5	4565.3	1.81	1.58	273.9	Infection
19	6.20E5	14.6	1.23	0.09	0.83	GBS-only Control
20	6.40E5	7.3	1.20	0.29	0.44	GBS-only Control
21	1.24E6	5.0	1.38	0.30	0.30	GBS-only Control
22	8.00E6	1.7	2.15	0.17	0.10	GBS-only Control

The expected two-band pattern representing the eukaryotic ribosomal subunit RNA (18S and 28S) was evident in most samples (FIGURE AP2.39). No secondary bands representing the bacterial ribosomal subunit RNA were detectable on the gel.

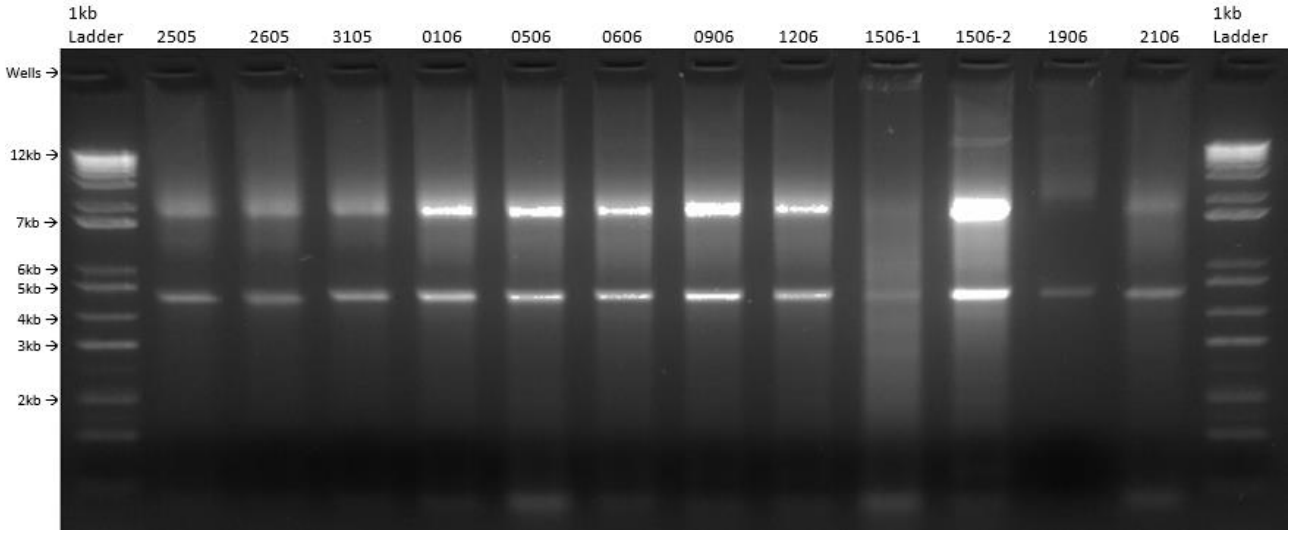

FIGURE AP2.39: Agarose gel showing separation of eukaryotic ribosomal subunits from 2µg RNA isolated from 12 selected infection samples.

Individual sample designations based on the date of RNA extraction. The ladder used was 1kb Plus DNA ladder (Invitrogen) with relevant sizes as indicated.

Interpretation

High amounts of good quality RNA is attainable through the TRIzol/Chloroform isolation method from GBS-challenged monocytes. However, only a very small portion of that RNA is bacterial.

Experiment 15: Test RNA for Bacterial DNA Contamination

GBS 874391 is characterised as Sequence Type 17 (ST17) and is thereby recognised as hypervirulent. There are several genes known to be common to ST17 GBS strains. One such gene is *spb1* – encoding a pilin backbone gene. Primers characterising this gene can therefore be utilised to test the RNA samples for contamination of bacterial DNA. The goal of this experiment was ensure the collected RNA samples are free of bacterial DNA contamination that may interfere with downstream applications.

PCR with Bacterial Gene *spb1*

Samples with high amounts of recorded RNA (Experiment 15) were selected for further testing. Standard PCR was performed using the Phusion High-Fidelity DNA polymerase (Thermo-Scientific) and following the manufacture's protocol; namely, the each 20µl reaction contained 4µl of 5X HF Phusion Polymerase Buffer (1.5mM $MgCl_2$), 0.4µl of 10mM dNTPs, 1µl of each 10µM primer, 0.2µl Phusion DNA Polymerase (2U/µl), 12.4µl of nuclease-free Ultrapure Distilled Water and 1µl of template RNA. The PCR program was 98°C for 30 seconds, followed by 35 cycles of 98°C for 10 seconds denaturation, 60°C for 30 seconds annealing, 72°C for 30 seconds extension, and then finally, a single 72°C extension for 5 minutes. Three PCRs were performed on the infection RNA samples and two on the GBS-only control RNA samples.

The *spb1* primers used in this PCR were;

Forward 5'-ATTGCGACATGGGCTAAATC (Designation: 1279 F1)

Reverse 5'-TGAAGCTTTTGTGGAACCATG (Designation: 1279 R1)

- generating an amplicon of ~762bp for the *spb1* gene specific to ST17 strains of GBS.

The synthesi from Ambion (Life Technologies) was utilised according to the manufactures instructions to DNase-treat each sample where bacterial DNA contamination was detected. PCR was subsequently re-performed on the DNase-treated samples. Amplification was analysed by gel electrophoresis.

Observations

No bacterial DNA contamination was readily detected (FIGURE AP2.40). However, in some samples, there was evident overlap between the sample smear and the *spb1* band size which may be hiding contamination. Therefore a further experiment was performed on for samples containing areas of overlap to clarify those regions.

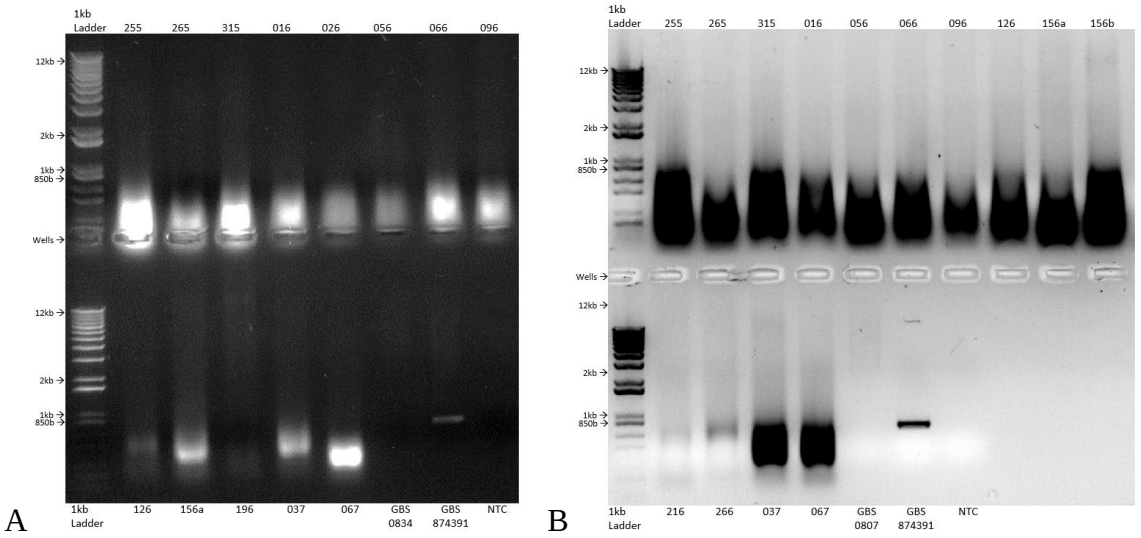

FIGURE AP2.40: Agarose gels of 2 independent PCRs testing for the presence of bacterial DNA in selected infection samples.

Electrophoresis was performed on putative PCR amplicons generated with spb1 bacterial DNA primers. GBS 874391 (ST17) serves as the positive control for both experiments. In addition to the No Template Control (NTC), non-ST17 strains of GBS serve as negative controls for each experiment; GBS 0834 in gel A and GBS 0807 in gel B. The ladder used was 1kb Plus DNA ladder (Invitrogen) with relevant sizes as indicated.

When repeated for those samples with smears overlapping the region of interest, the amplicon of interest was abundantly amplified in the positive PCR control, but not evident in the challenged samples (FIGURE AP2.41).

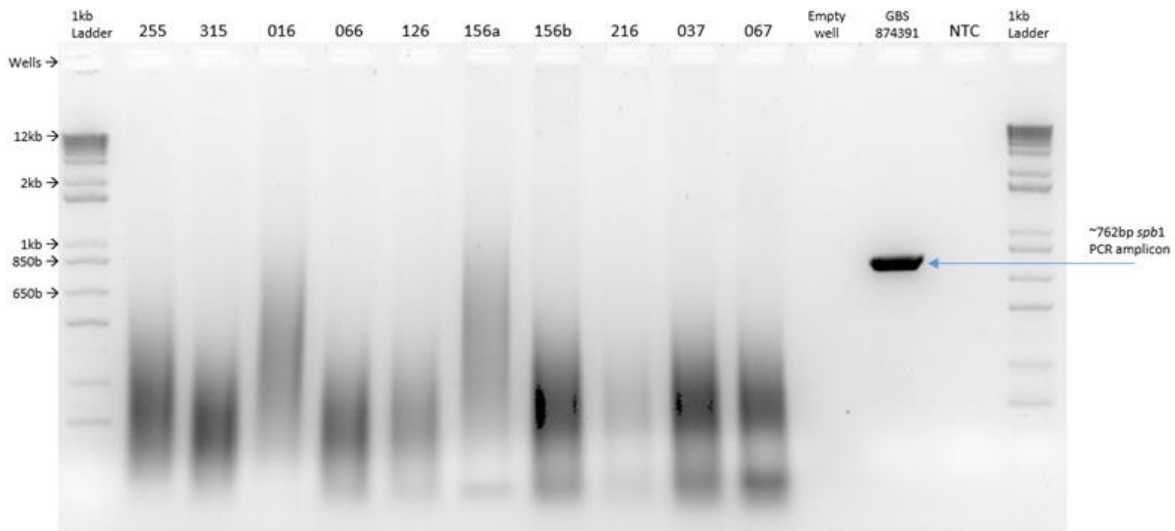

FIGURE AP2.41: Agarose gel of PCR rerun of 10 infection samples that previously demonstrated possible overlap with the amplified region of interest.

Electrophoresis was performed on putative PCR amplicons generated with spb1 bacterial DNA primers with GBS 874391 (ST17) serving as the positive control. The samples for this gel were selected based on possible overlap between the smear and amplicon in the previous gel (FIGURE AP2.40B). The ladder used was 1kb Plus DNA ladder (Invitrogen) with relevant sizes as indicated.

In all 4 GBS-only samples, there was obvious contamination of the RNA with GBS DNA (FIGURE AP2.42).

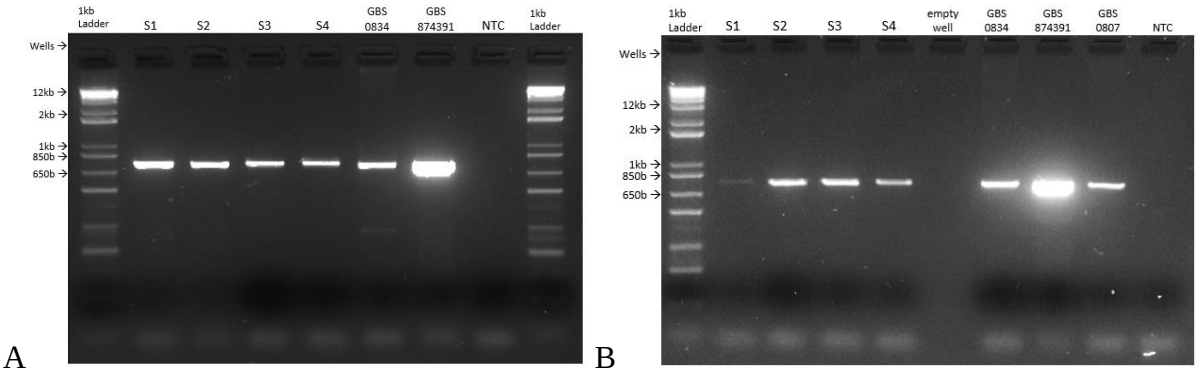

FIGURE AP2.42: Agarose gel showing bacterial DNA contamination of RNA isolated from 4 GBS-only control treatments.

Electrophoresis was performed on putative PCR amplicons generated with spb1 bacterial DNA primers. GBS 874391 (ST17) serving as the positive control. DNA contamination of all additional negative control strains (GBS 0834 and GBS 0807) was evident, however the primary negative control, the NTC, remained clear. The ladder used was 1kb Plus DNA ladder (Invitrogen) with relevant sizes as indicated.

After the DNase treatment, there was no PCR amplicon of the *spb1* bacterial gene evident in any of the DNase treated samples.

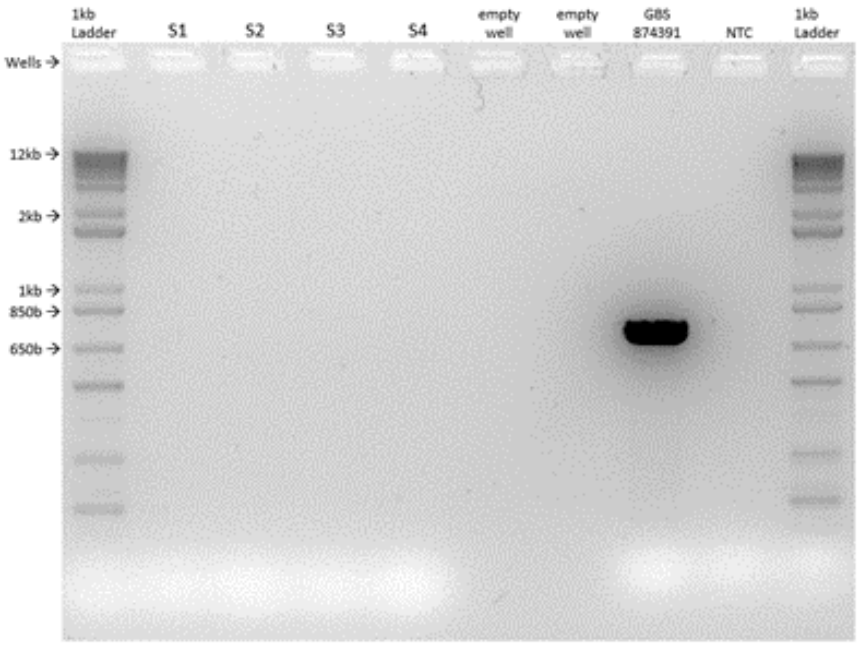

FIGURE AP2.43: Agarose gel of PCR results for 4 DNA-contaminated RNA samples after treatment with the Turbo DNAfree Kit.

Electrophoresis was performed on putative PCR amplicons generated with spb1 bacterial DNA primers. GBS 874391 (ST17) serving as the positive control. The ladder used was 1kb Plus DNA ladder (Invitrogen) with relevant sizes as indicated.

Interpretation

No bacterial DNA contamination was detected in the infection RNA samples. DNA contamination was overtly present in all four GBS-only RNA samples. The DNase enzyme in the Turbo DNAfree kit efficiently purified the RNA from DNA contamination.

Experiment 16: Test RNA for Eukaryotic DNA Contamination

The infection RNA samples further need to be examined for any possible contamination with eukaryotic/human DNA contributed by the human (U937) monocytes. *Beta-actin* (*β–actin* or *ACTB*) is a common eukaryotic housekeeping gene (Suzuki *et al.*, 2000). Primers targeting this gene can therefore be utilised to test the infection RNA samples for contamination with human DNA. The goal of this experiment was ensure the collected RNA samples are free of eukaryotic DNA contamination that may interfere with downstream applications.

PCR with Human Gene *Beta-actin* (*β-actin)*

Standard PCR was performed using the Phusion High-Fidelity DNA polymerase and the following the manufacture's protocol (see Experiment 15 for details). A PCR was performed on 12 infection RNA samples. A cDNA control (Olfactory Epithelial Cells) was supplied by Dr Deepak Ipe (Menzies Health Institute, Qld, Australia).

The *β–actin* primers (20nt) used in this PCR were;

Forward 5'-TCTACAATGAGCTGCGTGTG (Designation: Human Actin+GenomicF)

Reverse 5'-GGTGAGGATCTTCATGAGGT Designation: Human Actin+GenomicR)

This is an intron-intron primer set generating an expected genomic DNA amplicon of ~755bp for the human *β–actin* gene (and an expected amplicon of ~314bp for cDNA). These primers have been previously published (Castelruiz *et al.*, 1999, Sarobe *et al.*, 2002, Kethiri *et al.*, 2017).

Amplification was analysed by Electrophoresis run for 60 minutes at 100V on 2% agarose gels.

Observations

Some faint banding is evident around the expected gDNA size of 755bp (FIGURE AP2.44). The amplicon for the expected cDNA size is conspicuous in the cDNA sample.

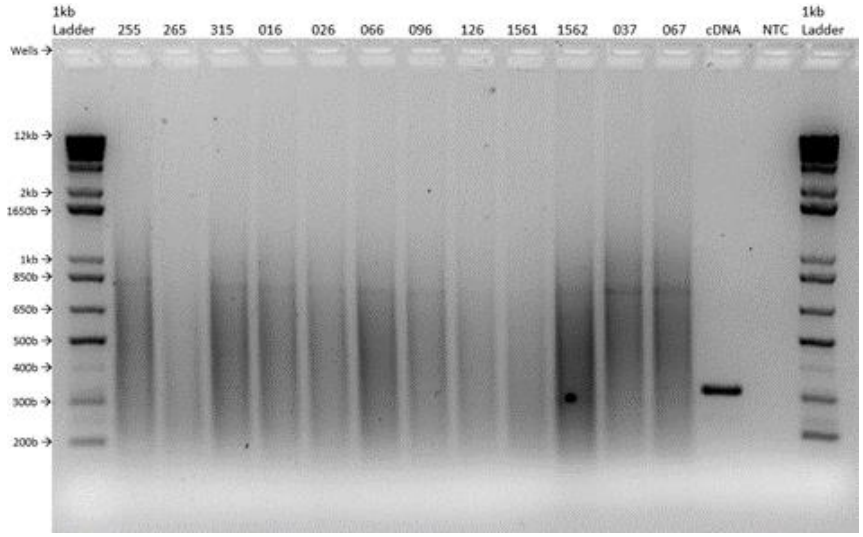

FIGURE AP2.44: Agarose gel of PCR testing for Human genomic DNA contamination of RNA isolated from 12 selected infections.

Electrophoresis was performed on putative PCR amplicons generated with β-actin eukaryotic (human) DNA primers and a cDNA sample serving as the positive control. The expected amplicon size for gDNA using these β-actin primers is 755bp. The ladder used was 1kb Plus DNA ladder (Invitrogen) with relevant sizes as indicated.

Interpretation

This PCR indicates that there is some gDNA in the infection RNA samples. However, the bands around the size of interest (755bp) are too light on the gel to be able to generate confidence in the subsequent gDNA removal procedure. Therefore optimisation of these primers is required to generate a more informative results for downstream use.

Experiment 17: Optimisation of PCR Procedures for *β-actin* primers

Due to the light bands of expected size from the previous experiment, various optimisations are employed to generate stronger amplicon bands on the gel. Stronger, more explicit bands at the expected size were expected to provide a baseline from which to increase confidence in the gDNA removal (RNA purification) procedure. The goal of this experiment was to optimise the PCR procedures for the *β-actin* primers to get a brighter, more explicit band on the gel.

PCR Optimisations

PCR Optimisation Overview

Using the *β-actin* primers from the previous experiment, the PCRs were optimised in the following ways;

PCR Optimisation 1 – 1:10 dilutions of the template were used to reduce the appearance of RNA smearing on the gel - to better distinguish amplicon bands from the background.

PCR Optimisation 2 – A 1:10 dilution of cDNA a control was added to the experiment.

PCR Optimisation 3 – Add dilutions of gDNA for another positive control.

PCR Optimisation 4 – Optimise PCR for annealing temperature and $MgCl_2$ concentrations.

PCR Optimisation 5 – Repeat PCR Optimisation 4, but with a higher resolution of the $MgCl_2$ concentrations.

Genomic DNA Preparation

Genomic DNA was isolated from an infection suspension stored at -80^{o}C in 0.5ml TRIzol. The Thermo Fisher/Invitrogen TRIzol Reagent User Guide for DNA isolation was generally followed; namely, chloroform was added to the TRIzol suspension, then centrifuged to separate into phases. After several rounds of re-centrifugation and washing from protein contaminants with ethanol, the DNA pellet was resuspended in 300µl nuclease-free Ultrapure Distilled Water. The DNA was incubated for 90 minutes at 65^{o}C, and then centrifuged at 12,000g for 10 minutes to remove any remaining contaminants. The supernatant containing the DNA was transferred to a new tube and quantified by absorbance on the Eppendorf Biospectrometer.

Observations

No 755bp band was evident at the 1:10 template concentrations used in these PCRs (FIGURE AP2.45). However, an unexpected band at the cDNA size (314bp) was present in both PCRs. For

unknown reasons, the cDNA control failed in PCR Optimisation 1, but was present in both dilutions in PCR Optimisation 2.

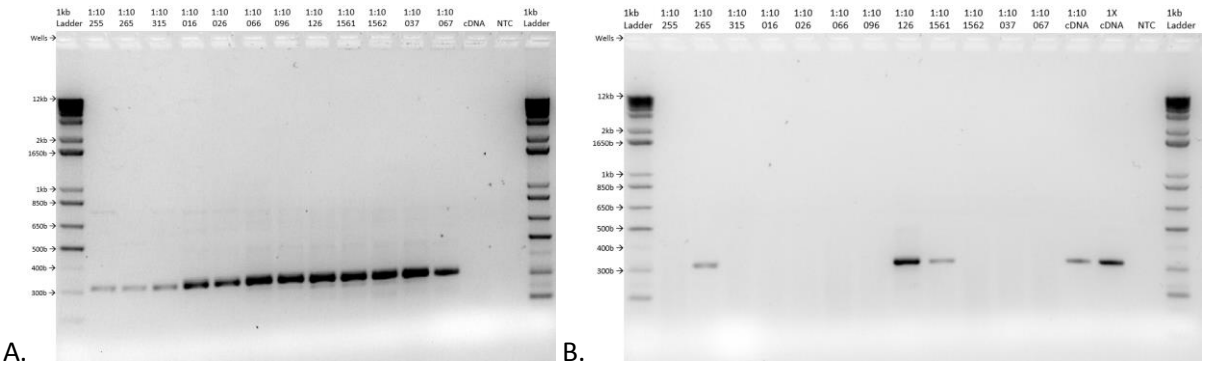

FIGURE AP2.45: PCR Optimisations 1 and 2. Agarose gels showing the results of 2 independent PCRs each testing the same 12 infection samples with β-actin primers - for gDNA contamination.
Templates of all samples are a 1 in 10 RNA dilutions for both gels. Gel A utilised a 1X cDNA control. Gel B utilised both a 1X and a 1:10 diluted cDNA control. The expected amplicon size for gDNA using these β-actin primers is 755bp. The ladder used was 1kb Plus DNA ladder (Invitrogen) with relevant sizes as indicated.

268.6µg of gDNA was prepared from an infection suspension and added to the PCR analysis as a positive control (FIGURE AP2.46). Even in the gDNA positive control, overt gel bands were only evident at the cDNA band size (314bp), but not the desired gDNA size (755bp).

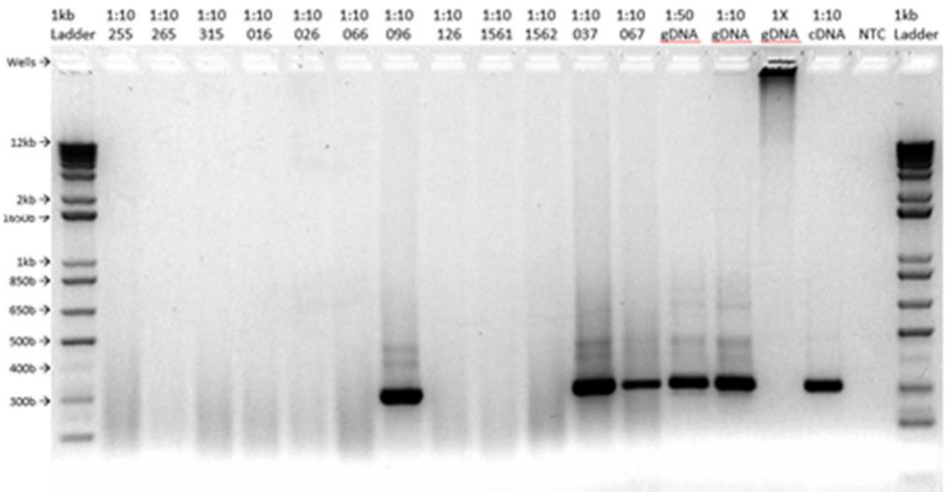

FIGURE AP2.46: PCR Optimisation 3. Agarose gels showing PCR results for 12 infection samples with β-actin primers – testing for gDNA contamination.
Templates of all samples are a 1: 10 RNA dilutions. Four positive controls were utilised; 3 dilutions of gDNA isolated from an infection sample (1X, 1:10, 1:50) and a 1:10 dilution of cDNA. The expected amplicon size for gDNA using these β-actin primers is 755bp. The ladder used was 1kb Plus DNA ladder (Invitrogen) with relevant sizes as indicated.

Having tested for varying PCR annealing temperatures and $MgCl_2$ concentrations on gDNA (FIGURES AP2.47-48), none of the optimisation measures revealed a clear band of desired size (755bp) from the gDNA template. A band at the size expected for cDNA continued to be overtly overrepresented in most of the tested conditions.

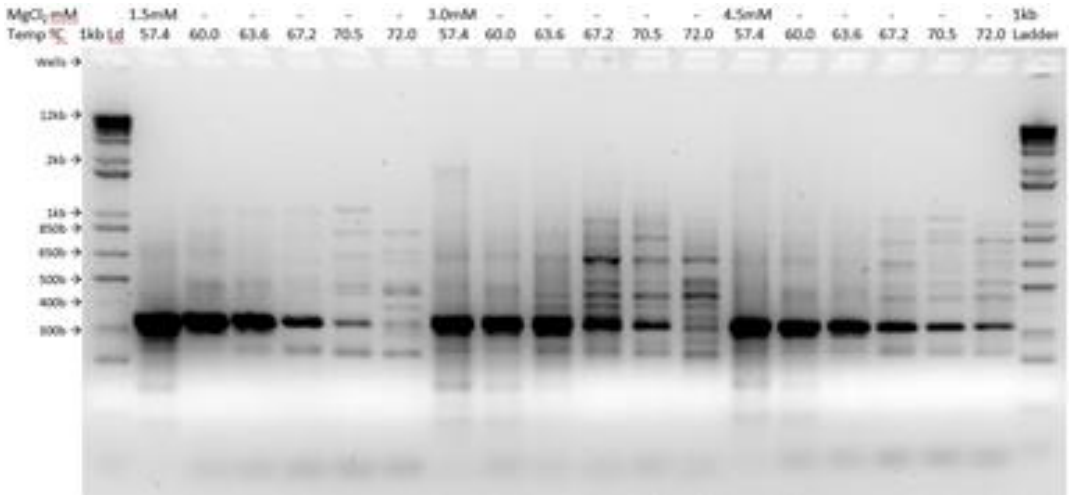

FIGURE AP2.47: PCR Optimisation 4. Agarose gel showing PCR optimisation results (optimising for annealing temperature and $MgCl_2$) for β-actin primers on a gDNA template.

Six annealing temperatures were tested (57.4°C, 60.0°C, 63.6°C, 67.2°C, 70.5°C and 72.0°C) each for 3 concentrations of $MgCl_2$ (1.5mM, 3.0mM and 4.5mM). The expected amplicon size for gDNA using these β-actin primers is 755bp. The ladder used was 1kb Plus DNA ladder (Invitrogen) with relevant sizes as indicated.

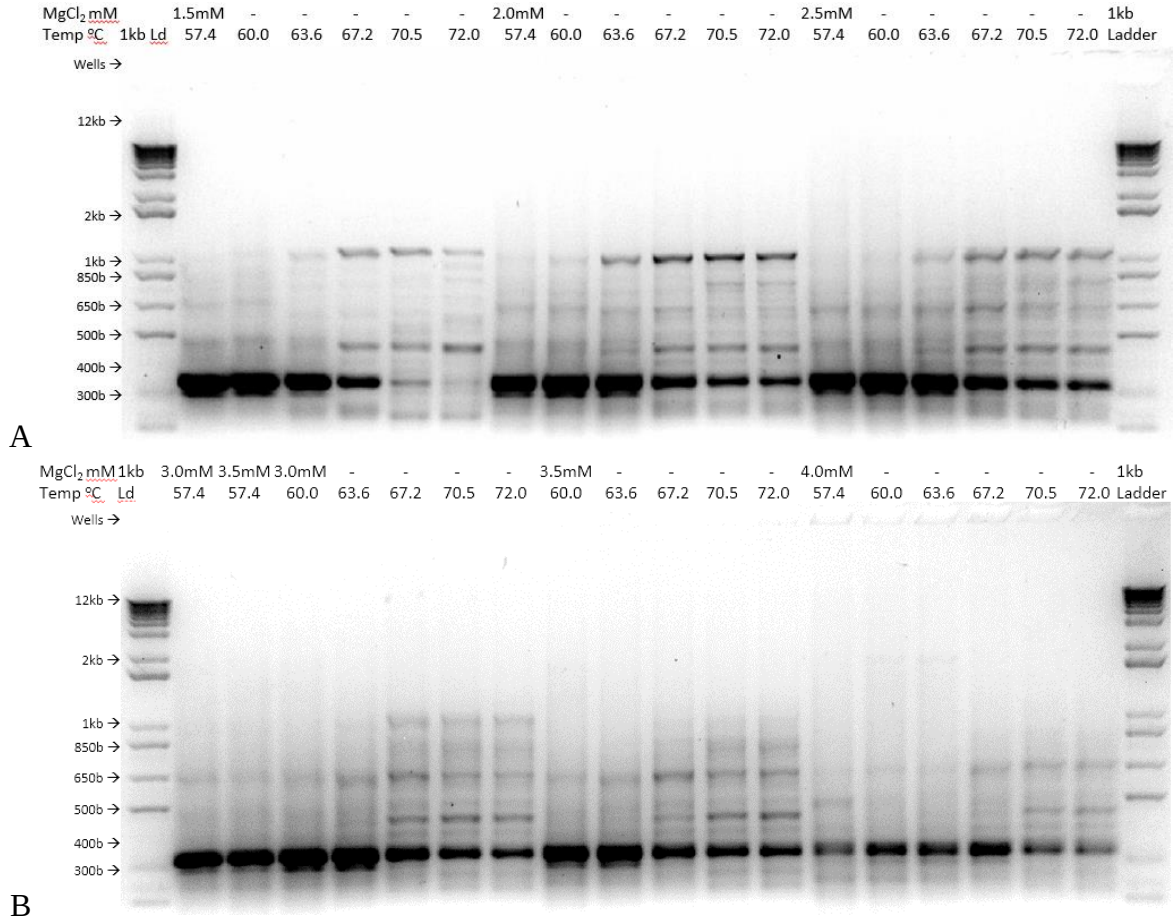

FIGURE AP2.48: PCR Optimisation 5. Agarose gel showing PCR optimisation results (further optimising for annealing temperature and $MgCl_2$) for β-actin primers on a gDNA template.

Higher resolution of $MgCl_2$ tested than previous PCR (FIGURE AP2.47). Six annealing temperatures were tested (57.4°C, 60.0°C, 63.6°C, 67.2°C, 70.5°C and 72.0°C) each for 6 concentrations of $MgCl_2$ (Gel A: 1.5mM, 2.0mM and 25.mM. Gel B: 3.0mM, 3.5mM and 4.0mM). The expected amplicon size for gDNA using these β-actin primers is 755bp. The ladder used was 1kb Plus DNA ladder (Invitrogen) with relevant sizes as indicated.

Interpretation

The primers used in these experiments are unsuitable to test the infection samples for human gDNA contamination.

Experiment 18: Optimisation of PCR Procedures for alternative *β-actin* primers

Being unable to optimise the *β–actin* primers used in the previous experiments, alternate *β–actin* primers were employed in a further attempt to test the samples for eukaryotic DNA contamination (Bas *et al.*, 2004).

PCR Optimisations (ii)

The *β–actin* primers (14-15nt) used in these experiments were;

Forward 5'- CCTCGCCTTTGCCGA (Designation: Human *Beta-Actin* Forward)

Reverse 5'- TGGTGCCTGGGGCG (Designation: Human *Beta Actin* Reverse)

This primer set is expected to generate a genomic DNA amplicon of 1030bp for the human *β–actin* gene (and 176bp for cDNA).

All amplicons were run on 2% agarose gel in TAE buffer at 100V for 60 minutes unless otherwise indicated. Template was added at a 1 in 10 dilutions unless otherwise indicated.

PCR optimisations were based on variations of Thermo-scientific Phusion High-Fidelity DNA polymerase protocol, namely;

PCR Optimisation 6 – Testing various $MgCl_2$ concentrations (from 1.5 to 4.5mM) and the annealing temperatures (57.4 to 72.0^{o}C) on gDNA

PCR Optimisation 7 – Testing various $MgCl_2$ concentrations (from 1.5 to 4.5mM) and the annealing temperatures (57.4 to 72.0^{o}C) on cDNA

PCR Optimisation 8 – Repeat PCR Optimisation 6 with increased resolution for both annealing temperature (from 2 to 1^{o}C increments between 63.0 and 66.9^{o}C) and $MgCl_2$ concentrations (from 1.5 to 0.5mM increments between 1.5 and 3.5mM), as well as increasing the PCR extension time (from 30 to 65 seconds).

PCR Optimisation 9 – Optimise PCR reactions for dimethyl sulfoxide (DMSO) - 0, 1, 3, 5, 7% per reaction volume).

PCR Optimisation 10 – Compare primary gDNA against infection gDNA using different buffers (GC vs. HF), annealing temperatures and $MgCl_2$ concentrations. The primary genomic extraction method is previously described (Ghatak *et al.*, 2013).

Observations

Having tested gDNA for varying PCR annealing temperatures and $MgCl_2$ concentrations (FIGURE AP2.49), many lanes contain a band around the desire size (1030bp). However, these also contain many other bands indicating alternate (non-specific) binding.

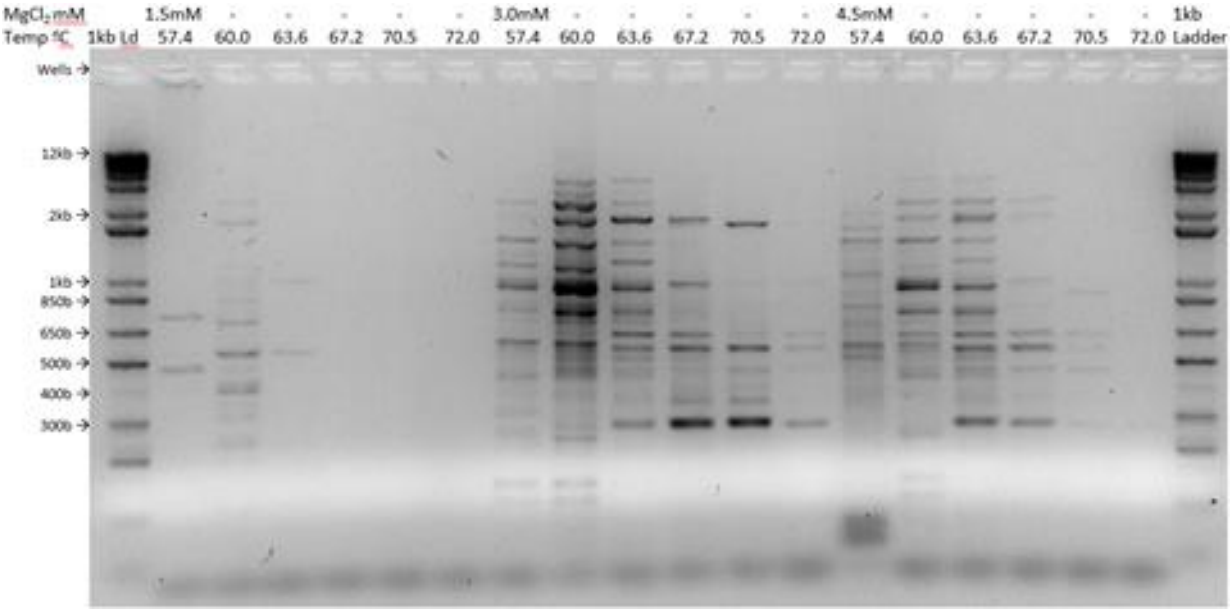

FIGURE AP2.49: PCR Optimisation 6 – Agarose gel showing PCR optimisation for alternative β-actin primers on gDNA for annealing temperature and $MgCl_2$.

Six annealing temperatures were tested (57.4°C, 60.0°C, 63.6°C, 67.2°C, 70.5°C and 72.0°C) each for 3 concentrations of $MgCl_2$ (1.5mM, 3.0mM and 4.5mM). The expected amplicon size for gDNA using these β-actin primers is around 1kb (1030bp). The ladder used was 1kb Plus DNA ladder (Invitrogen) with relevant sizes as indicated.

Having tested cDNA for varying PCR annealing temperatures and $MgCl_2$ concentrations (FIGURE AP2.50), the primers elucidate slight bands for cDNA at the expected size (176bp) at low temperatures (57.4°C and 60.0°C)and $MgCl_2$ concentrations reflecting the standard protocol for Phusion polymerase (i.e. 1.5mM). As the rest of the gel is clean, the primers can be assumed to specifically anneal to and amplify the predicted regions of the *β-actin* gene – though further optimisation was required to specifically amplify the longer gDNA region.

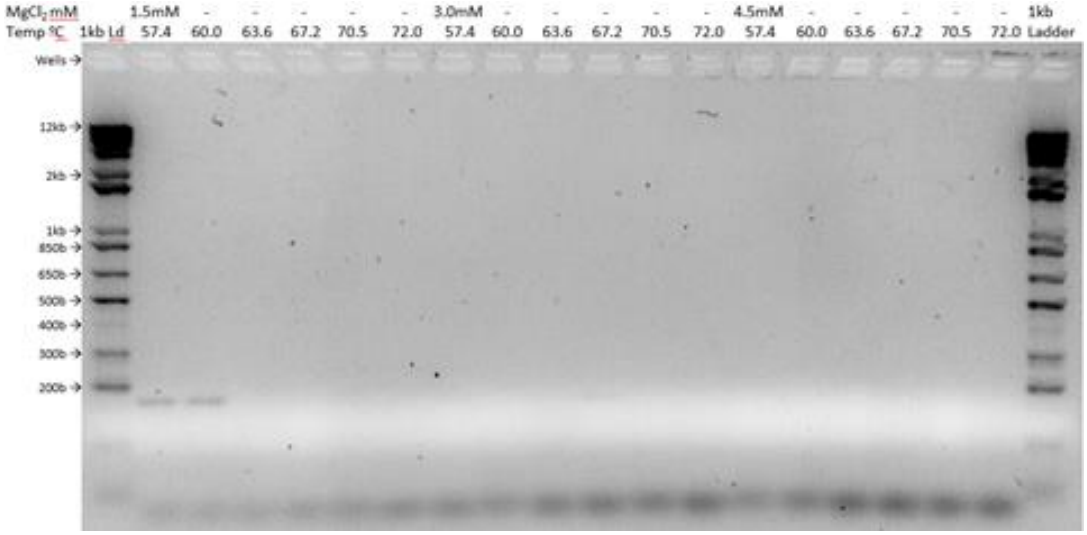

FIGURE AP2.50: PCR Optimisation 7 - Agarose gel showing PCR optimisation for alternative β-actin primers on cDNA for annealing temperature and $MgCl_2$.

Six annealing temperatures were tested (57.4°C, 60.0°C, 63.6°C, 67.2°C, 70.5°C and 72.0°C) each for 3 concentrations of $MgCl_2$ (1.5mM, 3.0mM and 4.5mM). The expected amplicon size for gDNA using these β-actin primers is 176bp. The ladder used was 1kb Plus DNA ladder (Invitrogen) with relevant sizes as indicated.

Increasing the extension time to 65 seconds for gDNA (FIGURE AP2.51) cleaned up the gel from some of the alternate binding observed in PCR Optimisation 6 (see FIGURE AP2.49). The clearest bands at the expected size (around 1kb) were observed at 2mM $MgCl_2$; with the least alternate binding at 64°C and 66°C.

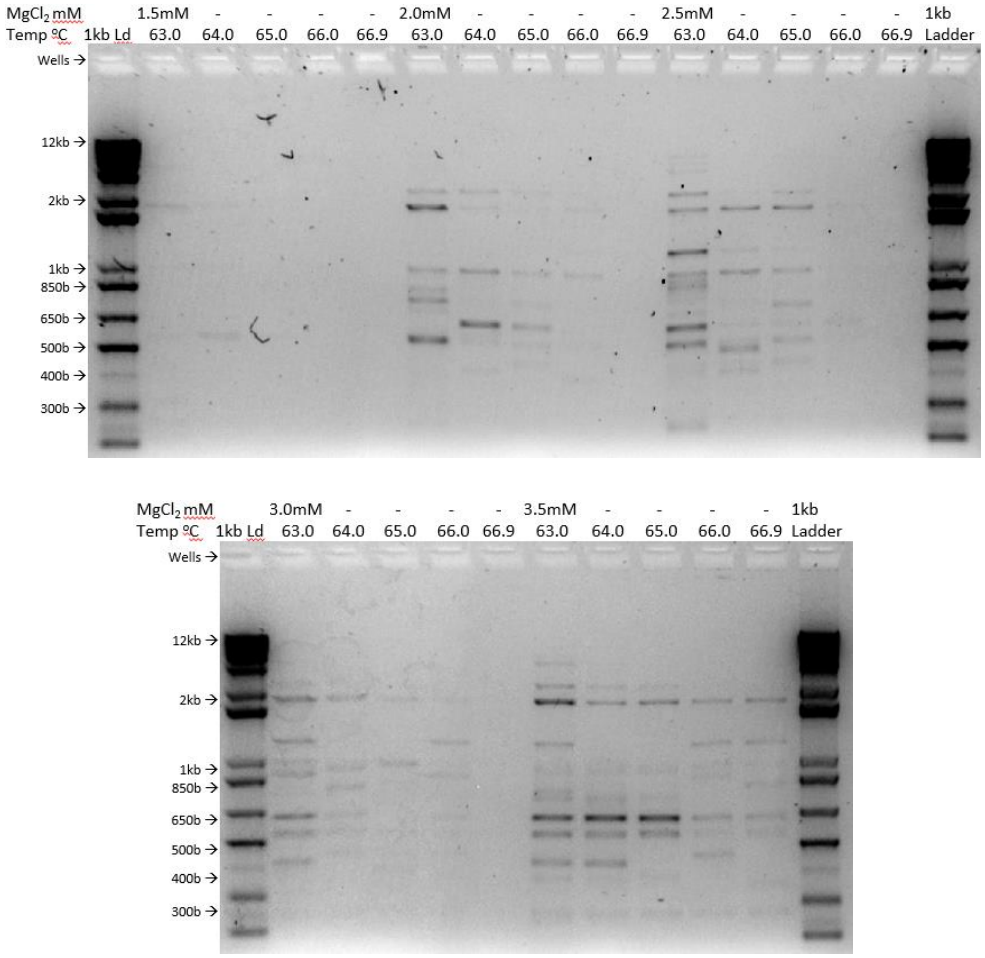

FIGURE AP2.51: PCR Optimisation 8 - Agarose gel showing PCR optimisation for alternative β-actin primers on gDNA for annealing temperature, $MgCl_2$ concentration and PCR extension time.
Five annealing temperatures were tested (63.0°C, 64.0°C, 65.0°C, 66.0°C and 66.9°C) each for 5 concentrations of $MgCl_2$ (1.5mM, 2.0mM, 2.5mM, 3.0mM and 3.5mM). The results of this PCR were loaded over 2 gels; the upper gel represents $MgCl_2$ concentrations 1.5mM, 2.0mM and 2.5mM, and the lower gel represents $MgCl_2$ concentrations 3.0mM and 3.5mM. The PCR extension time was 65 seconds (the extension time for previous PCRs was 30 seconds). The expected amplicon size for gDNA using these β-actin primers is around 1kb (1030bp). The ladder used was 1kb Plus DNA ladder (Invitrogen) with relevant sizes as indicated.

With DMSO added to the PCR reactions in varied concentrations, the brightest band at the desired size (~1kb) was observed in the control with no (0%) added DMSO (FIGURE AP2.52).

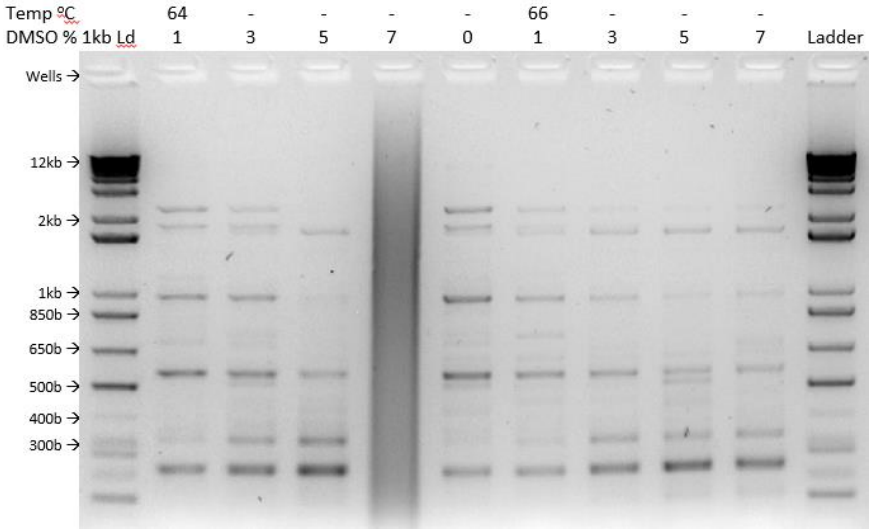

FIGURE AP2.52: Optimisation 9 – Agarose gel showing PCR optimisation results for alternate β-actin primers in 2mM $MgCl_2$ at annealing temperatures 64°C & 66°C for DMSO (% volume).
Two annealing temperatures were tested (64.0°C and 66.0°C) each for 4 concentrations of DMSO (1%, 3%, 5% and 7%). At 64°C, 1 reaction without any DMSO (i.e. 0%) was also tested. The expected amplicon size for gDNA using these β-actin primers is around 1kb (1030bp). The ladder used was 1kb Plus DNA ladder (Invitrogen) with relevant sizes as indicated.

The gDNA used up to this point was isolated from GBS-infected monocytes (i.e. a mixture of monocyte and GBS DNA from an infection sample), so gDNA was isolated from human cells to compare the effectiveness of the primers between the 2 preparations. A primary human DNA extraction yielded 514.8ng/µl (total 25.7µg in 50µl) of DNA. In PCR Optimisation 10, the *β-actin* primers were used to PCR-amplify primary genomic DNA (PgDNA – isolated from human cells) and genomic DNA isolated from infections (mixed gDNA or MgDNA). There are some bands at the expected size (~1kb) for both primary and mixed gDNA; especially from the 2.0 mM $MgCl_2$ reactions; however the gel is still characterised by excessive, non-specific banding (FIGURE AP2.53).

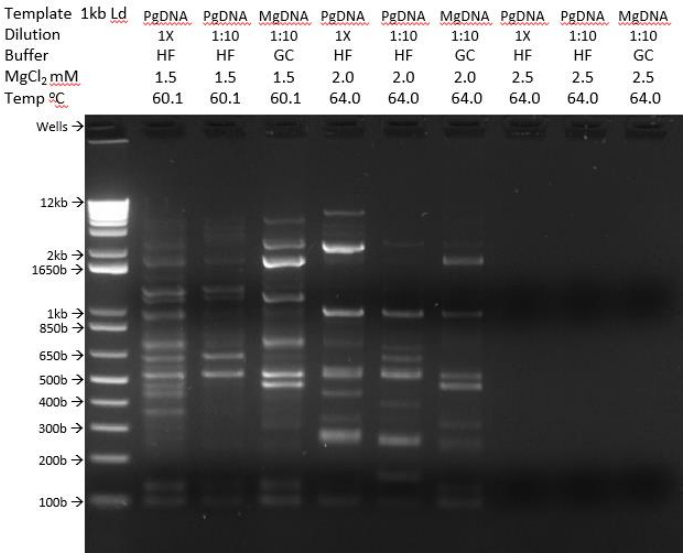

FIGURE AP2.53: Optimisation 10 – Agarose gel of PCR products comparing Primary genomic DNA (PgDNA) against mixed genomic DNA (MgDNA).

Primary genomic DNA was isolated from human cells. Mixed genomic DNA was isolated from GBS-infected monocytes. The PCR reactions were optimised for 2 template dilutions (1X and 1:10), 2 buffers (High Fidelity Phusion Buffer and GC Buffer), and 3 concentrations of $MgCl_2$ (1.5mM, 2.0mM and 2.5mM). The PCR programme was optimised for 2 annealing temperatures (60.1°C and 64.0°C). The ladder used was 1kb Plus DNA ladder (Invitrogen) with relevant sizes as indicated.

Interpretation

This primer set works to elucidate cDNA *β–actin* from a PCR reaction using the standard protocol for Phusion polymerase. Whether or not a reliable gDNA *β–actin* amplicon can be produced with these primers is less certain. A band around the desired 1030bp size for gDNA is evident in the gel when using these primers in an optimised PCR procedure (namely; 2mM $MgCl_2$, 64°C annealing temperature, 65 second extension time), however, the levels of non-specific binding observed through multiple gel bands mitigates confidence that this band is actually and exclusively *β–actin*.

Experiment 19: Sequencing of putative *β-actin* amplicon

After optimisation, an amplicon of the desired ~1kbp band is reproducible in the gel using the *β-actin* primer set from Experiment 18, however, the gels were not clean; with a lot of non-specific bands present. Further investigation is therefore required to confirm the identity of the amplicon through genetic sequencing of the band. The goal of this experiment was to sequence the putative *β-actin* amplicon to verify its identity.

Gel Extraction and Sequencing

Using the *β–actin* primers and PCR conditions developed in the previous experiment, the amplicon was extracted from the agarose gel and sent to Australian Genome Research Facility (AGRF), University of Queensland for Sanger sequencing. Briefly;

The standard Thermo-scientific Phusion High-Fidelity DNA polymerase protocol was followed with the following modifications. The PCR program used for the gDNA amplicon ran for 40 PCR cycles, with an annealing temperature of 64^{o}C and extension time of 65 seconds. The PCR program used for the cDNA amplicon ran for 35 PCR cycles, with an annealing temperature of 60^{o}C and extension time of 30 seconds.

QIAgen's QIAquick Gel Extraction Kit was used in accordance with the manufacturer's protocol to isolate the DNA from the agarose gel. Final elutions were performed in nuclease-free Ultrapure Distilled Water. The DNA was further concentrated using the QIAquick PCR Purification Kit in accordance with the manufacturer's instructions. Further concentration was achieved though dehydration using the Eppendorf Concentrator Plus at 30^{o}C (Mode: V-AQ). Between 30 and 120ng of the amplicon was sent to AGRF for both forward and reverse primer reactions for both gDNA and a cDNA amplicon.

Observations

PCRs performed on both gDNA and cDNA amplified bands around the desired sizes (1030 and 176bp respectively). The gDNA extracted from the gel was absorbance-measured to be 28.9ng/µl. The cDNA extracted from the gel was absorbance-measured to be 54.2ng/µl.

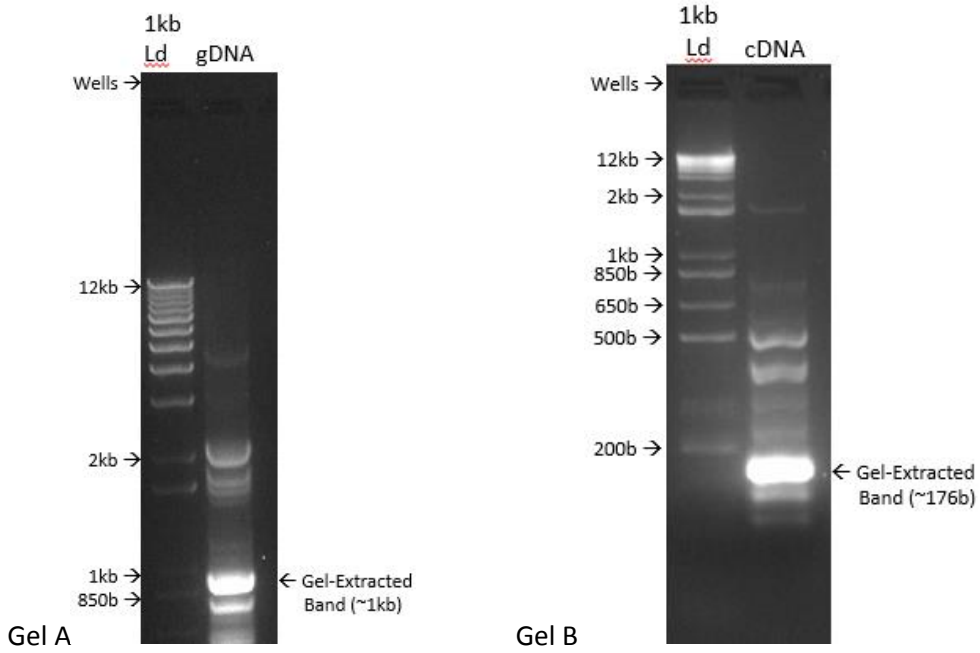

FIGURE AP2.54: Agarose gels of putative PCR-generated β-actin amplicons (Gel A: MgDNA. Gel B: cDNA) for gel-extraction and sequencing.

β-actin primers were used to generate amplicons for gDNA (Gel A) and cDNA (Gel B). The ladder used was 1kb Plus DNA ladder (Invitrogen) with relevant sizes as indicated.

The assembly for the cDNA was 178bp in length (FIGURE AP2.55). The forward sequence was 109 bases and the reverse sequence was 77 bases – with 79 bases overlapping (green). A nucleotide BLAST of both sequences identified the region as primate *β-actin* (*ACTB*).

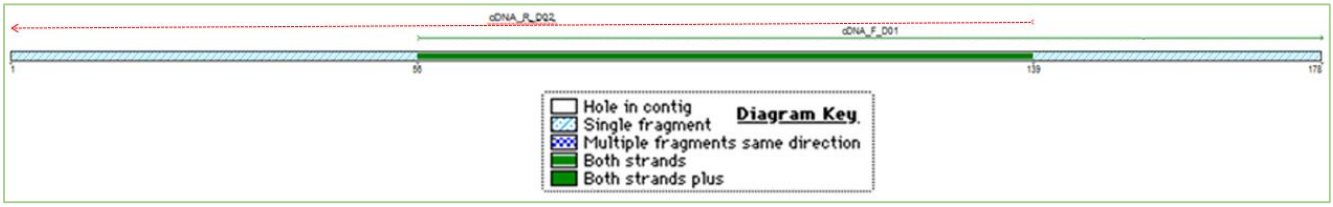

FIGURE AP2.55: cDNA sequence assembly generated in Sequencher 5.3.

Red and green arrows represent sequences generated using forward and reverse β-actin primers on a cDNA template. Both arrow colour (green) and direction indicate the direction of sequencing.

Using the most relaxed Sequencher parameters, no overlap was found for the gDNA sequences (FIGURE AP2.56). The nucleotide BLAST for the forward primer sequence predicted the sequence to be Homo sapiens exostosin-like glycosyltransferase 1 (EXTL1), transcript variant X2, mRNA. *β-actin* did not feature in the BLAST results (i.e. the top 82 BLAST hits). The nucleotide BLAST for the reverse primer gDNA sequence predicted the sequence to be Homo sapiens OTU deubiquitinase, ubiquitin aldehyde binding 1 (OTUB1), transcript variant 2, non-coding RNA. *β-actin* did not feature in the BLAST results (i.e. the top 100 BLAST hits).

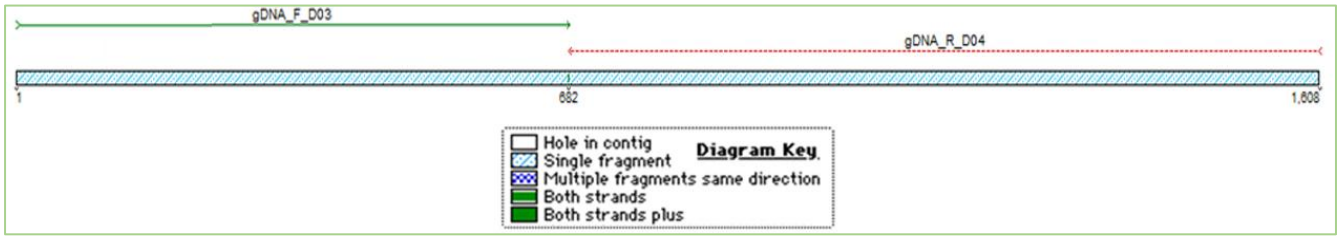

FIGURE AP2.56: gDNA sequence assembly generated in Sequencher 5.3.
Arrows represent sequences generated using forward and reverse β-actin primers on a gDNA template. Both arrow colour (green) and direction indicate the direction of sequencing.

After repeating the gel extraction and sequencing for the gDNA (FIGURE AP2.57), the assembly for the cDNA was 174bp in length – with 121 bases overlapping (green)(FIGURE AP2.58). A nucleotide BLAST of both sequences again identified the region as *β-actin* (*ACTB*).

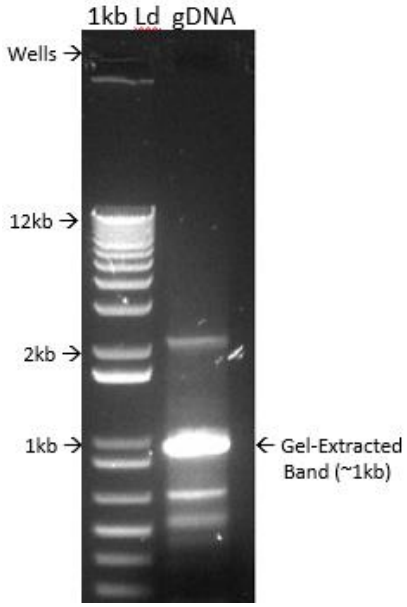

FIGURE AP2.57: Agarose gel of putative PCR-generated β-actin amplicons (gDNA) for gel-extraction and sequencing.
β-actin primers were used to generate amplicons for gDNA. The ladder used was 1kb Plus DNA ladder (Invitrogen) with relevant sizes as indicated.

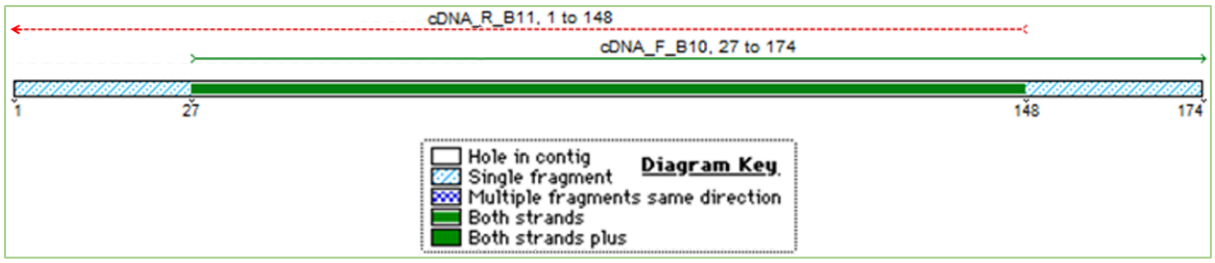

FIGURE AP2.58: cDNA (from first gel extraction) sequence assembly generated in Sequencher 5.3.
Arrows represent sequences generated using forward and reverse β-actin primers on a cDNA template. Both arrow colour (green) and direction indicate the direction of sequencing. Overlap in the assembly occurred between base 27 and base 148. The sequence template used was from the initial cDNA gel extraction (FIGURE AP2.54, Gel B) which was successfully sequenced and assembled to β-actin previously (FIGURE AP2.55).

Using the most relaxed Sequencher parameters, no overlap was again found for the gDNA sequences. The nucleotide BLAST for the forward primer sequence predicted the sequence to be primate *β-actin*. The nucleotide BLAST for the reverse primer gDNA sequence predicted the sequence to be Homo sapiens cDNA FLJ61195 complete cds, highly similar to Ubiquitin thioesterase protein OTUB1. *β-actin* did not feature in the BLAST results (i.e. the top 54 BLAST hits).

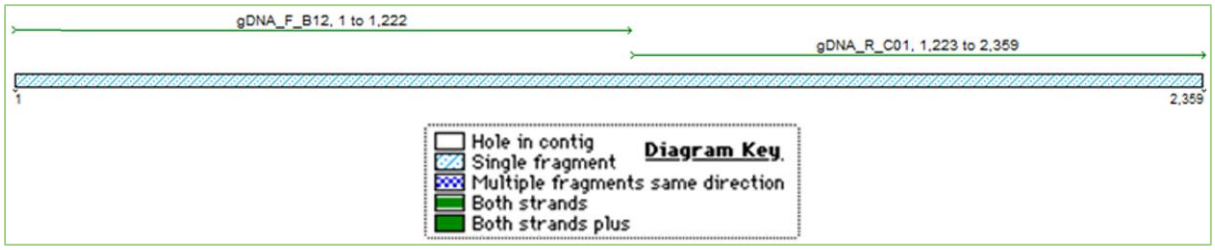

FIGURE AP2.59: gDNA (from repeated gel extraction) sequence assembly generated in Sequencher 5.3.
Arrows represent sequences generated using forward and reverse β-actin primers. Both arrow colour (green) and direction indicate the direction of sequencing. No overlap between the sequences was detected by the software – which assembled the 2 sequences one after the other.

Unidirectional analysis comparing forward and reverse sequences demonstrates complete overlap (blue) between the two sequences.

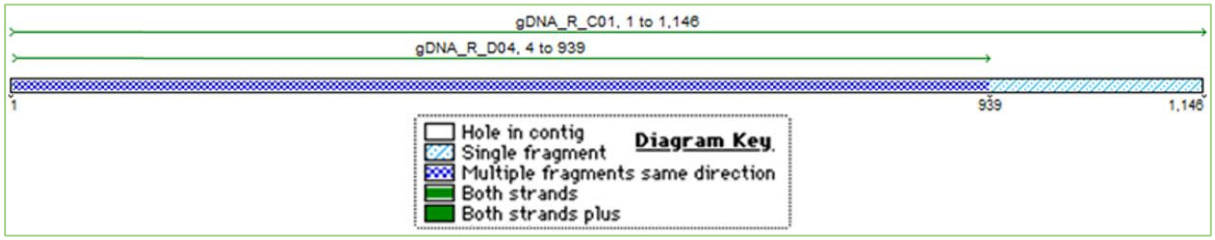

FIGURE AP2.60: Unidirectional assembly of gDNA sequences generated in Sequencher 5.3.
Arrows represent sequences generated using forward and reverse β-actin primers. Both arrow colour (green) and direction indicate the direction of sequencing. Complete overlap of the sequences by unidirectional analysis indicates that the primers are amplifying in the same direction; rather than from 2 directions flanking the region of interest.

Interpretation

The utility of these primers to successfully amplify *β-actin* from cDNA is confirmed. However the amplicon derived from using these primers on gDNA cannot be trusted to represent the *β-actin* gene; possibly due to the more complex structure of gDNA – with non-specific binding giving rise to multiple bands on the gel.

The unidirectional overlay of the gDNA sequencers indicates that the primers are amplifying the same gene region in one direction only; rather than straddling the region of interest as designed. One of the four gDNA sequences was identified as *β-actin* however the other three were identified as genes completely unrelated to *β-actin*. Given this ambiguity, this primer set is not appropriate for testing RNA for eukaryotic gDNA contamination.

Experiment 20: Design and testing *GAPDH* primers

Glyceraldehyde 3-phosphate dehydrogenase (*GAPDH*) is another recognised eukaryotic housekeeping gene performing multiple cellular functions (Suzuki *et al.*, 2000, Tristan *et al.*, 2011). In this experiment, *GAPDH* primers were designed and tested to provide a reliable eukaryotic DNA contamination test for infection RNA samples.

PCRs with Designed Primers

Ten primer sets were derived from three methods. Four primer sets were characterised manually using the Artemis 16.0.0 software, four others using the primer3plus.com website (Untergasser *et al.*, 2012), and two were derived from the literature. Primers were designed to be roughly 20 nucleotides long with a GC content around 50% (see Appendix 3, TABLE A for primer details).

Primers were tested using the standard PCR protocol for Phusion polymerase and the amplicons resolved on 2% agarose gels by electrophoresis for 60 minutes at 100V. The new primers were initially tested on mixed gDNA from an infection. Then selected primer sets were tested on both cDNA and gDNA before being applied to RNA extracted from infections. After the most sensitive

primer set was determined, the primers were used to compare their effect on different concentrations of RNA (0.1µg vs. 0.01µg). Samples at both of those concentrations were then DNase-treated using the Turbo DNAfree Kit according to the manufacturer's instructions on samples where DNA contamination was evident.

Observations

Appendix 3, TABLE A lists the details of primers designed in this experiment.

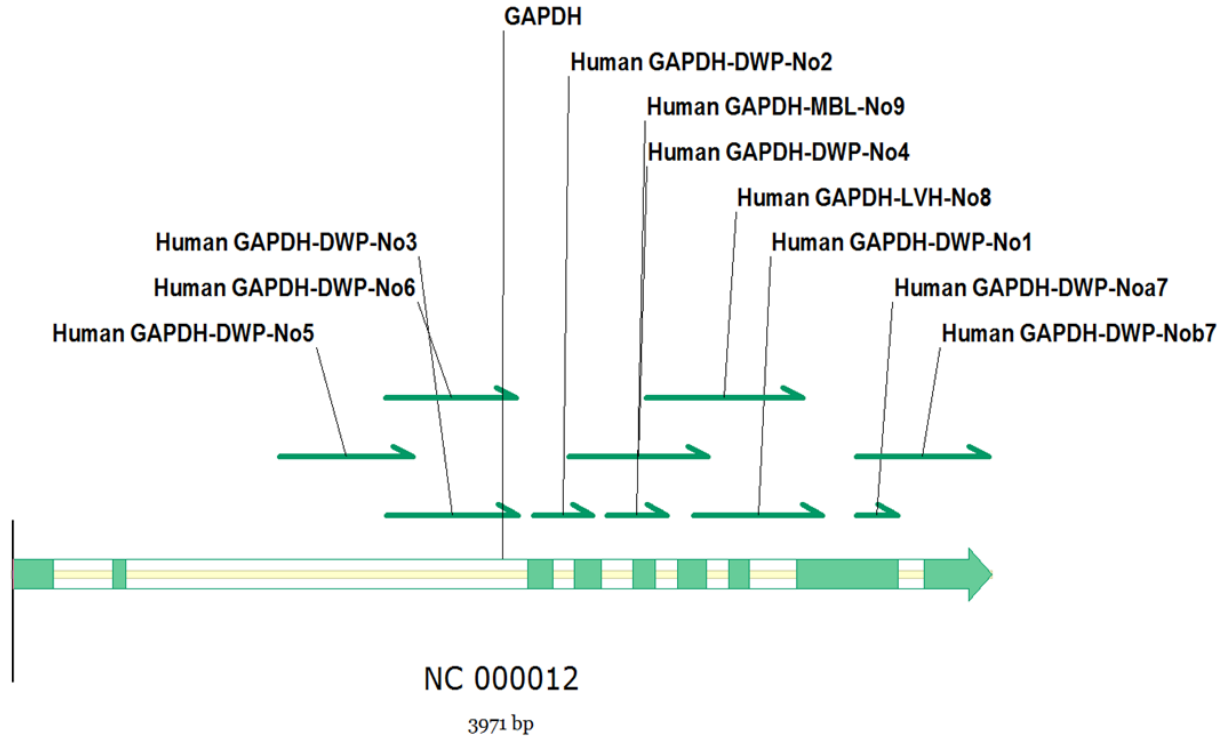

FIGURE AP2.61: Map of where the amplicons fit along the human GAPDH gene based on the newly designed primers.

Figure generated in Vector NTI 11.5.3. Large arrow represents the whole human GAPDH gene (3971bp) in the 5' to 3' direction – with exons blocked out in green and intron regions marked with a yellow line. Floating green arrows represent putative amplicons to be generated from the designed primers, as related to the GAPDH gene.

Testing these primers using the standard PCR protocol for Phusion polymerase (FIGURE AP2.62), only primer sets 4, 7a and 7b reliably amplify to the expected sizes (569, 171 and 543 respectively). Primers 1 and 2 amplified to sizes that were not expected. Primers 8a and 8b preferentially amplify cDNA. And Primers 3, 5, 6 and 9 displayed high levels of non-specific binding.

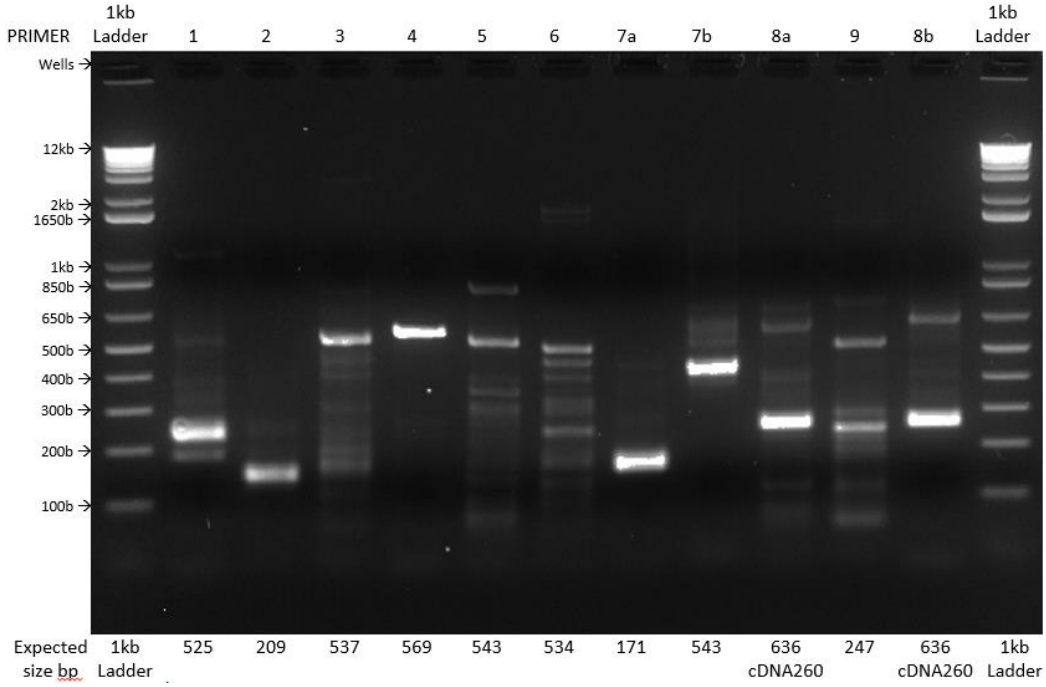

FIGURE AP2.62: Agarose gel showing putative GAPDH PCR-generated amplicons from newly designed primer sets on mixed gDNA.

Primer sets 7a and 7b use the same forward primer, but different reverse primers. Sample 8b is a repeat of 8a testing the impact of increasing the PCR extension time from 30 to 60 seconds. Expected amplicon sizes (under the image) are for gDNA unless otherwise specified. The ladder used was the 1kb Plus DNA ladder (Invitrogen) with relevant sizes as indicated.

After performing PCR on *GAPDH* primer sets 4, 7a and 7b against both gDNA and cDNA (FIGURE AP2.63*),* primer 4 revealed a clean band for gDNA only - which is in line with expectation. *GAPDH* 7a primers amplified strong bands at the same size for both gDNA and cDNA – which is also in line with expectation. Using the 7b primer set, there was only a slight band around the desired 543bp size for gDNA but a brighter band for the size expected for cDNA (439bp).

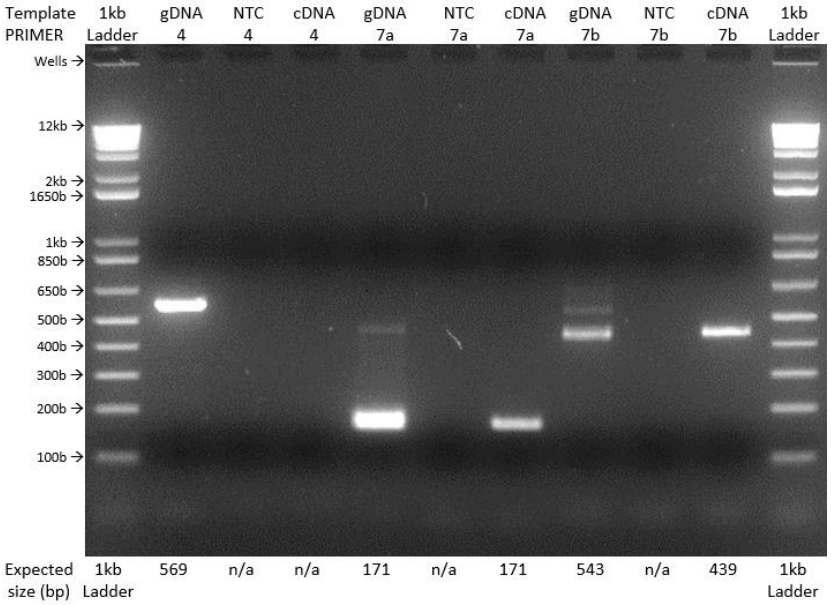

FIGURE AP2.63: Agarose gel showing putative GAPDH PCR-generated amplicons using newly designed primers 4, 7a and 7b on both gDNA and cDNA.

Primer set 4 spans from one intron to another, across an exon – and is therefore only expected to amplify gDNA (569bp). Primer set 7a is expected to amplify a region within a single exon – and is therefore expected to amplify the same size (171bp) for both gDNA and cDNA. Primer set 7b is expected to amplify from an exon to another exon, across an intron – and should therefore amplify a 543bp amplicon for gDNA and a 439bp amplicon for cDNA. The ladder used was the 1kb Plus DNA ladder (Invitrogen) with relevant sizes as indicated.

Both 4 and 7a primer sets were tested on RNA derived from infected samples (FIGURE AP2.64). *GAPDH* primer 4 presented a bright band for one infection sample (sample 166). *GAPDH* primer 7a generated amplicon bands for eight sample including sample 166. *GAPDH* primer 7a is therefore the more sensitive primer.

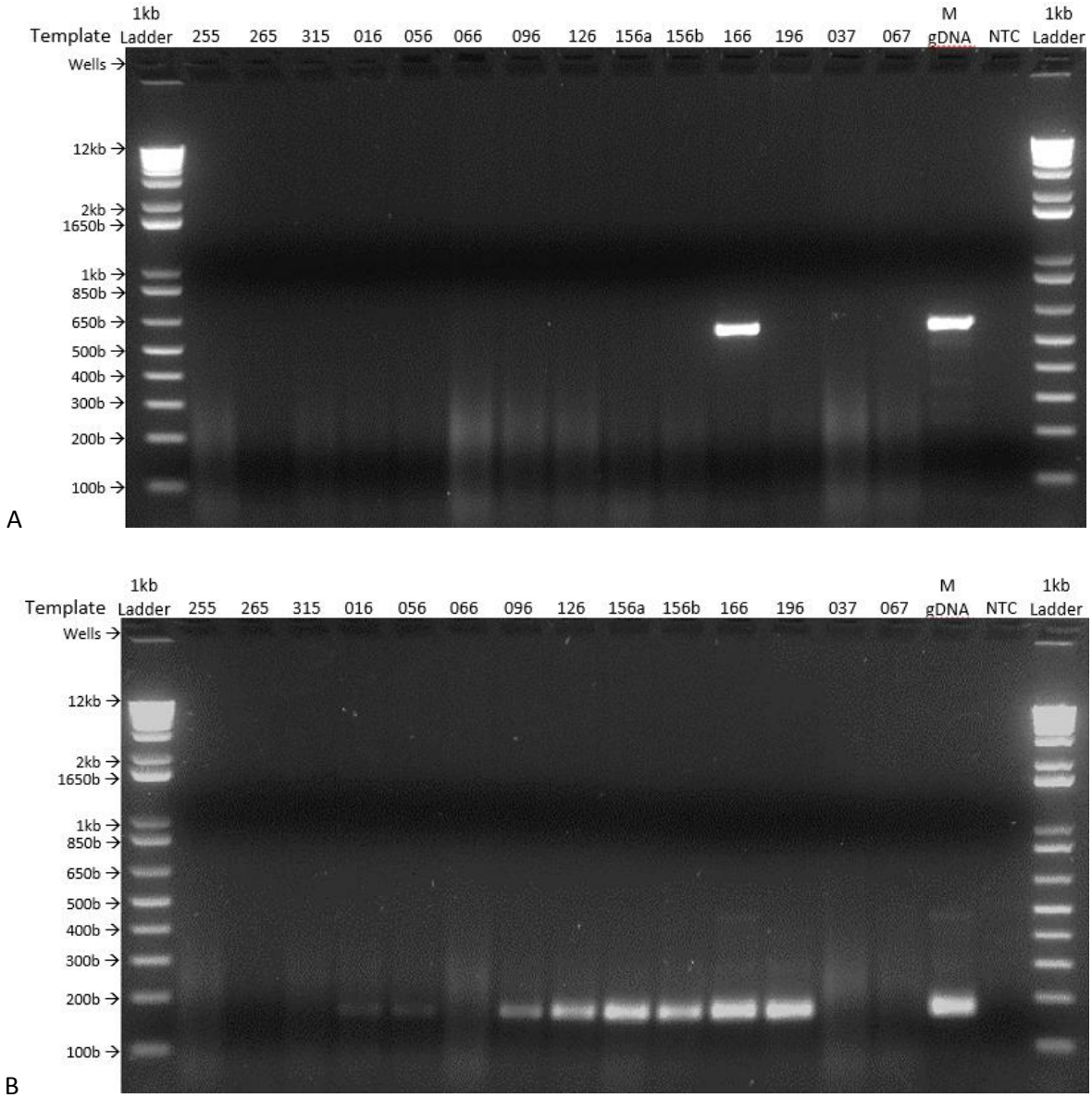

FIGURE AP2.64: Agarose gels testing 14 RNA samples for DNA contamination using 2 newly designed GAPDH primer sets.

Mixed gDNA (isolated from GBS-infected monocytes) was used as the positive control in both gels. The 14 RNA samples tested were also isolated from GBS-infected monocytes. Gel A shows the PCR results using primer set 4, generating an expected gDNA amplicon of 569bp. Gel B shows the PCR results using primer set 7a, generating an expected gDNA amplicon of 171bp. The ladder used in both gels was the 1kb Plus DNA ladder (Invitrogen) with relevant sizes as indicated.

GAPDH primer set 7a continues to be sensitive to DNA detection when amplifying 0.01µg of infection RNA (FIGURE AP2.65).

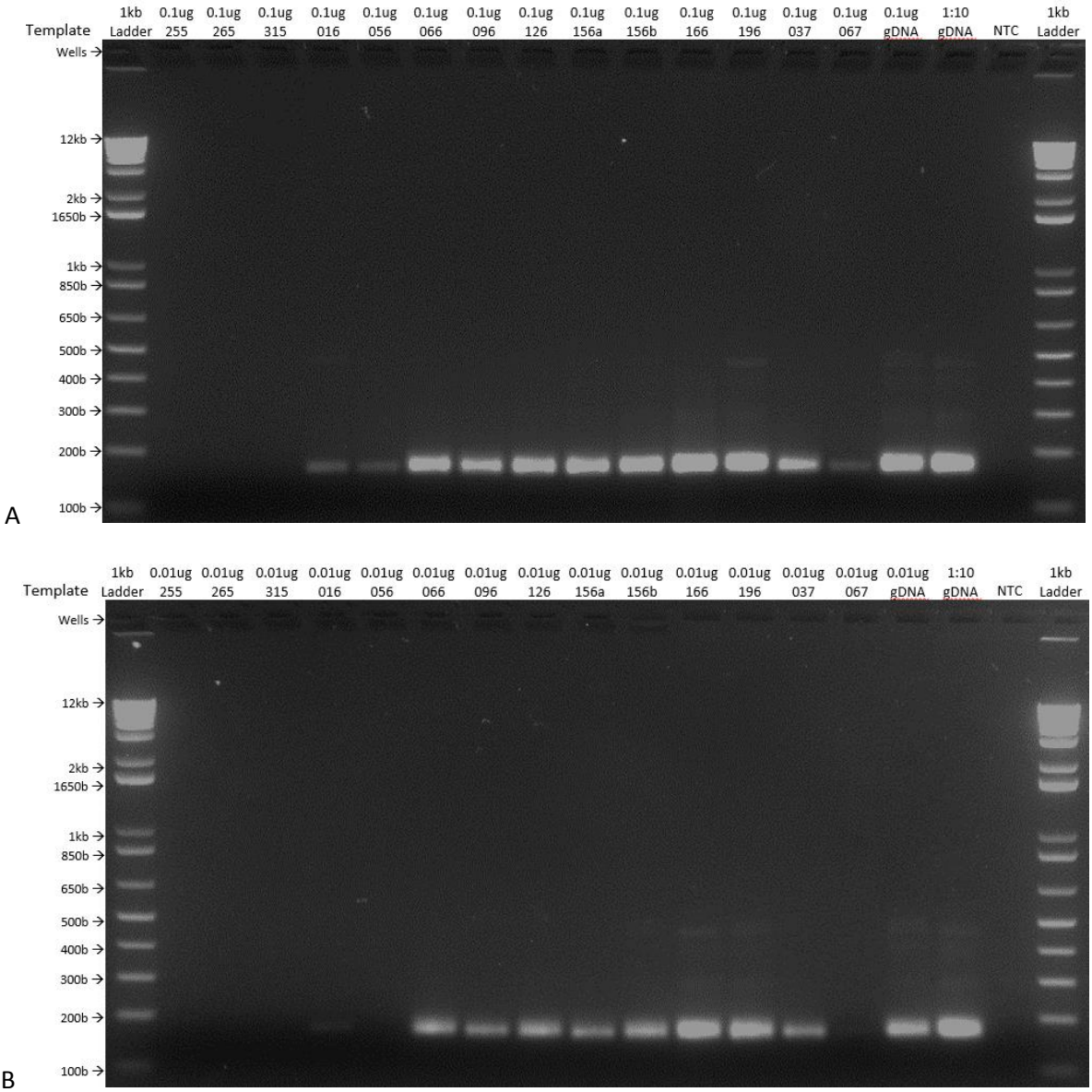

FIGURE AP2.65: Agarose gels testing the sensitivity of the GAPDH primer set 7a to detect human DNA contamination in RNA samples.

Mixed gDNA (isolated from GBS-infected monocytes) was used as the positive control in both gels. The 14 RNA samples tested were also isolated from GBS-infected monocytes. Primer set 7a is expected to produce an amplicon 171bp in size. Gel A shows the PCR results using primer set 7a on 0.1µg of RNA. Gel B shows the PCR results using primer set 7a on 0.01µg of RNA. The ladder used in both gels was the 1kb Plus DNA ladder (Invitrogen) with relevant sizes as indicated.

Very little DNA contamination is evident in the post-DNase-treated gel (FIGURE AP2.66). The DNase treatment efficiently degraded most of the DNA molecules present after the RNA extraction.

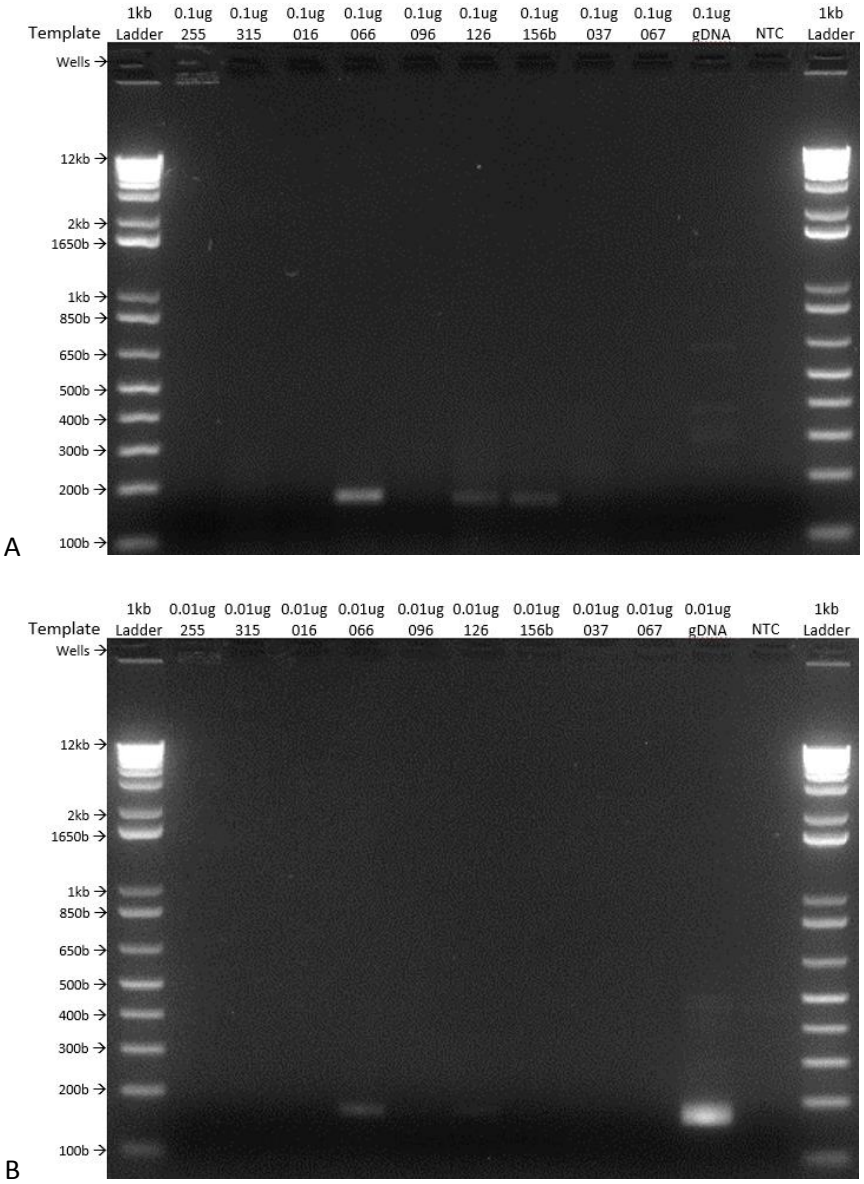

FIGURE AP2.66: Agarose gels testing the sensitivity of the GAPDH primer set 7a to detect human DNA contamination in RNA samples after being treated with DNase.

Nine RNA samples were tested for DNA contamination after being treated with DNase enzyme. Mixed gDNA (isolated from GBS-infected monocytes) was used as the positive control in both gels. The RNA samples tested were also isolated from GBS-infected monocytes. Primer set 7a is expected to produce an amplicon 171bp in size. Gel A shows the PCR results using primer set 7a on 0.1µg of RNA. Gel B shows the PCR results using primer set 7a on 0.01µg of RNA. The ladder used in both gels was the 1kb Plus DNA ladder (Invitrogen) with relevant sizes as indicated.

Interpretation

A primer pair was designed (7a) that successfully enabled specific and sensitive amplification of *GAPDH* from a template of DNA-contaminated RNA derived from GBS-infected U937 monocytes.

Using these newly designed primers, the infection RNA was revealed to have retained Human DNA contamination – requiring a further DNase treatment. Given the development and use of effective, sensitive *GAPDH* primers, it is now possible to conclude that the DNase enzyme in the Turbo DNAfree Kit efficiently purifies the infection RNA from residual DNA contamination.

Experiment 21: Upscaling the GBS-only Control

Unreliably low amounts of RNA were recovered from previous GBS-only attempts. Therefore the infection protocol for the GBS-only control was scaled up in an attempt to isolate higher numbers of GBS – and thereby more GBS-only RNA to provide a valid control for downstream applications.

584ml Infection

The established infection protocol was scaled up from 24ml in a single 6-well plate to 584ml in eight 175cm2 Corning cell culture flasks (a factor of 24.3). The same surface area/volume ratio used in the plates was applied to the flasks (73ml of infection per flask).

A variety of collection strategies and RNA isolation optimisations were attempted to increase the RNA yield using the TRIzol-chloroform RNA extraction method. Collection optimisations included increasing the collection centrifuge speed to 13,000g to ensure a larger, more stable pellet, altering the amount of TRIzol used to homogenize the cells, resuspending the pellets quickly in PBS to speed up processing time and mitigate pellet loss – followed by a 2 minute centrifuging before adding TRIzol to the pellet. RNA extraction optimisations included altering the amount of chloroform, adding ethanol washes, reducing the amount of water used to resuspend the RNA pellet – to increase RNA concentration, and removing the final heating stage to mitigate RNA degradation.

14 GBS-only samples were collected in TRIzol. Chloroform RNA preparations were performed on 12 of these samples.

Observations

Two of the preparations yielded good amounts of RNA (162.5 and 239.6ng/µl). However, these results could not be repeated. Two of the preparations yielded negative results. Six of the preparations yielded under 10ng/µl. The other two preparations yielded 16.1 and 26.7ng/µl.

Interpretation

Utilising established protocol, consistent yields of RNA could not be recovered from the GBS-only cells collected in TRIzol.

Experiment 22: RNA Preparations by Column Extraction

Given the failure of the TRIzol-chloroform method to yield consistently high enough amounts of GBS RNA from the GBS-controls, it was determined to change the RNA extraction method to a column extraction. The goal of this experiment was to further optimise the protocol to isolate sufficiently high amounts of GBS RNA from the assays.

Column RNA Isolation

RNA Column Extraction 1 – The GBS control assay was performed according to the established upscaled protocol (i.e. GBS in 584ml of sRPMI with 0.1% FBS). However, instead of homogenising the cells in TRIzol after the PBS wash, the cell pellet was quick-frozen on dry ice for 30 minutes, then stored at -80^{o}C. The Promega SV Total RNA Isolation System kit was used to column extract the GBS RNA. This kit incorporates and on-column DNase treatment. The cell pellet was thawed in ice before resuspension in 100µl RNase-free TE Buffer containing 30mg/ml Lysozyme. 100U of Mutanolysin was added to each resuspension before a 1 hour incubation at 37^{o}C. The remainder of the protocol was performed in accordance with the manufacturer's instructions. Elutions were performed with 100µl nuclease-free Ultrapure Distilled Water.

RNA Column Extraction 2: Column RNA Extraction 1 was repeated, but with the addition of a GBS overnight culture treatment to test the RNA extraction method on non-incubated GBS. 500µl of

washed GBS in bRPMI were centrifuged for 2 minutes at 13,000g were placed on ice after removing the supernatant (i.e. reflecting the final stage of cell collection in the incubation protocol). Pellets from the incubated sample and overnight culture were observed to be roughly the same size. Post-processing counts recovered 2.03E9 CFU/ml from the overnight culture and 1.25E9 CFU/ml from the incubated sample.

RNA Column Extraction 3 – Five conditions were tested; 1) a washed overnight culture of GBS, 2) a six hour incubation of GBS in PBS, 3) a six hour incubation of GBS in sRPMI with 0.1% FBS, 4) a six hour incubation of GBS in1.0% FBS, 5) a six hour incubation of GBS in 10% FBS. Treatments were scaled down to 250ml.

RNA Column Extraction 4 – Four treatments were tested, incubating GBS for six hours in sRPMI with 1% FBS; 190µl, 1.9ml, 19ml and 190ml. All samples were taken from the one, 250ml incubation treatment.

Observations

RNA Column Extraction 1 from the 584ml incubation in sRPMI with 0.1% FBS yielded only 5ng/µl RNA (0.5µg). In RNA column Extraction 2, 521ng/µl (52.1µg) RNA was isolated from the overnight culture pellet while only 15ng/µl (1.5µg) RNA was isolated from the cells after six hours incubation in the 0.1% FBS media.

TABLE AP2.01: RNA Column Extraction 3. Absorbance measures of RNA yield from GBS cells incubated under various media conditions.

Collection Conditions	**RNA concentration (ng/µl)**	**Total RNA (µg) - in 100µl**
Washed cells from Overnight Culture	49.0	4.9
Incubated 6 hours in PBS	2.4	0.2
Incubated 6 hours in sRPMI with 0.1% FBS	7.0	0.7
Incubated 6 hours in sRPMI with 1.0% FBS	105.3	10.5
Incubated 6 hours in sRPMI with 10.0% FBS	164.0	16.4

Increasing the FBS concentration in the media from 0.1% to 1% increased the RNA isolated by more than ten-fold.

TABLE AP2.02: RNA Column Extraction 4. Absorbance measures of RNA yield from varying numbers of GBS incubated in sRPMI with 1% FBS.

Treatment Volume	GBS (Total CFU)	Mean RNA concentration (ng/µl)	Total RNA (µg) - in 100µl
190µl	2.01E6	0.4	0.04
1.9ml	2.01E7	2.5	0.25
19ml	2.01E8	11.3	1.13
190ml	2.01E9	62.6	6.26

When plotting GBS CFU against RNA concentration (FIGURE AP2.67), RNA yields for 2.01E6 CFU GBS deviated from the trend line, and were both very low and highly variable between duplicate readings (0.1 to 0.7ng/µl) - and were therefore be considered uninformative noise. Readings Even though the RNA yields for GBS numbers ≥2.01E7 total CFU were low, the values sit on the trend line, and were therefore be considered representative; regardless of the scale. That is, it could be assumed that the RNA measured at this lower scale was of similar quality to that attained at from higher amounts of GBS.

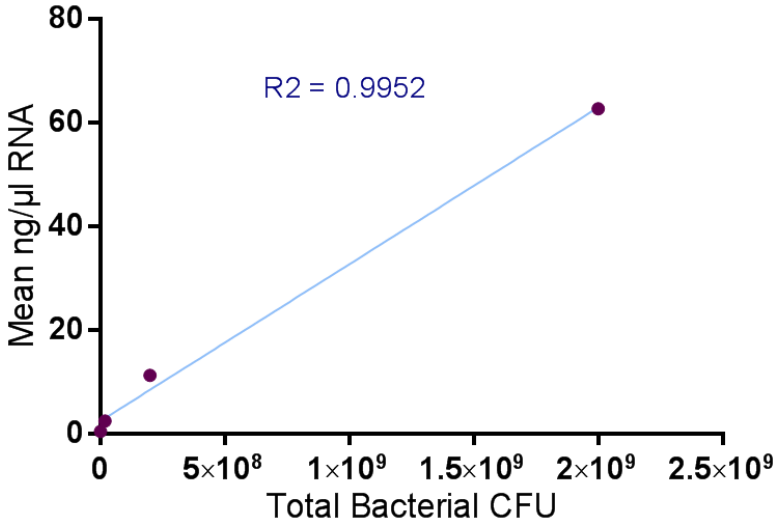

FIGURE AP2.67: RNA Column Extraction 4. Trend line demonstrating the correlation between cell numbers and RNA yield for 6-hour incubated, GBS-only treatment in sRPMI with 1% FBS.

Interpretation

Changing to a column extraction method did not increase DNA yield – even from the scaled up collections with vastly more GBS available for the RNA isolation. RNA Column Extraction 2 demonstrated that the method of column extraction is sound when performed on GBS from an overnight culture; i.e. those that haven't been undergone 6 hours of incubation in sRPMI with 0.1% FBS. This indicates that cells numbers are not the limiting factor to RNA yield, but rather some biological condition is interfering with transcription levels. Changing the incubation media to include 1% FBS from 0.1% promoted a substantial increase in transcription (as indicated by RNA yield). The previous media formulation was therefore too nutrient restrictive to serve as an incubation media for the infections and controls. RNA Column Extraction 4 demonstrated that RNA of sufficient quality and quantity can be isolated from at least 2.01E7 total CFU of GBS – despite lower RNA yields at this end of the scale.

Experiment 23: RNA Extraction, DNAse Treatment, cDNA Synthesis and preliminary RT-qPCR

Having established a protocol for the GBS control, the protocol needed to be tested for suitability for downstream applications such as RT-qPCR. This involves taking the GBS 874391 from overnight cultures, incubating them for six hours in the prescribed media formulation (sRPMI with 1% FBS) at 37^{o}C in 5% CO_2, collecting the GBS from the incubation, isolating the RNA from the cells, testing for and removing any DNA contamination, synthesising cDNA from the RNA, and amplifying specific GBS genes from the cDNA by RT-qPCR. The goal of this experiment was to demonstrate the viability of the optimised protocol for use on RNA derived from the GBS control and the infection assays for use with RT-qPCR.

RT-qPCR

Twelve samples of RNA were extracted from GBS-only incubated cells according to the established protocol - scaled to 7ml to ensure that at least 2.01E7 total GBS CFU were available for RNA

isolation. RNA samples were tested for DNA contamination using *spb1* primers and DNased if necessary using the Turbo DNAfree Kit (see Experiment 15). RNA quality was then analysed using an Experion RNA StdSens Reagents (BIO-RAD) and Experion RNA StdSens Chips (BIO-RAD) on an Experion Automated Electrophoresis Station (BIO RAD). A cDNA synthesis was performed on the RNA samples using the SuperScript III Reverse Transcriptase kit (Invitrogen) in accordance with the manufacturer's instructions. RNA going into the cDNA synthesis for all samples was normalised to the amount of RNA in the sample containing the lowest concentration of RNA.

RT-qPCR was performed in 96-well plates on a Lightcycler 480 II (Roche) in 20µl reactions (in triplicate) using the SensiFAST SYBR No-ROX kit (BIOLINE) in accordance with the manufacturer's instructions. The cDNA templates were diluted 1:5 before use. Ten-fold dilutions of a previous gDNA preparation of GBS 874391 were used as standards for the RT-qPCR (neat = 79.5ng/µl). Twelve GBS-specific genes were analysed for amplification by RT-qPCR.

TABLE AP2.03: The 12 GBS genes used in this study for RT-qPCR and their primers.

Locus Tag (Gene)	Designation	Primers (5' to 3')	Amplicon size (bp)	Function
CHF_00796 ***(cylE)***	cylE-2F	GGAAGTTACCCGATTGAGCA	114	Haemolysin Cytolysin promoter
	cylE-2R	TGCCAGGAGGAGAATAGGAA		
CHF17_00570 ***(rib)***	Rib-1F	AGGCGGCAATTATTTCACAC	113	Cell surface Protease resistance
	Rib-1R	ACTTGTCCATCAGGCTTCGT		
CHF17_01108	1010-1F	CACCGACAACTTCAGGGACT	125	Iron ABC transporter permease
	1010-1R	GCGATCCTAAAATGGCAAAA		
CHF17_00567 ***(czcD)***	czcD-1F	TCAATATCTGGTCAATGGATGG	114	Heavy Metal (zinc) importer
	czcD-1R	TAATGTTGGCAAATCGTTCG		
CHF17_01463-4 ***(pil2B)***	pil2B-2F	ATCGCTGTTAGTGGCGAGTT	116	Pilin gene cluster
	pil2B-2R	TAGGTTGCGCCTTTTTGAGT		
CHF17_01258 ***(cpsE)***	cpsE-1F	ATGGTGGACCGGCTATCTTT	137	Glycosal Transferase
	cpsE-1R	GCCCTGTCATTTGATTGTGA		
CHF17_01326 ***(scpB)***	scpB-1F	CACACGTGTCAGGGATCTTG	111	C5a Peptidase
	scpB-1R	ACAATTTCGACACGCATCAA		
CHF17_01323 ***(htp)***	1233-1F	TCCATGTCGTTCCGTATTCA	112	Cell surface Histidine Triad Protein
	1233-1F	CTCTTCATGCCCTGGCTTAG		
CHF17_02031 ***(cfb)***	cfb-1F	CTCTAGTGGCTGGTGCATTG	126	CAMP factor
	cfb-1R	AGCTTTTGAGCCATTTGCTG		
CHF17_00278 ***(rpoB)***	GBSrpoB-1F	TATCATGAGTGAGCGCCTTG	80	RNA Polymerase subunit beta
	GBSrpoB-1R	TATCACGCGTTTCAGATTCG		
CHF17_00002 ***(dnaN)***	GBSdnaN-1F	CAACAAGAAAGCCGTCCAAT	80	DNA Polymerase III subunit beta
	GBSdnaN-1R	TCTGTCGCAACAGCCTTAAA		
CHF17_02051 ***(hvgA)***	hvgA-3F	TTTGGAATGGTCAGGAAGGA	147	Cell surface Adhesin
	hvgA-3R	GCTGGTTTTGCAGCTTCTGT		

An infection sample (Sample M266 – "Mixed" sample No. 266 – see Chapter 4) was also tested for RT-qPCR amplification with GBS housekeeping genes *ropB* and *dnaN* to ensure that bacterial genes could be amplified from mixed cDNA samples.

Observations

TABLE AP2.04: Summary of RNA derived from 12 GBS-only samples.

Sample No.	Sample ID	GBS Cells CFU/ml	GBS Cells CFU in 6.8ml	RNA ng/µl	A260/280	Total RNA (µg) in 60ul
1	175A	2.26E7	1.54E8	21.9	2.10	1.3
2	175B	2.14E7	1.46E8	12.2	2.02	0.7
3	185A	1.80E7	1.26E8	19.5	2.00	1.8
4	185B	1.54E7	1.04E8	17.8	2.12	1.1
5	195A	1.80E7	1.22E8	15.0	1.94	0.9
6	195B	2.20E7	1.50E8	17.3	2.09	1.0
7	195C	2.54E7	1.73E8	20.8	1.96	1.24
8	195D	1.80E7	1.22E8	17.0	1.98	1.0
9	225A	2.20E7	1.50E8	18.2	1.88	1.1
10	225B	1.74E7	1.18E8	7.2	1.87	0.43
11	225C	2.94E7	2.00E8	9.8	1.79	0.59
12	225D	2.66E7	1.81E8	8.8	1.77	0.53

Using primers for the GBS gene *spb1* (FIGURE AP2.68) on GBS-only control samples, there was sufficient DNA contamination in 5 of the 12 samples to warrant subjecting them to a further DNase treatment (i.e. beyond the on-column DNase treatment performed during RNA isolation).

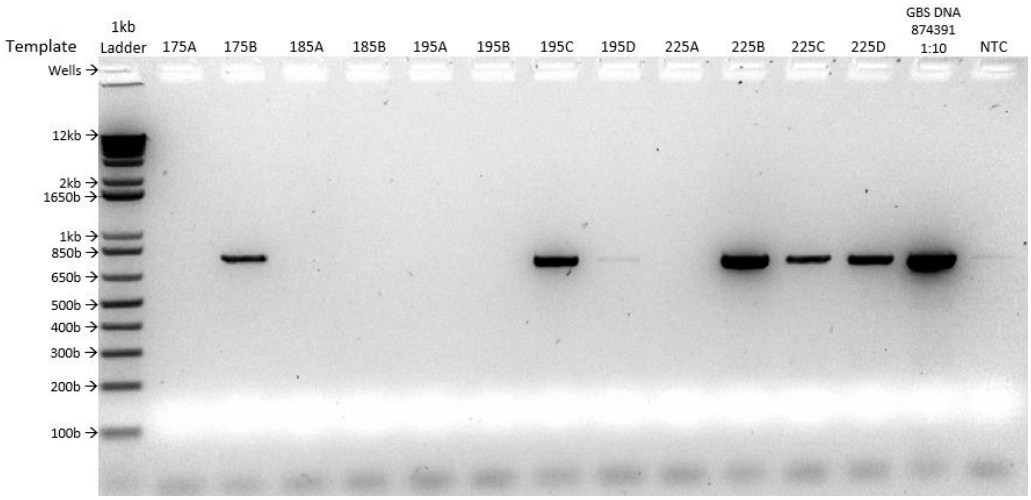

FIGURE AP2.68: Agarose gel showing spb1 DNA contamination test of 12 GBS-only RNA samples. *Gel shows the PCR-derived amplicon generated using the bacterial primer set spb1. The expected amplicon size for these primers is 762bp. The templates were 1X RNA samples derived from 12 GBS-only control (mock infection) samples. A 1:10 dilution of GBS 874391 served as the positive control. Clear spb1 amplicons indicating DNA contamination for 5 samples (175B, 195C, 225B. 225C and 225D). A light band indicating slight DNA contamination is also evident for sample 195D. The ladder used in both gels was the 1kb Plus DNA ladder (Invitrogen) with relevant sizes as indicated.*

The DNase enzyme effectively degraded the DNA beyond standard PCR detection (FIGURE AP2.69).

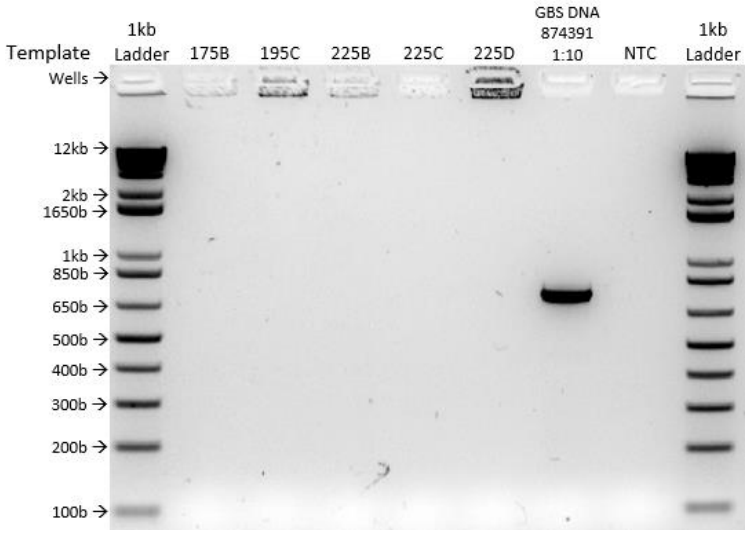

FIGURE AP2.69: Agarose gel showing DNA contamination test of 5 GBS-only RNA samples after undergoing DNase treatment.

Gel shows the PCR-derived amplicon generated using the bacterial primer set spb1. The expected amplicon size for these primers is 762bp. The templates were 1X RNA samples derived from 5 GBS-only control (mock infection) samples. Selected samples are those previously indicating clear DNA contamination (FIGURE AP2.68). A 1:10 dilution of GBS 874391 served as the positive control. The ladder used in both gels was the 1kb Plus DNA ladder (Invitrogen) with relevant sizes as indicated.

All GBS-only samples showed quality RNA in the Experion gel (FIGURE AP2.70) – as indicated by clean bands representing the higher concentrations of ribosomal RNA in each well. Samples that had undergone DNase treatment had lighter bands than the other samples – possibly indicating some RNA degradation.

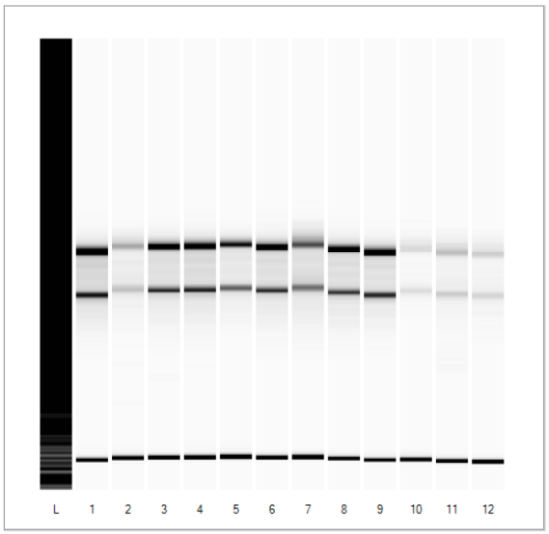

FIGURE AP2.70: Experion gel image showing prokaryotic ribosomal RNA.

Three clear bands on a relatively clean background for 12 GBS-only RNA samples demonstrating quality RNA. RAN subunits represented are 23S, 16S and 5S. The ladder failed for unknown reasons.

1:5 dilutions of cDNA template all amplified all 12 GBS genes trialled in the RT-qPCR runs in less than 35 cycles (FIGURE AP2.71).

A 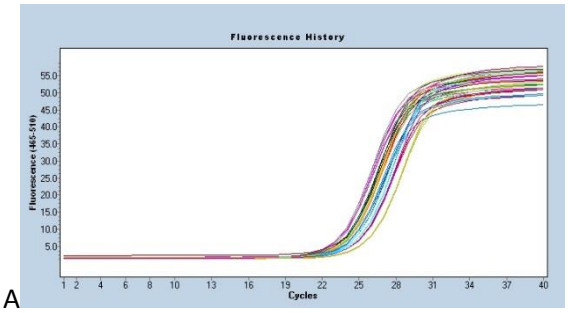

B 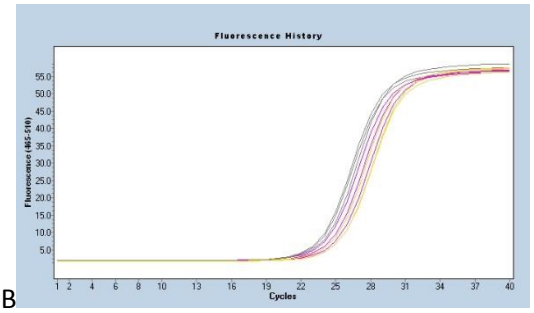

C 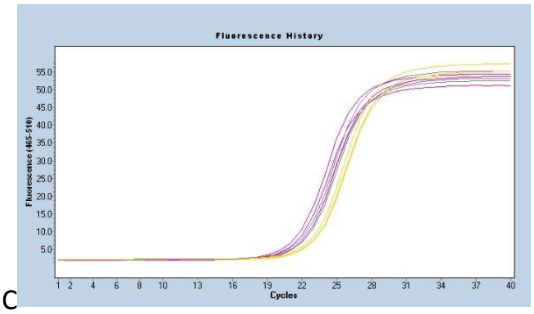

D 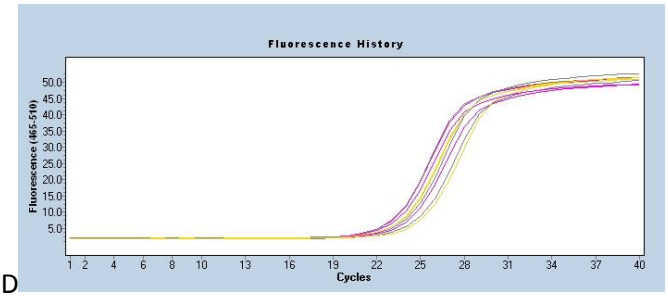

E 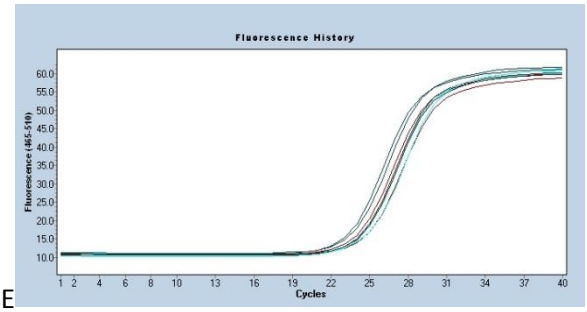

F 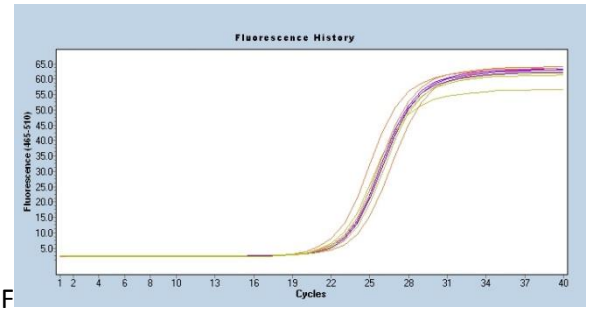

G 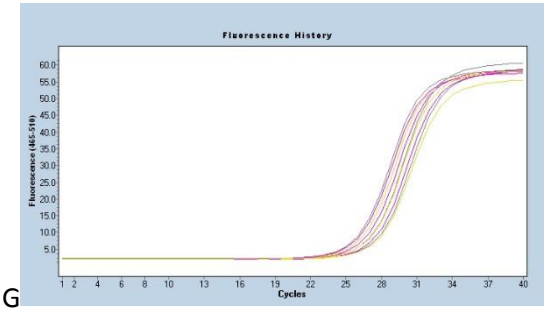

H 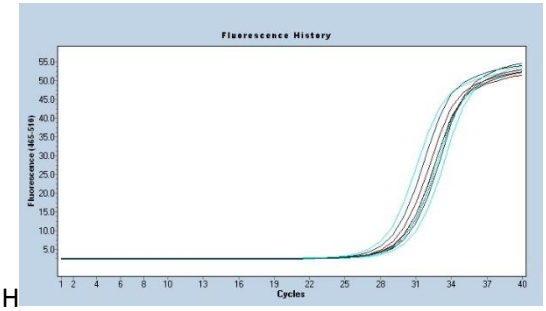

I 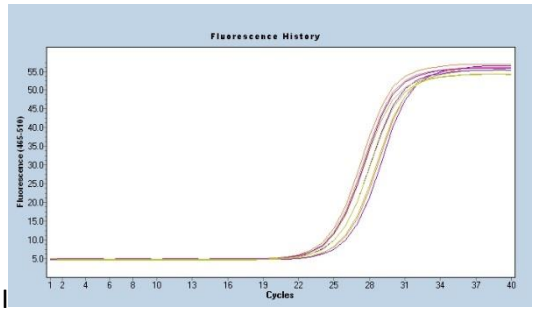

J 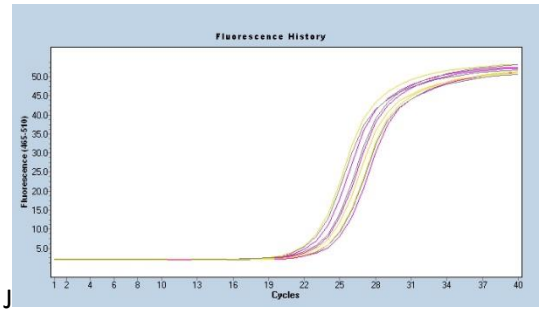

K 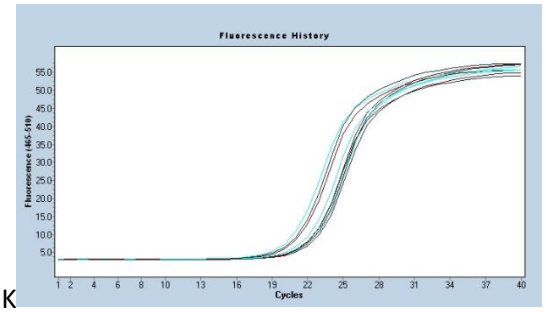

L 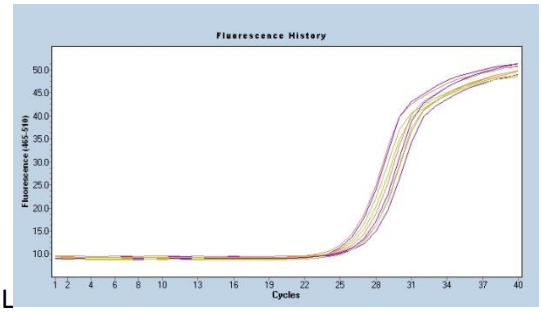

FIGURE AP2.71: RT-qPCR performed on GBS-only cDNA samples.

Images generated in Lightcycler 480 software. Genes: A cylE, B 1010, C rib, D czcD, E pil2B, F cpsE, G scpB, H htp, I cfb, J ropB, K dnaN, L hvgA.

Both housekeeping genes were amplified in the neat infection cDNA in less than 25 amplification cycles (FIGURE AP2.72).

A

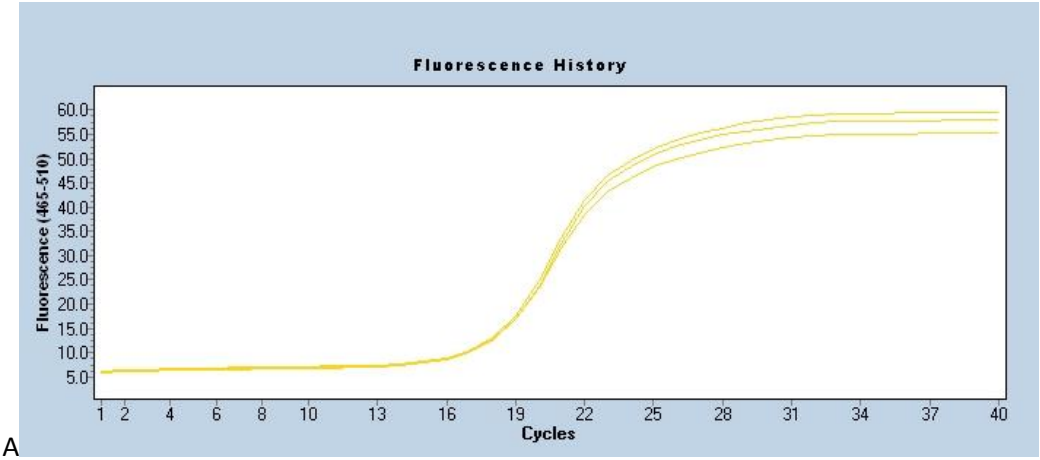

B

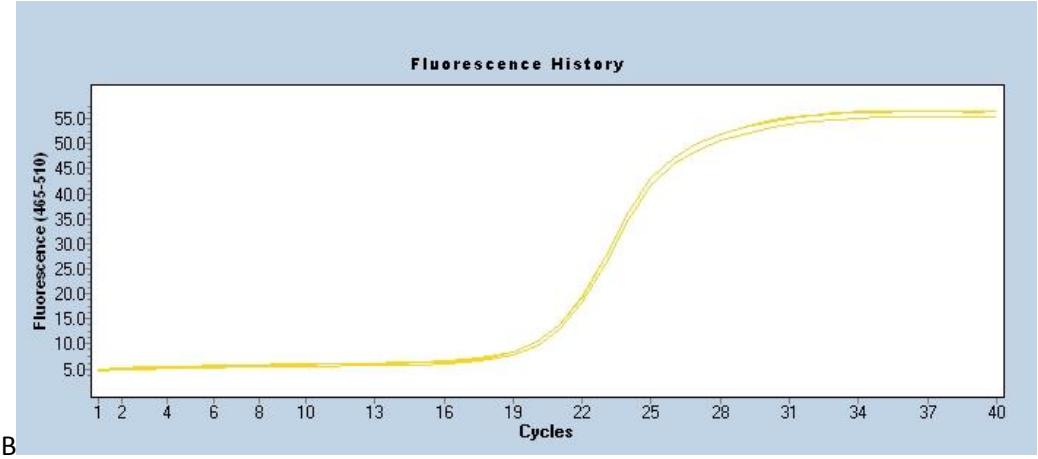

FIGURE AP2.72: RT-qPCR performed on a single sample of mixed cDNA amplifying GBS housekeeping genes.

Images generated by Lightcycler 480 software. Genes: A dnaN, B ropB.

Interpretation

The optimised protocol can be used to generate sufficient, high quality GBS RNA and cDNA from GBS-only controls and GBS-infected monocytes for successful RT-qPCR amplification of bacterial genes.

Experiment 24: Optimising RNA extraction from monocytes

In Chapter 3, a protocol was optimised to derive RNA from limited bacterial numbers (5.40E3 – 1.86E6 CFU/ml) for RT-qPCR amplification. The protocol included the addition of Mutanolysin (Sigma) to the RNA extraction digest for the purpose of breaking down the bacterial wall. As the bacteria from infections are presumed to be intracellular in monocytes, a non-chemical, mechanical means of eukaryotic cellular breakdown was tested to provide optimal access for the Mutanolysin to the bacterial calls during the digest.

Monocyte Bead Lysis

For the initial experiment, 50mg (1mg/10µl of reaction) of 425-600µM acid-washed glass beads (Sigma) were added to three 2ml nuclease-free, cap-lock tubes (Eppendorf). A fourth tube was also used for the no-treatment control. 10ml of U937 monocytes (from at least passage 5) were centrifuged at 300g for 5 minutes and resuspended in 2ml bRPMI. 500µl of the resuspended cells was aliquoted into the four 2ml tubes (three containing 50mg of beads). Note that this 500µl reflected approximately 1E6 monocytes and a scaling up of the RNA digest protocol by a factor of five (to account for the larger pellet in the monocyte-only and infection treatments). The non-treatment control tube was left on the bench at room temperature while the other three tube were bead-beaten on a Tissue Lyser II (QIAGEN) at 30bps for 10, 30 and 60 seconds respectively. Monocytes were then counted on a NucleoCounter NC-200 (Chemometec) for total (i.e. non-fragmented) cells.

Three subsequent experiments took an additional 5ml of passaged monocytes for an additional two treatments of bead-beating for 90 and 120 seconds.

Observations

Data for 4 independent experiments and summary statistics are found in Appendix 3, TABLES B and C.

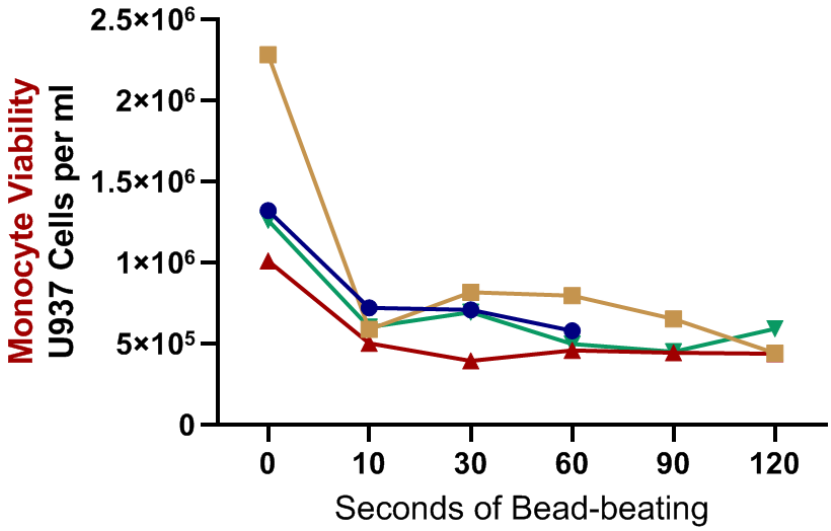

FIGURE AP2.73: U937 monocyte cell count data for viability estimates after bead-beating.
Data points are single viable monocyte readings derived for each bead-beating treatment on the NucleoCounter NC-200.

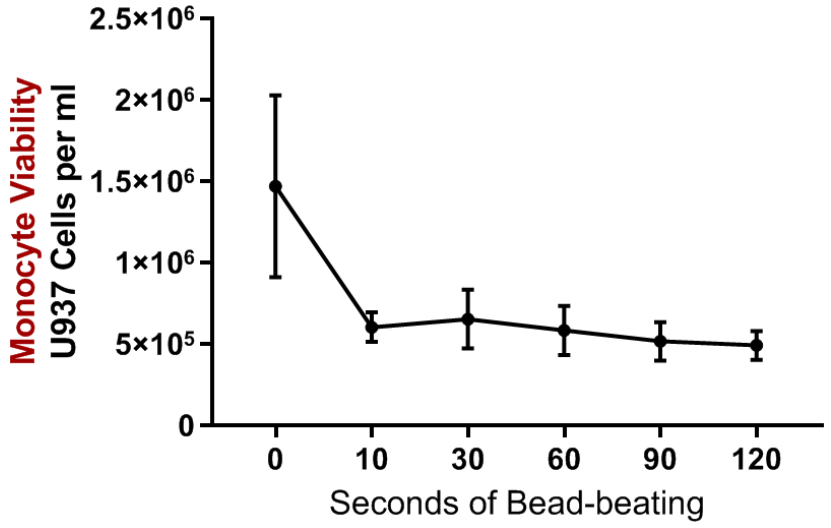

FIGURE AP2.74: Mean and standard deviation for cell count of viable monocyte across four independent bead-beating experiments.
Data points are means data from the 4 independent experiments represented in figure 4.01.

Regardless of how many monocytes went into the experiment, after 10 seconds of bead-beating, the concentration of viable (i.e. total counted) cells settled at or under 8E5 cells/ml – and did not decrease thereafter below 4E5 cells/ml.

Interpretation

Given that the total monocyte concentrations from the infections exceeds 2E6 cells/ml, a roughly 60-80% monocyte lysis rate can be expected from 10 seconds of bead beating. We also assume that many of the non-viable cells will likely be sufficiently lysed to permit Mutanolysin access to the bacteria. Furthermore, monocyte lysis is expected to occur as a result of the freeze-thaw between cell collection and RNA isolation. Therefore, 10 second of bead beating exerts minimal mechanical interference to the RNA isolation and provides optimal access of Mutanolysin to the internalised GBS bacteria.

Appendix 3 – Ancillary Information

Table A: GAPDH primers designed for this study to test infection-derived RNA for human DNA contamination.

Primer Designation	Sequence (5'-3')	Length (nt)	gDNA Amplicon length (bp)	GC%	Tm (°C)	Location on gene
Human_GAPDH-DWP-F1	CGTCATGGGTGTGAACCATGAG	22	525	54.6	61.5	2762..2783
Human_GAPDH-DWP-R1	GTAGAGGCAGGGATGATGTTCTGG	24	525	54.2	62.5	c3263..3286
Human_GAPDH-DWP-F2	CACCAGGGCTGCTTTTAACTCTGG	24	209	54.2	63.9	2114..2137
Human_GAPDH-DWP-R2	CAAGCTTCCCGTTCTCAGCCTTG	23	209	56.5	64.0	c2330..2352
Human_GAPDH-DWP-F3	GAAAAGAGCTAGGAAGGACAGG	22	537	50.0	58.1	1515..1536
Human_GAPDH-DWP-R3	CTCCTCCAGAATATGTGAGCAG	22	537	50.0	58.0	c2030..2051
Human_GAPDH-DWP-F4	CTTCATACCCTCACGTATTCCC	22	569	50.0	58.0	2254..2275
Human_GAPDH-DWP-R4	CCTTCCTCACCTGATGATCTTG	22	569	50.0	58.2	c2801..2822
Human_GAPDH-DWP-F5	GGTTTATGGAGGTCCTCTTGTG	22	543	50.0	58.4	1082..1103
Human_GAPDH-DWP-R5	CTACAAAAGGGACAGAGACTGG	22	543	50.0	58.1	c1603..1624
Human_GAPDH-DWP-F6	CTGGAAAAGAGCTAGGAAGGAC	22	534	50.0	58.1	1512..1533
Human_GAPDH-DWP-R6	CAGAATATGTGAGCAGCCCTAG	22	534	50.0	58.3	c2024..2045
Human_GAPDH-DWP-F7	GATGACATCAAGAAGGTGGTG	21	171	47.6	56.6	3420..3440
Human_GAPDH-DWP-Ra7	GGAAATGAGCTTGACAAAGTGG	22	171	45.5	58.1	c3569..3590
Human_GAPDH-DWP-Rb7	GAGCACAGGGTACTTTATTGATGG	24	543	45.8	59.4	c3939..3962
Human_GAPDH-LVH-F8	GTCCACTGGCGTCTTCACCA	20	636	60.0	62.4	2570..2589
Human_GAPDH-LVH-R8	GTGGCAGTGATGGCATGGAC	20	636	60.0	61.7	c3186..3205
Human_GAPDH-MBL-F9	GAAATGTGCTTTGGGGAGGCA	21	247	52.4	61.4	2409..2429
Human_GAPDH-MBL-R9	TTTGCAGGGCTGAGTCAGCTTC	22	247	54.6	63.3	c2634..2655

TABLE B: Monocyte cell viability after bead-beating.

Experiment	Cells	Control	10 second bead-beat	30 second bead-beat	60 second bead-beat	90 second bead-beat	120 second bead-beat
1	**Viable**	**1.22E6**	**5.44E5**	**4.05E5**	**2.46E5**	n/a	n/a
	Viability %	92.5%	75.6%	57.4%	42.4%	n/a	n/a
	non-Viable	9.88E4	1.70E5	3.01E5	3.34E5	n/a	n/a
	Total	**1.32E6**	**7.20E5**	**7.07E5**	**5.79E5**	n/a	n/a
2	**Viable**	**2.15E6**	**2.97E5**	**1.53E5**	**1.05E5**	**2.10E5**	**1.32E5**
	Viability %	94.3%	50.7%	18.8%	13.2%	32.2%	29.9%
	non-Viable	1.31E5	2.88E5	6.62E5	6.90E5	4.41E5	3.09E5
	Total	**2.28E6**	**5.86E5**	**8.15E5**	**7.95E5**	**6.51E5**	**4.41E6**
3	**Viable**	**9.57E5**	**3.54E5**	**2.03E5**	**2.97E5**	**2.53E5**	**2.35E5**
	Viability %	94.6%	70.5%	51.7%	65.8%	57.1%	53.8%
	non-Viable	5.43E4	1.48E5	1.90E5	1.54E5	1.90E5	2.02E5
	Total	**1.01E6**	**5.02E5**	**3.93E5**	**4.57E5**	**4.43E5**	**4.37E5**
4	**Viable**	**1.20E6**	**4.01E5**	**4.83E5**	**2.61E5**	**2.48E5**	**3.57E5**
	Viability %	95.3%	66.8%	69.7%	52.6%	55.2%	60.5%
	non-Viable	5.97E4	1.99E5	2.10E5	2.35E5	2.02E5	2.33E5
	Total	**1.26E6**	**6.00E5**	**6.93E5**	**4.96E5**	**4.50E5**	**5.91E5**

TABLE C: Summary statistics of 4 bead-beating experiments (i.e. summary data from TABLE B).

10 second beat (n=4)		30 second beat (n=4)		60 second beat (n=4)		90 second beat (n=3)		120 second beat (n=3)	
Mean	**SD**	**Mean**	**SD**	**Mean**	**SD**	**Mean**	**SD**	**Mean**	**SD**
602,000	89,785	652,000	181,067	581,750	150,995	514,667	118,120	489,667	87,780
6.0E5	9.0E4	6.5E5	1.8E5	5.8E5	1.5E5	5.1E5	1.2E5	4.9E5	8.8E4

TABLE D: Cell collection data from infection model optimisations.

No.	Collection Type	Designation	Viable Monocytes cells/ml	Bacterial CFU/ml	Volume (ml)	Total Viable Monocytes	Total Bacterial CFU
01	GBS-only	G175A		2.26E7	6.8ml		**1.54E8**
02	GBS-only	G175B		2.14E7	6.8ml		**1.46E8**
03	GBS-only	G185A		1.86E7	6.8ml		**1.26E8**
04	GBS-only	G185B		1.54E7	6.8ml		**1.04E8**
05	GBS-only	G195A		1.80E7	6.8ml		**1.22E8**
06	GBS-only	G195B		2.20E7	6.8ml		**1.50E8**
07	GBS-only	G195C		2.54E7	6.8ml		**1.73E8**
08	GBS-only	G195D		1.80E7	6.8ml		**1.22E8**
09	GBS-only	G225A		2.20E7	6.8ml		**1.50E8**
10	GBS-only	G225B		1.74E7	6.8ml		**1.18E8**
11	GBS-only	G225C		2.94E7	6.8ml		**2.00E8**
12	GBS-only	G225D		2.66E7	6.8ml		**1.81E8**
13	Mixed	M266	2.33E6	1.80E6	22.9ml	**5.34E7**	**4.10E7**
14	Mixed	M286	1.75E6	unknown	22.9ml	**4.00E7**	unknown
15	Mixed	M296	2.00E6	1.20E6	22.9ml	**4.58E7**	**2.74E7**
16	Mixed	M306	2.30E6	1.27E6	22.9ml	**5.27E7**	**2.90E7**
17	U937-only	U237A1	2.93E6		7.5ml	**2.20E7**	
18	U937-only	U237A2	3.51E6		7.5ml	**2.62E7**	
19	U937-only	U237A3	2.68E6		7.5ml	**2.01E7**	
20	U937-only	U247B1	3.38E6		7.5ml	**2.54E7**	
21	U937-only	U247B2	3.02E6		7.5ml	**2.27E7**	
22	U937-only	U247B3	2.82E6		7.5ml	**2.11E7**	

TABLE E: RNA isolation, quantification and cDNA synthesis data from infection model optimisations.

Sample	Combined Elutions (ng/µl)	Elution Volume (µl)	Total RNA (µg)	260/280	260/230	Turbo DNased	cDNA Synthesis
G175A	21.9	60	**1.3**	2.10	0.99	-	
G175B	12.2	60	**0.7**	2.02	0.75	17µl	172.8ng
G185A	19.5	60	**1.8**	2.00	0.68	-	172.8ng
G185B	17.8	60	**1.1**	2.12	0.81	-	172.8ng
G195A	15.0	60	**0.9**	1.94	0.78	-	172.8ng
G195B	17.3	60	**1.0**	2.09	0.46	-	172.8ng
G195C	20.8	60	**1.24**	1.96	0.86	17µl	172.8ng
G195D	17.0	60	**1.0**	1.98	0.75	-	172.8ng
G225A	18.2	60	**1.1**	1.88	1.17	-	172.8ng
G225B	7.2	60	**0.43**	1.87	0.44	16µl	172.8ng
G225C	9.8	60	**0.59**	1.79	0.70	17µl	172.8ng
G225D	8.8	60	**0.53**	1.77	0.42	18µl	172.8ng
M266	399.1	1000	**399.1**	2.07	2.17	100µl	5µg
M286	212.2	1000	**212.2**	2.02	2.11	100µl	5µg
M296	484.8	1000	**484.8**	2.05	2.18	100µl	5µg
M306	508.5	1000	**508.5**	2.06	2.18	100µl	5µg
U237A1	383.7	400	**153.5**	2.05	1.99	100µl	5µg
U237A2	393.5	400	**158.2**	2.04	2.08	100µl	5µg
U237A3	670.9	300	**201.3**	2.06	2.13	100µl	5µg
U247B1	352.6	400	**141.0**	2.04	2.18	100µl	5µg
U247B2	615.6	300	**184.7**	2.04	2.17	100µl	5µg
U247B3	625.8	300	**187.7**	2.05	2.11	100µl	5µg

TABLE F: Results Summary generated by Quantstudio Real-Time PCR Software for dnaN amplification of various cDNA dilutions from 4 infection samples.

Results Summary

Sample	Target	CT (Mean)	CT (Std Dev)	Normalized Qty (Mean)	Normalized Qty (Std Err)	RQ	RQ (Min)	RQ (Max)
M266_1:10 *	dnaN †	20.085	0.174					
M266_1:20	dnaN †	21.038	0.084					
M266_1:40	dnaN †	22.288	0.167					
M266_1:80	dnaN †	22.953	0.054					
M286_1:20	dnaN †	23.666	0.142					
M286_1:40	dnaN †	24.705	0.228					
M286_1:80	dnaN †	25.167	0.243					
M286__1:10	dnaN †	23.774	0.592					
M296_1:10	dnaN †	20.382	0.343					
M296_1:20	dnaN †	20.622	0.178					
M296_1:40	dnaN †	21.070	0.077					
M296_1:80	dnaN †	22.301	0.401					
M306_1:10	dnaN †	21.116	0.066					
M306_1:20	dnaN †	20.409	0.255					
M306_1:40	dnaN †	21.344	0.511					
M306_1:80	dnaN †	21.731	0.297					
NTC	dnaN †							

Notes:

(*) denotes Calibrator

(†) denotes Endogenous Control

TABLE G: Results Summary generated by Quantstudio Real-Time PCR Software for cylE amplification of various cDNA dilutions from 4 infection samples and 2 GBS-only samples.

Results Summary

Sample	Target	C_T (Mean)	C_T (Std Dev)	Normalized Qty (Mean)	Normalized Qty (Std Err)	RQ	RQ (Min)	RQ (Max)
G175A 1:10	cylE †	24.196	0.230					
G175A 1:20	cylE †	24.930	0.053					
G175A 1:40	cylE †	25.776	0.088					
G175A 1:80	cylE †	26.547	0.054					
G175B 1:10	cylE †	25.057	0.088					
G175B 1:20	cylE †	25.989	0.051					
G175B 1:40	cylE †	26.634	0.076					
G175B 1:80	cylE †	27.606	0.231					
M266 1:10 *	cylE †	22.322	0.061					
M266 1:20	cylE †	22.829	0.017					
M266 1:40	cylE †	23.918	0.049					
M266 1:80	cylE †	25.338	0.225					
M286 1:10	cylE †	25.003	0.015					
M286 1:20	cylE †	25.855	0.099					
M286 1:40	cylE †	26.463	0.041					
M286 1:80	cylE †	26.981	0.121					
M296 1:10	cylE †	23.361	0.019					
M296 1:20	cylE †	23.979	0.113					
M296 1:40	cylE †	24.076	0.021					
M296 1:80	cylE †	24.764	0.090					
M306 1:10	cylE †	23.462	0.063					
M306 1:20	cylE †	23.765	0.021					
M306 1:40	cylE †	24.341	0.077					
M306 1:80	cylE †	24.153	0.113					
NTC	cylE †							

Notes:

(*) denotes Calibrator

(†) denotes Endogenous Control

TABLE H: Results Summary tables generated by Quantstudio Real-Time PCR Software for all human genes over 5 separate runs of qPCR.

Results Summary

Sample	Target	CT (Mean)	CT (Std Dev)	Normalized Qty (Mean)	Normalized Qty (Std Err)	RQ	RQ (Min)	RQ (Max)
M266 *	ACTB †	23.949	0.082					
M286	ACTB †	21.817	0.161					
M296	ACTB †	22.821	0.065					
M306	ACTB †	22.603	0.144					
NTC	ACTB †							
U237A1	ACTB †	21.517	0.224					
U237A2	ACTB †	21.185	0.047					
U237A3	ACTB †	21.967	0.108					
U247B1	ACTB †	21.051	0.097					
U247B2	ACTB †	22.123	0.044					
U247B3	ACTB †	23.300	0.076					
M266 *	GAPDH	25.637	0.084			1.000	0.894	1.118
M286	GAPDH	23.201	0.154			1.074	0.869	1.328
M296	GAPDH	24.656	0.076			0.826	0.751	0.908
M306	GAPDH	24.783	0.058			0.630	0.540	0.734
NTC	GAPDH							
U237A1	GAPDH	23.656	0.141			0.600	0.464	0.777
U237A2	GAPDH	22.981	0.065			0.756	0.701	0.815
U237A3	GAPDH	23.436	0.150			1.019	0.857	1.212
U247B1	GAPDH	23.084	0.084			0.628	0.555	0.710
U247B2	GAPDH	23.346	0.073			1.237	1.143	1.340
U247B3	GAPDH	24.281	0.090			1.612	1.442	1.802
M266 *	IL1A	35.876						
M286	IL1A	34.594	2.830					
M296	IL1A	30.779	0.975			3.403	2.053	5.641
M306	IL1A	36.437				0.264		

Notes:

(*) denotes Calibrator

(†) denotes Endogenous Control

Sample	Target	CT (Mean)	CT (Std Dev)	Normalized Qty (Mean)	Normalized Qty (Std Err)	RQ	RQ (Min)	RQ (Max)
NTC	IL1A							
U237A1	IL1A	36.234	2.404			0.119	0.034	0.418
U237A2	IL1A	36.964	2.007			0.067	0.024	0.188
U237A3	IL1A	33.373						
U247B1	IL1A	32.320						
U247B2	IL1A	37.308				0.124		
U247B3	IL1A	38.511	1.837			0.195	0.043	0.889
M266 *	IL1B	30.171	0.451			1.000	0.675	1.482
M286	IL1B	27.879	0.150			0.873	0.711	1.073
M296	IL1B	29.858	0.289			0.497	0.385	0.641
M306	IL1B	29.575	0.299			0.507	0.378	0.680
NTC	IL1B							
U237A1	IL1B	30.265	0.467			0.129	0.082	0.204
U237A2	IL1B	29.795	0.244			0.137	0.111	0.170
U237A3	IL1B	30.562	0.432			0.152	0.096	0.241
U247B1	IL1B	29.649	0.636			0.136	0.078	0.236
U247B2	IL1B	30.186	0.503			0.224	0.146	0.345
U247B3	IL1B							
M266 *	IL6	35.499	1.733					
M286	IL6	32.901	1.558			1.596	0.223	11.413
M296	IL6	33.696	2.925			1.841	0.046	73.070
M306	IL6	28.875	5.558			91.863	0.009	957,819.062
NTC	IL6							
U237A1	IL6	35.928				0.096		
U237A2	IL6							
U237A3	IL6							
U247B1	IL6							

Notes:

(*) denotes Calibrator

(†) denotes Endogenous Control

Sample	Target	CT (Mean)	CT (Std Dev)	Normalized Qty (Mean)	Normalized Qty (Std Err)	RQ	RQ (Min)	RQ (Max)
U247B2	IL6	38.115						
U247B3	IL6	33.351				3.643		
M266 *	IL8	24.789	0.102			1.000	0.879	1.138
M286	IL8	21.746	0.250			2.065	1.537	2.773
M296	IL8	23.922	0.268			0.805	0.613	1.057
M306	IL8	24.397	0.127			0.460	0.380	0.556
NTC	IL8							
U237A1	IL8	31.650	1.149			0.001	0.000	0.002
U237A2	IL8	30.735	0.434			0.001	0.001	0.001
U237A3	IL8	31.341	0.381			0.001	0.001	0.001
U247B1	IL8	30.154	0.436			0.001	0.001	0.002
U247B2	IL8	31.129	0.545			0.001	0.001	0.003
U247B3	IL8	31.823	1.410			0.002	0.000	0.008

Notes:

(*) denotes Calibrator

(†) denotes Endogenous Control

Results Summary

Sample	Target	CT (Mean)	CT (Std Dev)	Normalized Qty (Mean)	Normalized Qty (Std Err)	RQ	RQ (Min)	RQ (Max)
M266 *	ACTB	23.482	0.147			1.000	0.009	115.444
M286	ACTB	21.355	0.219			0.045	0.006	0.357
M296	ACTB	21.654	0.114			0.923	0.324	2.631
M306	ACTB	18.767	0.487			0.000	0.000	0.000
NTC	ACTB							
U237A1	ACTB	21.438	0.061			0.329	0.016	6.939
U237A2	ACTB	21.354	0.269			2.588	1.283	5.221
U237A3	ACTB	21.974	0.012			29.755	0.005	196,247.531
U247B1	ACTB	21.163	0.123			3.400	1.531	7.549
U247B2	ACTB	22.148	0.073			0.263	0.003	26.984
U247B3	ACTB	23.460	0.119					
M266 *	GAPDH	23.220	0.154			1.000	0.009	115.251
M286	GAPDH	21.257	0.228			0.022	0.003	0.172
M296	GAPDH	21.710	0.120			0.435	0.153	1.236
M306	GAPDH	23.872	0.344			0.000	0.000	0.000
NTC	GAPDH							
U237A1	GAPDH	21.728	0.046			0.123	0.006	2.594
U237A2	GAPDH	21.389	0.173			1.139	0.603	2.152
U237A3	GAPDH	21.746	0.120			18.913	0.003	124,826.188
U247B1	GAPDH	21.398	0.150			1.225	0.554	2.709
U247B2	GAPDH	21.460	0.145			0.246	0.002	25.252
U247B3	GAPDH	22.740	0.130					
M266 *	IL10 †	34.187	1.525					
M286	IL10 †	31.684	0.796					
M296	IL10 †	33.264	0.405					

Notes:

(*) denotes Calibrator

(†) denotes Endogenous Control

Sample	Target	CT (Mean)	CT (Std Dev)	Normalized Qty (Mean)	Normalized Qty (Std Err)	RQ	RQ (Min)	RQ (Max)
M306	IL10 †	20.629	1.284					
NTC	IL10 †							
U237A1	IL10 †	32.668	0.740					
U237A2	IL10 †	33.611	0.241					
U237A3	IL10 †	35.075	2.826					
U247B1	IL10 †	33.649	0.251					
U247B2	IL10 †	32.905	1.124					
U247B3	IL10 †							
M266 *	IL12A	32.441	0.900			1.000	0.007	135.121
M286	IL12A	32.608	0.919			0.004	0.000	0.047
M296	IL12A	33.496	0.055			0.046	0.016	0.138
M306	IL12A	26.128	0.234			0.000	0.000	0.000
NTC	IL12A							
U237A1	IL12A	31.990	1.273			0.067	0.002	2.454
U237A2	IL12A	31.991	1.162			0.486	0.093	2.540
U237A3	IL12A	32.932	0.770			3.795	0.001	26,698.229
U247B1	IL12A	31.333	0.886			1.070	0.249	4.587
U247B2	IL12A	32.102	1.706			0.098	0.000	19.408
U247B3	IL12A	33.465	0.103					
M266 *	IL12B	37.460				1.000		
M286	IL12B	36.416	4.572					
M296	IL12B	36.222	3.504					
M306	IL12B	20.190	0.584			0.000	0.000	0.000
NTC	IL12B							
U237A1	IL12B							
U237A2	IL12B							
U237A3	IL12B	33.687						

Notes:

(*) denotes Calibrator

(†) denotes Endogenous Control

Sample	Target	CT (Mean)	CT (Std Dev)	Normalized Qty (Mean)	Normalized Qty (Std Err)	RQ	RQ (Min)	RQ (Max)
U247B1	IL12B							
U247B2	IL12B	38.433				0.028		
U247B3	IL12B							
M266 *	IL17	32.477	2.975					
M286	IL17							
M296	IL17	38.341						
M306	IL17	22.507	4.234			0.037	0.000	25,673.635
NTC	IL17							
U237A1	IL17	33.779						
U237A2	IL17	37.022						
U237A3	IL17							
U247B1	IL17	34.770	6.869			0.001	0.000	83,153,116,987,392.000
U247B2	IL17							
U247B3	IL17	20.163	19.912					

Notes:

(*) denotes Calibrator

(†) denotes Endogenous Control

Results Summary

Sample	Target	CT (Mean)	CT (Std Dev)	Normalized Qty (Mean)	Normalized Qty (Std Err)	RQ	RQ (Min)	RQ (Max)
M266 *	ACTB	22.409	0.187			1.000	0.664	1.506
M286	ACTB	21.516	0.151			0.371	0.301	0.456
M296	ACTB	21.710	0.379			1.184	0.823	1.702
M306	ACTB	21.690	0.126			0.677	0.535	0.855
NTC	ACTB							
U237A1	ACTB	21.852	0.090			2.925	1.670	5.122
U237A2	ACTB	21.810	0.062			1.450	1.177	1.787
U237A3	ACTB	22.049	0.088			4.798	3.557	6.471
U247B1	ACTB	21.425	0.116			1.785	1.276	2.497
U247B2	ACTB	22.512	0.136			2.819	1.552	5.121
U247B3	ACTB	23.585	0.102			2.021	1.521	2.684
M266 *	CXCL1	36.637				1.000		
M286	CXCL1	37.584	4.853			0.131	0.008	2.034
M296	CXCL1	43.883	0.959					
M306	CXCL1	43.665	0.583			0.016	0.010	0.026
NTC	CXCL1							
U237A1	CXCL1	44.656	0.171					
U237A2	CXCL1							
U237A3	CXCL1	40.132	5.380			0.752	0.036	15.838
U247B1	CXCL1	36.947						
U247B2	CXCL1	44.032				0.100		
U247B3	CXCL1	36.572				4.603		
M266 *	GAPDH	22.470	0.146			1.000	0.672	1.487
M286	GAPDH	21.300	0.250			0.434	0.335	0.562
M296	GAPDH	22.026	0.328			0.986	0.716	1.356
M306	GAPDH	22.153	0.119			0.512	0.407	0.644

Notes:

(*) denotes Calibrator

(†) denotes Endogenous Control

Sample	Target	CT (Mean)	CT (Std Dev)	Normalized Qty (Mean)	Normalized Qty (Std Err)	RQ	RQ (Min)	RQ (Max)
NTC	GAPDH							
U237A1	GAPDH	22.269	0.154			2.289	1.296	4.044
U237A2	GAPDH	21.828	0.080			1.469	1.188	1.816
U237A3	GAPDH	22.086	0.190			4.832	3.484	6.703
U247B1	GAPDH	21.658	0.145			1.558	1.107	2.193
U247B2	GAPDH	21.857	0.121			4.503	2.485	8.159
U247B3	GAPDH	22.894	0.112			3.392	2.549	4.513
M266 *	LMO2	27.894	0.276			1.000	0.639	1.565
M286	LMO2	26.844	0.228			0.424	0.328	0.548
M296	LMO2	27.244	0.111			1.166	0.948	1.435
M306	LMO2	27.231	0.207			0.664	0.504	0.874
NTC	LMO2							
U237A1	LMO2	28.921	0.723			0.977	0.425	2.247
U237A2	LMO2	27.999	0.254			0.899	0.668	1.211
U237A3	LMO2	29.057	0.124			1.663	1.221	2.266
U247B1	LMO2	27.849	0.222			0.948	0.653	1.379
U247B2	LMO2	28.288	0.289			2.292	1.212	4.333
U247B3	LMO2	29.715	0.531			1.244	0.718	2.155
M266 *	MCP-1 †	29.001	0.406					
M286	MCP-1 †	26.917	0.176					
M296	MCP-1 †	28.605	0.197					
M306	MCP-1 †	27.857	0.224					
NTC	MCP-1 †							
U237A1	MCP-1 †	29.913	0.593					
U237A2	MCP-1 †	28.959	0.216					
U237A3	MCP-1 †	30.734	0.310					
U247B1	MCP-1 †	28.891	0.344					
U247B2	MCP-1 †	30.447	0.626					

Notes:

(*) denotes Calibrator

(†) denotes Endogenous Control

Sample	Target	CT (Mean)	CT (Std Dev)	Normalized Qty (Mean)	Normalized Qty (Std Err)	RQ	RQ (Min)	RQ (Max)
U247B3	MCP-1 †	30.957	0.238					
M266 *	TNF	28.148	0.057			1.000	0.683	1.465
M286	TNF	28.047	0.092			0.215	0.180	0.257
M296	TNF	29.078	0.255			0.427	0.329	0.554
M306	TNF	28.324	0.122			0.376	0.299	0.471
NTC	TNF							
U237A1	TNF	31.220	0.505			0.329	0.169	0.638
U237A2	TNF	31.431	0.408			0.140	0.098	0.200
U237A3	TNF	30.807	0.106			0.786	0.582	1.061
U247B1	TNF	30.810	0.552			0.192	0.115	0.320
U247B2	TNF	31.359	0.332			0.456	0.242	0.858
U247B3	TNF	31.918	0.606			0.484	0.255	0.921

Notes:

(*) denotes Calibrator

(†) denotes Endogenous Control

Results Summary

Sample	Target	CT (Mean)	CT (Std Dev)	Normalized Qty (Mean)	Normalized Qty (Std Err)	RQ	RQ (Min)	RQ (Max)
M266 *	ACTB	22.791	0.108			1.000		
M286	ACTB	21.729	0.222			1.088	0.754	1.571
M296	ACTB	21.845	0.147			3.083	1.679	5.661
M306	ACTB	21.793	0.083			1.660	1.529	1.802
NTC	ACTB							
U237A1	ACTB	21.503	0.097			3.884	2.889	5.221
U237A2	ACTB	21.585	0.129			3.583	2.507	5.121
U237A3	ACTB	21.905	0.139			5.152	1.436	18.486
U247B1	ACTB	21.402	0.114			2.476	1.326	4.624
U247B2	ACTB	22.304	0.161			1.882	1.220	2.902
U247B3	ACTB	23.270	0.076			0.762		
M266 *	GAPDH	22.575	0.176			1.000		
M286	GAPDH	21.236	0.299			1.332	0.888	1.998
M296	GAPDH	21.991	0.127			2.432	1.329	4.449
M306	GAPDH	22.104	0.129			1.170	1.037	1.320
NTC	GAPDH							
U237A1	GAPDH	21.897	0.188			2.594	1.868	3.602
U237A2	GAPDH	21.555	0.142			3.198	2.226	4.594
U237A3	GAPDH	21.797	0.133			4.832	1.347	17.333
U247B1	GAPDH	21.507	0.241			2.018	1.051	3.875
U247B2	GAPDH	21.621	0.153			2.607	1.694	4.013
U247B3	GAPDH	22.488	0.167			1.117		
M266 *	IL10 †	34.571						
M286	IL10 †	33.476	0.451					
M296	IL10 †							
M306	IL10 †	34.283	0.046					

Notes:

(*) denotes Calibrator

(†) denotes Endogenous Control

Sample	Target	CT (Mean)	CT (Std Dev)	Normalized Qty (Mean)	Normalized Qty (Std Err)	RQ	RQ (Min)	RQ (Max)
NTC	IL10 †							
U237A1	IL10 †	35.417	0.331					
U237A2	IL10 †							
U237A3	IL10 †	36.377	1.802					
U247B1	IL10 †	34.519	0.720					
U247B2	IL10 †	35.098	0.358					
U247B3	IL10 †							
M266 *	IL12A	35.021	0.744			1.000		
M286	IL12A	34.114	0.804			1.085	0.470	2.504
M296	IL12A	35.545	1.364			1.080	0.218	5.357
M306	IL12A	44.374	0.030			0.001	0.001	0.001
NTC	IL12A							
U237A1	IL12A	34.403	0.346			2.649	1.554	4.515
U237A2	IL12A	34.639	0.433			2.146	1.202	3.834
U237A3	IL12A	35.718	0.731			1.640	0.336	8.006
U247B1	IL12A	34.290	1.268			1.725	0.416	7.153
U247B2	IL12A	34.265	0.519			2.457	1.017	5.938
U247B3	IL12A	35.429	0.521			0.764		
M266 *	IL12B							
M286	IL12B	34.826						
M296	IL12B	35.833	1.322					
M306	IL12B	38.764	5.549					
NTC	IL12B							
U237A1	IL12B							
U237A2	IL12B							
U237A3	IL12B							
U247B1	IL12B	44.240						
U247B2	IL12B	35.835	1.889					

Notes:

(*) denotes Calibrator

(†) denotes Endogenous Control

Sample	Target	CT (Mean)	CT (Std Dev)	Normalized Qty (Mean)	Normalized Qty (Std Err)	RQ	RQ (Min)	RQ (Max)
U247B3	IL12B							
M266 *	IL17	32.249						
M286	IL17							
M296	IL17	39.427						
M306	IL17	38.836						
NTC	IL17							
U237A1	IL17	38.091	2.186					
U237A2	IL17	41.390						
U237A3	IL17	38.895	4.734			0.007	0.000	34.704
U247B1	IL17	39.220	0.137			0.002	0.001	0.004
U247B2	IL17	38.105	0.634					
U247B3	IL17	38.758						

Notes:

(*) denotes Calibrator

(†) denotes Endogenous Control

Results Summary

Sample	Target	CT (Mean)	CT (Std Dev)	Normalized Qty (Mean)	Normalized Qty (Std Err)	RQ	RQ (Min)	RQ (Max)
M266 *	ACTB †	23.228	0.169					
M286	ACTB †	22.147	0.257					
M296	ACTB †	21.934	0.111					
M306	ACTB †	22.049	0.145					
NTC	ACTB †							
U237A1	ACTB †	22.002	0.196					
U237A2	ACTB †	22.065	0.195					
U237A3	ACTB †	21.812	0.204					
U247B1	ACTB †	21.666	0.249					
U247B2	ACTB †	22.376	0.201					
U247B3	ACTB †	23.321	0.099					
M266 *	CXCL1	39.261						
M286	CXCL1	39.761	4.896			0.374	0.008	17.587
M296	CXCL1	37.625	9.490					
M306	CXCL1	44.765				0.025		
NTC	CXCL1							
U237A1	CXCL1							
U237A2	CXCL1							
U237A3	CXCL1	41.006						
U247B1	CXCL1	39.751	4.279					
U247B2	CXCL1							
U247B3	CXCL1							
M266 *	GAPDH	24.044	0.173			1.000	0.831	1.203
M286	GAPDH	22.725	0.075			1.054	0.850	1.308
M296	GAPDH	23.291	0.108			0.658	0.584	0.741
M306	GAPDH	23.231	0.035			0.735	0.652	0.829

Notes:

(*) denotes Calibrator

(†) denotes Endogenous Control

Sample	Target	CT (Mean)	CT (Std Dev)	Normalized Qty (Mean)	Normalized Qty (Std Err)	RQ	RQ (Min)	RQ (Max)
NTC	GAPDH							
U237A1	GAPDH	23.150	0.074			0.747	0.631	0.884
U237A2	GAPDH	22.917	0.147			0.893	0.738	1.080
U237A3	GAPDH	22.749	0.121			0.833	0.691	1.004
U247B1	GAPDH	22.554	0.087			0.847	0.685	1.046
U247B2	GAPDH	22.663	0.172			1.273	1.038	1.561
U247B3	GAPDH	23.367	0.175			1.580	1.361	1.834
M266 *	IL1A	39.102	2.737			1.000	0.119	8.418
M286	IL1A	39.403	1.816			0.403	0.097	1.676
M296	IL1A	35.658	2.603			3.769	0.498	28.530
M306	IL1A	35.288	4.301			5.146	0.182	145.660
NTC	IL1A							
U237A1	IL1A	39.806	1.776			0.283	0.071	1.135
U237A2	IL1A	38.503	5.770					
U237A3	IL1A	40.008	5.897					
U247B1	IL1A	41.410	2.438			0.082	0.004	1.724
U247B2	IL1A	39.100	0.909			0.569	0.237	1.362
U247B3	IL1A	35.401						
M266 *	IL6	37.603	5.722					
M286	IL6	34.418	1.589					
M296	IL6	33.238				14.533		
M306	IL6	33.483						
NTC	IL6							
U237A1	IL6							
U237A2	IL6							
U237A3	IL6	35.221						
U247B1	IL6							
U247B2	IL6	39.950						

Notes:

(*) denotes Calibrator

(†) denotes Endogenous Control

Sample	Target	CT (Mean)	CT (Std Dev)	Normalized Qty (Mean)	Normalized Qty (Std Err)	RQ	RQ (Min)	RQ (Max)
U247B3	IL6	36.248						

Notes:

(*) denotes Calibrator

(†) denotes Endogenous Control

TABLE I: Results Summary tables generated by Quantstudio Real-Time PCR Software for all GBS genes over 6 separate runs of qPCR.

Results Summary

Sample	Target	CT (Mean)	CT (Std Dev)	Normalized Qty (Mean)	Normalized Qty (Std Err)	RQ	RQ (Min)	RQ (Max)
G175A *	cylE	28.836	0.459	0.114	1.162	1.000	0.692	1.445
G185A	cylE	28.171	0.445	0.103	1.181	0.906	0.604	1.361
G185B	cylE	28.299	0.314	0.173	1.111	1.521	1.177	1.967
G195B	cylE	28.517	0.673	0.112	1.251	0.984	0.569	1.704
G195C	cylE	29.224	0.276	0.076	1.110	0.670	0.519	0.866
G225A	cylE	28.111	0.218	0.110	1.119	0.964	0.733	1.268
M266	cylE	25.667	0.290	0.236	1.104	2.077	1.632	2.643
M286	cylE	29.595	0.337	0.144	1.130	1.266	0.940	1.706
M296	cylE	24.088	2.849	0.193	2.527	1.695	0.175	16.369
M306	cylE	26.733	0.503	0.150	1.215	1.322	0.802	2.181
NTC	cylE							
G175A *	czcD	28.116	0.153	0.202	1.054	1.000	0.878	1.138
G185A	czcD	27.699	0.319	0.155	1.140	0.768	0.558	1.058
G185B	czcD	28.137	0.173	0.214	1.063	1.059	0.912	1.228
G195B	czcD	28.398	0.249	0.135	1.098	0.668	0.531	0.840
G195C	czcD	28.217	0.268	0.163	1.107	0.808	0.631	1.036
G225A	czcD	28.259	0.227	0.111	1.120	0.549	0.416	0.725
M266	czcD	23.151	0.057	1.284	1.035	6.347	5.840	6.898
M286	czcD	26.518	0.187	1.165	1.084	5.760	4.733	7.010
M296	czcD	23.379	0.060	0.325	1.053	1.606	1.413	1.824
M306	czcD	24.183	0.121	0.845	1.063	4.176	3.593	4.855
NTC	czcD							
G175A *	dnaN †	26.906						
G185A	dnaN †	26.047						
G185B	dnaN †	27.021						
G195B	dnaN †	26.545						

Notes:

(*) denotes Calibrator

(†) denotes Endogenous Control

Sample	Target	CT (Mean)	CT (Std Dev)	Normalized Qty (Mean)	Normalized Qty (Std Err)	RQ	RQ (Min)	RQ (Max)
G195C	dnaN †	26.666						
G225A	dnaN †	26.084						
M266	dnaN †	24.753						
M286	dnaN †	28.088						
M296	dnaN †	22.762						
M306	dnaN †	25.145						
NTC	dnaN †							
G175A *	pil2B	29.128	0.597	0.166	1.210	1.000	0.627	1.595
G185A	pil2B	27.900	0.340	0.213	1.145	1.285	0.922	1.791
G185B	pil2B	28.878	0.087	0.209	1.038	1.258	1.150	1.377
G195B	pil2B	28.204	0.292	0.239	1.111	1.439	1.112	1.863
G195C	pil2B	28.150	0.247	0.266	1.100	1.606	1.272	2.027
G225A	pil2B	27.798	0.193	0.232	1.112	1.402	1.081	1.819
M266	pil2B	26.794	0.122	0.194	1.049	1.167	1.038	1.313
M286	pil2B	28.936	0.317	0.388	1.121	2.342	1.772	3.095
M296	pil2B	22.113	0.309	1.109	1.116	6.687	5.117	8.740
M306	pil2B	27.174	0.099	0.194	1.059	1.168	1.015	1.344
NTC	pil2B							
G175A *	rib	25.716	0.426	1.166	1.142	1.000	0.722	1.385
G185A	rib	25.542	0.178	0.764	1.104	0.655	0.514	0.834
G185B	rib	26.045	0.217	1.021	1.074	0.876	0.735	1.043
G195B	rib	26.053	0.085	0.758	1.058	0.650	0.566	0.746
G195C	rib	26.112	0.087	0.787	1.062	0.675	0.582	0.782
G225A	rib	25.970	0.133	0.600	1.101	0.514	0.407	0.651
M266	rib	22.022	0.074	3.019	1.037	2.588	2.367	2.831
M286	rib	25.786	0.072	2.314	1.060	1.984	1.722	2.286
M296	rib	22.539	0.340	0.642	1.123	0.550	0.415	0.730
M306	rib	22.860	0.233	2.292	1.090	1.965	1.591	2.428

Notes:

(*) denotes Calibrator

(†) denotes Endogenous Control

Sample	Target	CT (Mean)	CT (Std Dev)	Normalized Qty (Mean)	Normalized Qty (Std Err)	RQ	RQ (Min)	RQ (Max)
NTC	rib							
G175A *	ropB	28.045	0.109	0.345	1.041	1.000	0.906	1.104
G185A	ropB	27.156	0.209	0.359	1.112	1.040	0.803	1.347
G185B	ropB	27.752	0.163	0.447	1.059	1.294	1.124	1.490
G195B	ropB	27.895	0.237	0.304	1.095	0.881	0.706	1.099
G195C	ropB	28.110	0.222	0.286	1.093	0.827	0.665	1.029
G225A	ropB	27.334	0.235	0.328	1.122	0.949	0.716	1.257
M266	ropB	26.868	0.167	0.194	1.063	0.563	0.485	0.653
M286	ropB	29.835	0.356	0.228	1.134	0.659	0.484	0.896
M296	ropB	22.514	0.148	0.924	1.070	2.676	2.267	3.158
M306	ropB	27.203	0.133	0.200	1.066	0.578	0.494	0.677
NTC	ropB							

Notes:

(*) denotes Calibrator

(†) denotes Endogenous Control

Results Summary

Sample	Target	CT (Mean)	CT (Std Dev)	Normalized Qty (Mean)	Normalized Qty (Std Err)	RQ	RQ (Min)	RQ (Max)
G175A *	1010	27.671	0.662	0.187	1.221	1.000	0.614	1.630
G185A	1010	27.819	0.369	0.153	1.136	0.819	0.599	1.120
G185B	1010	28.198	0.234	0.213	1.078	1.138	0.947	1.368
G195B	1010	28.647	0.396	0.139	1.195	0.742	0.479	1.148
G195C	1010	29.040	0.582	0.125	1.223	0.666	0.407	1.089
G225A	1010	27.775	0.433	0.139	1.170	0.743	0.506	1.092
M266	1010	25.032	0.152	0.357	1.135	1.908	1.401	2.599
M286	1010	28.324	0.524	0.499	1.267	2.666	1.493	4.758
M296	1010	25.784	0.385	1.730	6.386	9.243	0.099	863.177
M306	1010	25.228	0.451	0.500	1.198	2.671	1.715	4.158
NTC	1010							
G175A *	cpsE	27.214	0.540	0.291	1.216	1.000	0.619	1.615
G185A	cpsE	26.810	0.524	0.346	1.217	1.188	0.734	1.921
G185B	cpsE	27.771	0.562	0.305	1.222	1.046	0.641	1.708
G195B	cpsE	27.733	0.778	0.265	1.357	0.912	0.432	1.926
G195C	cpsE	28.292	0.541	0.202	1.244	0.695	0.407	1.186
G225A	cpsE	26.803	0.531	0.307	1.232	1.055	0.633	1.758
M266	cpsE	26.837	0.408	0.155	1.204	0.531	0.337	0.836
M286	cpsE	30.261	0.456	0.133	1.273	0.457	0.253	0.826
M296	cpsE	26.609	0.675	1.365	6.461	4.688	0.049	450.527
M306	cpsE	26.850	0.961	0.240	1.434	0.825	0.342	1.993
NTC	cpsE							
G175A *	dnaN †	26.806						
G185A	dnaN †	26.621						
G185B	dnaN †	27.527						
G195B	dnaN †	27.255						

Notes:

(*) denotes Calibrator

(†) denotes Endogenous Control

Sample	Target	CT (Mean)	CT (Std Dev)	Normalized Qty (Mean)	Normalized Qty (Std Err)	RQ	RQ (Min)	RQ (Max)
G195C	dnaN †	27.455						
G225A	dnaN †	26.418						
M266	dnaN †	25.325						
M286	dnaN †	29.050						
M296	dnaN †	28.649						
M306	dnaN †	26.067						
NTC	dnaN †							
G175A *	htp	33.616	0.773	0.006	1.274	1.000	0.553	1.809
G185A	htp	33.512	1.178	0.005	1.446	0.953	0.387	2.347
G185B	htp	33.959	0.435	0.007	1.147	1.255	0.897	1.755
G195B	htp	33.153	0.471	0.010	1.219	1.746	1.075	2.837
G195C	htp	33.066	1.437	0.011	1.684	2.080	0.545	7.940
G225A	htp	31.379	0.509	0.017	1.200	3.126	2.001	4.881
M266	htp	27.669	0.755	0.087	1.298	15.763	8.332	29.824
M286	htp	31.511	1.075	0.078	1.457	14.252	5.674	35.794
M296	htp	28.858	0.930	0.314	6.505	57.088	0.584	5,578.175
M306	htp	28.708	0.842	0.072	1.332	13.059	6.470	26.356
NTC	htp							
G175A *	ropB	27.973	0.217	0.240	1.087	1.000	0.816	1.225
G185A	ropB	27.909	0.192	0.223	1.096	0.931	0.744	1.164
G185B	ropB	28.398	0.314	0.285	1.109	1.185	0.920	1.527
G195B	ropB	28.481	0.114	0.229	1.151	0.954	0.677	1.345
G195C	ropB	28.646	0.378	0.233	1.174	0.971	0.656	1.437
G225A	ropB	27.436	0.131	0.266	1.107	1.108	0.864	1.422
M266	ropB	27.040	0.435	0.176	1.199	0.733	0.471	1.142
M286	ropB	30.506	0.357	0.190	1.237	0.791	0.470	1.331
M296	ropB	27.420	0.298	1.042	6.379	4.339	0.047	404.194
M306	ropB	27.904	0.217	0.160	1.152	0.667	0.472	0.943

Notes:

(*) denotes Calibrator

(†) denotes Endogenous Control

Sample	Target	CT (Mean)	CT (Std Dev)	Normalized Qty (Mean)	Normalized Qty (Std Err)	RQ	RQ (Min)	RQ (Max)
NTC	ropB							
G175A *	scpB	30.796	0.226	0.048	1.087	1.000	0.815	1.227
G185A	scpB	29.925	0.460	0.073	1.169	1.521	1.038	2.229
G185B	scpB	31.444	0.451	0.050	1.151	1.044	0.739	1.473
G195B	scpB	31.008	0.453	0.055	1.214	1.155	0.719	1.854
G195C	scpB	31.637	0.563	0.042	1.225	0.888	0.541	1.458
G225A	scpB	30.163	0.544	0.056	1.210	1.163	0.730	1.853
M266	scpB	26.591	0.233	0.253	1.148	5.301	3.783	7.428
M286	scpB	30.255	0.613	0.260	1.297	5.437	2.880	10.265
M296	scpB	27.016	0.223	1.470	6.372	30.766	0.331	2,857.860
M306	scpB	27.571	0.456	0.219	1.205	4.575	2.901	7.216
NTC	scpB							

Notes:

(*) denotes Calibrator

(†) denotes Endogenous Control

Results Summary

Sample	Target	CT (Mean)	CT (Std Dev)	Normalized Qty (Mean)	Normalized Qty (Std Err)	RQ	RQ (Min)	RQ (Max)
G175A *	cylE	29.104	0.575			1.000	0.643	1.556
G185A	cylE	29.072	0.060			0.539	0.486	0.599
G185B	cylE	28.947	0.469			1.522	1.063	2.180
G195B	cylE	29.545	0.358			0.701	0.454	1.082
G195C	cylE	29.654	0.402			0.831	0.593	1.165
G225A	cylE	30.152	0.650			0.428	0.222	0.825
M266	cylE	26.339	0.218			1.422	1.026	1.972
M286	cylE							
M296	cylE	27.014	0.138			1.223	0.960	1.558
M306	cylE	27.145	0.138			1.299	0.918	1.838
NTC	cylE							
G175A *	czcD	29.056	0.205			1.000	0.846	1.182
G185A	czcD	28.500	0.299			0.736	0.583	0.929
G185B	czcD	29.378	0.171			1.141	0.997	1.306
G195B	czcD	29.631	0.440			0.655	0.411	1.044
G195C	czcD	29.308	0.205			1.007	0.818	1.240
G225A	czcD	29.410	0.463			0.664	0.434	1.015
M266	czcD	23.968	0.141			5.261	4.032	6.864
M286	czcD	27.604	0.497			6.204	3.831	10.047
M296	czcD	24.601	0.135			4.721	3.791	5.878
M306	czcD	25.324	0.749			3.541	1.895	6.617
NTC	czcD							
G175A *	dnaN †	27.356	0.110					
G185A	dnaN †	26.238	0.122					
G185B	dnaN †	27.924	0.074					
G195B	dnaN †	27.212	0.488					

Notes:

(*) denotes Calibrator

(†) denotes Endogenous Control

Sample	Target	CT (Mean)	CT (Std Dev)	Normalized Qty (Mean)	Normalized Qty (Std Err)	RQ	RQ (Min)	RQ (Max)
G195C	dnaN †	27.631	0.208					
G225A	dnaN †	27.006	0.372					
M266	dnaN †	24.968	0.352					
M286	dnaN †	29.047	0.458					
M296	dnaN †	25.437	0.281					
M306	dnaN †	25.686	0.442					
NTC	dnaN †							
G175A *	pil2B	29.446	0.425			1.000	0.730	1.369
G185A	pil2B	27.875	0.398			1.328	0.986	1.788
G185B	pil2B	29.978	0.112			1.011	0.919	1.112
G195B	pil2B	28.945	0.258			1.235	0.810	1.883
G195C	pil2B	29.076	0.253			1.453	1.152	1.833
G225A	pil2B							
M266	pil2B	27.407	0.241			0.847	0.628	1.144
M286	pil2B	29.368	0.471			2.741	1.723	4.362
M296	pil2B	27.304	0.249			1.176	0.902	1.532
M306	pil2B	27.250	0.300			1.398	0.960	2.035
NTC	pil2B							
G175A *	rib	26.828	0.253			1.000	0.819	1.221
G185A	rib	26.615	0.499			0.601	0.382	0.944
G185B	rib	27.025	0.256			1.228	1.011	1.492
G195B	rib	27.162	0.187			0.755	0.509	1.118
G195C	rib	27.129	0.160			0.977	0.811	1.177
G225A	rib	26.993	0.159			0.742	0.559	0.986
M266	rib	22.672	0.147			3.074	2.352	4.019
M286	rib	26.902	0.245			2.507	1.738	3.615
M296	rib	23.370	0.077			2.648	2.159	3.247
M306	rib	24.166	0.661			1.896	1.069	3.361

Notes:

(*) denotes Calibrator

(†) denotes Endogenous Control

Sample	Target	CT (Mean)	CT (Std Dev)	Normalized Qty (Mean)	Normalized Qty (Std Err)	RQ	RQ (Min)	RQ (Max)
NTC	rib							
G175A *	rpoB	28.460	0.257			1.000	0.817	1.224
G185A	rpoB							
G185B	rpoB	28.574	0.238			1.291	1.078	1.546
G195B	rpoB							
G195C	rpoB	28.649	0.275			1.045	0.817	1.337
G225A	rpoB							
M266	rpoB	27.241	0.410			0.529	0.359	0.777
M286	rpoB	28.826	0.795			2.107	0.969	4.582
M296	rpoB	26.954	0.163			0.819	0.651	1.030
M306	rpoB							
NTC	rpoB							

Notes:

(*) denotes Calibrator

(†) denotes Endogenous Control

Results Summary

Sample	Target	CT (Mean)	CT (Std Dev)	Normalized Qty (Mean)	Normalized Qty (Std Err)	RQ	RQ (Min)	RQ (Max)
G175A	1010	29.288	0.274			1.010	0.821	1.243
G185A	1010	28.457	0.179			1.001	0.876	1.143
G185B	1010	29.280	0.199			1.183	1.029	1.362
G195B	1010	28.923	0.082			1.039	0.887	1.218
G195C	1010	29.735	0.276			0.812	0.627	1.053
G225A *	1010	28.371	0.075			1.000	0.886	1.129
M266	1010	25.588	0.189			2.977	2.423	3.659
M286	1010							
M296	1010	25.795	0.103			2.257	2.076	2.455
M306	1010	25.850	0.316			2.858	2.246	3.636
NTC	1010							
G175A	cpsE	27.838	0.284			0.964	0.780	1.191
G185A	cpsE	27.020	0.199			0.946	0.819	1.092
G185B	cpsE	27.644	0.187			1.255	1.099	1.434
G195B	cpsE	27.506	0.084			0.972	0.834	1.134
G195C	cpsE	27.794	0.219			1.027	0.835	1.264
G225A *	cpsE	26.835	0.133			1.000	0.869	1.150
M266	cpsE	26.645	0.102			0.671	0.561	0.803
M286	cpsE	29.294	0.164			0.579	0.474	0.708
M296	cpsE	25.879	0.081			0.888	0.826	0.956
M306	cpsE	25.890	0.176			1.153	0.971	1.370
NTC	cpsE							
G175A	dnaN	26.638	0.138					
G185A	dnaN	25.837	0.100					
G185B	dnaN	27.054	0.086					
G195B	dnaN	26.369	0.124					

Notes:

(*) denotes Calibrator

(†) denotes Endogenous Control

Sample	Target	CT (Mean)	CT (Std Dev)	Normalized Qty (Mean)	Normalized Qty (Std Err)	RQ	RQ (Min)	RQ (Max)
G195C	dnaN	26.629	0.135					
G225A *	dnaN	25.754	0.107					
M266	dnaN	24.407	0.375					
M286	dnaN	27.140	0.242					
M296	dnaN	24.168	0.104					
M306	dnaN	24.525	0.192					
NTC	dnaN							
G175A	htp	32.740	0.110			0.574	0.499	0.660
G185A	htp	31.172	0.379			0.884	0.656	1.190
G185B	htp	31.675	0.810			1.248	0.670	2.326
G195B	htp	31.408	0.197			1.044	0.847	1.288
G195C	htp							
G225A *	htp	30.874	0.502			1.000	0.670	1.492
M266	htp	26.283	0.057			8.847	7.455	10.498
M286	htp	29.472	0.444			5.374	3.840	7.520
M296	htp	26.865	0.156			5.375	4.796	6.024
M306	htp	26.943	0.250			6.707	5.442	8.266
NTC	htp							
G175A	rpoB	28.248	0.202					
G185A	rpoB	27.342	0.112					
G185B	rpoB	28.373	0.098					
G195B	rpoB	27.881	0.293					
G195C	rpoB	28.391	0.312					
G225A *	rpoB	27.249	0.222					
M266	rpoB	26.806	0.023					
M286	rpoB	28.880	0.293					
M296	rpoB	26.493	0.050					
M306	rpoB	27.071	0.218					

Notes:

(*) denotes Calibrator

(†) denotes Endogenous Control

Sample	Target	CT (Mean)	CT (Std Dev)	Normalized Qty (Mean)	Normalized Qty (Std Err)	RQ	RQ (Min)	RQ (Max)
NTC	rpoB							
G175A	scpB	31.168	0.257			0.861	0.711	1.043
G185A	scpB	30.154	0.125			0.922	0.832	1.021
G185B	scpB	30.585	0.288			1.381	1.115	1.710
G195B	scpB							
G195C	scpB	31.077	0.199			0.941	0.773	1.144
G225A *	scpB	29.913	0.438			1.000	0.749	1.335
M266	scpB	26.358	0.124			4.205	3.500	5.051
M286	scpB	29.341	0.226			3.233	2.596	4.027
M296	scpB	26.188	0.095			3.942	3.647	4.260
M306	scpB	26.888	0.436			3.511	2.503	4.926
NTC	scpB							

Notes:

(*) denotes Calibrator

(†) denotes Endogenous Control

Results Summary

Sample	Target	CT (Mean)	CT (Std Dev)	Normalized Qty (Mean)	Normalized Qty (Std Err)	RQ	RQ (Min)	RQ (Max)
G175A	cfb	29.103	0.266			1.462	1.198	1.784
G185A	cfb	28.014	0.195			1.651	1.434	1.901
G185B	cfb	28.674	0.248			2.005	1.600	2.513
G195B	cfb	29.359	0.349			1.253	0.995	1.577
G195C	cfb	29.537	0.200			1.337	1.156	1.547
G225A *	cfb	28.619	0.223			1.000	0.824	1.214
M266	cfb	27.044	0.229			1.516	1.305	1.761
M286	cfb	29.027	0.301			2.140	1.729	2.648
M296	cfb	26.866	0.267			1.369	1.147	1.633
M306	cfb	27.441	0.245			1.405	1.149	1.717
NTC	cfb							
G175A	copA	29.958	0.493			1.193	0.854	1.667
G185A	copA	29.290	0.059			1.067	0.983	1.157
G185B	copA	29.859	0.439			1.357	0.980	1.879
G195B	copA	29.922	0.394			1.208	0.930	1.569
G195C	copA	30.610	0.189			0.958	0.832	1.104
G225A *	copA	29.129	0.285			1.000	0.797	1.254
M266	copA	28.076	0.082			1.138	1.066	1.214
M286	copA	27.703	0.313			6.143	4.916	7.676
M296	copA	28.717	0.250			0.641	0.541	0.759
M306	copA	28.801	0.220			0.869	0.718	1.051
NTC	copA							
G175A	dnaN	27.427	0.146					
G185A	dnaN	26.670	0.076					
G185B	dnaN	27.800	0.113					
G195B	dnaN	27.484	0.111					

Notes:

(*) denotes Calibrator

(†) denotes Endogenous Control

Sample	Target	CT (Mean)	CT (Std Dev)	Normalized Qty (Mean)	Normalized Qty (Std Err)	RQ	RQ (Min)	RQ (Max)
G195C	dnaN	27.632	0.123					
G225A *	dnaN	26.582	0.172					
M266	dnaN	25.020	0.068					
M286	dnaN	27.913	0.109					
M296	dnaN	24.856	0.025					
M306	dnaN	25.390	0.084					
NTC	dnaN							
G175A	hvgA	31.882	0.218			0.853	0.699	1.041
G185A	hvgA	30.484	0.116			1.178	1.064	1.303
G185B	hvgA	31.836	0.895			0.942	0.513	1.728
G195B	hvgA	31.305	0.500			1.187	0.804	1.751
G195C	hvgA							
G225A *	hvgA	30.495	0.246			1.000	0.811	1.232
M266	hvgA	27.834	0.241			2.951	2.510	3.470
M286	hvgA	29.117	0.330			6.055	4.783	7.666
M296	hvgA	28.181	0.272			1.963	1.631	2.363
M306	hvgA	28.393	0.047			2.467	2.157	2.821
NTC	hvgA							
G175A	maeE	31.568	0.135			1.205	1.052	1.379
G185A	maeE	31.233	0.432			0.883	0.670	1.164
G185B	maeE	32.029	0.344			1.002	0.766	1.310
G195B	maeE							
G195C	maeE	32.498	0.039			0.841	0.777	0.910
G225A *	maeE	30.726	0.316			1.000	0.766	1.306
M266	maeE	29.118	0.250			1.516	1.293	1.779
M286	maeE	29.336	0.244			5.847	4.889	6.992
M296	maeE	30.027	0.273			0.745	0.624	0.890
M306	maeE	30.871	0.379			0.663	0.508	0.867

Notes:

(*) denotes Calibrator

(†) denotes Endogenous Control

Sample	Target	CT (Mean)	CT (Std Dev)	Normalized Qty (Mean)	Normalized Qty (Std Err)	RQ	RQ (Min)	RQ (Max)
NTC	maeE							
G175A	ropB	28.558	0.178					
G185A	ropB	27.624	0.124					
G185B	ropB	28.434	0.329					
G195B	ropB	28.474	0.087					
G195C	ropB	28.890	0.097					
G225A *	ropB	27.178	0.230					
M266	ropB	27.097	0.047					
M286	ropB	29.220	0.174					
M296	ropB	26.569	0.108					
M306	ropB	27.235	0.260					
NTC	ropB							

Notes:

(*) denotes Calibrator

(†) denotes Endogenous Control

Results Summary

Sample	Target	CT (Mean)	CT (Std Dev)	Normalized Qty (Mean)	Normalized Qty (Std Err)	RQ	RQ (Min)	RQ (Max)
G175A *	cfb	28.917	0.365			1.000	0.729	1.371
G185A	cfb	27.808	0.252			1.099	0.866	1.395
G185B	cfb	28.430	0.430			1.649	1.156	2.352
G195B	cfb	29.335	0.184			0.846	0.686	1.043
G195C	cfb	29.737	0.631			0.737	0.435	1.249
G225A	cfb	28.166	0.199			0.693	0.563	0.853
M266	cfb	26.916	0.152			0.859	0.743	0.992
M286	cfb	28.439	0.176			1.868	1.491	2.340
M296	cfb	26.711	0.109			0.876	0.800	0.959
M306	cfb	27.083	0.070			0.994	0.883	1.119
NTC	cfb							
G175A *	copA	30.063	0.187			1.000	0.828	1.208
G185A	copA	28.887	0.244			1.159	0.917	1.466
G185B	copA	29.744	0.344			1.478	1.107	1.975
G195B	copA	30.081	0.149			1.102	0.911	1.334
G195C	copA	30.143	0.395			1.201	0.847	1.703
G225A	copA	28.961	0.181			0.880	0.722	1.073
M266	copA	28.174	0.276			0.808	0.637	1.025
M286	copA	27.453	0.070			7.794	6.487	9.365
M296	copA	28.429	0.107			0.607	0.555	0.664
M306	copA	28.473	0.359			0.855	0.627	1.167
NTC	copA							
G175A *	dnaN †	27.108	0.139					
G185A	dnaN †	26.127	0.154					
G185B	dnaN †	27.382	0.086					
G195B	dnaN †	27.276	0.184					

Notes:

(*) denotes Calibrator

(†) denotes Endogenous Control

Sample	Target	CT (Mean)	CT (Std Dev)	Normalized Qty (Mean)	Normalized Qty (Std Err)	RQ	RQ (Min)	RQ (Max)
G195C	dnaN †	27.472	0.166					
G225A	dnaN †	25.780	0.165					
M266	dnaN †	24.840	0.094					
M286	dnaN †	27.582	0.219					
M296	dnaN †	24.662	0.026					
M306	dnaN †	25.235	0.130					
NTC	dnaN †							
G175A *	hvgA	31.401	0.772			1.000	0.524	1.908
G185A	hvgA	30.518	0.348			0.957	0.701	1.308
G185B	hvgA	31.440	1.329			1.164	0.389	3.489
G195B	hvgA	31.328	0.160			1.172	0.938	1.463
G195C	hvgA	31.861	0.452			0.930	0.580	1.491
G225A	hvgA	29.879	0.150			1.175	0.959	1.441
M266	hvgA	27.742	0.279			2.687	2.110	3.423
M286	hvgA							
M296	hvgA	27.688	0.247			2.484	2.024	3.047
M306	hvgA	28.070	0.173			2.787	2.338	3.324
NTC	hvgA							
G175A *	maeE	31.656	0.554			1.000	0.578	1.729
G185A	maeE							
G185B	maeE	31.463	0.583			1.355	0.847	2.167
G195B	maeE	32.008	0.619			0.887	0.530	1.484
G195C	maeE	31.933	0.400			1.058	0.749	1.493
G225A	maeE	30.298	0.313			1.020	0.770	1.353
M266	maeE	28.766	0.213			1.500	1.246	1.806
M286	maeE	28.755	0.233			9.005	6.978	11.620
M296	maeE	29.641	0.174			0.756	0.657	0.870
M306	maeE	30.474	0.486			0.638	0.427	0.952

Notes:

(*) denotes Calibrator

(†) denotes Endogenous Control

Sample	Target	CT (Mean)	CT (Std Dev)	Normalized Qty (Mean)	Normalized Qty (Std Err)	RQ	RQ (Min)	RQ (Max)
NTC	maeE							
G175A *	rpoB	28.134	0.165			1.000	0.840	1.190
G185A	rpoB	27.370	0.198			0.879	0.718	1.077
G185B	rpoB	28.301	0.198			1.068	0.896	1.274
G195B	rpoB	28.481	0.104			0.885	0.747	1.048
G195C	rpoB	29.033	0.287			0.695	0.531	0.909
G225A	rpoB	27.082	0.244			0.851	0.670	1.080
M266	rpoB	27.136	0.103			0.445	0.397	0.498
M286	rpoB	29.124	0.396			0.703	0.486	1.015
M296	rpoB	26.587	0.200			0.572	0.485	0.675
M306	rpoB	27.285	0.085			0.521	0.460	0.590
NTC	rpoB							

Notes:

(*) denotes Calibrator

(†) denotes Endogenous Control

TABLE J: Assembled contig of htp mutant GV6_177 – FASTA file format.

```
>Contig_GV6_177
cattatccgctcaatgtctcgaaaaggaacacctgcagataatgcctgtattgaatggtt
tcacaccgtcctaaagactgaaacctttatttccataataggagaaaatacaacaaaga
tagtataacaaatattgttaaaaattacattacattttataatgaaactagaattcaaca
gagattaaacgaccagtcgcctgtacagtacagaaaactgattgcctaaaagtgtttttc
ttgcgtctcactattagggtgcagtgccaatatcatgcattctttttctaatcctggata
tccttatgataatgccgtaactgaagcatttttcaagtatttaaagcatagacaaatcaa
ccgaaaacattatcaaaatatcaaacaggttcaattagactgctttgaatacattgagaa
tttttataacaattacaacccacatacggctaatctaggactaacccctaatcagaaaga
agaaaattattttaactcaataaaataacacagttttctgtctacttatttgacattagt
ccaagaatcctcctctttttttactattctaacatggataccatttctttgcaaaagaaa
accgctattatccaacttttatcactactcgttacatagaatgacttcaaaatcaccgta
acttgctttgacaaagcagtgctttaacaatgagatcttcttttggtttagttcaacaaa
cgaaaattggataaagtgggatattagtttaacaatatatatttatgttacagtaatatt
gacttttaaaaaaggattgattataatgaagaaagcagacaagtaagcctcctaaattca
ctttagataaaaatttaggaggcatatcaaatgaactttaataaaattcactttagataa
aaatttaggaggcatatcaaatgaactttaataaaattgatttagacaattggaagagaa
aagagatatttaatcattatttgaaccaacaaacgacttttagtataaccacagaaattg
atattagtgttttataccgaaacataaaacaagaaggatataaattttaccctgcattta
ttttcttagtgacaagggtgataaactcaaatacagcttttagaactggttacaatagcg
acggagagttaggttattgggataagttagagccactttatacaatttttgatggtgtat
ctaaaacattctctggtatttggactcctgtaaagaatgacttcaaagagttttatgatt
tatacctttctgatgtagagaaatataatggttcggggaaattgtttcccaaaacaccta
tacctgaaaatgctttttctctttctattattccatggacttcatttactgggtttaact
taaatatcaataataatagtaattaccttctacccattattacagcaggaaaattcatta
ataaaggtaattcaatatatttaccgctatctttacaggtacatcattctgtttgtgatg
gttatcatgcaggattgtttatgaactctattcaggaattgtcagataggcctaatgact
ggcttttataatatgagataatgccgactgtacttttacagtcggttttctaatgtcac
taacctgcccctaataatctcctttacttcaactgttgatagagcacttccaaatttgct
ctaagattttctagatatgtcttgtttccgcttggagcagcttcaagtggacttaatgtc
tttactttagctcctgttgatttcgcaatagcatgagcaattttggggttgacgttgtct
tctgcaaaaatagtcttgacgttgtattctttaacaaagtcttgaatttctttcaattgg
cgaggagagggctcttgctctggagaaatacccgagataccaagttgtttcaagccgaat
cgtttagccagataagaaaatgccgtgtgttgcgtcacaaatgtttttgagcgcaccttt
ttaaatttttgagtgtattcttcagttagttgctctgcttctttttttgaaagccttagcc
tttttagtgtaactgtctttgtgtttaggatccaaatgtcctagctctttagcgatatta
acagcttcctcaccagctaaaacgggatccgtccaggtatgtgggtcataaagtgtcgca
gggtcaatgccttgtgtgacttccatatcttctagccctttgactctatctagtgtcaga
ggttt
```

TABLE K: Assembled contig of htp mutant GV12_8 – FASTA file format.

```
>Contig_GV12_8
ggcttactaccaggcttgcacggaaaaagacattatccgctcaatgtctcgaaaaggaac
acctgcagataatgcctgtattgaatggtttcacaccgtcctaaagactgaaacctttta
tttccataataggagaaaatacaacaaagatagtataacaaatattgttaaaaattacat
tacattttataatgaaactagaattcaacagagattaaacgaccagtcgcctgtacagta
cagaaaactgattgcctaaaagtgtttttcttgcgtctcactattagggtgcagtgccaa
tatcatgcattctttttctaatcctggatatccttatgataatgccgtaactgaagcatt
tttcaagtatttaaagcatagacaaatcaaccgaaaacattatcaaaatatcaaacaggt
tcaattagactgctttgaatacattgagaatttttataacaattacaaacccacatacgg
ctaatctaggactaacccctaatcagaaagaagaaaattattttaactcaataaaataac
acagttttctgtctacttatttgacattagtccaagaatcctcctctttttttactattc
taacatggataccatttctttgcaaaagaaaaccgctattatccaacttttatcactact
cgttacatagaatgacttcaaaatcaccgtaacttgctttgacaaagcagtgctttaaca
atgagatcttcttttggtttagttcaacaaacgaaaattggataaagtgggatattttta
aaatatatatttatgttcacagtaatattgacttttataaaaaggattgattataatgaa
gaaagtcatgttacaagtaatattgcctcctaaattcactttagataaaaatttaggagg
catatcaaatgaactttaataaaattcactttagataaaaatttaggaggcatatcaaat
gaactttaataaaattgatttagacaattggaagagaaaagagatatttaatcattattt
gaaccaacaaacgacttttagtataaccacagaaattgatattagtgttttataccgaaa
cataaaacaagaaggatataaattttaccctgcatttattttcttagtgacaagggtgat
aaactcaaatacagcttttagaactggttacaatagcgacggagagttaggttattggga
taagttagagccactttatacaatttttgatggtgtatctaaaacattctctggtatttg
gactcctgtaaagaatgacttcaaagagttttatgatttatacctttctgatgtagagaa
atataatggttcggggaaattgtttcccaaaacacctatacctgaaaatgctttttctct
ttctattattccatggacttcatttactgggtttaacttaaatatcaataataatagtaa
ttaccttctacccattattacagcaggaaaattcattaataaaggtaattcaatatattt
accgctatctttacaggtacatcattctgtttgtgatggttatcatgcaggattgtttat
gaactctattcaggaattgtcagataggcctaatgactggcttttataatatgagataat
gccgactgtacttttacagtcggttttctaatgtcactaacctgcccctaataatctcc
tttacttcaactgttgatagagcacttccaaatttgctctaagattttctagatatgtct
tgtttccgcttggagcagcttcaagtggacttaatgtctttactttagctcctgttgatt
tcgcaatagcatgagcaattttggggttgacgttgtcttctgcaaaaatagtcttgacgt
tgtattctttaacaaagtcttgaatttctttcaattggcgaggagagggctcttgctctg
gagaaatacccgagataccaagttgtttcaagccgaatcgtttagccagataagaaaatg
ccgtgtgttgcgtcacaaatgtttttgagcgcacctttttaaatttttgagtgtattctt
cagttagttgctctgcttctttttttgaaagccttagccttttttagtgtaactgtctttgt
gtttaggatccaaatgtcctagctctttagcgatattaacagcttcctcaccagctaaaa
cgggatccgtccaggtatgtgggtcataaagtgtcgcagggtcaatgccttgtgtgactt
ccatatcttctagccctttgactctatctagtgtcagaggtt
```

TABLE L: Assembled contig of WT GBS 874391 – FASTA file format.

```
>Contig_WT_htp
gttatgtgtttgagcgtcaaaacctctgacactagatagagtcaaagggctagaagatat
ggaagtcacacaaggcattgaccctgcgacactttatgacccacatacctggacggatcc
cgttttagctggtgaggaagctgttaatatcgctaaagagctaggacatttggatcctaa
acacaaagacagttacactaaaaaggctaaggctttcaaaaaagaagcagagcaactaac
tgaagaatacactcaaaaatttaaaaaggtgcgctcaaaaacatttgtgacgcaacacac
ggcattttcttatctggctaaacgattcggcttgaaacaacttggtatctcgggtatttc
tccagagcaagagccctctcctcgccaattgaaagaaattcaagactttgttaaagaata
caacgtcaagactatttttgcagaagacaacgtcaaccccaaaattgctcatgctattgc
gaaatcaacaggagctaaagtaaagacattaagtccacttgaagctgctccaagcggaaa
caagacatatctagaaaatcttagagcaaatttggaagtgctctatcaacagttgaagta
aaggagattattagtgaagaaaacatatggttatatcggctcagttgctgctattttact
agctactcatattggaagttaccagcttggtaagcatcatatgggtctagcaacaaagga
caatcagattgcctatattgatgatagcaaaggtaaggtaaaagcccctaaaacaaacaa
aacgatggatcaaatcagtgctgaagaaggcatctctgctgaacagatcgtagtcaaaat
tactgaccaaggttatgttacctcacacggtgaccattatcatttttacaatgggaaagt
tccttatgatgcgattattagtgaagagttgttgatgacggatcctaattaccatttaa
acaatcagacgttatcaatgaaatcttagacggttacgttattaaagtcaatggcaacta
ttatgtttacctcaagccaggtagtaagcgcaaaaacattcgaaccaaacaacaaattgc
tgagcaagtagccaaaggaactaaagaagctaaagaaaaaggtttagctcaagtggccca
tctcagtaaagaagaagttgcggcagtcaatgaagcaaaaagacaaggacgctatactac
agacgatggctatatttttagtccgacagatatcattgatgatttaggagatgcttattt
agtacctcatggtaatcactatcattatattcctaaaaaagatttgtctccaagtgarct
agctgctgcaaagcctactggartcaaaaacaaggtcaaggtgctagaccgtctgattac
cgcccgamaccagccccaggtsgtargaaagccccaattccggatgggacgcctaacccb
ggacaaggtcmtcmsccagawaacggkggttatcatccmssgcctcctaggccaaakgat
gcgtcacaaaacaaacaccmaagagatgagtttaaaggaaaaaccctttaaggaactttta
gatcaactacaccgycttgatttgaaataccgtcmtgkggaagaagawgggttgrttttt
kaaccgactcmmgtgaksaaatcaaacgctttkgggtatgkggtgsswmatggaratywt
tccccaawmawattatncccmwkargtyagwwawmacctcykgnmrakggaatwmgcagr
tcgmtacwwarmcrrmmaaactkwtkacmacgacycargttsagatmamwmaaaamsatn
nncakattaaakwmgkgnnnnrsrcgayacctttytatkktmattygcwtcttaaarmww
acggaaaaggcttagatggtaaaccatatgatacgagtgatgcttatgtttttagtaaag
aatccattcattcagtggataaatcaggagttacagctaaacacggagatcatttccact
atataggatttggagaacttgaacaatatgagttggatgaggtcgctaactgggtgaaag
caaaaggtcaagctgatgagcttgttgctgctttggatcaggaacaaggcaaagaaaaac
cactctttgacactaaaaaagtgagtcgcaaagtaacaaawkmtggkaargkggrctwtg
rttwtkcsaaaagatggcaarrmctatwwmwawgctcrwwatmaackkgaggttttkacw
magagttgcctttkyckwacaagaaytwwtnngyttwwmsawaaraagcwttwmmrwwaw
gmcmtysttnncckwtrcasscattgagccacsacttgctgtagatrtgtcaagtctkcc
satrcaygckggwaanttkytaswwasgnawatytggwwkttccccrtttgtttatycca
crtrttgatcrtatycakgtcgttcsgyawtcatggttgacrcgcaatcaagatnnatgc
aacaaycmmgtawgtgwtkcmrsayymcgaakttmryccggrygtatrgwctmagsywgg
kcattcsaaragtmagsttcggtsatnwmcarrtgktaygccaawctkgmwaawygtsca
tkktrtgmmraastgkcaaattatccattctgcwgmagaagktcarwwwgcmsyascaga
mggctmkwtttkcagcaycasacggctakattttygrymmamgaractkttgtatggmaa
gatrgmwmctttwgyatssmaagatggctcctttagcatcccaagagcagatggcagttc
attgagaaccattaataaatccgatctatcccaagctgagtggcaacaagctcaagagtt
attggcaaagaaaaatgctggtgatgctactgatacggataaacctgaagaaaagcaaca
ggcagataagagcaatgaaaaccaacagccaagtgaagccagtaaagaagaaaaagaatc
agatgactttatagacagtttaccagactatggtctagatagagcaaccctagaagatca
tatcaatcaattagcacaaaaagctaatatcgatcctaagtatctcattttccaaccaga
aggtgtccaatttataataaaaatggtgaattggtaacttatgatatcaagacacttca
acaaataaacccttaaccaaaagaagatctcattgttaaagcactgctttgtcaaagcaa
```

gttacggtgattttgaagtcattctatgtaacgagtagtgataaaagttggataatagcg
gttttcttttgcaaagaaatggtatccatgttagaatagtaaaaaaagaggaggattctt
ggactaatgtcaaataagtagacagaaaactgtgttattttattgagttaaaataatttt
cttctttctgattaggggttagtcctagattagccgtatgtgggttgtaattgttataaa
aattctcaatgtattcaaagcagtctaattgaacctgtttgatattttgataatgttttc
ggttgatttgtctatgctttaaatacttgaaaaatgcttcagttacggcattatcataag
gatatccaggattagaaaaagaatgcatgatattggcactgcaccctaatagtgagacgc
aagaaaaacacttttaggcaatcagttttctgtactgtacaggcgactggtcgtttaatc
tctgttgaattctagtttcattataaaatgtaatgtaatttttaacaatatttgttatac
tatctttgttgtattttctcctattatggaaataaaaggtttcagtctttaggacggtgt
gaaaccattcaatacaggcattatctgcaggtgttccttttcgagacattgagcggataa
tgtctttttccgtgcaagcctggtagtaagccatagaagtatacactgagc